Abstract

Background. *Necator americanus* is one of the major causes of human hookworm infection, affecting over 800 million people worldwide. Hookworm infections cause gastro-intestinal bleeding, anaemia and iron deficiency, and are associated with high rates of morbidity, especially in children. Although chemotherapy has proven effective, high rates of reinfection are reported in socioeconomically developing countries, possibly due to the short-term efficacy of anthelmintic drugs in addition to individual predisposition to these infections, raising interests in developing suitable alternatives to chemotherapy which are capable of providing complete, long-term protection against hookworms. Understanding of the molecular mechanisms used by *Necator americanus* larvae to penetrate the human skin and the vasculature would therefore aid the development of effective vaccines against this important pathogen.

Methods. First, *Necator americanus* larval exsheathing fluid (EF) and excretory/secretory products (ES) were profiled using gel electrophoresis and enzyme assays. Protease inhibitors against the main protease classes were used to determine which proteases are present in larval products. Second, the interaction of larval EF and ES products with human skin and extracellular matrix (ECM) macromolecules including collagens I, III, IV and V, fibronectin and laminin was investigated using western blots and protein separation by gel electrophoresis. Third, the impact of *Necator americanus* larval EF and ES on the endothelial barrier was examined using human umbilical vein endothelial cells (HUVEC). Permeability, an essential endothelial barrier function, was

assessed during treatment with larval products, using transendothelial electrical resistance (TEER), and post-treatment using albumin-tracer flux. Finally, at the cellular level, responses to treatment with larval products were assessed by investigating molecular changes at cell-cell vascular endothelial (VE)-cadherin junctions and actin filaments, and by determining levels of secreted inflammatory cytokines, IL-6 and IL-8, and vascular endothelial growth factor (VEGF) in the culture medium.

Results. It would appear that a repertoire of larval proteases, including serine, cysteine, aspartyl and metalloprotinases, caused partial degradation of skin macromolecules, collagens I, III, IV and laminin while fibronectin was fully degraded. Proteolysis of skin- and ECM macromolecules was related to the characteristic presence of proteolytic enzymes in larval products. The presence of transglutaminase activity was confirmed in both EF and ES products.

Larval proteases caused a dose related increase in endothelial permeability, characterised by a decrease in monolayer resistance (TEER) with increased permeation of albumin tracer, which was minimal in the presence of a cocktail of protease inhibitors. These barrier changes were associated with disruption of junctional VE-cadherin and F-actin, the formation of intercellular gaps and an increase in endothelial secretion of IL-6 and IL-8.

Conclusions. *Necator americanus* larvae produce a repertoire of proteolytic enzymes which could play an important role in negotiating the skin and breaching the endothelium to gain access to the host's blood circulation.

List of publications

Souadkia N, Brown A, Leach L and Pritchard D (2010). <u>Hookworm (*Necator americanus*) larval enzymes disrupt human vascular endothelium</u>. The American Journal of Tropical Medicine and Hygiene (in press).

Souadkia N, Pritchard D and Leach L (2009). <u>Studies into *Necator americanus* L3 larvae and human endothelium interactions</u>. The British Microcirculation Society at the 59th annual meeting, Birmingham.

Acknowledgment

It is an honour for me to thank the people who made this experience enjoyable and this thesis possible.

I owe my deepest gratitude to my supervisors, Professor David Pritchard and Dr Lopa Leach, for their support, guidance and constructive criticism throughout my studies and during my writing up.

I would like to thank Dr Alan Brown for his invaluable advice and using his precious time to read this thesis and answer all my questions. I would also like to acknowledge every member of Professor Pritchard's and Dr Leach's groups for providing their support and help when needed. I would also like to thank the Algerian government for funding this project.

I am grateful for everyone who was there for me when I needed help and support, but special 'thanks' to my friends Ouannassa Rached, Sabrina Dey, Asma Yahyouche and Abdennour Bouhroum for their caring and continuous support and best of luck with their writing up.

I am grateful in every possible way for being blessed with a family that supported me throughout my undergraduate and my PhD studies. For my oldest siblings, Zouha and Abdelfiad, for being supportive and taking care of me whenever I visited home. For my brother, Mohamed Kheir Allah, for his inspiring courage and determination. For my sisters Manar Sana and Chemse el Assil, for keeping me smiling with their jokes and encouraging comments. For my nephew, Nizar, for making the writing up much easier since I have his picture as a background on my laptop. However, I can never be grateful enough for my grand-mother, Aisha, my father, Aziz, and my mother, Louisa, for their prayers, support and encouragement throughout my studies.

Thank you to everyone who believed in me and made a difference in my life.

Table of Content

Abbreviations

α	Alpha
APS	Ammonium persulphate
AMC	7-amino-4-methylcoumarin
Ala	Alanine
APR	Aspartic Protease
Arg	Arginine
ASP	"*Ancylostoma*" Secreted Protein
BSA	Bovine Serum Albumin
cm	Centimeter
CO$_2$	Carbon dioxide
CaCl$_2$	Calcium chloride
˚C	Degree Celsius
DTT	Dithiothreitol
ES	Excretory/Secretory
EF	Exsheathing fluid
EU	Endotoxin unit
EDTA	Ethylene-diaminetetraacetic acid
ELISA	Enzyme Linked ImmunoSorbent Assay
ECM	Extracellular matrix
ECGS	Endothelial cell growth supplements
FITC	Fluorescein isothiocyanate
FU	Fluorescence unit
FBS	Fetal Bovine Serum
F-actin	Actin filaments
g	Gram
g	Gravity
Glu	Glutamic acid
HCl	Hydrochloric acid
h	Hour
HUVEC	Human umbilical vein endothelial cells
IgG	Immunoglobulin
IU	International unit
IEF	Isoelectric focusing
IPG	Immobilized pH gradient
IL	Interleukin
kDa	Kilodalton
L	Litre
LPS	Lipopolysaccharide
Leu	Leucine
L3	Stage-3 larvae
L4	Stage-4 larvae
mL	Milliliter
mg	Milligram
mA	Milli Ampere
M	Molar

mm	Millimeter
mM	Millimolar
MALDI	Matrix-assisted laser desorption ionization
MgCl$_2$	Magnesium chloride
M199	Medium 199
M0	Medium 199 supplemented with 200 IU/mL penicillin, 200 μg/mL streptomycin, 2 μg/mL fungizone
M20	M0 supplemented with 20% fetal bovine serum (FBS)
MMPs	Matrix metalloproteases
nm	Nanometer
NaCl	Sodium chloride
NTZ	Nitroblue tetrazolium
ng	Nanogram
Ω	Ohm
%	Per cent
PBS	Phosphate buffered saline
PMSF	Phenyl methane sulphonyl fluoride
PNG	Papua New Guinea
P	Probability value
PFA	Paraformaldehyde
pg	Picogram
rpm	Revolutions per minute
SDS-PAGE	Sodium dodecyl sulphate polyacrylamide gel electrophoresis
SEM	Standard error of the mean
TEMED	N'N'N'-tetramethylethylenediamine
TAA	Tert-amyl alcohol
TCA	Trichloroacetic acid
TBS	Tris buffered saline
TMB	3,3',5,5'-tetramethylbenzidine dihydrochloride
TEER	Transendothelial electrical resistance
TRITC	Tetramethylrhodamine isothiocyanate
2DE	Two dimensional gel electrophoresis
U	Unit
μg	Microgram
μL	Microliter
μA	Micro Ampere
μM	Micromolar
μm	Micrometer
V	Volt
v/v	Volume/volume
VEGF	Vascular endothelial growth factor
VE-cadherin	Vascular endothelial-cadherin
w/v	Weight/volume

1. General Introduction

The interest in studying the journey of *Necator americanus* larvae through the skin and the underlying vasculature necessitates a deep understanding of *Necator americanus* infection and the structure of the skin and the vascular endothelium, the two major barriers controlling larval entry into the host's microcirculation.

1.1 Necator americanus

Human hookworm infection is one of the most devastating gastro-intestinal infections, affecting over 800 million people worldwide (Haas *et al*, 2005; Bethony *et al*, 2006). The two main species that account for almost all human infections, *Ancylostoma duodenale* and *Necator americanus*, are among the most prevalent nematodes (Williamson *et al*, 2003) and occur in most warm-temperature regions with *Necator americanus* largely thriving in sub-Saharan Africa, Southeast Asia, Melanesia, and Latin America (Hoagland and Schad, 1978; Loukas and Prociv, 2001) and *Ancylostoma duodenale* favouring cooler and drier, tropical regions of the world (Albonico *et al*, 1998). Hookworms are highly host specific, obligate blood-feeders (Williamson *et al*, 2003a), causing gastro-intestinal bleeding, anaemia and iron deficiency in most chronic infections (Hotez and Pritchard, 1995; Albonico *et al*, 1998; Devaney, 2005). The severity of these outstanding features can lead to retardation of growth as well as physical and cognitive impairment in children with chronic conditions depending on the intensity and prevalence of infection (Crompton, 2000; Williamson *et al*, 2003a), which in turn is influenced by the susceptibility of individuals at all ages to hookworm infections (Timothy and Behnke, 1993; Bethony *et al*, 2002). Since hookworms do not replicate in the human host, the intensity of *Necator americanus* infection is estimated using a quantitative faecal egg count as a practical marker for worm burden (Hotez *et al*, 2005). Hookworm infections are defined by the World Health Organization (WHO) to be moderate in individuals producing 2,000 to 3,999 eggs per gram of faeces (epg) while heavily infected individuals produce over 4,000 epg.

At high intensity, hookworm infections can cause significant morbidity and mortality (Hotez and Pritchard, 1995). However, there is increasing evidence suggesting that a tolerated *Necator americanus* infection (at ~ 50 epg), as described by Mortimer *et al* (2006), might be associated with therapeutic benefits to autoimmune conditions such as Crohn's disease (Reddy and Fried, 2007; Reddy and Fried, 2009), allergic disorders including asthma (Pritchard *et al*, 1995; Quinnell *et al*, 2004; Falcone and Pritchard, 2005) and atopic dermatitis (Cooper *et al*, 2003; Wordemann *et al*, 2008; Flohr *et al*, 2009). Despite being of major importance to humankind, little is actually known about parasite-host interactions, parasite invasion strategies and the importance of the generated immune responses in terms of host protection and/ or parasite survival (Loukas and Prociv, 2001).

1.1.1 Life cycle of *Necator americanus*

Necator americanus is an obligate skin-penetrating hookworm (Hawdon *et al*, 1993) which resides in the jejunum and duodenum (Pritchard *et al*, 1990). Following sexual pairing between adult worms, female worms start producing eggs by days 42—49 post-infection (Jian *et al*, 2003, Bethony *et al*, 2006), which undergo several cell divisions prior to being passed out in host faeces (Pritchard *et al*, 1990; Loukas and Prociv, 2001). Under humidified and warm (25—28°C) conditions (Schad *et al*, 1973), the embryonated eggs hatch within 1 to 2 days. The hatched first-stage larvae (L1) feed on organic debris and faecal microflora to grow and develop as shown in Figure 1.1 (Pritchard *et al*, 1990; Bethony *et al*, 2006), moulting twice to form the infective non-feeding third-stage (L3) larvae, ensheathed in a loose outer cuticle left over from the second moult (Loukas and Prociv, 2001; Brooker *et al*, 2004; Bethony *et al*,

2006). In the presence of appropriate conditions such as moisture, warmth and shade (Schad *et al*, 1973; Hotez and Pritchard, 1995), infective L3 larvae will crawl onto vegetation, soil particles and rocks to maximize their chances of contacting a new host, the so-called 'questing behaviour' (Hotez and Pritchard, 1995; Hotez *et al*, 2004).

Upon contact with infective L3 larvae, key molecules in the skin can provide a trigger to the invading larvae, allowing them to actively penetrate the skin and reach the bloodstream, mainly through the vasculature (Hotez and Pritchard, 1995) and/ or possibly through the lymphatic system (Pritchard *et al*, 1990). Infective L3 larvae migrate to the lungs, through the vasculature, where they break out into the alveolar spaces and migrate up the trachea mostly by coughing (Hawdon *et al*, 1993; Devaney, 2005). Finally, L3 larvae are swallowed, arriving in the small intestine where maturation to the L4 stage takes place (Devaney, 2005). During the larval stages, *Necator americanus* encounter the endothelium in the skin, as they penetrate into the blood circulation and as they migrate out into the lungs.
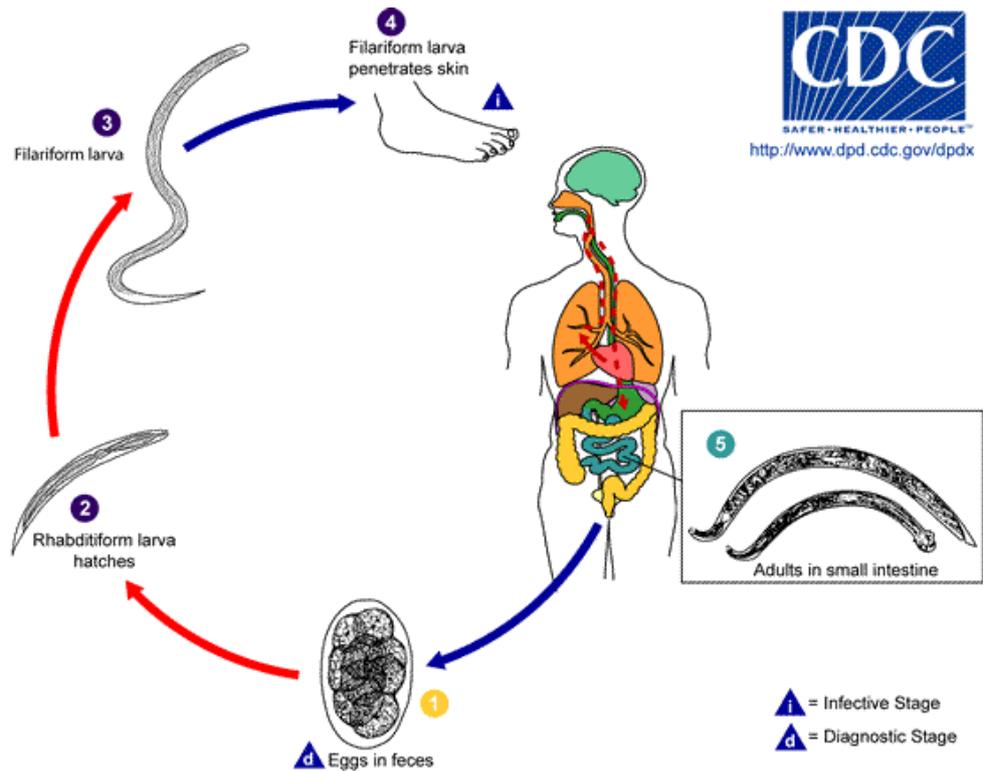
Figure 1.1   Life cycle of *Necator americanus*.

❶ Eggs are passed in the stool. ❷ Larvae hatch in 1 to 2 days, and grow in the faeces and or the soil, to become infective (third-stage) larvae ❸ within 5 to 10 days. ❹ On contact with the human host, the larvae penetrate the skin and are carried through the blood vessels to the heart and then to the lungs. They penetrate into the pulmonary alveoli, ascend the bronchial tree to the pharynx, and are swallowed. ❺ Once they reach the small intestine, larvae reside and mature into adults. Adult worms attach to the intestinal wall and feed on intestinal mucosa and blood. Female worms then start laying eggs.

From http://www.dpd.cdc.gov/dpdx/HTML/Hookworm.htm.

The L4 larvae are characterised by a false buccal cavity which is shed following the final moult to the adult worm stage (Behnke *et al*, 1986; Pritchard *et al*, 1990). Within six weeks post-infection, adult worms reach sexual maturity and are easily distinguished as adult males show a rounded posterior end in addition to a copulatory bursa while females have a sharp, needle-like tail and a vulva located anterior to the middle of the body (Pritchard *et al*, 1990; Jian *et al*, 2003). Adult worms then mate and females start laying eggs, completing the life cycle of *Necator americanus*.

1.1.2   The course of *Necator americanus* infection

Human hookworm infection is usually stimulated by ecological factors at the transmission sites (Haas *et al*, 2005). *Necator americanus* larvae often adopt a motionless resting posture, also known as developmental arrest (Hotez *et al*, 2004), to minimise unnecessary energy expenditures in the soil. Stimuli including humidity (Haas *et al*, 2005), radiating warmth from hosts, and lights (Haas *et al*, 2005a) contribute to the 'ambushing strategy' as infective, non-feeding L3 larvae position themselves on top of soil particles and blades of grass and wait for the appropriate host. L3 larvae are then activated to the searching (in which larvae raise their anterior ends and move in all directions) and waving (in which one third of the larval body is erected) behaviours which are essential for these species to locate and reach the appropriate host. Other factors such as vibration, carbon dioxide and chemical gradients seem to cause little to no activation of larvae (Sasa *et al*, 1960; Sciacca *et al*, 2002), which is regarded as a beneficial way for saving energy during the frequent contact with soil-living habitats (Schad, 1991).

Although thin, the outer layer of human skin is considered a highly efficient barrier to the majority of infective parasites including human hookworms (Matthews, 1982). In the presence of a thin water-film, *Necator americanus* infective larvae crawl on the surface and penetrate the human skin by pressing their anterior ends vertically on the skin and 'nictating' or 'waving' their elevated neck laterally (Haas *et al*, 2005), a process that is largely stimulated in the presence of chloroform soluble lipids of human skin surface (Matthews, 1982; Salafsky *et al*, 1990). Initial invasion, which is believed to be totally mechanical (possibly driven by surface lipids), occurs as fast as 5 minutes and is often accomplished in 1 to 2 hours after being exposed to the skin (Matthews, 1982). Exsheathment, described as the loss of the loose sheath of infective L3 larvae, is apparently not essential during larval invasion as ensheathed L3 larvae were also capable of penetrating the skin (Figure 1.2) (Kumar and Pritchard, 1992). *Necator americanus* larvae remain in the skin for 48 to 72 hours post-infection (Behnke *et al*, 1986; Hawdon *et al*, 1993), a period that is required to resume larval feeding and reactivate developmental changes to facilitate the parasitic infection in mice (Hawdon *et al*, 1993; Hawdon and Hotez, 1996). Activated L3 larvae negotiate through the lower epidermal and dermal layers, using a repertoire of enzymatic secretions (Matthews, 1975; Matthews, 1982; Kumar and Pritchard, 1992a; Loukas and Prociv, 2001; Williamson *et al*, 2004), and enter the capillaries to be carried to the lungs via the blood circulation. Parasitic developmental changes are usually observed a few hours after arrival in the lungs including acquiring pigments in the parasitic intestine and the rounding of their anterior end (Jian *et al*, 2003),

and are indicative of the obligatory lung mediated phase in *Necator americanus* infection (Hoagland and Schad, 1978; Behnke *et al*, 1986).
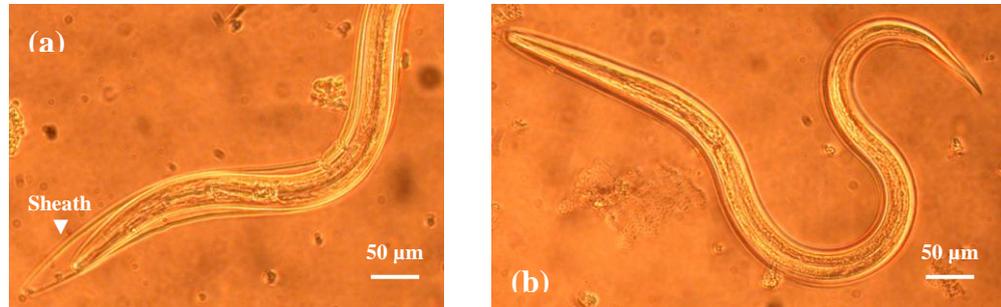
Figure 1.2   Micrographs of *Necator americanus* L3 (a) ensheathed, and (b) exsheathed larvae under phase contrast microscopy.

Necator americanus larvae enter the gastrointestinal tract, finally arriving in the small intestine where they mature into adult worms (Hawdon and Schad, 1990). Migration of *Necator americanus* larvae either from the skin to the lungs or from the lungs to the small intestine is believed to occur in response to local triggers (Timothy and Behnke, 1993; Zhan *et al*, 2002; Hawdon and Datu, 2003). At this stage, maturation into juvenile adult worms is usually accomplished and worms exhibit a full buccal cavity, a pharynx connecting this cavity to the intestine (Jian *et al*, 2003), a dorsal pair of ventral cutting plates (Figure 1.3), a concave median tooth and a pair of sub-ventral lancets (Pritchard *et al*, 1990). Adult worms attach to the intestinal wall and feed on intestinal mucosa and blood and are estimated to cause a blood loss of approximately 40 µL per day per single worm (Devaney, 2005). Despite being mechanical, attachment to the intestinal wall and degradation of host tissue is also explained by the enzymatic activity of these worms, allowing the release

of nourishing components of the wall through a cascade of haemoglobinases (Williamson *et al*, 2004) and other proteolytic enzymes (Williamson *et al*, 2003).
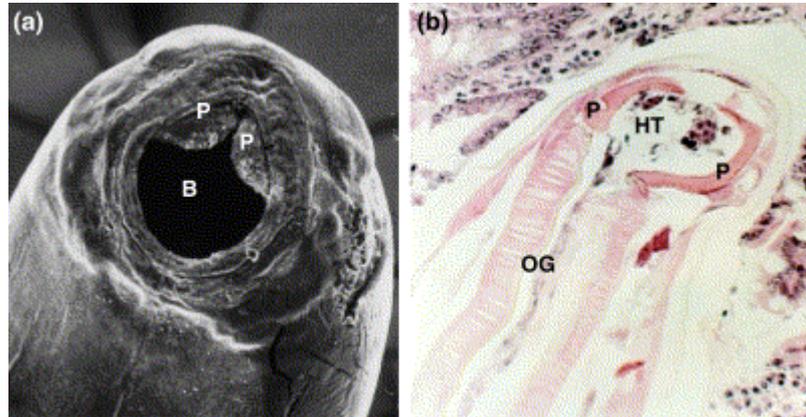
Figure 1.3   Two faces of *Necator americanus*. (a) Micrograph showing the buccal cavity (B) and plates (P) used for attachment and feeding in the gut. Micrograph courtesy of Bernard Matthews. (b) *Necator americanus* attached to the intestinal mucosa, stained with haematoxylin and eosin. Host tissue (HT) is drawn into the buccal cavity prior to digestion in the oesophagus (OG). In addition, parasite-protective molecules are secreted at the site of attachment (Adapted from Pritchard and Brown, 2001).

1.1.3   *Necator americanus* secreted products

According to Loukas and Prociv (2001), secretions of *Necator americanus* are believed to come into contact with the human host not only anatomically during penetration and feeding, but also physiologically during immune responses. These secretions are supposed to boost hookworm infection by modulating the immune response to the parasitic existence. Recent studies have

revealed numerous larval and adult proteins with potential antigenic and immunoevasive properties (Carr and Pritchard, 1986; Loukas and Prociv, 2001). Antioxidants are functional molecules which might provide some protection to cuticle-exposed antigens including neutralizing host free radicals such as superoxide dismutases (SOD) and counteracting the effects of lipid hydroperoxides such as glutathione-S-transferases (GST) (Hotez and Pritchard, 1995; Brophy *et al*, 1995; Loukas and Prociv, 2001). Parasite derived C type lectins, which are present in serum and on surface of immune effector cells, could be responsible for switching off the local inflammatory responses to feeding in the small intestine as they compete with host lectins to bind to immune cells (Loukas and Prociv, 2001). Furthermore, the secretion of a neutrophil inhibitory factor (NIF), which blocks the adhesion of activated human neutrophils to vascular endothelial cells at feeding sites, have been reported in adult *Necator americanus* but its functional properties are yet to be investigated (Daub *et al*, 2000). This factor was said to antagonize naturally occurring CR3 receptors and affect the migration of monocytes to the inflammatory sites, hence providing a mechanism for immune evasion (Asojo *et al*, 2005). Calreticulin, an extracellular calcium binding protein with lectin like features, has been purified from *Necator americanus* secreted products. Calreticulin, which shows an association with the complement system (Cq1) as well as integrins (Reilly *et al*, 2004), is also believed to act as an immune modulator during the parasitic infection (Hotez and Pritchard, 1995; Kasper *et al*, 2001). *Necator americanus* adult worms are also known to secrete acetylcholinesterase (Pritchard *et al*, 1991), possibly to degrade acetylcholine produced in the intestinal wall, as well as anti-coagulant (Rogers and

Sommerville, 1963; Schad, 1991) and anti-platelet (Zhan *et al*, 2005) proteins at the site of attachment in the small intestine, which would delay the formation of blood clot and enhance the blood loss.

Evidence suggests that *Necator americanus* larvae are capable of releasing a wide range of pre-synthesized proteolytic enzymes at any stage of their development (Sasa *et al*, 1960; Matthews, 1975; Williamson *et al*, 2004). These enzymes are believed to be stored in secretory granules, present within the oesophageal glands of these parasites (Smith, 1976), and contribute to parasitic developmental processes. To date, the infective larvae of *Necator americanus* were shown to facilitate skin penetration, larval migration and intestinal attachment (Matthews, 1982; Brown *et al*, 1999; Williamson *et al*, 2003) by secreting a mixture of proteolytic enzymes including aspartyl, metalloproteases, serine and cysteine proteases (Kumar and Pritchard, 1992; Kumar and Pritchard, 1992a; Brown *et al*, 1999; Quinnell *et al*, 2004). Most of these proteases are gelatinolytic in nature (Kumar and Pritchard, 1992a) and have an ability to degrade a number of skin macromolecules such as collagens I—V, fibronectin and laminin (Brown *et al*, 1999), and host haemoglobin (Williamson *et al*, 2003). In addition, cysteine proteases including *Ancylostoma* secreted proteins (ASP-1 and ASP-2) are very immunogenic and play different roles in the biology of *Necator americanus* including tissue invasion and immune evasion (Hawdon and Hotez, 1996; Bin *et al*, 1999; Loukas *et al*, 2000). Furthermore, aspartic proteases, which are expressed at all developmental stages of *Necator americanus* such as *Na*-APR-1 and -2 (Brown *et al*, 1999; Bethony *et al*, 2005), are also capable of hydrolyzing human

haemoglobin and serum proteins in a multi-protease cascade (Williamson *et al*, 2002; Williamson *et al*, 2003).

Proteases are also known to cause the most ubiquitous effects on the immune system than all other *Necator americanus* secreted proteins. As such, metalloproteases have been shown to specifically cleave the chemo-attractant eotaxin-1 (Culley *et al*, 2000), therefore interfering with the role of eosinophils at all inflammatory sites of feeding while cysteine proteases can selectively cleave CD23, a host lectin, from the surface of B-cells and are therefore responsible for the enhanced IgE synthesis (i.e. Hypersensitivity type I), observed in *Necator americanus* infection (Hewitt *et al*, 1995; Loukas and Prociv, 2001).

1.1.4   Immunogenicity of *Necator americanus*

Necator americanus larval entry is often associated with mild clinical inflammatory responses such as static ground itch lesions, migratory creeping eruption and skin redness, which could last for a few weeks post-infection (Hotez *et al*, 2004, Wright and Bickle, 2005). Upon arrival into the lungs, *Necator americanus* larvae can cause central haemorrhagic and inflammatory lesions, which may be evident clinically depending on the intensity of the hookworm infection, possibly with cough and sore throat (Hotez *et al*, 2004). Following migration to the small intestine, occasional mild nausea and moderate abdominal pain could be experienced, in addition to weight loss and intestinal bleeding, the main pathological effects of hookworm infection. Less commonly occurring features include oedema in both feet and the right arm as

previously stated by Wright and Bickle (2005). These symptoms are less likely to occur on the second infection with the exception of the skin irritation.

During their life cycles, *Necator americanus* are in close contact with the immune system as they circulate in the vasculature (Hotez and Pritchard, 1995), offering the parasite and host several opportunities to interact at the cellular level. The skin, lungs and gut are considered as critical obstacles to these parasites, where most immune activation and immune modulation is likely to happen (Loukas and Prociv, 2001; Pritchard and Brown, 2001). Antigenic stimulation of the host's immune system may afford a degree of early protection in pre-exposed hosts, especially during the skin invasive phase (Kumar and Pritchard, 1992). Although hookworm antigenic expression is stage-specific, antibodies developed in individuals infected with *Necator americanus* failed to recognize exsheathed L3, but succeeded to detect antigens on the surface of ensheathed L3 larvae (Pritchard *et al*, 1990). These observations would explain the diversionary role of larval surface antigens in bypassing the immune response in the skin and allowing the defenceless, exsheathed parasite to remain unrecognized (Kumar and Pritchard, 1992; Loukas and Prociv, 2001).

1.1.4.1 Immune responses to *Necator americanus* infection

Necator americanus infection elicit a strong, stage-specific, Th2 response which is characterized by increased activation of CD19$^+$ B-cells and CD3$^+$ and CD4$^+$ T-cells corresponding to elevated levels of total and antigen-specific immunoglobulin, particularly IgGs, IgM and IgE (Pritchard and Walsh, 1995; Loukas and Prociv, 2001; Quinnell *et al*, 2004; Geiger *et al*, 2007). Some

antibody responses, such as IgG4 and IgE, are more species-specific and appear to correlate with the intensity of hookworm infection (Pritchard and Walsh, 1995; Palmer *et al*, 1996; Loukas *et al*, 1996; Xue *et al*, 1999) while down-regulation of others, such as IgA, is possibly due to the proteolytic breakdown of this antibody (Behnke, 1991; Pritchard, 1995). Infections are also associated with a mixed Th1/Th2 cytokine response in which both Th1 (gamma interferon (INF-γ) and IL-12) and Th2 (IL-4, IL-5 and IL-13) are produced (Pit *et al*, 2001; Quinnell *et al*, 2004a), emphasising the significance of a mixed Th1/Th2 cell response to *Necator americanus* infection intensity. In addition, *Necator americanus* infection is accompanied by an increase in the levels of IL-10, an anti-inflammatory cytokine with a regulatory role to play in the immune response, and a down-regulation of cellular reactivity (Geiger *et al*, 2004; Bethony *et al*, 2006; Geiger *et al*, 2007). However, Wright and Bickle (2005) reported a transient elevation in IL-5 and IL-13 production in infected individuals but no IFN-γ or IL-10 mediated responses were observed.

Eosinophilia, a characteristic response to *Necator americanus* infection (Culley *et al*, 2002; Wright and Bickle, 2005), is known to predominate the inflammatory response to larval and adult parasites (Behnke, 1991; Loukas and Prociv, 2001; Quinnell *et al*, 2004). In a self infection study, an increase in eosinophil counts was recorded as early as day 3 post-infection, implicating the involvement of non-specific responses, and was shown to persist for up to 2 years post-infection (Wright and Bickle, 2005). Evidence suggests that eosinophils bind to *Necator americanus* larvae in the presence of the

complement system (Desakorn *et al*, 1987), thus being able to eliminate these parasites only at the larval stage (Meeusen and Balic, 2000).

1.1.4.2   Immune modulation in *Necator americanus* infection

Necator americanus is known to survive in the human host, mainly as adult worms, for an average of 5 to 7 years with recent evidence showing the intensity of hookworm infection to increase with age (Beaver *et al*, 1984; Bethony *et al*, 2002). *Necator americanus* species, which live in close contact with the host immune system, secrete a number of stage-specific molecules such as eotaxin metalloproteinase, calreticulin, antioxidants and neutrophil inhibitory factor (NIF), with immuno-modulatory properties capable of redirecting the immune response during hookworm infection (Kumar and Pritchard, 1992a; Quinnell *et al*, 2004a; Loukas *et al*, 2005).

Immuno-modulation of the host immune system, reported to date, include parasite-mediated suppression of antigen-specific immune responses, divergence of the host immune responses from protective against these parasites to non-protective, and inactivation of immune effector mechanisms which are mainly responsible for expulsion of these parasites (Quinnell *et al*, 2004a). Immuno-suppression was supported by the increase in immune responsiveness following chemotherapy-induced removal of parasites. This is described by a decline in antigen-specific antibody responses, including IgGs and IgE, and eosinophilia to pre-infection levels while a significant increase in anti-adult IgD (Pritchard *et al*, 1992) and anti-larval IgA was observed (Kumar *et al*, 1980; Quinnell *et al*, 2004a).

During *Necator americanus* establishment in the gut, natural killer (NK) cells are attracted to the site of infection by protein secretions from adult worms (Hsieh *et al*, 2004). NK cells selectively bind to excretory/secretory (ES) products which cause these cells to become activated and secrete INF-γ locally, a mechanism that is likely to modulate host immune responses and contribute to the longevity of infection (Teixeira-Carvalho *et al*, 2008). In addition, the high levels of IL-10 and regulatory T_{reg} cells are believed to play a pivotal role in the down-regulation of cellular reactivity and the inhibition of protective immune responses against these parasites (Taylor *et al*, 2005; Geiger *et al*, 2007). Cellular reactivity, which is reduced during the adult-phase of hookworm infection, is probably induced by adult ES proteins to inhibit killing of incoming L3 and L4 larvae, therefore prolonging the survival of *Necator americanus* in the human host (Croese *et al*, 2006).

1.1.5   Treatments for *Necator americanus* infection

The World Health Organization has approved four anthelmintic drugs for morbidity control against soil transmitted infections (STI) including albendazole, mebendazole, levamisole, and pyrantel pamoate (WHO, 1997). These drugs have demonstrated a broad spectrum of activity and have been used effectively for more than 30 years (Keiser and Utzinger, 2008). Albendazole and mebendazole, which are derivatives of the benzimidazole class, are associated with a cure rate of 66% in patients treated with a 400 mg single dose of albendazole (Cline *et al*, 1984) and about 31% cure rates in Mafia Island, following treatment with a 500 mg single oral dose of mebendazole (Albonico *et al*, 2002). A recent study investigating the efficacy of albendazole, pyrantel pamoate and tribendimidine against *Necator*

americanus infection, in hamsters, demonstrated an equal activity of all drugs at doses as high as 100 mg/kg (Xue *et al*, 2005). In clinical trials, tribendimidine exhibited a safe, broad spectrum of activity with a promising effect against *Necator americanus*. A 400 mg single oral dose of tribendimidine and albendazole, which was administered to patients infected with *Necator americanus*, resulted in cure rates of about 86% and 66% respectively, indicating that tribendimidine may become the drug of choice (Xiao *et al*, 2005; Wu *et al*, 2006). Unlike ivermectin (Campbell *et al*, 1984), the only macrocyclic lactone anthelmintic approved for human use, drugs such as nitazoxanide and amidantel have revealed no activity against *Necator americanus* despite being effective against other human intestinal protozoa and nematodes (Xiao *et al*, 2005).

Because of their high efficacy, low costs and ease of use, albendazole and mebendazole are widely used in control programmes for intestinal nematode infections, raising concerns about potential emergence of drug resistance. The likelihood of developing drug resistance among intestinal parasites is greater than all other parasites as the density of sexual stages resides in the small intestine. To date, resistance to mebendazole and pyrantel pamoate has been reported in human hookworm infection in Australia and Africa (Horton, 2003; Albonico *et al*, 2003). Since anthelmintic drugs do not provide complete and long-lasting protection, naturally acquired immunity is not common in individuals with a history of *Necator americanus* infection, possibly accounting for the high rates of reinfection within 4 to 12 months post-infection (Quinnell *et al*, 1993; Albonico *et al*, 1995). Additional factors,

including individual predisposition (Hotez *et al*, 2004) and the geo-distribution of hookworm infections in socioeconomically developing countries (Loukas and Prociv, 2001; Hotez *et al*, 2007), may also increase the potential for reinfection.

1.1.6   Vaccines

Although anthelmintic treatments are widely used to control human intestinal infections, the prevalence of hookworm infection remains of major concern from a public health standpoint. Therefore, developing an effective vaccine against hookworm infections is a suitable alternative to chemotherapy and provide early protection against these parasites. Vaccination with irradiated *Necator americanus* larvae resulted in almost complete protective immunity against challenge infection (i.e. Th2 response associated with high IgG, IgE and IL-5), and reduced the pathology associated with hookworm infections in mice (Brown, 2000; Culley *et al*, 2001). Although immunization with irradiated larvae was effective and supported the feasibility of hookworm vaccination, an ideal vaccine would mimic the effect of live, attenuated larvae with larval-derived antigens, which could be genetically engineered on a large scale.

Since *Necator americanus* antigens are stage-specific (Pritchard *et al*, 1990; Williamson *et al*, 2004), the ultimate hookworm vaccine should consist of at least two different antigens, one that targets penetrating and migrating larvae to reduce the number of larvae entering the gastrointestinal tract, and the other targeting adult stage to interrupt blood feeding and hence minimize the pathology associated with hookworms (Girod *et al*, 2003; Loukas *et al*, 2005a).

Based on this theory, larval proteins such as ASPs (Loukas and Prociv, 2001; Goud *et al*, 2005; Bower *et al*, 2008), metalloproteases (Hotez *et al*, 2003; Goud *et al*, 2005) and calreticulin (Winter *et al*, 2005) appear to be attractive as larval vaccines while adult haemoglobinases (Daub *et al*, 2000; Pearson *et al*, 2009), and glutathione-S-transferase (GST) (Zhan *et al*, 2005) have shown great promise as adult vaccine candidates.

According to Bethony *et al* (2005), vaccination against the aspartic protease *Na*-ASP-2 elicited a strong antibody response in rats including IgG1, IgG2a and IgM levels, which were durable and easily boosted with a single dose of as low as 50 micrograms. *Na*-ASP-2 vaccines also reduced the worm burden (Xiao *et al*, 2008), and was therefore selected to undergo process development in clinical trials (Bethony *et al*, 2006; Bower *et al*, 2008). Calreticulin, another lead vaccine candidate which was selected based on its role as an immune evasion protein, induced a strong Th2 response, characterised by high levels of specific IgE (Winter *et al*, 2005). Free calreticulin vaccine also provided great protection against *Necator americanus* infection with reduced worm burdens in the lungs of vaccinated mice. Unlike encapsulated calreticulin, lower levels of eosinophlia, IgG1, IgG2a and IgE were observed following free calreticulin vaccines, indicating that these findings require further investigations to identify the nature of protection generated by free calreticulin vaccines (Winter *et al*, 2005).

Ac-GST-1, an enzyme that is involved in the detoxification of host-generated free radicals during haemoglobin digestion, presents a promising vaccine

candidate to prevent the establishment of *Necator americanus* larvae in the small intestine (Zhan *et al*, 2005; Devaney, 2005). *Ac*-GST-1 vaccine induced strong antibody responses (IgG1 and IgG2) and elevated levels of IFN-γ and IL-4 responses, characteristic of a mixed Th1/Th2 response (Zhan *et al*, 2005; Pearson *et al*, 2009). *Na*-APR-1, an aspartic protease responsible for initiating the cascade of haemoglobin digestion (Williamson *et al*, 2002), is another vaccine candidate with high potentials to target the adult stage of these parasites (Loukas *et al*, 2005; Pearson *et al*, 2009). Immunisation with recombinant *Na*-APR-1 was associated with a significant protection against blood loss and low worm burdens and egg counts in dogs (Loukas *et al*, 2005). Immunisation with anti-adult *Na*-APR-1 was reported to partially inhibit *Necator americanus* larvae from passage through skin (16- 26%) while anti-larval *Na*-APR-2 vaccines caused over 50% inhibition of larval migration through the skin (Williamson *et al*, 2003), signifying that stage-specificity of these antigens possibly accounts for their potentials to inhibit *Necator americanus* infection at different stage.

1.1.7   Overviews

Understanding the molecular biology of hookworms represents an excellent opportunity for studying the fundamental, parasite-specific processes in the host, including the entry of *Necator americanus* larvae into the host's blood circulation. Migration of hookworm larvae through the skin has been described in some detail in the literature. The skin, the major barrier that protects the host against hookworms and all other parasites, is introduced and the available knowledge of the parasitic mechanisms to negotiate the skin is discussed.

1.2   The Skin

The skin is the largest, outermost organ of the human body, accounting for approximately 15% of the total body weight in adults. It acts as a multifunctional barrier between the body and the environment, mainly to protect the human body against external physical, chemical and biological factors. By serving as an anatomical barrier, the skin prevents pathogenic invasion of the body, controls the loss of fluids, absorbs the harmful, ultraviolet (UV) radiation from the sun, and has an immunological role in host defences. It also contributes to the thermo-regulation of the human body through radiation, convection and evaporation and plays a role in sensation to incoming stimuli of touch, pain, pressure, heat and cold and others.

The skin is organised into two major compartments, the epidermis and the dermis, separated by the dermal-epidermal junction. Below the dermis is a fatty layer, known as the hypodermis, which attaches the skin to the rest of the body. This introduction focuses on the structure and the major components of the skin and briefly highlights the available knowledge with concerns to the interaction of hookworms and the skin.

1.2.1   The epidermis

The epidermis is the outermost layer of the skin which consists of terminally differentiated, stratified epithelium (Figure 1.4). The major cells, making up to 95% of the total epidermal structure, are the keratinocytes in which keratin filaments form the cytoskeleton (Wolff and Schreiner, 1968; Mackenzie, 1975; Sun and Green, 1978). Based on the arrangement of epidermal cells, the epidermis can be divided into four morphologically distinct layers (Holbrook

and Odland, 1975; McGrath *et al*, 2008), comprising from the inside to the outside:

- <u>The basal layer</u>, also known as the stratum basale, which is characterised by small and cubical cells with large, dark nuclei, dense cytoplasm and tono-filament keratin bundles. The basal cells, mainly keratinocytes and stem cells, form a single layer by aligning perpendicularly to the underlying basement membrane to which they attach through the hemidesmosomes. Hemidesmosomes are asymmetrical cellular structures capable of anchoring cells to the underlying extracellular matrix through integrin adhesion proteins (Shienvold and Kelly, 1976). Epithelial cells are generated at the basal layer by mitotic divisions, and new cells migrate outwards to form the prickle cell layer (Yasuno *et al*, 1980).

- <u>The prickle cell layer</u>, also known as the stratum spinosum, is a multilayered region (5 to 15 layers) which contains larger, polygonal keratinocytes with eosiniphilic cytoplasm and vesicular nuclei (Staiano-Coico *et al*, 1986).

- <u>The granular layer</u>, also known as the stratum granulosum, which is characterised by flattened keratinocytes with dense, keratohyalin granules made of histidine-rich proteins (such as profilaggrin) and keratin (Lavker and Matoltsy, 1971). Lamellar bodies, which migrate to the periphery of cells in the granular layer, are involved in the desquamation process as they discharge of their lipid components into the intercellular space which contributes to the formation of the cornified envelope (Odland and Holbrook, 1981; Odland, 1991).

- <u>The horny layer</u>, also known as the stratum corneum, is the outermost layer of the epidermis where cells, now flattened corneocytes, are devoid of nucleus and cytoplasmic organelles. The cornified envelope, which is made of cross-linked proteins from the keratohyalin granules, contributes to the barrier properties of the skin (Lynley and Dale, 1983; Ishida-Yamamoto and Iizuka, 1998).

The cellular diversity within the epidermis represents 5 to 10% of the total, with each type playing a role in the skin. Langerhans cells are mobile, dendritic antigen presenting cells which originate from the bone marrow. These cells are capable of accumulating foreign antigens and presenting them to naïve T-cells, in the basal layer, and therefore are thought to play a role in recognition and defence against foreign pathogens (Kiistala and Mustakallio, 1968; Girolomoni *et al*, 2002). In addition, the epidermis contains melanocytes which produce melanin and donate pigment to the keratinocytes (Szabo, 1954; Jimbow *et al*, 1976), and Merkel cells which form synaptic junctions with dermal sensory axons and seem to serve as mechano-receptors (Kidd *et al*, 1971; Lacour *et al*, 1991).

1.2.2 The dermal-epidermal junction

The epidermis is anchored to the underlying dermis through the dermal-epidermal junction, also known as the basement membrane, which is synthesised by basal keratinocytes and dermal fibroblasts. The junction provides mechanical support for epidermis and plays an additional role during wound healing and inflammatory processes by regulating the exchange of large

molecules and cell trafficking (Heaphy and Winkelmann, 1977; Schechter, 1989).

The dermal-epidermal junction is composed primarily of laminin and collagen IV, the structural scaffolds of all basement membranes, which align in four distinct layers comprising, the cell membrane through which basal keratinocytes attach to the underlying layers, the lamina lucida, the lamina densa, and the sub-basal lamina which is directly connected to the dermis. Anchoring filaments, made of either collagen XVII or collagen VII, connect these layers and maintain the integrity of the junction (Ghohestani *et al*, 2001).

1.2.3   The dermis

The dermis is a dense connective tissue layer which originates from the dermal fibroblast and contains the vascular network, glands i.e. sweat and sebaceous, and the hair follicles (Figure 1.4). The main structural macromolecules of the dermis are collagens, elastin, fibronectin and laminin, arranged in the extracellular matrix, primarily contributing to the structural complexity and multifunctional nature of the skin (Pearce, 1968; Swanson and Helwig, 1968). The dermis provides a mechanical support for the overlaying epidermis and is structurally divided into two main areas (Briggaman and Wheeler, 1968; Rodrigo and Cotta-Pereira, 1979):

-   <u>A superficial, papillary region</u>, connected to the epidermis through the dermal-epidermal junction. The layer is composed of collagen fibres arranged in loose bundles and of thin elastic fibres anchored to the junction.

- <u>A deep, reticular region</u>, made of coarser collagen bundles and thicker elastin fibres and accounting for the strength, extensibility, and elasticity of the dermis.

The dermis has a rich vascular network which plays a key role in thermo-regulation, wound healing, and immunological defences. Cutaneous vessels, which originate from the underlying muscle vasculature, traverse the dermis vertically forming a superficial plexus at the interface between the papillary and reticular layers, and a deep plexus lying close to the hypodermis and providing nutritional supply to sweat glands and hair follicles (Yen and Braverman, 1976; Braverman, 2000). The dermis also contains a lymphatic system with an active role in the protection of the body against invasive pathogens. The major cellular constituents of the dermis are fibroblasts, which mainly reside in the papillary region and are responsible for the synthesis of all types of fibres in the connective tissue (Saalbach *et al*, 1996). Other cells in the dermis are associated with immunological functions and include dermal dendrocytes (Narvaez *et al*, 1996), Langerhans cells, mast cells, microphages and T-cells (Bos and Kapsenberg, 1995).
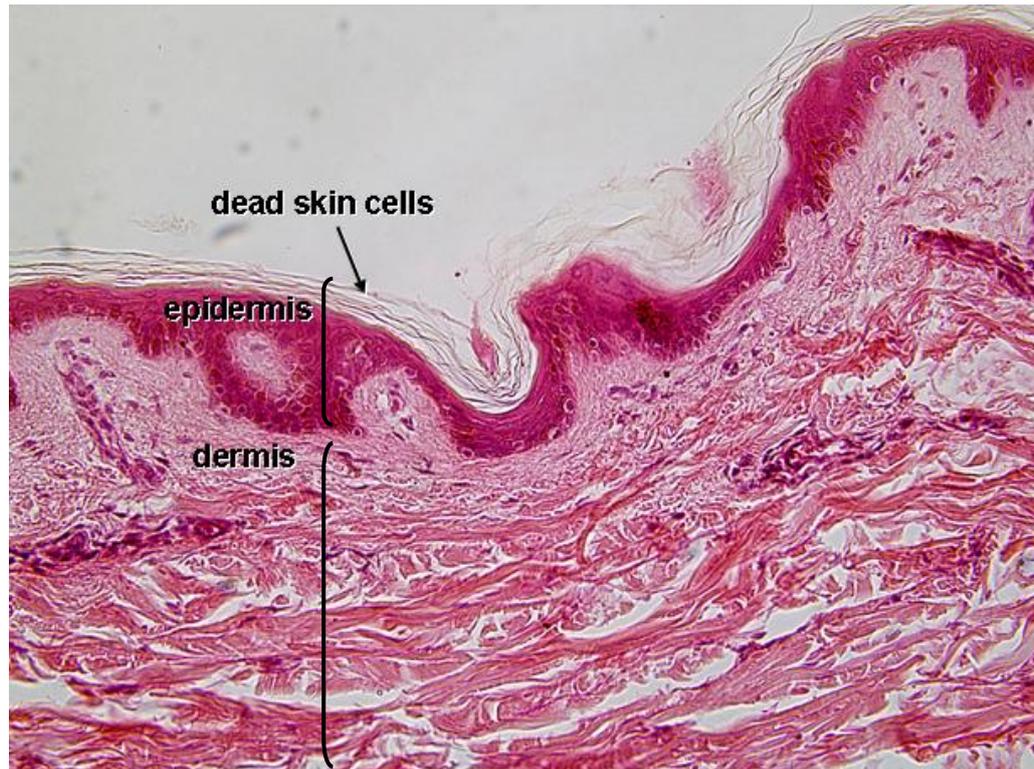
Figure 1.4   Micrograph showing the histology of the skin.

From http://faculty.irsc.edu/FACULTY/TFischer/Default.htm.

1.2.4   Extracellular matrix

The extracellular matrix (ECM) is the fundamental element of all connective tissues which is composed of structural fibres, embedded in an interlocking mesh, known as the ground substance. The latter consists mainly of water, for communication and transport purposes between tissues, and a complex of glycosaminoglycans (GAGs), such as heparin sulfate, which forms proteoglycans when attached to matrix proteins particularly, perlecan and collagen XVIII (Del Forno *et al*, 1978). The ground substance also comprises hyaluronic acid, a non-proteoglycan polysaccharide which serves as cell to cell adhesion bridges and regulates cell behaviour during healing, inflammation and

tumor development (Miyake *et al*, 1990). In this context, *Necator americanus* have been shown to secrete a wide range of proteolytic enzymes capable of degrading the main fibrous and non fibrous components of the dermis (Hotez *et al*, 1990; Kumar and Pritchard, 1992a; Brown *et al*, 1999), including:

1.2.4.1 <u>Collagen</u>

Collagen is the most abundant constituent of the extracellular matrix, accounting for about 98% of the total mass of the dried dermis. To date, the skin has been associated with the largest diversity of collagens, with over ten types divided based on their structure and function into two main subgroups (Garrone *et al*, 1997): fibril and FACIT, fibril-associated collagens with interrupted helices (Gordon and Olsen, 1990).

Fibril collagens, including types I, III and V, are characterised by a long central triple helical domains with a periodicity of 64—67 nm and Glycine-X-Y repeating sequences (Garrone *et al*, 1997; Ruggiero *et al*, 2005). Collagens I and III, being the major constituents of the dermis, co-exist as individually banded fibrils that are loose in the papillary region and become thicker in the reticular region of the dermis, hence accounting for their resistance to proteolytic degradation and maintaining the stability of the skin. Collagens V, VI and VII have also been shown to occur in the form of fibrils and serve as molecular bridges with a role to play in anchoring principal fibres to the surrounding matrix components and cells (Fichard *et al*, 1997). Collagen V has been detected in the dermis, forming heterotypic fibrils with collagens I and III, and occasionally in the dermal-epidermal junction with a potential function during cell migration to the epidermis (Ruggiero *et al*, 1994; Garrone *et al*,

1997). Although less abundant, collagen VI is believed to play an important role in bridging elements in the dermis such as cells and proteoglycans (Bonaldo *et al*, 1990; Tillet *et al*, 1994), while the presence of collagen VII at the dermal-epidermal junction is involved in anchoring fibril components of the junction (Ruggiero *et al*, 2005).

Unlike other types of collagen, collagen IV is a non fibrillar molecule, from the FACIT group which forms the framework of the dermal-epidermal junction and basement membranes around blood vessels, nerves and dermal appendages (Timpl, 1996). Collagen IV is primarily involved in securing the basement membrane and dermal cells into the dermis and maintaining the integrity of the dermal-epidermal junction. The FACIT group also include collagens XII and XIV (Van der Rest and Garrone, 1991) and collagen XVI (Ruggiero *et al*, 2005). These collagens are preferentially distributed in tissues containing banded collagen I fibrils, including the dermis, and are believed to mediate interactions of collagenous fibrils and possibly mediate cell-matrix adhesion during development (Brown *et al*, 1993; Nishiyama *et al*, 1994).

1.2.4.2   Elastin

Elastin, a component of the connective tissue, is responsible for retractile properties of the dermis and provides elasticity to the skin, lungs, tendons and blood vessels. Elastin is synthesised by dermal fibroblasts as proelastin which, upon proteolytic degradation, leads to the formation of tropoelastin, the monomer of elastin fibres (Smith and Wood, 1991). Tropoelastins are then deaminated, upon contact with a mature elastin fibre, allowing these molecules to be cross-linked to the elastin strand (Plopper, 2007). Elastin fibres, which

are thin in the papillary dermis become thicker in the reticular dermis and interweave between collagen fibres to prevent overstretching and subsequent damage to the skin structure.

1.2.4.3   Fibronectin

The extracellular matrix is rich in fibronectin, a multifunctional glycoprotein with a major role in cellular adhesion (Ruoslahti, 1988), growth and wound healing (Peltonen *et al*, 1989) and cross-linking of the matrix fibres. It consists of two similar polypeptide chains, which by enfolding in several domains, mediate binding to cell surface receptor molecules from the integrin family (Yamada, 1988) and collagen fibres (Timpl and Martin, 1997). By binding to collagens and cell surface integrins, fibronectin facilitates cell movement during tissue injury and wound healing by triggering reorganisation of the cellular cytoskeleton.

1.2.4.4   Laminin

Laminin, a non-collagenous glycoprotein, is an essential constituent of all basement membranes which promotes a variety of biological functions including cell adhesion, cross-linking of extracellular molecules (Terranova *et al*, 1980; Sollberg *et al*, 1992; Timpl and Brown, 1996), proliferation and differentiation, as well as neurite outgrowth (Martin and Timpl, 1987). Laminin, synthesised by keratinocytes and dermal fibroblasts, is capable of interacting with collagen IV, nidogen and heparin sulfate proteoglycan through the multi-domain structure of this protein which also have high affinity for some cell types such as endothelial and epithelial cells (Marinkovich *et al*, 1992; Nishiyama *et al*, 2000). Hence, laminin plays an essential role in

anchoring the dermal-epidermal junction to the surrounding tissue and stabilising the skin layers.

1.2.5 *Necator americanus* and the human skin

Necator americanus larvae penetrate the skin using mechanical forces and enzymatic activities to migrate through the different layers and gain access to the host's microcirculation (Matthews, 1982; Kumar and Pritchard, 1992). Larvae have been shown to remain in the skin of mice for up to 48 hours post-infection (Figure 1.5) (Behnke *et al*, 1986; Hawdon *et al*, 1993), during which time they resume larval feeding and reactivate developmental changes to facilitate the parasitic invasion of the host (Hawdon *et al*, 1993; Hawdon and Hotez, 1996). *Necator americanus* secrete a repertoire of proteolytic enzymes which allow them to degrade collagens I to V, elastin, laminin and fibronectin, the main components of the extracellular matrix and all basement membranes (Hotez *et al*, 1990; Kumar and Pritchard, 1992a; Brown *et al*, 1999; Loukas and Prociv, 2001; Williamson *et al*, 2006) and reach the dermal blood vessels.
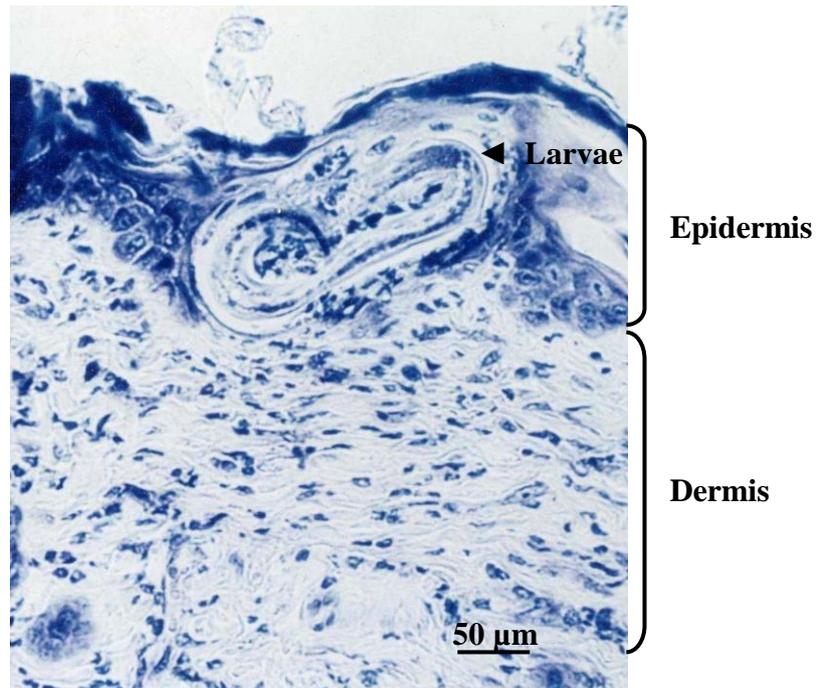
Figure 1.5 *Necator americanus* **larvae residing in the hamster skin.**

The skin is rich in vascular capillaries which consist of a single layer of endothelial cells, surrounded by a simple vascular basement membrane while the post-capillary venules have a similar structure with a multilayered basement membrane, allowing the later to accommodate inflammatory responses (Ruggiero *et al*, 2005). Entry into the blood circulation necessitates *Necator americanus* larvae to pass through the vascular basement membrane and negotiate the endothelium, the innermost lining of all blood vessels and dermal capillaries which plays a major role in regulating the vascular permeability. In order to understand the work presented in this thesis, the reader is introduced to the endothelium and vascular permeability.

1.3   The endothelium

The endothelium is the innermost cellular lining of the vasculature and the lymphatic vessels. As a selective, semi-permeable barrier, the endothelium plays an important role in maintaining vascular homeostasis (Stevens *et al*, 2000; Aurrand-Lions *et al*, 2002) and regulating other physiological functions including permeability and cellular trafficking (Ruffer *et al*, 2004; Aird, 2007; Vandenbroucke *et al*, 2008), cell polarity (Bazzoni and Dejana, 2004), and signal transduction (Mehta and Malik, 2006).

Endothelial cells express a considerable heterogeneity which is characterised by structural diversity across the vascular tree (Kumar *et al*, 1987; Garlanda and Dejana, 1997; Simionescu, 2000; Ruffer *et al*, 2004). The vasculature is lined with continuous, non-fenestrated endothelium, rich in tight junctions, in organs with a strict control of permeability between the blood and surrounding tissues, such as the brain, skin and heart, whereas fenestrated continuous endothelium is characteristic of vascular beds with increased transendothelial transport such as the pancreas, kidney, exocrine and endocrine glands and intestinal mucosa. The endothelium can also be sinusoidal, or discontinuous, which is found in vascular beds with selective filtration properties such as the liver, spleen and bone marrow (Rubin and Staddon, 1999; Aird, 2007). Endothelial heterogeneity is also evident within the microcirculation, where endothelial junctions are more restrictive in arterioles, therefore maintaining the laminar blood flow, compared with capillaries, the main site of molecular exchange, and less mature in post-capillary venules (Leach, 2002; Bazzoni and Dejana, 2004; Aird, 2007a). The latter, containing simple intercellular junction,

are therefore considered as the preferred site for cellular transport during inflammation (Muro *et al*, 2004; Miyasaka and Tanaka, 2004; Aird, 2007a), in response to permeability-increasing agents (Bazzoni and Dejana, 2004) and possibly during parasitic invasion. However, proteolytic activity of *Necator americanus* secretions is likely to mediate disruption of endothelial integrity at the molecular level, possibly allowing larvae to breach the endothelium at the capillary plexus. The structure of the endothelium and its role in regulating the vascular permeability are introduced here.

1.3.1 Vascular permeability

The endothelium is a semi-permeable, physical barrier which regulates the exchange of fluids, solutes, plasma proteins and macromolecules between the blood and the interstitial space, in a process known as vascular permeability. This is a continuous process that occurs at the microcirculation site, the capillaries, in two pathways, that is the transcellular and paracellular pathway (Lum and Malik, 1994; Leach, 2002).

1.3.1.1 <u>Transcellular permeability</u>

Transcellular transport or transcytosis, is a route by which macromolecules (less than 3 nm in diameter) and plasma proteins, such as albumin, are shuttled across the endothelium (Simionescu *et al*, 1978). Based on the physical properties of the transported molecules, transcytosis can be mediated by special structures, including caveolae (Predescu and Palade, 1993; Minshall *et al*, 2002) and vesiculo-vacuolar organelles (VVOs). Caveolae, 70 nm membrane-bound vesicles, are particularly prevalent in capillaries and transport molecules from the luminal space either by non-specific fluid-phase uptake (Vogel *et al*,

2001; Schubert *et al*, 2001) or via receptor-dependent binding to the molecule

(Dejana *et al*, 1999; Minshall *et al*, 2002; Aird, 2007). Albumin, for instance,

has been shown to bind to a 60 kDa endothelial cell surface glycoprotein, gp60,

which is believed to initiate transcytosis (Minshall *et al*, 2002). Caveolae,

which pinch off and shuttle across the cytoplasm, merge with the membrane

and liberate their content on the abluminal side of the endothelium. VVOs, on

the other hand, are specifically present in venular endothelial cells and consist

of groups of vesicles, possibly arising from the fusion of individual caveolae to

allow transport across the much thicker cytoplasm of venular endothelium

compared with capillaries (Dvorak and Feng, 2001; Aird, 2007). Transcellular

channels may also be involved in transport of amino acids, glucose and other

ions including nitric oxide and prostacyclin (Bazzoni, 2006).
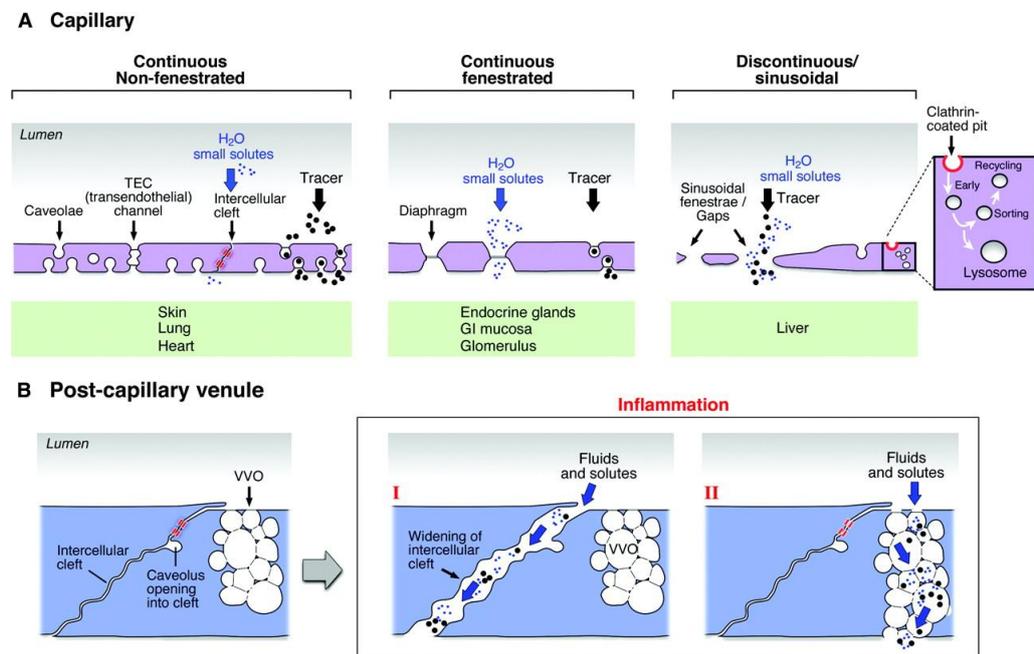
Figure 1.6   Permeability pathways through the vascular endothelium.

A) Capillaries mediate transfer of solutes and fluids between blood and

underlying tissue. Water and small solutes pass through the intercellular

cleft, whereas larger solutes pass through endothelial cells either via transendothelial channels or transcytosis which is primarily mediated by caveolae. B) In response to inflammation, post-capillary venules accommodate inducible transfer of water and solutes through the paracellular route which involves formation of gaps between endothelial cells (I), and/or the transcellular route (II) through VVO-mediated formation of transcellular channels (Adapted from Aird, 2007).

1.3.1.2   Paracellular permeability

The paracellular pathway is a structural equivalent of the 'small pore' theory, which explains transport of hydrophilic solutes through the endothelium (Pappenheimer *et al*, 1951). Paracellular transport was first reported by Majno and Palade (1961) and supported through tracer studies by Williams *et al* (1975). Anatomically, paracellular channels made of an intercellular junction complex, are located between adjacent endothelial cells and act as a regulated barrier for passive diffusion of fluids and small, hydrophilic solutes as well as cell trafficking through the paracellular space (Bazzoni and Dejana, 2004; Aird, 2007). Adhesion of endothelial cells, through the paracellular junctions, also mediates cellular communications and cross-talking which maintains the homeostatic balance and regulates other physiological functions in the endothelium such as proliferation and survival (Hordijk *et al*, 1999; Edens and Parkos, 2000; Taddei *et al*, 2008; Vandenbroucke *et al*, 2008). Paracellular permeability is therefore an essential measure to evaluate the integrity of the endothelium and its physiological importance as an active barrier between the blood and the surrounding tissues.

Techniques used to analyse paracellular permeability are based on the biophysical properties of the endothelium and include the transendothelial electrical resistance (TEER) and tracer flux across the endothelial layer (Spring, 1998; Bazzoni and Dejana, 2004). Resistance, which is calculated using Ohm's law, is based on the ability of ionic currents in the aqueous medium to carry a pulse of an electrical current across the endothelial monolayer, and is measured as the change in voltage between the apical and basal compartments of the cell layer (Rutten *et al*, 1987). Tracer flux, however, is used to determine the flow of non-electrolyte, tracers which usually are not transported by the paracellular routes. Fluorescent albumin or dextrans, of known molecular weight, are the most common tracers used to determine the size of the paracellular pathways as a function of their molecular size and radius (Huxley and Curry, 1991; Balda *et al*, 1996; Minshall *et al*, 2002). TEER and tracer fluxes are often inversely related, and used as indicative of the integrity of the paracellular junctions and the barrier properties of the endothelium (Bazzoni and Dejana, 2004).

1.3.2   The molecular organisation of the endothelial cell to cell junctions

Inter-endothelial cell junctions are specialised regions of the endothelial membrane, where cells come into close contact to establish structural integrity and regulate endothelial permeability (Leach and Firth, 1995; Vestweber, 2000; Dejana *et al*, 2000; Dejana *et al*, 2008). Permeability, which is regulated by the dynamic opening and closing of these adhesive structures, is mediated by adhesion molecules which are primarily organised into two classical groups, adherens and tight junctions (Karnovsky, 1967; Karnovsky, 1968; Dejana *et al*, 1995). Adhesion, in both junctions, is mediated by transmembrane proteins

which promote homophilic interactions between adjacent cells as well as promoting stabilisation and dynamic control of these junctions by binding to cellular cytoskeleton (Gonzalez-Mariscal *et al*, 2008; Dejana *et al*, 2009). Gap junctions, which are also present in the endothelium, are not involved in the control of permeability (Dejana *et al*, 2009) and will not be addressed here.

1.3.2.1   <u>Adherens junctions</u>

Adherens junctions (AJs), representing the majority of junctions within the endothelial barrier, are cellular membrane contacts formed by transmembrane glycoproteins of the cadherin family (Dejana *et al*, 1995; Ruffer *et al*, 2004; Villasante *et al*, 2007). Cadherins are single-chain transmembrane proteins which mediate homophilic, calcium dependent adhesion and are able to form multimeric complexes with cytoplasmic binding proteins (Bazzoni and Dejana, 2004; Villasante *et al*, 2007). Vascular endothelial (VE) cadherin, the major constituent of AJs in the vascular endothelium, is expressed in essentially all vessels (Lampugnani *et al*, 1992; Ayalon *et al*, 1994; Bazzoni and Dejana, 2004), whereas neuronal (N) cadherin is distributed diffusely over the cell surface, possibly maintaining endothelial integrity by anchoring endothelial cells to other cell types expressing N-cadherin (such as pericytes), and therefore has no major role to play in regulating endothelial permeability (Lampugnani and Dejana, 1997, Hordijk *et al*, 1999).

VE-cadherin, also known as cadherin-5 or CD144, is structured in an extracellular domain, consisting of five calcium binding repeats that associate homophilically with VE-cadherin on the adjacent cell (Lampugnani *et al*, 1995; Hordijk *et al*, 1999; Vandenbroucke *et al*, 2008). The cytoplasmic tail of VE-

cadherin comprises a C-terminal domain (CTD) which forms complexes with β-catenin and plakoglobin (γ-catenin), linking VE-cadherin to α-catenin, which in turn is anchored with the actin cytoskeleton to promote stabilisation of the junctional complex (Lampugnani *et al*, 1995; Dejana *et al*, 2000) while the juxtamembrane domain (JMD) binds p120-catenin to further stabilise AJs by anchoring VE-cadherin with endothelial microtubules, known as kinesin (Lampugnani *et al*, 1995). Dynamic interactions between the AJs proteins and the actin cytoskeleton are believed to maintain the stability of AJs and regulate junctional permeability while microtubules are believed to ensure the stability of the cytoskeleton by connecting actin filaments to other cellular components and mediating dynamic cellular processes including the opening and closing of these junctions (Figure 1.7) (Dejana *et al*, 2008; Vandenbroucke *et al*, 2008). The association of VE-cadherin with desmosomal proteins including desmoplakin and vimentin is mediated by plakoglobin, forming desmosomal-like structures at the membrane which are known as complexus adherentes (Kowalczyk *et al*, 1998; Schmelz *et al*, 1994). These structures are specific for endothelial cells mostly in the lymphatic vessels (Girard and Springer, 1995), and therefore will not be addressed in this work.
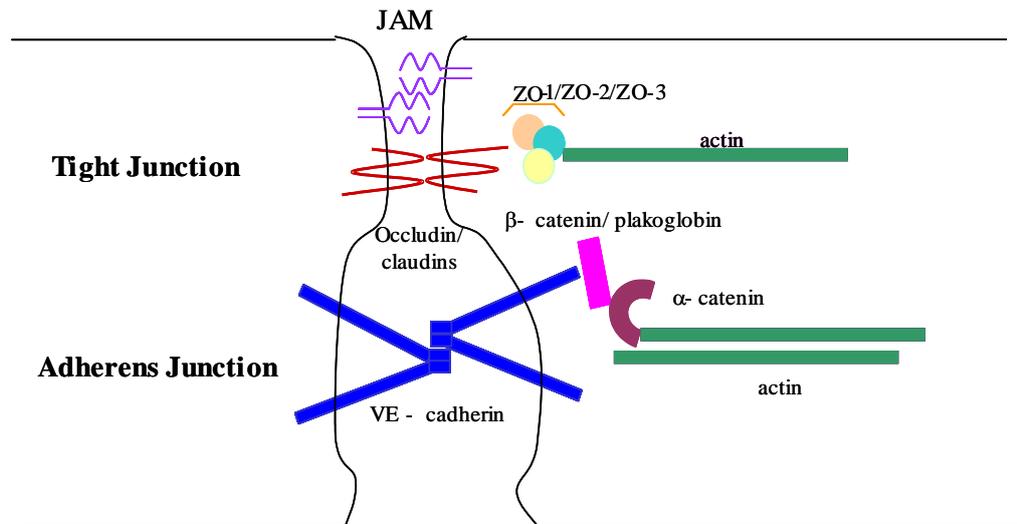
Figure 1.7   Molecular structure of endothelial cell to cell junctions (Adapted from Leach *et al*, 2009).

Besides VE-cadherin, nectin-afadin complex which binds to the actin cytoskeleton through α-catenin, co-localises with cadherins and may be involved in the assembly of AJs (Bazzoni and Dejana, 2004). Other junctional proteins such as VE-cadherin-2, which shows similar homology and adhesive properties to the cadherin family, has been identified at the AJs but had no ability to modulate vascular permeability or interact with cellular signalling pathways (Telo *et al*, 1998).

1.3.2.2   Tight junctions

Tight junctions (TJs), or zonula occludens, form a very close contact between adjacent endothelial cells representing around 20% of total inter-endothelial junctional complexes (Mehta and Malik, 2006). The density of TJs is believed to account for unique barrier properties within different vascular beds (Harhaj and Antonetti, 2004; Aird, 2007). For instance, the blood brain barrier and

arteries, which require a strict control of permeability, are rich in well organised TJs, whereas these junctions are poorly developed in post-capillary venules, which accommodate the dynamic transport of immune cells and plasma proteins during inflammation (Bazzoni *et al*, 1999; Bazzoni and Dejana, 2004).

Structural organisation of TJs comprises two principal groups; the tetrahelical molecules including occludin (Furuse *et al*, 1993) and claudins (Furuse *et al*, 1998), and the immunoglobulin gene superfamily involving junctional adhesion molecules (JAMs) (Dejana *et al*, 2000; Aurrand-Lions *et al*, 2002). While occludin is considered as an accessory junctional protein (Furuse *et al*, 1993; Leach, 2002; Harhaj and Antonetti, 2004), claudins (especially claudin-5) are a large family of transmembrane proteins which form the building units of tight junctional strands (Furuse *et al*, 1998; Bazzoni, 2006). Both occludin and claudins are structured in four membrane-spanning domains (Jiang *et al*, 1998), two extracellular loops through which they interact homophilically and heterophilically, therefore contributing to the assembly of endothelial TJs (Mehta and Malik, 2006), and two cytoplasmic termini which are capable of interacting with the zonula occludens ZO-1 and other actin binding proteins (Figure 1.7) (Furuse *et al*, 1994; Ruffer *et al*, 2004). Through their interaction with ZOs and actin cytoskeleton, both occludin and claudins establish an essential role in promoting better stability of inter-endothelial junctions and in regulating paracellular permeability (Bazzoni and Dejana, 2004; Bazzoni, 2006; Vandenbroucke *et al*, 2008). Junction adhesion molecules (JAMs), mono-spanning membrane proteins with two extracellular immunoglobulin

domains and a short cytoplasmic tail, represent the third class of TJs associated integral proteins (Bazzoni and Dejana, 2004; Weber *et al*, 2007). To date, four members of the JAM family have been identified in endothelial cells (JAM 1—3 and endothelial cell-selective adhesion molecule, ESAM), all capable of establishing homophilic and heterophilic interactions (Bazzoni and Dejana, 2004; Dejana *et al*, 2009), which is likely to be involved in TJs assembly as well as in regulation of paracellular permeability and cellular trafficking (Mehta and Malik, 2006).

1.3.2.3 <u>Intracellular and non-junctional proteins</u>

Endothelial cells express different proteins with adhesive properties which are localised either outside the junctions or in the cytoplasm. Two proteins, which have been extensively studied, are reviewed here. However, it is worth noting that a set of other proteins including actin polymerising formin (Goode and Eck, 2007), vasodilator-stimulated phosphoprotein, VASP (Huttelmaier *et al*, 1999), vinculin (Wilkins and Lin, 1986) and cingulin (Cordenonsi *et al*, 1999) which are localised outside the AJs and TJs, form connections between actin cytoskeleton and junctional molecules to provide mechanical stability of inter-endothelial junctions and maintain the integrity of the endothelium (Mehta and Malik, 2006).

Platelet endothelial cell adhesion molecule (PECAM-1 or CD31) is a member of the immunoglobulin superfamily, which plays a major role in leukocyte transendothelial migration and permeability regulation (Albelda *et al*, 1991; DeLisser *et al*, 1994; Newman, 1999; Muller, 2003). PECAM-1, a mono-spanning protein, exhibits six external immunoglobulin-like domains to

mediate homophilic interaction with circulating blood cells, which is thought to mediate leukocyte migration across the endothelium (Sun *et al*, 1996). In addition, PECAM-1 is capable of establishing heterophilic bindings, through its cytoplasmic tail, with matrix adhesion receptors such as integrins, to modulate cell adhesion and migration (Albelda *et al*, 1991; Jackson *et al*, 1997). Through its cytoplasmic tail, PECAM-1 also associates with intracellular β-catenin and protein tyrosine phophatase containing SRC homology-2 domain (SHP-2) which is likely to influence endothelial barrier integrity and intracellular signalling processes (Ilan *et al*, 2000; Bazzoni and Dejana, 2004; Mehta and Malik, 2006).

Zonula occludens (ZOs) are members of the membrane associated guanylate kinase homologues (MAGUKs). ZOs (1—3) are known to stabilise tight junctions by means of bridging intracellular proteins with claudins, occludin and JAMs. However, recent evidence suggests that ZOs, particularly ZO-1 could also bind to α-catenin (Muller *et al*, 2005) and connexin-43 (Toyofuku *et al*, 1998), thus linking TJs through their cytoplasmic associated proteins to AJs and gap junctions, respectively (Bazzoni and Dejana, 2004). ZOs which form hetero-dimeric complexes either with actin cytoskeleton or with other members of the MAGUKs family through their multiple domains, including PDZ, SH-3 and guanylate kinase (GUK), may play a potential role in modulation of intracellular adhesion and paracellular permeability (Mehta and Malik, 2006).

1.3.3   Junctional structures regulate the vascular permeability

Molecular heterogeneity, which is observed along the vascular tree, is an essential determinant of structural and functional differences in the

endothelium. TJs, which are predominant in vascular beds with a strict control of permeability such as the blood brain barrier and heart, are poorly developed in the post-capillary venules where most inflammatory responses take place. AJs and VE-cadherin in particular, play an important role in mediating and controlling site-specific permeability as evidenced by *in vivo* studies in which the systemic administration of blocking antibodies to VE-cadherin resulted in preferential alterations in vascular permeability in the lung and heart (Dejana *et al*, 2008; Dejana *et al*, 2009). Moreover, truncated VE-cadherin lacking its cytoplasmic tail was associated with partial disassembly of AJs and an incontrollable increase in permeability, further supporting the major role of the VE-cadherin-catenin complex in regulating endothelial permeability (Navarro *et al*, 1995; Dejana *et al*, 2008). AJs, which are known to interconnect with TJs at the intracellular level, possibly through ZO-1 and ZO-2 molecules, were found to control TJs by VE-cadherin-mediated upregulation of claudin-5, the building unit of endothelial TJs (Taddei *et al*, 2008). Therefore, VE-cadherin expression is a crucial factor which determines the junctional stability and regulates vascular permeability.

Endothelial junctions are dynamic structures which undergo continuous remodelling and maintenance in rest and upon exposure to haemodynamic stimuli (Dejana *et al*, 2009). Paracellular exchange, which is controlled by the opening and closing of these junctions, is associated with dynamic contractions resulting in small gaps at the cellular cleft without complete cell separation (Figure 1.8, A and B) (Dudek and Garcia, 2001). The contractile status of endothelial cells, as most other cells, is the result of myosin light chain (MLC)

phosphorylation which is mediated by MLC kinase (MLCK) in a Ca^{+2}/calmodulin-dependent manner (Garcia *et al*, 1995), RhoA from the small GTPase Rho family which controls actin organisation (Noda *et al*, 1995; Yoshioka *et al*, 2007), and by vascular endothelial protein tyrosine phosphatase (VE-PTP), an endothelial receptor-type phosphatase that interacts specifically with VE-cadherin (Nawroth *et al*, 2002). MLC phosphorylation generates a contractile force which induces actin reorganisation and dissociation of VE-cadherin homophilic and heterophilic interactions, forcing these molecules to be internalised (Mehta and Malik, 2006). VE-cadherin re-localisation to the surface is possibly modulated by cytosolic p120-catenin, which is considered as a crucial feedback mechanism promoting VE-cadherin expression and assembly of intact AJs (Xiao *et al*, 2003; Reynolds and Carnahan, 2004; Vandenbroucke *et al*, 2008). Upon VE-cadherin re-establishment in AJs, members of the GTPases Rho family including Cdc-42 and Rac-1 are activated to further stabilise AJs by anchoring VE-cadherin with the actin cytoskeleton. Activated Cdc-42 and Rac-1 also inhibit the binding of IQRas GTPase activating protein (IQGAP-1) to β-catenin, thereby enhancing the accessibility of β-catenin to its partners including VE-cadherin, p120-catenin and α-catenin, and regulating AJs assembly (Mehta and Malik, 2006). An additional binding of VE-cadherin with vascular endothelial growth factor receptor (VEGFR-2) forms a multiprotein complex which limits its internalisation and improves the junctional stability (Lampugnani *et al*, 2006).
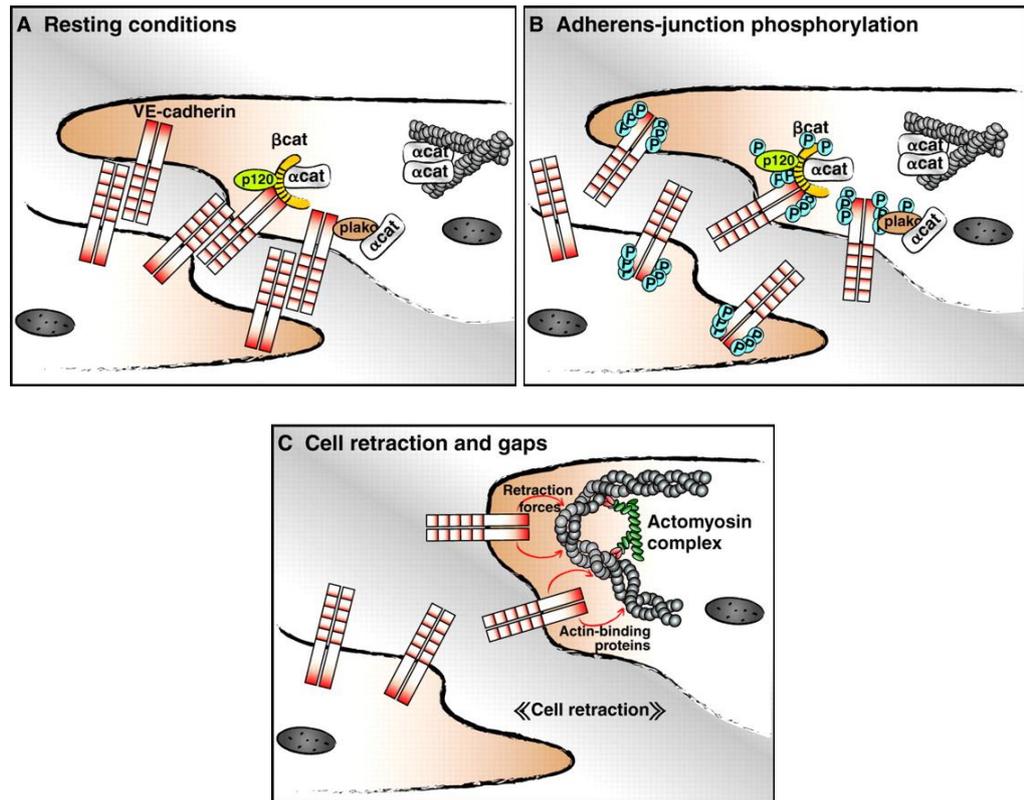
Figure 1.8   Mechanism of gap formation and inducible permeability in the endothelium. A) VE-cadherin associates with p120, β-catenin (βcat) and plakoglobin (plako) which in turn bind to actin filaments through α-catenin (α-cat). B) Phosphorylation (P) of VE-cadherin complex mediates VE-cadherin internalisation and increased vascular permeability. C) Inducible permeability is mediated by formation of intercellular gaps which is caused by cell retraction (Adapted from Dejana *et al*, 2008).

TJs assembly is partially regulated by an atypical protein kinase C (PKC) in complex with other intracellular proteins such as Cdc-42 from the GTPase Rho family and PAR-3/PAR-6, the PDZ-containing proteins (Ruffer *et al*, 2004; Bazzoni and Dejana, 2004). JAM-3, which is known to increase endothelial permeability when expressed in endothelial cells, plays a potential role in

promoting continuous organisation and maintenance of TJs (Orlova *et al*, 2006). Phosphorylation of TJs components by ZO-1-associated kinase (ZAK), protein kinase C (PKC) affecting ZO-1 and casein kinase II, which acts on occludin molecules, induces reorganisation of TJs and modulate junctional permeability. In addition, phosphorylation of AJs and actin cytoskeleton by protein kinase C (PKC) and GTPases (Rho and Rac), indirectly affect the stability of TJs, therefore contributing to regulation of vascular permeability (Bazzoni and Dejana, 2004).

1.3.4 Modulation of vascular permeability

The endothelium is capable of meditating inducible permeability in response to patho-physiological factors affecting endothelial cells (Figure 1.8, C). Inflammation, both in acute and chronic conditions, occurs predominantly in post-capillary venules where junctional complexity is low (Mehta and Malik, 2006; Aird, 2007a). Most permeability-related studies use endothelial cells from large vessels such as the human umbilical vein (HUVEC) as they are easily obtainable and grown *in vitro*. The HUVEC model, as primary endothelial cells, is known to maintain the basic properties of all endothelial cells, including plasticity and molecular structure, and is generally used *in vitro* to mimic endothelial activity *in vivo* (Aird, 2007). Other cell lines, such as human dermal microvascular endothelial cells (HDMEC) and immortalised human microvascular endothelial cells (HMED-1), have been shown to express distinct phenotypic differences compared to HUVEC model, and are usually used to investigate site-related characteristics of the endothelium (Swerlick *et al*, 1992; Xu *et al*, 1994; Bonnefoy *et al*, 2001). A typical increase in vascular permeability, which is controlled by a dynamic balance of junctional

complexes and contractile forces (Dudek and Garcia, 2001), is usually mediated by phosphorylation of junctional proteins causing their dissociation from the actin cytoskeleton and possibly the formation of frank's intercellular gaps (Budworth *et al*, 1999; Andriopoulou *et al*, 1999; Bazzoni and Dejana, 2004). Stimulation of endothelial cells by permeability increasing agents has been shown to target the adhesive VE-cadherin-catenin complex, emphasising the crucial role of VE-cadherin in regulating endothelial permeability.

Vascular endothelial growth factor (VEGF) is an endothelial-specific mitogen which plays an important role in angiogenesis during development of the vasculature. VEGF induces an increase in vascular permeability, evidenced by *in vivo* studies in which exogenous administration of VEGF induced fenestration in vascular beds that normally do not have fenestrae including capillaries and venules of skin (Roberts and Palade, 1995). VEGF binds to VEGF receptors 1—3 on endothelial cells which initiates phosphorylation of VE-cadherin by kinases from the SRC family leading to the internalisation of VE-cadherin molecules and a subsequent increase in permeability (Wright *et al*, 2002; Weis *et al*, 2004; Gavard and Gutkind, 2006). VEGF also activates tyrosine phosphorylation of VE-cadherin and its associates, β-catenin and p120-catenin, which in turn induces actin reorganisation and alters junctional structure and permeability (Esser *et al*, 1998; Dejana *et al*, 2008).

Thrombin, a serine protease primarily involved in the coagulation cascade, is known to bind protease-activated receptor (PAR)-1 on endothelial cells causing an increase in vascular permeability and cellular trafficking during an

inflammation. Activation of PAR-1 initiates multiple phosphorylation cascades including myosin light chain (MLC) phosphorylation (Garcia *et al*, 1995; Verin *et al*, 2001), RhoA and protein kinase C (PKC) phosphorylation of VE-cadherin complexes (Sandoval *et al*, 2001; Bogatcheva *et al*, 2002; Vandenbroucke *et al*, 2008). Disassembly of VE-cadherin junctional complex, including dissociation of SHP-2 phosphatase (Bazzoni and Dejana, 2004), is followed by internalisation of VE-cadherin which induces reorganisation of the actin cytoskeleton leading to cellular contraction and formation of intercellular gaps, which in turn is associated with increased vascular permeability (Mehta and Malik, 2006).

Junctional complexes, VE-cadherin in particular, have shown susceptibility to proteolysis which is said to promote junctional disruption and modulate vascular permeability (Bazzoni and Dejana, 2004; Dejana *et al*, 2008). Thrombin and dengue virus infection have been shown to activate endothelial cells, promoting the production of acute inflammatory cytokines including IL-6 (Day *et al*, 2006; Dewi *et al*, 2008) and IL-8 (Talavera *et al*, 2004), which in turn triggers tyrosine phosphorylation of junctional molecules (Nwariaku *et al*, 2004) and modulate endothelial permeability. In addition, neutrophil derived proteolytic activities and gingipains, cysteine proteases derived from *Porphyromonas gingivalis*, have been shown to mediate increased vascular permeability and enhanced transmigration of monocytes through disruption of endothelial junctions and production of IL-8 (Lukacs *et al*, 1995; Moll *et al*, 1998; Inomata *et al*, 2007). Protease-related alterations in the vascular permeability are also associated with reorganisation of actin filaments and

formation of intercellular gaps in the endothelial barrier as previously described (Blum *et al*, 1997; Moll *et al*, 1998; Hordijk *et al*, 1999; Young *et al*, 2003). For instance, *Schistosoma mansoni* enzymatic extracts were shown to mediate paracellular permeability through a cAMP/protein kinase A pathway leading to increased phosphorylation of the MLCK (Trottein *et al*, 1999). For the reasons outlined above, this thesis addresses the interaction between *Necator americanus* larval enzymes and the endothelium and the effects of these parasites on vascular permeability.

Hypothesis and Aims

The hypothesis of this thesis proposes that *Necator americanus* L3 larvae produce exsheathing and secretory enzymes to negotiate the skin and breach the paracellular integrity of the endothelium, the innermost lining of dermal vasculature, allowing larvae to gain access to the bloodstream.

The primary aims of this work were:

- To study the enzymatic profiles of *Necator americanus* larval exsheathing fluid (EF) and excretory/secretory (ES) products.
- To investigate the effects of larval EF and ES products on extracellular (ECM) and skin macromolecules.
- To study the interaction of larval EF and ES products with monolayers of human umbilical vein endothelial cells (HUVEC) as an "*in vitro*" model of the endothelium, specifically by investigating their effects on paracellular integrity of the endothelial barrier and the molecular mechanisms employed therein.

2. Characterisation of *Necator americanus* larval products

2.1 Introduction

Although *Necator americanus* larvae are believed to infect the human host both mechanically and by secreting a mixture of enzymes (Kumar and Pritchard, 1992a; Loukas and Prociv, 2001), knowledge of the mechanisms by which these parasites enter the underlying vasculature is not well documented. *Necator americanus* larvae have been shown to express a wide range of enzymatic secretions, presumably with roles to play in the infection process (Matthews, 1975; Kumar and Pritchard, 1992; Williamson *et al*, 2004). Characterisation of these secretions is therefore crucial to understand their impact in the context of negotiating the human vascular endothelium.

Classification of *Necator americanus* larval proteases was previously investigated using protease inhibitors against distinct classes of proteases (Kumar and Pritchard, 1992a; Brown *et al*, 1999). *Necator americanus* infective larval excretory/secretory (ES) products have been shown to contain serine, cysteinyl, aspartyl, and metalloproteases (Kumar and Pritchard, 1992a; Brown *et al*, 1999; Quinnell *et al*, 2004) whereas cysteinyl proteases were the only proteolytic enzymes reported by Kumar and Pritchard (1992a) in *Necator americanus* exsheathing fluid (EF). Metalloproteases such as aminopeptidases have been previously detected in the intestine of *Necator americanus* adult worms (McLaren *et al*, 1974) and later identified in the exsheathing fluid of the blood feeding nematode, *Haemonchus contortus* (Rogers and Brooks, 1978), setting a potential role for these enzymes to play in the exsheathment and penetration processes of the human hookworm *Necator americanus*.

Most of these proteases are gelatinolytic in nature (Kumar and Pritchard, 1992a) and have an ability to degrade a number of skin macromolecules (Brown *et al*, 1999) and host haemoglobin (Williamson *et al*, 2003). Therefore, investigating the proteolysis of both gelatin and haemoglobin would be of major importance in describing protease profiles of larval enzymatic mixtures and determining their involvement in the process of infection. Casein, labelled with fluorescein isothiocyanate would also be beneficial as a quantitative indicator of proteolytic activities through the precise and sensitive measurement of casein degradation (Twining, 1984).

The work presented here aimed at producing a detailed profile of *Necator americanus* larval proteases using protein and substrate gel electrophoresis and enzyme assays. Further characterisation of larval products was performed using different protease inhibitors. Treatment of larval products with anti worm IgG antibodies was also conducted to investigate their possible protective role against *Necator americanus* infection.

2.2 Methods

2.2.1 Culture of infective *Necator americanus* larvae

Infective *Necator americanus* larvae were cultured as described by Kumar and Pritchard (1992). Faecal material was collected from a *Necator americanus* infected individual, mixed with charcoal, 1% fungizone, and water to form a smooth paste which was applied as a thin layer on the upper half of 0.5 x 8 cm strips of Whatman chromatography paper. Each strip was then placed in a 15 mL centrifuge tube (containing ~ 2 mL of distilled water) and incubated at room temperature for 8—10 days. The strips were carefully removed and the water containing the larvae transferred to a larger measuring cylinder. The larvae were allowed to settle for 1—2 hours and excess water was aspirated off. The concentrated larvae were washed extensively in RPMI 1640 medium containing penicillin (100 IU/mL), streptomycin (100 μg/mL) and 1% fungizone, counted (~ 3 live larvae/μL), and stored in the dark at room temperature until needed.

2.2.2 Preparation of larval *Necator americanus* exsheathing fluid and excretory/secretory products

Larval exsheathing fluid (EF) was prepared by bubbling carbon dioxide (100% CO_2) through the larval suspension in media (RPMI 1640 medium containing penicillin (100 IU/mL), streptomycin (100 μg/mL) and 1% fungizone) for 2 hours at room temperature. The media containing the EF was collected after centrifugation at 52 x g for 45 minutes, filter-sterilised and stored at -20˚C. The exsheathed larvae were then cultured for an additional 72 hours at 37˚C and the excretory/secretory products (ES) were collected every 24 hours after

centrifugation at 52 x g for 45 minutes. ES products were pooled, dialyzed against water for 48 hours at 4˚C, filter-sterilised and stored at -20˚C until needed.

The presence of lipopolysaccharide (LPS) in larval EF and ES products was estimated using an E-TOXATE kit, following the manufacturer's recommendations and was not detected or else present at a level below the detection limits of this assay (0.015 EU/mL).

2.2.3   Protein estimation

The protein content of larval EF and ES products was estimated using the BioRad protein assay. A solution of bovine serum albumin (BSA) in media (RPMI 1640 medium containing penicillin (100 IU/mL), streptomycin (100 µg/mL) and 1% fungizone) was used at a concentration of 25 mg/mL to prepare protein standards at a range of 0—25 µg/mL. In a 96 well Nunc plate, 20 µL triplicates of BioRad protein dye reagent was added to 80 µL triplicates of both BSA standards and neat EF or ES samples. After mixing, the absorbance of all samples was measured using DYNEX MRX Microplate Reader at 595 nm. The absorbance of BSA standards was plotted against their known protein content and the protein concentrations of EF and ES samples were calculated using the equation of the standard curve.

2.2.4 Characterisation of *Necator americanus* larval products using Sodium Dodecyl Sulphate Polyacrylamide Gel Electrophoresis (SDS-PAGE)

2.2.4.1 Preparation of SDS-PAGE gels

In this project, proteins were separated on 10% acrylamide resolving gels under reducing conditions, unless otherwise described. Glass plates were carefully cleaned with distilled water, then ethanol and allowed to air-dry. To 12 mL of 10% resolving gel solution, 60 µL of 10% ammonium persulphate (APS) and 6 µL of N'N'N'-tetramethylethylenediamine (TEMED) were added and the gel solution was quickly poured between the gel plates. Air bubbles were carefully removed by applying an overlay of tert-amyl alcohol (TAA) to the top surface of the gel and allowed to polymerise at room temperature for 1 hour. The gel was thoroughly washed with distilled water and excess moisture removed with filter paper before applying the stacking gel. For all SDS-PAGE gels, 1 mL of 4% acrylamide solution was used as a stacking gel to which 10 µL of 10% APS and 4 µL of TEMED were added. A well forming comb was then inserted between the glass plates avoiding the formation of air bubbles and the stacking gel left to polymerise for 30 minutes.

2.2.4.2 Sample preparation

Samples were concentrated either by acetone or trichloroacetic acid (TCA) precipitation and loaded at 20 µg per lane. In brief, EF and ES samples were mixed with 1:4 (v/v) of ice cold acetone or 5:3 (v/v) of 5% TCA and precipitated overnight at 4°C (TCA) or at -20°C (acetone). Samples were then centrifuged at 13000 x g for 10 minutes and the precipitate resuspended in 20

μL of 2 x reducing sample buffer. Samples were reduced by boiling at 100˚C for 10 minutes and loaded onto the gel. Five to ten microliter of a protein molecular mass standard (EZ-Run Prestained Rec Protein Ladder) were also loaded on a single well per gel prior to running each gel at 20 mA constant current for 60—90 minutes, using BioRad PowerPac 200.

2.2.4.3   Separation of proteins by two dimensional gel electrophoresis (2DE)

EF and ES samples were concentrated as described above (using TCA) and approximately 100 μg of protein was resuspended in 125 μL of BioRad rehydration buffer. Samples were then loaded into the PROTEAN IEF focusing tray and ReadyStrip IPG strips (7 cm, pH 3—10) placed gel side down in the tray, avoiding the formation of air bubbles. Strips were overlaid with 2 mL of BioRad mineral oil and allowed to passively rehydrate overnight at room temperature. Isoelectric focusing (IEF) was programmed to commence automatically following rehydration with a maximum current of 50 μA/IPG strip and an end voltage of 4000 V (at 20˚C). When the electrophoresis was completed, strips were drained for 5 seconds then transferred gel side up to a clean equilibration tray. Two milliliters of BioRad equilibration I with 2% dithiothreitol (DTT) and bromophenol blue was added to each IPG strip and the tray was gently shaken for 10 minutes. Buffer I was carefully discarded and replaced with 2 mL of BioRad equilibration buffer II with 2.5% iodoacetamide and bromophenol blue for 10 minutes. IPG strips were then dipped briefly in SDS-PAGE running buffer and placed gel side up on the back plate of a 10% SDS-PAGE gel. Strips were carefully pushed into the well, overlaid with 0.25% agarose in 0.5 M Tris buffer (pH 6.8) and left for 5 minutes to allow the

agarose to solidify. Gels were then run at a constant current of 20 mA per gel for 60 minutes.

2.2.4.4   Protein visualisation

One and two dimensional SDS-PAGE gels were silver stained using a modified method by Yan *et al* (2000). Gels were washed three times in distilled water (5 minutes per wash) prior to fixing in destain solution (25% methanol, 10% glacial acetic acid and distilled water) for 1 hour. To improve the contrast of the silver staining, gels were washed and left in distilled water overnight. Gels were then sensitized with 0.02% sodium thiosulphate for 1 minute and rinsed three times with distilled water (20 seconds each). 0.2% silver nitrate was added for 20—40 minutes and gels were washed twice (20 seconds each) and developed with a solution of 3% sodium carbonate, 0.05% formaldehyde and 0.0004% sodium thiosulphate on an orbital shaker. The developer solution was discarded and the reaction stopped with 2% ethylene-diaminetetraacetic acid (EDTA) for 20 minutes. Finally, silver stained gels were washed and stored in distilled water if required.

2.2.4.5   Protein identification

Protein bands, separated on silver stained gels, were carefully excised and stored in PBS. Samples were analysed and proteins identified using matrix-assisted laser desorption/ionization (MALDI) peptide mass fingerprinting as described by Gonnet *et al* (2003).

2.2.5 Detection of *Necator americanus* larval protease activity using substrate SDS-PAGE

2.2.5.1 Preparation of substrate SDS-PAGE gels

Following a method by Kumar and Pritchard (1992a), 10% substrate SDS-PAGE gels were prepared by including 0.1% (w/v) of either gelatin or haemoglobin in the 10% resolving gel. Hyaluronidase activity was also assessed by incorporating 0.1% (w/v) of hyaluronic acid into a 12% SDS-PAGE gel in a method modified from Hotez *et al* (1992). Substrate gels were run under non reducing conditions. EF and ES samples were concentrated using StrataClean Resin and centrifuged at 13000 x g for 10 minutes. Protein pellets were then resuspended in 20 µL of 2 x non reducing sample buffer (without DTT), incubated at 37˚C for 30 minutes and loaded at 5—10 µg per lane. Substrate gels were run at a constant current of 20 mA per gel for 60—90 minutes then washed in 2.5% Triton X-100 for 20 minutes at room temperature. Gels were then washed twice in distilled water for 20 minutes each.

2.2.5.2 Treatment of substrate SDS-PAGE gels

After being washed, protease activity was observed by incubating substrate gels in phosphate buffered saline (PBS) with 5 mM of cysteine for 48 hours at 37˚C and refreshing the buffer every 24 hours. Other substrate gels were cut into individual strips, each strip was incubated with PBS/5 mM cysteine in the presence or absence of the protease inhibitors shown in Table 2.1, individually or in combination. Substrate gels containing hyaluronic acid were incubated in 0.05 M sodium acetate buffer (pH 6) overnight at 37˚C.

Table 2.1   Protease inhibitors used for substrate gel electrophoresis

Protease inhibitors	Concentrations used
E64 (cysteine proteases)	1 μM, 100 μM
Pepstatin A (aspartyl proteases)	1 μM, 100 μM
1, 10- Phenanthroline (metalloproteases)	1 mM, 100 mM
Phenyl methane sulphonyl fluoride (PMSF, serine proteases)	1 mM, 100 mM

2.2.5.3   Protein visualisation

Larval protease activity was visualised by fixing substrate gels for 30 minutes in destain solution before being stained with 1% Coomassie Brilliant Blue R250 overnight while hyaluronidase activity was stained with 0.1% Stain-All, dissolved in 50% formamide. Activity was detected by destaining the gels for 5—6 hours and was observed as clear bands against a blue background.

2.2.6   Determination of *Necator americanus* larval protease activity using enzyme assays

2.2.6.1   Preparation of Fluorescein Isothiocyanate (FITC) labelled casein

Fluorescein isothiocyanate labelled casein was prepared by dissolving 1 g of casein and 40 mg of fluorescein isothiocyanate (FITC) in 100 mL of 50 mM sodium carbonate, 150 mM NaCl buffer, pH 9.6. The solution was stirred for 1 hour at room temperature before being extensively dialysed against distilled water for 48 hours at 4˚C. The protein concentration of FITC-labelled casein was then adjusted to 5 mg/mL, aliquoted and stored at -20˚C until needed.

2.2.6.2 Protease assays using FITC-labelled casein

The effect of pH on protease activity present in larval EF and ES products was studied as previously described by Brown *et al* (1999). Briefly, larval EF/ES products (1 µg, 50 µL) were mixed with 10 µL of fluorescein isothiocyanate-casein (FITC-casein, to a final concentration of 250 µg/mL) and 140 µL of buffer (pH 3—5.5, 0.1 M citric acid/sodium citrate buffer; pH 6—8, 0.1 M phosphate buffer; pH 8—10, 0.05 M 2-amino-2-methyl-1:3-propanediol-HCl buffer) containing 5 mM cysteine and incubated at 37˚C for 2 hours. The reaction was stopped by adding 120 µL of 5% trichloracetic acid (TCA) and the undigested protein was removed by centrifugation at 13000 x g for 10 minutes. In a black 96 well microtitre plate, 20 µL of the supernatant were added to 80 µL of 0.5 M Tris- Cl (pH 8.5) and the fluorescence was measured in triplicates using DYNEX Microtiter Plate MFX Fluorometer (excitation = 490 nm, emission detection = 525 nm).

Using the same protocol, larval EF/ES products (1 µg, 50 µL) were incubated with 10 µL of FITC-labelled casein (250 µg/mL) at 37˚C for up to 2 hours and the reactions were stopped one by one by adding 120 µL of 5% TCA at intervals of 30 minutes. 0.1 M phosphate buffer was used at pH 6, 6.5, 8 and 8.5.

To characterise the proteases present in larval secretions, EF/ES products (1 µg, 50 µL) were pre-incubated with 20 µL of protease inhibitors E64 (1 µM), 1, 10-phenanthroline (1 mM), pepstatin A (1 µM) and phenyl-methane sulfonyl fluoride (PMSF, 1 mM), individually or in a mixture for 30 minutes prior to the

addition of 10 μL of FITC-casein as described above. In this assay, only phosphate buffer (0.1 M, at pH 6.5 and 8) was used. A concentration-response assay was also carried using protease inhibitors at 1, 5, 10 and 100 times the concentration used above. Specific protease activity was obtained by subtracting values for a blank buffer control and presented as fluorescence units per hour per microgram of larval products (FU/h/μg).

2.2.6.3 Detection of aminopeptidase activity in *Necator americanus* larval EF/ES products

Aminopeptidase activity was studied by monitoring the release of 7-amino-4-methylcoumarin (AMC) from a range of synthetic peptide substrates including H-Arg-AMC, H-Leu-AMC, H-Ala-AMC and H-Glu-AMC. Peptide substrates were prepared in PBS containing 1 mM $CaCl_2$ and 1 mM $MgCl_2$ and used at a concentration of 5 μM. In a black 96 well plate, 180 μL of each substrate solution was placed per well, to which 20 μL of larval EF/ES products (10 μg/mL) were added. The samples were incubated at 37°C overnight and the release of AMC fluorescence was measured using DYNEX Microtiter Plate MFX Revelation Fluorometer (excitation = 360 nm, emission detection = 460 nm).

2.2.7 Inhibition of *Necator americanus* larval activity using IgG from post-infected individuals

2.2.7.1 Preparation of IgG using protein G sepharose

Plasmas were collected from control and individuals from Papua New Guinea (PNG), naturally infected with *Necator americanus* and specific IgG antibodies were prepared following a method by Pritchard *et al* (1990). Plasmas were

dialysed against PBS (pH 7.2) and passed down a protein G column. The column was extensively washed with PBS and the bound IgG antibodies were eluted with 0.1 M glycine buffer (pH 2.5) and collected in 1 M Tris buffer (pH 9.5). The concentration of antibody solutions was measured using DYNEX MRX Microplate Reader at 405 nm and IgG samples were stored at -20˚C until required.

2.2.7.2 Detection of activity of IgG against larval EF/ES products using Western blot

Larval EF/ES and adult ES products were concentrated and prepared as described in section 2.2.4.2. Twenty micrograms of each product (20 µL per lane) were then loaded on a 10% SDS-PAGE gel and the gel was run at a constant current of 20 mA for 60—90 minutes. Proteins separated by SDS-PAGE electrophoresis were transferred onto nitrocellulose membrane at a constant voltage of 26 V overnight, using a BioRad Mini Protean II Transfer Cell. Westerns blots were then blocked with 5% dried milk powder in Tris buffered saline (TBS) for 2 hours before being incubated overnight at 4˚C with primary antibody (20 µg/mL of either control sera or post-hookworm infection IgG antibodies diluted in blocking buffer). Blots were extensively washed with TBS containing 0.05% Tween 20, and then incubated for 2 hours with a secondary anti human IgG conjugated to peroxidase and diluted 1:1000 (v/v) in blocking buffer. After being washed with TBS/0.05% Tween 20, antibody binding was visualised by incubating blots with horseradish peroxidase substrate chlornapthol (5 mg of chlornapthol dissolved in 1: 5 (v/v) ethanol/TBS and 3 µL of hydrogen peroxide added before use). Subsequent washing of Western blots in distilled water was used to stop the reaction.

2.2.7.3   Detection of activity of IgG against larval EF/ES products using

Enzyme Linked ImmunoSorbent Assay (ELISA)

A 96 well Nunc MaxiSorb plate was coated overnight at 4°C with 50 µL of

larval EF/ES, adult ES and adult homogenate per well (5 µg/mL diluted in 0.05

M carbonate/bicarbonate buffer, pH 9.6). The plate was then gently washed in

TBS/0.05% Tween 20 and blocked for 1 hour with 200 µL of 5% dried milk

powder/ TBS per well. The plate was washed and incubated with 50 µL of

either Papua New Guinea pooled plasma (PNG, as a control) or post-infection

IgG, diluted in blocking buffer to a concentration of 20 µg/mL. The plate was

washed again and an anti human-peroxidase IgG antibody was diluted 1:1000

(v/v) in blocking buffer, added to individual wells (100 µL each) and incubated

for 2 hours at room temperature. The antibody binding was then visualised by

the addition of 100 µL of 3,3',5,5'-tetramethylbenzidine dihydrochloride per

well (TMB, prepared by dissolving 1 tablet in 10 mL of 0.1 M sodium acetate

(pH 6) and 2 µL of 30% hydrogen peroxide). After 30 minutes, the reaction

was stopped by adding 50 µL per well of 2.5 M sulphuric acid and the

absorbance measured using DYNEX MRX Microplate Reader at 450 nm.

2.2.7.4   Inhibition of larval protease activity with post-infection anti worm

IgG using FITC-labelled casein assay

Larval EF/ES products (1 µg, 50 µL) were pre-incubated overnight at 37°C

with either control or post-infection anti worm IgG antibodies (at a final

concentration of 0.5—50 µg/mL) as described in section 2.2.6.2. Phosphate

buffer (0.1 M) was used at pH 6.5 and 8 only. FITC-labelled casein (10 µL,

final concentration of 250 µg/mL) was then added and the mixture incubated

for 2 hours at 37°C. The reaction was then stopped as described before and the

absorbance measured using DYNEX Microtiter Plate MFX Fluorometer (excitation = 490 nm, emission detection = 525 nm) and presented as fluorescence units per hour per microgram of larval products (FU/h/µg).

2.2.8   Statistical analysis

Data were analyzed with GraphPad Prism version 5.01. Values are presented as means ± SEM and statistical significance was determined by two-way ANOVA tests followed by Bonferroni post-tests. Statistical significance was defined as $P < 0.05$.

2.3 Results

2.3.1 Characterisation of *Necator americanus* larval products using gel electrophoresis

Necator americanus larval exsheathing fluid (EF) and excretory/secretory products (ES) were initially analysed using protein electrophoresis (Figure 2.1). Separated proteins were never observed with Coomassie Blue while protein bands were detected with silver staining. Proteins were differentiated based on sample preparation (i.e. precipitation) showing difference in number of bands, bandwidth and band intensity. EF products showed a total of eight bands with molecular masses ranging from 20—135 kDa and twelve bands with molecular weight from 13—170 kDa using acetone and trichloroacetic acid (TCA) precipitation, respectively. Similarly, ES products showed a difference in protein profile, having eight to nine bands with molecular weight from 17—135 kDa or 11—60 kDa for acetone and TCA precipitation, respectively. Divergence among larval products was also observed unrelated to differences associated with sample preparation. In that prospect, EF proteins were mainly observed at molecular weights of 55—170 kDa whereas ES protein bands were concentrated at molecular weights from 11—60 kDa. Although these profiles established a difference in proteins present in larval EF and ES products, further investigation and characterisation of larval products was required.
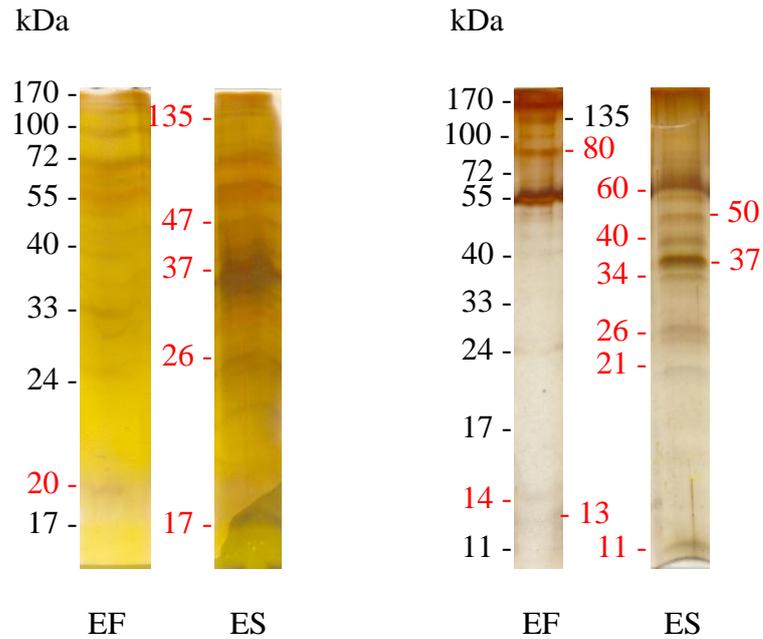
a- Precipitation with acetone   b- Precipitation with 5% TCA

Figure 2.1 Larval products separated on SDS-PAGE gels and prepared by (a) acetone precipitation; (b) 5% TCA precipitations. Gels were silver stained as described in the Methods. Molecular weights represent the protein ladder (black) and extra protein bands (red).

Larval products were further characterised using two-dimensional electrophoresis (Figure 2.2). Proteins, which were loaded at approximately 100 micrograms per gel, showed partial separation for ES products at acidic pH (pointed by arrow heads). In contrast, no protein spots were observed with EF products. Similar results were obtained when repeated. In addition, protein fingerprinting was less informative since no proteins were detected. These findings suggested that higher total protein contents might be required for better protein profiling and accurate characterisation of larval products.
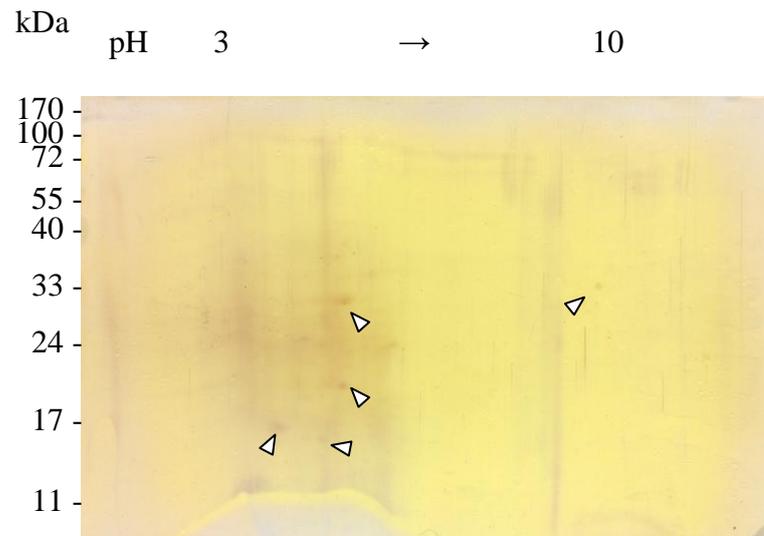
a- ES products
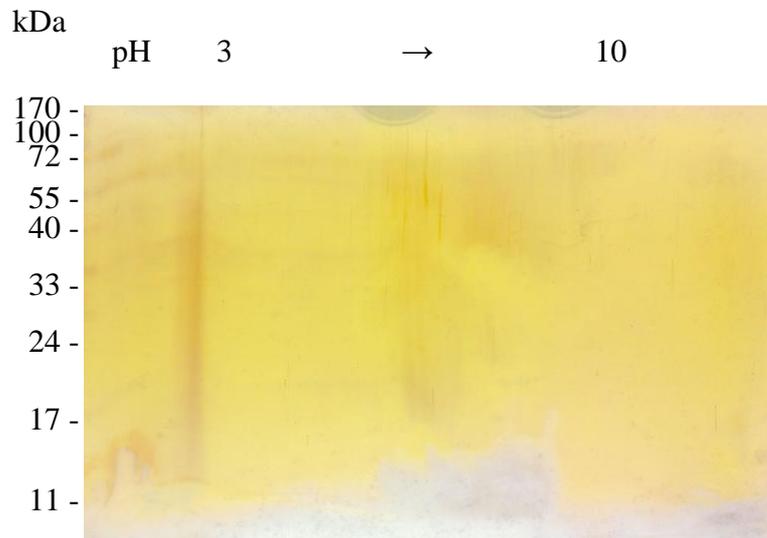
b- EF products

Figure 2.2 **Larval products separated on two dimensional SDS-PAGE gels, (a) ES products; (b) EF larval products. The optimised TCA precitipation was used to concentrate larval samples. Following separation, gels were silver stained and labelled with arrow heads pointing at protein spots.**

2.3.2 Characterisation of protease activity in *Necator americanus* larval products using substrate gels

Protease activity present in *Necator americanus* larval products was examined using substrate gel electrophoresis. Gelatin and haemoglobin were used as substrates as described in the Methods. Protease activity is detected as clear bands against a dark background, as evidence for substrates being degraded by larval products (Figure 2.3). Since larval products were equally loaded on gel wells, differences in number, bandwidth and intensity of the clear band was proportional to the protease activity per sample. Gelatin was degraded by EF and ES products, resulting in a single clear band at 25 kDa while two clear bands (20 and 27 kDa) were observed on haemoglobin gels. Degradation of substrates indicated the presence of active proteases in larval products at molecular weights of 20, 25 and 27 kDa. Based on the intensity of the clear bands, ES products demonstrated a greater ability to degrade both gelatin and haemoglobin (only at 27 kDa) than EF products. Results suggested that compared to EF products, ES proteases were either stronger or present in larger quantities. Both EF and ES products demonstrated no ability to degrade hyaluronic acid as shown in Figure 2.3 (c).

a- Gelatin

b- Haemoglobin
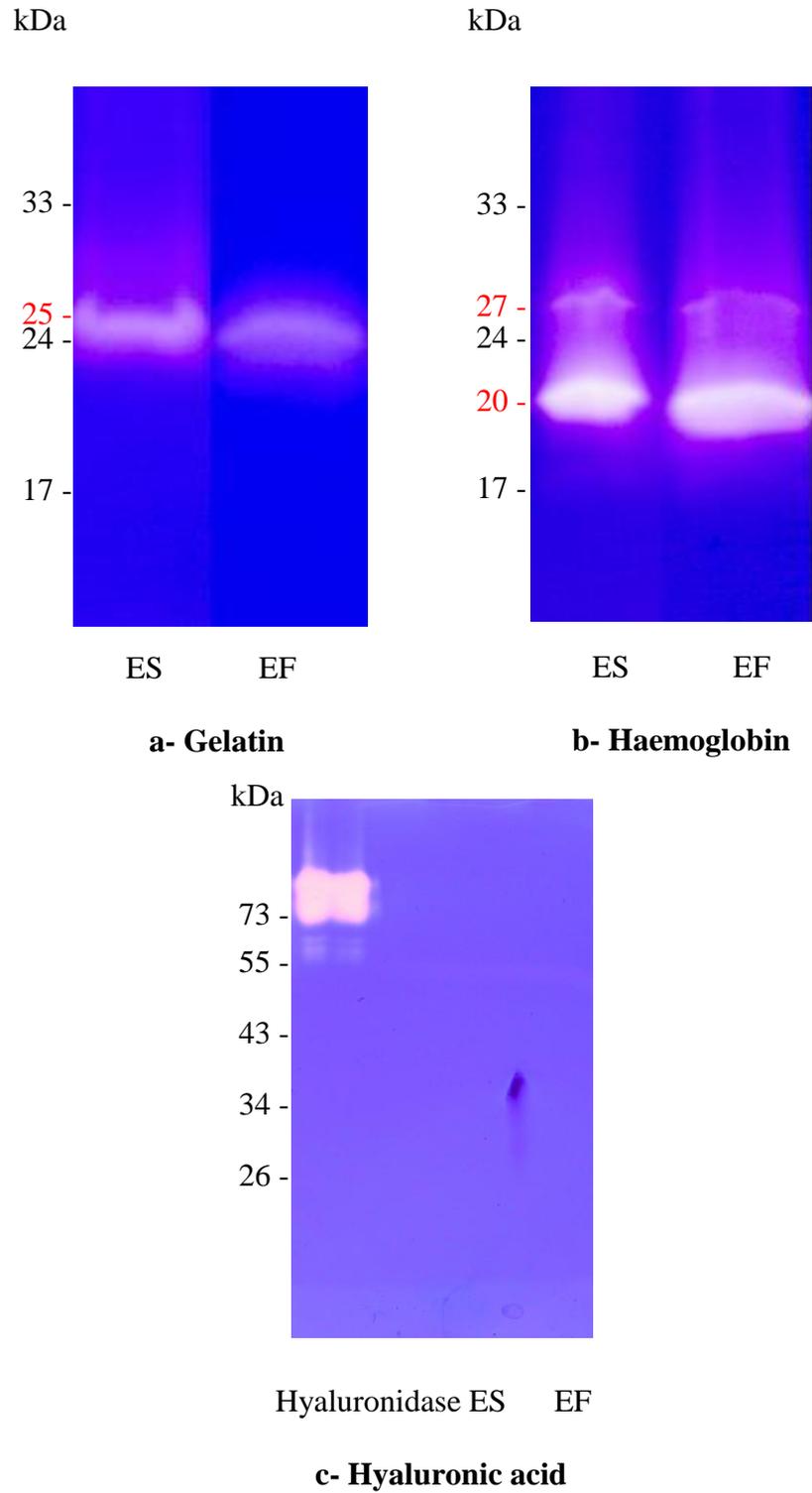
c- Hyaluronic acid

Figure 2.3   Substrate gels showing degradation of (a) gelatin; (b) haemoglobin; (c) hyaluronic acid by *Necator americanus* larval products. Equal quantities of larval products were loaded per lane and protease activity was evident, appearing as clear bands against a dark background.

Protease activity was further characterised using specific protease inhibitors (Figure 2.4). Degradation of gelatin was inhibited by 1, 10-phenanthroline (partially when used at 10 mM and completely when used at 100 mM), indicating that metalloproteases were primarily present in EF products. Protease activity was also inhibited by PMSF, only when used at a high dose (100 mM), indicating the presence of a serine protease in larval EF products at low quantities. The use of other protease inhibitors was slightly effective when used at high doses (only E64 at 100 μM) as little to no inhibition of protease activity was observed. Similar results were reported using ES products as shown in Figure 2.4 (b). These results suggested that substrate gel electrophoresis was inconclusive and therefore other techniques should be used to further characterise protease activity present in larval products.
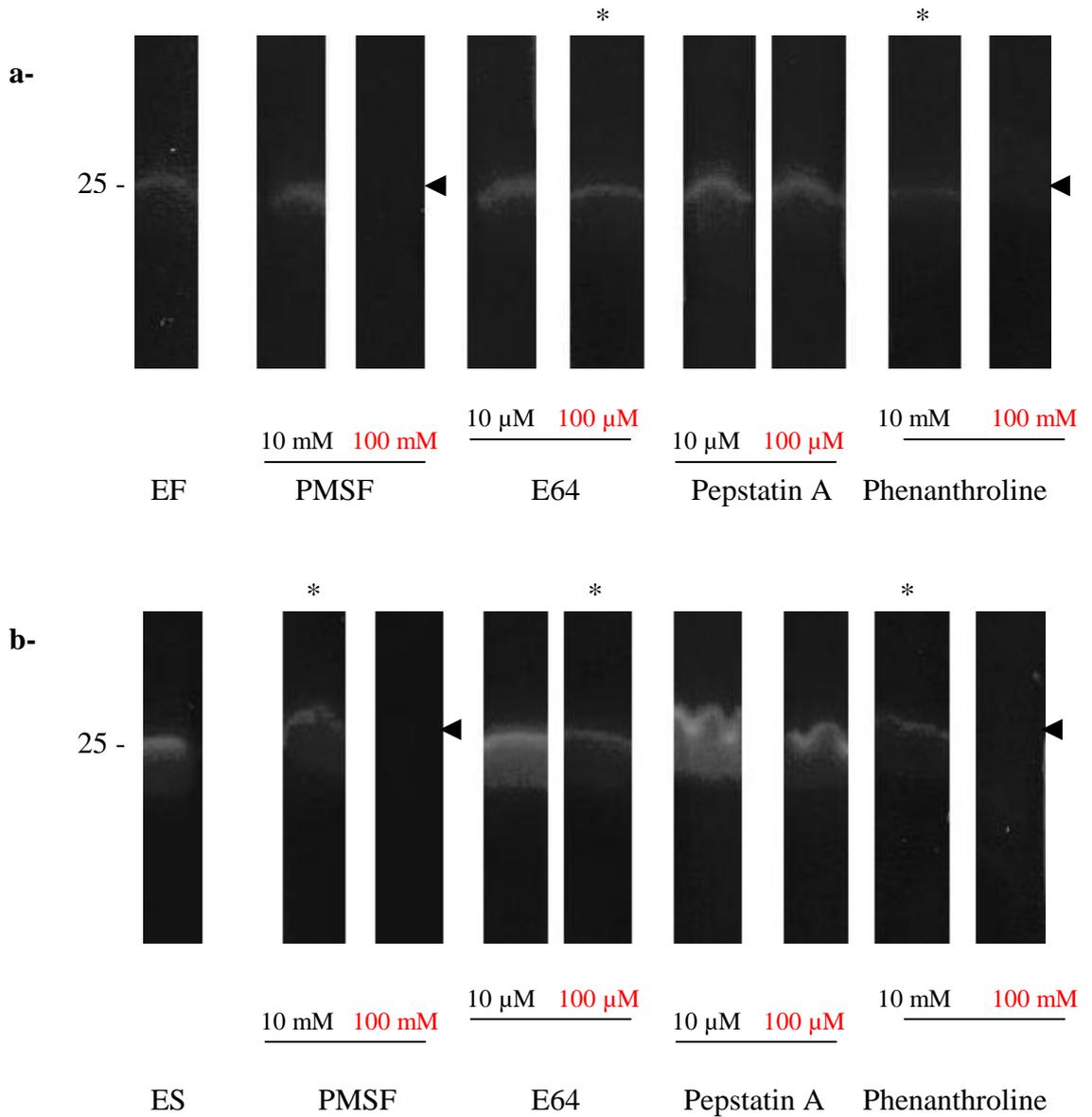
Figure 2.4   Effect of protease inhibitors on degradation of gelatin by larval: (a) EF products and (b) ES products. Inhibition of protease activity was detected when clear bands disappeared (arrowheads) or appeared smaller in size (*).

2.3.3   Characterisation of protease activity in *Necator americanus* larval products using enzyme assays

2.3.3.1   <u>Effect of pH on larval protease activity</u>

The proteolysis of FITC-labelled casein as a function of pH is shown in Figure 2.5. Optimal pH for protease activity ranged between 6 and 8.5 with two peaks appearing at pH 6.5 and 8. At optimal pH, protease activity was found to be proportional to time of incubation and the highest specific activity was obtained after running the reaction for 2 hours (Figure 2.6). Overall, protease activity was significantly higher in ES products (Figure 2.7). These results are in line with both protein separation (Figure 2.1, b) and substrate gel electrophoresis (Figure 2.3, a and b) emphasising that proteases present in larval ES secretions are either more active or present at higher quantities compared to exsheathing products (EF).
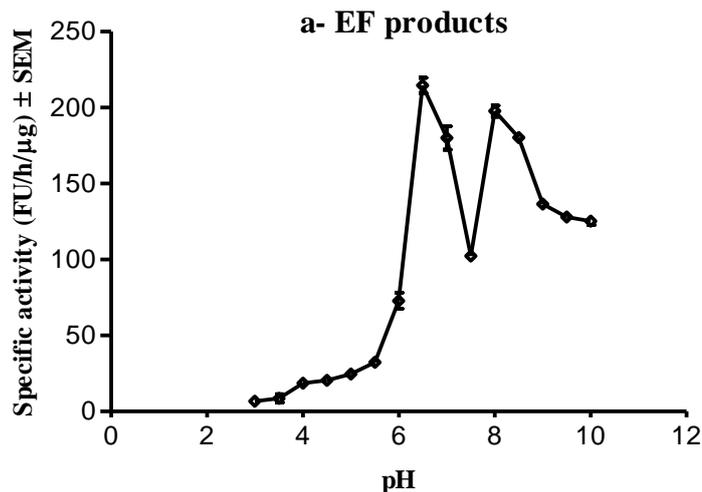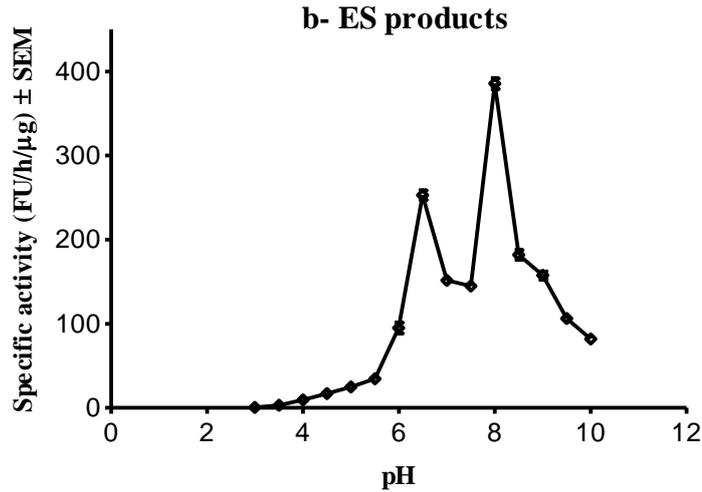
b- ES products

Figure 2.5 **Effect of pH on protease activities present in *Necator americanus* larval (a) EF products; (b) ES products. FITC-casein was used as a substrate and protease activity was presented as the mean ± SEM of fluorescence units/microgram of products/hour. SEM bars are not visible in (b) because of the reproducibility of the assay.**

a- EF products
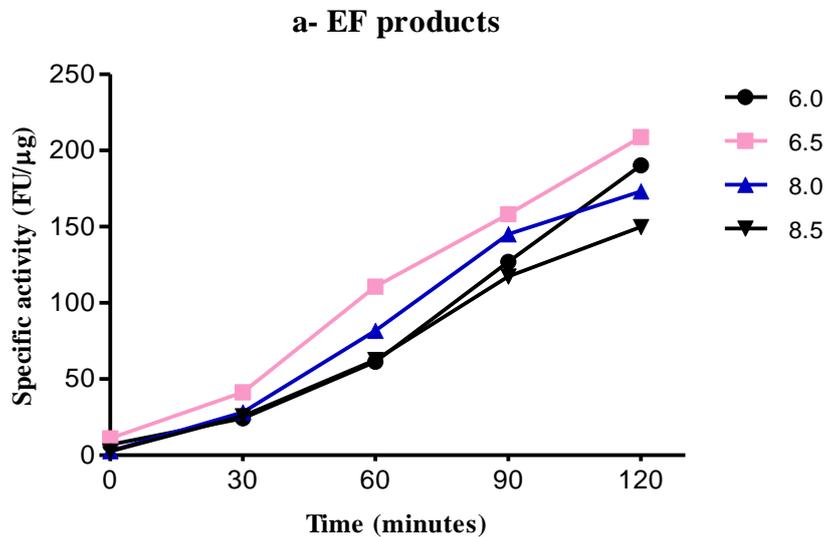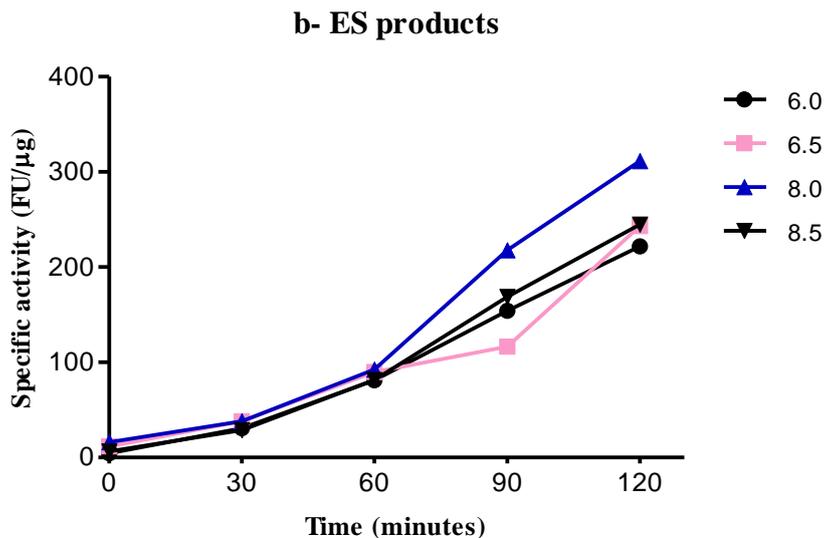
b- ES products

Figure 2.6   Time-related changes of protease activity in (a) EF products; (b) ES products. Specific activity was determined at optimal pH over a period of 2 hours.
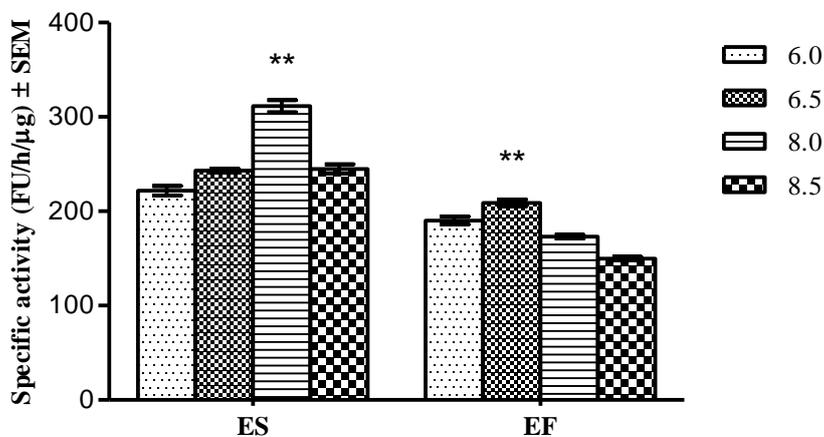
Figure 2.7   Protease activities in larval products at optimal pH. Products were incubated with FITC-casein substrate. Specific activity was measured after 2 hours and presented as the mean ± SEM of fluorescence units/microgram of products/hour. ** = $P < 0.001$, compared to protease activities of the same product at different pH.

2.3.3.2   <u>Characterisation of protease activity using FITC-labelled casein</u>

Protease inhibitors were used to further characterise the protease activities in *Necator americanus* larval EF and ES products. Inhibitors were quality controlled by assaying them against their class specific proteases (Table 2.2). Inhibitors were reported to cause a reduction of at least 90% in protease activities, except for 1, 10-phenanthroline (~ 59%). Percentage of inhibition indicated that protease inhibitors might be useful for further identification and classification of larval proteases.

Table 2.2   Inhibition of specific protease activities. Inhibitors were used at their optimal pH and inhibition was determined as the percentage of reduction in protease activity to the total specific activity.

Protease	Protease inhibitor	% Inhibition
Trypsin (serine proteases, 5 µg)	PMSF used at 1 mM, pH 8	88%
Papain (cysteine proteases, 5 µg)	E64 used at 1 µM, pH 6	95.5%
Leucine aminopeptidase (metalloprotease, 5 µg)	1, 10-Phenanthroline used at 1 mM, pH 7.2	59%
Pepsin (aspartyl proteases, 5 µg)	Pepstatin A used at 1 µM, pH 5	91.5%

The contribution of different protease classes to larval EF and ES proteolytic activities was examined at their optimal pH (6.5 and 8). Overall, protease activity in both EF and ES products was decreased by individual inhibitors especially PMSF (at pH 6.5 and 8). Reduction was most significant when all inhibitors (PMSF, E64, pepstatin A, and 1, 10-phenanthroline) were combined together, as shown in Figure 2.8. Table 2.3 summaries the inhibition of protease activities (Figure 2.8) as the percentage of reduction in proteolysis of FITC-casein to the specific activity observed with larval products. Protease activity in ES products was noticeably inhibited by PMSF at pH 6.5 and 8 while EF proteases were significantly inhibited at pH 8. These results indicate the presence of serine proteases in both EF and ES products, which are primarily active not only at pH 8 (optimal pH for PMSF), but also at pH 6.5. Inhibition of cysteine proteases by E64 was highest at pH 6.5 suggesting that cysteine proteases are markedly active in larval products at this pH. Unlike EF products, cysteine proteases were considerably inhibited by E64 in ES products at pH 8, signifying that cysteine proteolytic activity in ES products was not affected by pH. These findings indicated that cysteine proteases were distinctly present in larval ES products and to a lesser extent in EF products.

At pH 6.5 and 8, a modest inhibition of protease activity by pepstatin A (optimal pH for pepstatin A is 5) was indicative of the partial involvement of aspartyl proteases in both EF and ES products. Inhibition by 1, 10-phenanthroline was higher with ES products and highest at pH 6.5 indicating that although metalloproteases were present in both larval products, proteases were exceptionally more active in ES products at pH 6.5. In addition, the use of all protease inhibitors in combination which resulted in the greatest inhibition

a- EF products
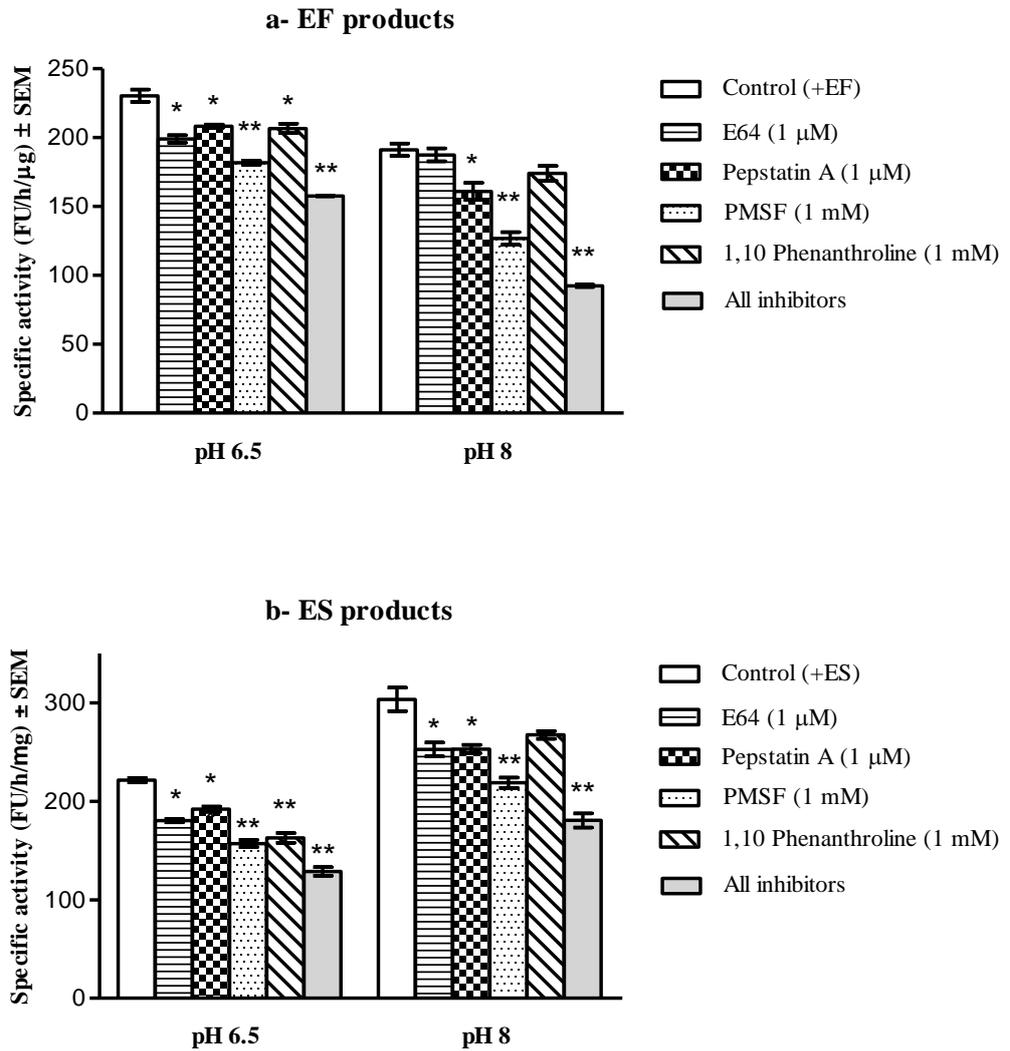
b- ES products

Figure 2.8   Characterisation of protease activities present in *Necator americanus* larval products at their optimal pH; a) EF and b) ES products. The specific activity was obtained by subtracting values for a blank buffer control and presented as the mean ± SEM of fluorescence units/ microgram of products/ hour. ** = P < 0.001, * = P < 0.01 by comparing each sample to their control (+ EF (a) or ES (b) at the same pH).

of proteolytic activity, confirming the presence of the four main protease classes; serine, cysteine, aspartyl and metalloproteases in larval EF and ES products.

Table 2.3   Summary of inhibition of protease activities present in *Necator americanus* larval products. Inhibition was determined as the percentage of reduction in protease activity to the total specific activity in larval products at their optimal pH.

Protease Inhibitors	EF products		ES products	
	pH 6.5	pH 8	pH 6.5	pH 8
E64 (1 µM)	- 13.6	- 1.97	- 18.58	- 16.69
Pepstatin A (1 µM)	- 9.62	- 15.88	- 13.31	- 16.56
PMSF (1 mM)	- 21.11	- 33.72	- 28.07	- 27.83
1, 10-phenanthroline (1 mM)	- 10.31	- 8.96	- 26.5	- 11.82
All inhibitors	- 31.58	- 51.66	- 41.87	- 40.49

A dose-response inhibition assay was carried out using protease inhibitors at 1—100 times their recommended doses (Figure 2.9). Evidently, no complete inhibition of protease activity was observed with individual inhibitors. Responses to the 100 x doses were statistically similar to those of 1, 10 and 50 x recommended doses as higher dosage produced slightly further inhibition of protease activities.

a- EF products, pH 6.5

b- ES products, pH 6.5

c- EF products, pH 8
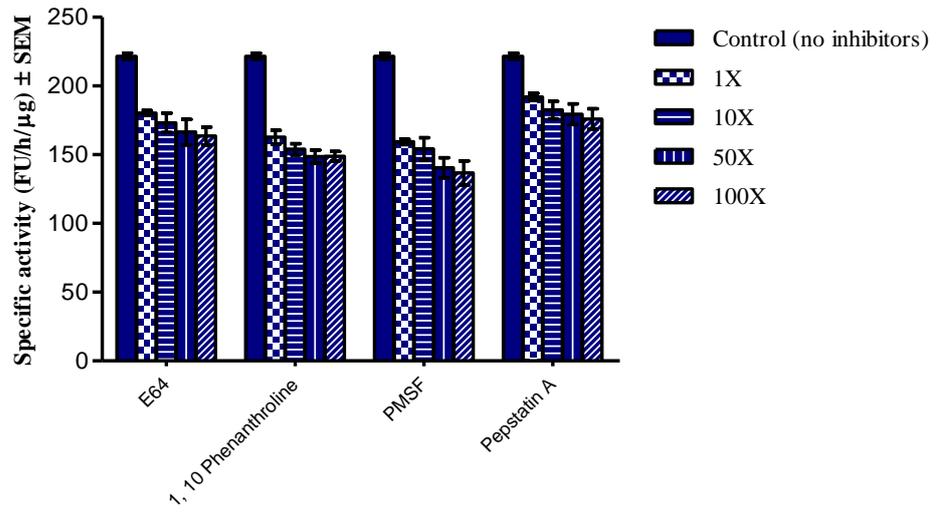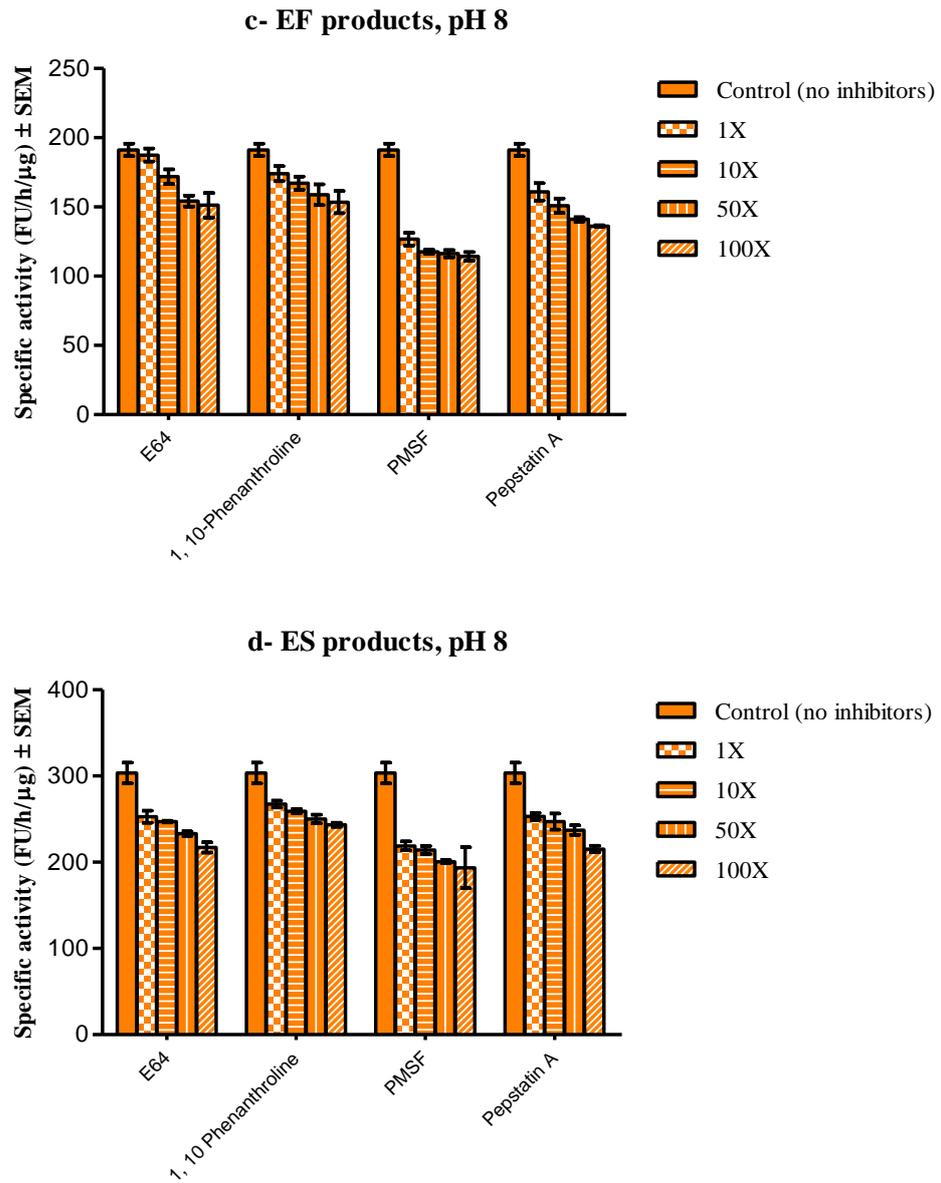
d- ES products, pH 8

Figure 2.9 **Dose-response inhibition of protease activities in *Necator americanus* larval products, (a) EF products at pH 6.5; (b) ES products at pH 6.5; (c) EF products at pH 8; (d) ES products at pH 8. Protease inhibitors were used at 1—100 times the recommended dose and protease activities were determined using FITC-casein as a substrate. Results are presented as the mean ± SEM of fluorescence units/microgram of products/hour.**

Table 2.4 Summary of the dose-response inhibition of protease activities of *Necator americanus* larval products. Inhibition was presented as the percentage of reduction in protease activity (FITC-casein) to the total control activity in larval products at the highest and lowest dosage of inhibitors.

Protease Inhibitors	EF products				ES products			
	pH 6.5		pH 8		pH 6.5		pH 8	
	1 X	100X	1X	100 X	1 X	100 X	1 X	100 X
E64	13.6	**22.4**	1.9	**20.9**	18.5	**26.2**	16.6	**28.4**
Pepstatin A	9.6	**23.1**	15.8	**19.7**	13.3	**32.7**	16.5	**18.4**
PMSF	21.1	**28.4**	33.7	**40.2**	28.0	**38.3**	27.8	**36.2**
1, 10-phenanthroline	10.3	**20.8**	8.9	**28.8**	26.5	**20.6**	11.8	**29.1**

Table 2.4 summarises the dose-response relationship of specific protease activities and the use of protease inhibitors at 1 x and 100 x their recommended dosage. Although further inhibition of protease activities was detected at 100 x doses (maximum of approximately 40%), complete inhibition of proteolytic activity in larval products was never observed. Data suggested that other factors possibly including pH optima for each protease inhibitor and emergence of resistance might account for the low inhibition levels.

Thus far, *Necator americanus* larval EF and ES products:

- Exhibited a characteristic difference in their protein and proteolytic profiles in a quantitative and a qualitative manner.

- Demonstrated pH dependent proteolytic activities against FITC-casein substrate with the optimal pH ranging between 6 and 8.5.

- Demonstrated the presence of serine, cysteine, aspartyl and metalloproteases, and complete inhibition of their activities was not observed even in the presence of all protease inhibitors in a cocktail.

- Using gel electrophoresis and enzyme assays, ES proteolytic activity was shown to involve either more/ or more active proteases than EF activity.

2.3.3.3   Further characterisation of enzymatic activity in *Necator americanus*
          larval products using synthetic substrates

The enzymatic activity against a number of aminopeptidase substrates was
determined after 24 hours of incubation with larval products (Figure 2.10).
Results demonstrated a significant increase of leucine and arginine
aminopeptidase activities in EF products ($P < 0.001$), assayed with H-Leu-
AMC and H-Arg-AMC. Alanine aminopeptidase activity was also
considerably increased in EF products while glutamate aminopeptidases were
not significantly active. Unlike EF products, aminopeptidase activities were
markedly reduced after 24 hours incubation with ES products with the
exception of leucine aminopeptidase activity which was significantly
increased.

a- EF products

b- ES products

AMC substrates
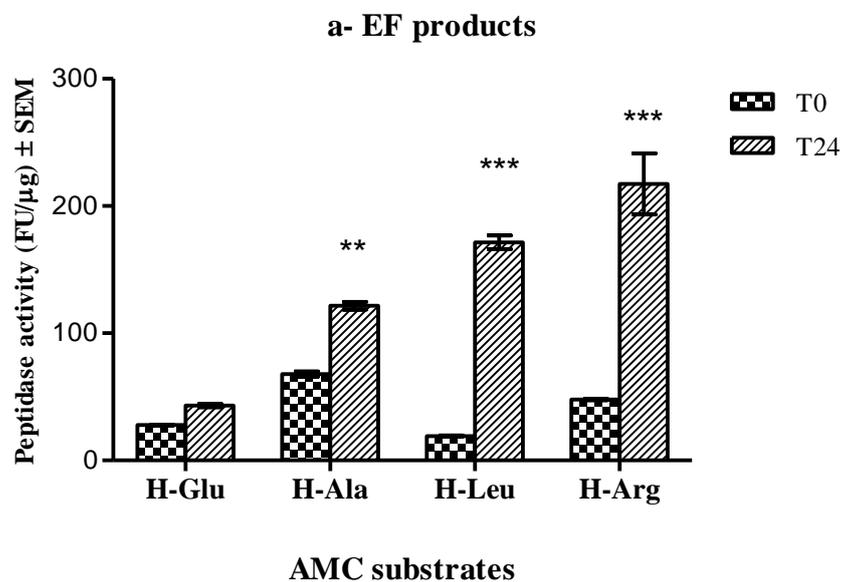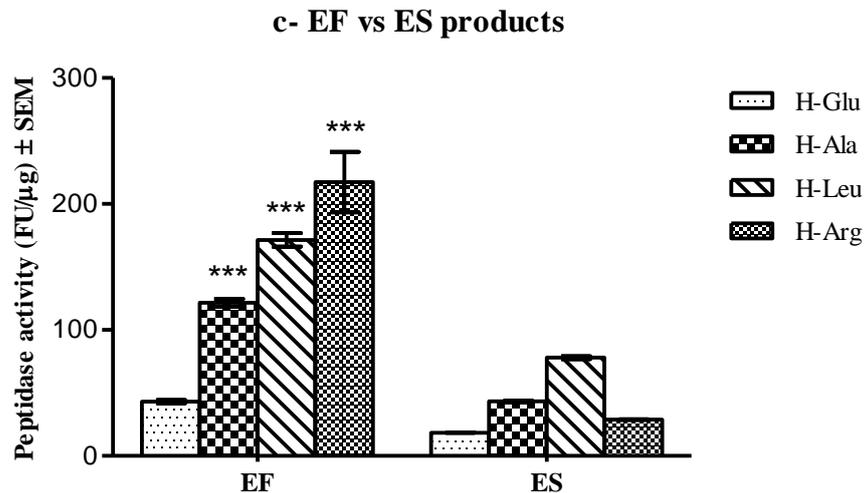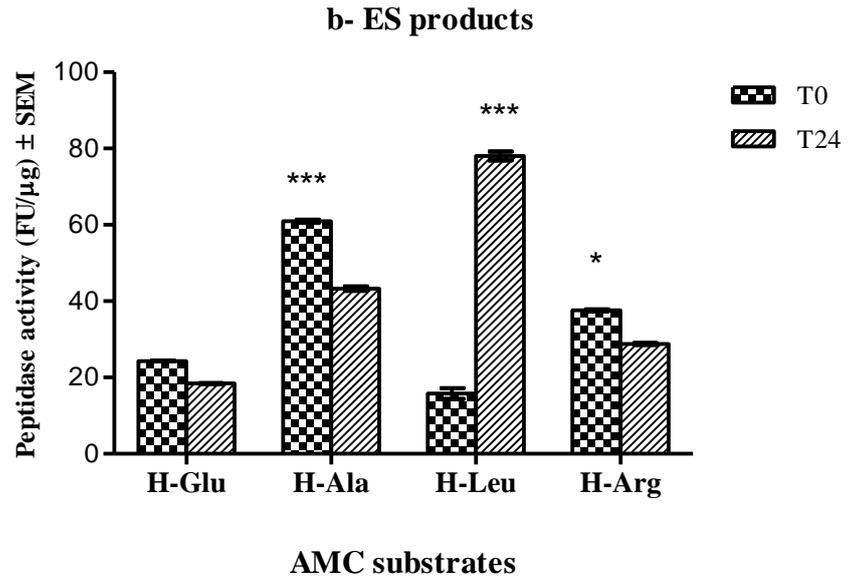
c- EF vs ES products

Figure 2.10 **Aminopeptidase activity in *Necator americanus* larval, (a) EF products; (b) ES products; (c) EF vs ES products. Activity is presented as the mean ± SEM of fluorescence units/ microgram of larval product. Significance was defined as * = P < 0.05, ** = P < 0.01 and *** = P < 0.001.**

Aminopeptidase substrates were hydrolysed to a higher degree (P < 0.001) with EF than ES products indicating the predominant presence of these aminopeptidases in EF products.

2.3.4 Inhibition of *Necator americanus* larval activity using IgG from individuals post-infection

2.3.4.1   <u>Characterisation of post-infection anti worm IgG antibodies</u>

Western blots were used to detect larval antigens using post-infection anti worm IgG antibodies, developed against adult ES antigens. A band of 37 kDa was observed with adult ES and larval ES products while EF antigens were not detected (Figure 2.11). Sera from uninfected individuals was used as a control and was found unable to detect antigens in larval EF and ES as well as adult ES (Figure not included here). In an ELISA assay (Figure 2.12), only adult ES and homogenate antigens were statistically recognised by post-infection IgG antibodies. Larval ES antigens were detected to a smaller degree while EF antigens were not recognised, supporting data from the Western blots. Papua
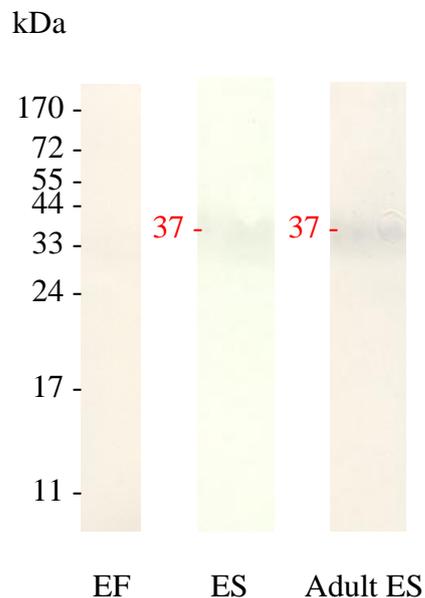
Figure 2.11   Detection of *Necator americanus* larval antigens using post-infection antiworm IgG antibodies, developed against adult ES antigens. Sera was collected from naturally infected individuals and prepared as described in the Methods.
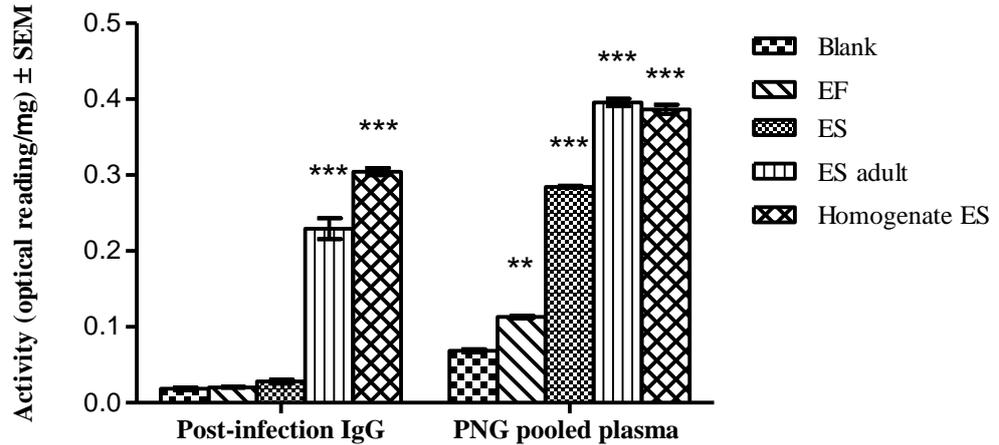
Figure 2.12 **Interaction of post-infection anti worm IgG antibodies with *Necator americanus* products. Significance is determined against blank and between samples and recognised as ** = P < 0.01 and *** = P < 0.001.**

New Guinea (PNG) pooled plasmas were used as a positive control to confirm the presence of antigens in larval, adult and homogenate products. Detection of antigens was significantly higher with PNG pooled IgG antibodies especially in larval ES, adult ES and homogenate products.

2.3.4.2 <u>Effect of post-infection anti worm IgG antibodies on *Necator americanus* larval activity</u>

The effect of treatment of *Necator americanus* larval products with antibodies is described in Table 2.5. Control sera produced a decrease in proteolysis of FITC-casein, not exceeding 5% at all doses. Post-infection IgG antibodies caused a considerable increase in inhibition of both EF and ES activity, mirrored by a significant decrease in proteolysis of FITC-casein at doses of antibodies from 0.1—10 μg/sample.

Although inhibition levels were markedly higher at pH 8, they did not exceed 50% of the total activity in larval products, raising the possibility that anti worm IgG antibodies were pH sensitive and possibly acting as a competitive substrate to larval enzymes.

Table 2.5   Effect on *Necator americanus* larval activity following treatment with post-infection IgG antibodies, presented as the percentage of reduction in proteolysis of FITC-casein to the total control activity in larval products. Antibodies were used at different concentrations and at optimal pH. AW: anti worm IgG, CT: control sera.

IgG Concentration (µg/sample)	EF products				ES products			
	pH 6.5		pH 8		pH 6.5		pH 8	
	AW	CT	AW	CT	AW	CT	AW	CT
0.1	-19.5	**-3.6**	-38.8	**-0.6**	-8.3	**-0.8**	-19.6	**-0.3**
0.5	-23.9	**-4.5**	-41.5	**-0.8**	-15.3	**-0.9**	-28.4	**-0.5**
1	-27.3	**-2.9**	-45.1	**-2.3**	-18.5	**-1.1**	-28.0	**-0.7**
5	-28.8	**-3.4**	-41.9	**-1.9**	-19.5	**-0.4**	-32.5	**-1.4**
10	-30.4	**-3.6**	-49.0	**-4.1**	-25.9	**-1.5**	-35.3	**-0.6**

2.4 Discussion

The electrophoretic separation of *Necator americanus* larval products demonstrated the presence of most proteins within a molecular weight range of 11—60 kDa in the excretory/secretory products (ES) while the exsheathing fluid (EF) contained essentially proteins of 55—170 kDa. Based on the proteolytic activity observed at ~ 21 kDa (Figures 2.1, b and 2.3, b), the band could possibly be assigned to the aspartic APR-1 as previously reported by Williamson *et al* (2002) while the 40 kDa protein (Figure 2.1, b) is likely the cysteine ASP-2 proteases following previous work by Goud *et al* (2005). In addition, a zinc-dependent metalloprotease is probably resolving at 50 kDa as shown in previous work by Hawdon *et al* (1995). Moreover, the occurrence of a 55—56 kDa protein is likely to reflect the presence of calreticulin in both EF and ES products (to a lesser degree), which was previously reported by Pritchard *et al* (1999) and Winter *et al* (2005). Further investigation of larval products using two-dimensional gel electrophoresis demonstrated a partial separation of ES products with few protein spots resolving at 11—27 kDa (acidic pH) and a single protein spot at 30 kDa (basic pH). Peptide fingerprinting was also less informative as a result of the low detection levels of larval products, suggesting that larger quantities of total larval proteins should be used for better protein profiling.

The involvement of proteases in larval EF and ES products was studied using gelatin and haemoglobin on substrate gels. The degradation of gelatin was caused by gelatinolytic proteases with an apparent molecular weight of 25 kDa while haemoglobin was hydrolysed by proteases of 20 and 27 kDa. Variation

in the number, size and intensity of clear bands suggested the involvement of a number of proteases in the degradation of substrates, which was more evident with ES products. These findings supported the involvement of a multi-protease cascade in the degradation of haemoglobin reported by Williamson *et al* (2002 and 2003) as well as the gelatinolytic activity of larval products, previously described by Kumar and Pritchard (1992a). Unlike the infective *Ancylostoma* larval extracts, hyaluronidase activity was not present in both EF and ES products indicating that migration of *Necator americanus* larvae through the skin is not mediated by the activity of this class of enzymes as described previously by Hotez *et al* (1992). Gelatinolytic activity in EF products was considerably inhibited by 1, 10-phenanthroline while partial inhibition was only observed with PMSF and E64 at doses outside the recommended range, indicating that this gelatinolytic enzyme is a mixture of metallo-, serine and cysteine proteases. Since similar results were observed with ES products (also using haemoglobin), classification of larval proteases using substrate gels was limited therefore requiring a better protein profiling method.

Since generating EF and ES products in large scale was both complicated and time consuming, enzyme assays using FITC-labelled casein as a substrate were used as a better technique for the characterisation of *Necator americanus* larval products. Results demonstrated a pH related protease activity which was optimal between pH 6 and 8.5 with sharp peaks at pH 6.5 and 8 for both the exsheathing fluid (EF) and the excretory/secretory products (ES). The effect of pH on protease activity was most evident after 2 hours of incubation with

FITC-casein and proteolysis was significantly high with EF products at pH 6.5 and higher with ES products at pH 8. Knowing the normal skin pH ranges between 4.5 and 6.5 (Yosipovitch *et al*, 1993), these results suggest that protease activity in the exsheathing fluid (EF) is likely to be involved in the penetration process at the skin surface whereas the excretory/secretory products (ES) are believed to help the larvae move deeper in the skin, finally arriving at the blood microcirculation.

Using protease inhibition assay, proteolytic activity in larval products was primarily inhibited by PMSF at pH 6.5 and 8. The predominant presence of serine proteases in both EF and ES products at optimal pH suggested a potential role of serine proteases during the exsheathment of *Necator americanus* larvae and the penetration of skin. The presence of cysteine proteases in larval products was reflected by the inhibition of proteolytic activity using E64 which was highest in ES products at pH 6.5. Findings indicated that cysteine proteases may be involved in the exsheathment of larvae as previously described by Kumar and Pritchard (1992a) and during the penetration process.

Activity of aspartyl and metalloproteases were also pH dependent and considerably different in EF and ES products. Although moderately present in larval products as mirrored by the partial inhibition of activity by 1, 10-phenanthroline, metalloproteases were noticeably present in ES products and exceptionally more active at pH 6.5 indicating they may be important for *Necator americanus* larvae to negotiate the different layers of the skin. The

presence of aspartyl proteases in larval products was modest at pH 6.5 and 8, unlike previous findings by Brown *et al* (1999) which described these proteases to be predominant in larval ES products. Previous studies illustrated the major role of this class of proteases as digestive enzymes to the blood-feeding behaviour of most nematodes including *Necator americanus* species (Brown *et al*, 1995; Williamson *et al*, 2002). However at early stages of larval invasion, aspartyl proteases are likely to be involved in the penetration process, ultimately allowing species to enter the host.

In addition, the use of all protease inhibitors in combination indicated that no protease is singly essential and that the penetration process may be mediated by the contribution of all proteolytic activities in the larval products. The involvement of more than one protease is likely due to the complexity of and the need to negotiate the different layers of skin (i.e. epidermis and dermis) to reach the vasculature. The use of protease inhibitors in combination was expected to cause complete inhibition of proteolytic activities in larval products. This is probably due to the fact that individual inhibitors work best at their optimal pH (Table 2.2), while this assay was carried out at pH 6.5 and 8 only. Since complete inhibition of protease activities was never observed (Brown *et al*, 1999), a dose-response inhibition assay was performed to determine if total inhibition of protease activity could be obtained. The use of higher doses of each inhibitor caused further increase in inhibition levels but proteolytic activities were never eliminated. Data emphasised that other factors possibly including the involvement of additional larval enzymes in FITC-

casein proteolysis and emergence of resistance against protease inhibitors might account for the considerably partial inhibition of proteolytic activities. *Necator americanus* larval products were also examined using a number of aminopeptidase substrates. Exsheathing fluids demonstrated a significant presence of leucine, arginine and to a lesser extent alanine aminopeptidase while enzymatic activity in ES products was moderate and contained leucine aminopeptidase only. The presence of leucine aminopeptidases in adult *Necator americanus* species was previously confirmed by McLaren *et al* (1974) and later in the exsheathing fluid of other nematodes by Rogers and Brooks (1977 and 1978). The large presence of aminopeptidases in EF products suggested an important role of these enzymes during and after exsheathment as proposed by Kumar and Pritchard (1992a) while the presence of leucine aminopeptidases in ES products indicated their potential involvement in the hydrolysis of both skin and serum molecules (Williamson *et al*, 2003).

Proteolytic enzymes have been suggested as a potential mechanism for *Necator americanus* infection, allowing larvae to gain access to the host's microcirculation and protect themselves against the host's immune system (Pritchard *et al*, 1990). Targeting these proteases using IgG antibodies, developed against adult ES products aimed at providing total inhibition of larval activities and early protection against *Necator americanus* infection. The interaction of post-infection anti worm IgG antibodies and larval products was initially determined using Western blots, in which only adult and larval ES products were detected. The use of ELISA assay demonstrated a major ability

of these antibodies to capture adult ES antigens while detection of larval ES antigens was minimal. Although the presence of antigens in larval EF products was confirmed using PNG pooled plasmas, EF antigens were not detected using post-infection IgG antibodies. Being specific to adult and to a lesser extent, larval excretory/secretory products suggested a partial similarity in antigens present in both adult and larval ES product. Previous knowledge showed larval ES products to contain certain antigens including calreticulin (Pritchard *et al*, 1999; Kasper *et al*, 2001), aspartic *Na*-APR-1 (Williamson *et al*, 2002; Pearson *et al*, 2009) and cysteine *Na*-ASP-2 (Hawdon *et al*, 1999) proteases, previously reported in adult ES product.

Although specificity of post-infection anti worm IgG antibodies was limited, treatment of *Necator americanus* larval products with these antibodies produced a considerable decrease in the proteolysis of FITC-casein, indicated by a parallel increase in inhibition of both EF and ES activity. Although inhibition levels were highest using 10 μg of antibodies per sample, reduction in proteolysis of casein never exceeded 50%. Inhibition is possibly due to anti worm IgG acting as a competitive substrate to larval enzymes rather than targeting specific, functional connections in their structures. Thus, the use of antibodies with better specificity to target active sites of larval EF and ES antigens would be more beneficial in inhibiting the infection at early stages and providing total protection against these species.

In conclusion, the characteristic presence of serine, cysteine, aspartyl and metalloproteases in larval EF and ES products and the potential role of protease

inhibitors and post-infection IgG antibodies in inhibiting larval proteolytic activities will be considered in studying the involvement of *Necator americanus* larval enzymes in penetrating the skin and the underlying vasculature.

3. Interaction between *Necator americanus* larval products and the human skin

3.1 Introduction

As obligate skin penetrators, *Necator americanus* species are believed to combine mechanical forces and enzymatic activities to migrate through the skin and gain access to the host's microcirculation (Matthews, 1982). Previous work by Hawdon *et al* (1993) indicates that *Necator americanus* L3 larvae remain in the skin for up to 48 hours post infection, during which time larvae are believed to alter their enzymatic repertoire to penetrate the skin and migrate to the blood circulation. Thus, understanding the molecular structure of the skin would be beneficial to investigate the mechanisms behind skin penetration by *Necator americanus* larvae.

Skin is the largest organ of the body, and serves as a protective barrier against environmental factors and foreign pathogens. Two major functional layers are characteristic of the human skin, each with a specific role to play. The epidermis is the outermost stratified, keratinizing epithelium anchored to a basement membrane which is in turn connected to the underlying layer, the dermis. The latter is a dense connective tissue layer containing the vascular network, the glands i.e. sweat and sebaceous and the hair follicles and originates from the dermal fibroblast. The main structural macromolecules of the dermis are collagens, elastin, fibronectin and laminin, primarily contributing to the structural complexity and multifunctional nature of the skin. Collagens I and III, being the major components of the dermis, co-exist as individually banded fibrils and play important roles in maintaining the stability of the skin. Collagens V, VI and VII have also been shown to occur in the skin in the form of fibrils with a role to play in anchoring principal fibres to the

surrounding matrix components and cells. Unlike other types of collagen, collagen IV is a non fibrillar molecule with a primary role in securing the basement membrane to the dermis and keratinocytes. Other matrix molecules including fibronectin and laminin are multifunctional proteins with a major role in cellular adhesion (Ruoslahti, 1988; Terranova *et al*, 1980) and cross linking of the extracellular matrix (Timpl and Martin, 1997) and basement membranes (Kucharz, 1992), respectively.

The aim of this section of the work is to explore the possible involvement of larval enzymes in skin penetration, by studying their proteolytic effects on both individual and skin-derived extracellular matrix macromolecules. This was performed using electrophoretic separation (SDS-PAGE) in combination with Western blotting.

3.2 Methods

3.2.1 Preparation of human skin extracts

Human skin samples were obtained from the forearm of healthy volunteers with no skin complications. Skin samples were collected as 4 mm-diameter punch biopsies (i.e. 0.125 cm^2, ~ 5 mg wet weight), extracted in 250 µL of 0.1 M phosphate buffer pH 6 and stored at -20˚C in aliquots of 20 µL until needed. Before use, skin aliquots were thawed and precipitated by adding 4 volumes of ice cold acetone and freezing for 1—2 hours at -20˚C. Precipitated protein was obtained by centrifuging at 13000 x g for 10 minutes and resuspended in 20 µL of 2 x reducing sample buffer per sample. Extracted proteins were reduced by boiling for 10 minutes at 100˚C and separated by SDS-PAGE electrophoresis.

3.2.2 Effect of larval EF/ES products on the degradation of human skin/extracellular matrix (ECM) molecules

3.2.2.1 Preparation of SDS-PAGE gels

SDS-PAGE gels were prepared as described in section 2.2.4.1. Protein separation of skin extracts and all extracellular matrix molecules (ECM) was carried on 10% SDS-PAGE gels except for laminin which was loaded on 6% SDS-PAGE gels.

3.2.2.2 Treatment of skin/ECM with *Necator americanus* larval products

Extracellular matrix molecules (ECM) were incubated with *Necator americanus* larval products following a modified method from Brown *et al* (1999). Ten micrograms of human collagen I, III, IV, V, fibronectin and laminin were incubated overnight at 37˚C in the presence or absence (controls)

of 2 µg of larval EF/ES products. Proteins were then precipitated with ice cold acetone as described in section 2.2.4.2 and the precipitate was resuspended in 20 µL of 2 x reducing sample buffer. Finally, proteins were reduced by boiling for 10 minutes at 100˚C and separated using SDS-PAGE electrophoresis. Skin extracts (20 µL, ~ 0.4 mg wet weight) were also treated as before in the presence or absence (controls) of 2 µg of larval EF/ES products individually and processed as for ECM molecules.

3.2.2.3 <u>Treatment of skin/ECM molecules with larval products in the presence of protease inhibitors</u>

Prior to incubation with larval EF/ES products, both skin extracts and ECM molecules were pre-incubated for 2 hours at 37˚C with a mixture of protease inhibitors containing E64 (1 µM), pepstatin A (1 µM), 1, 10-phenanthroline (1 mM) and PMSF (1 mM). Upon addition of 2 µg of larval EF/ES products, samples were treated and processed as described in section 3.2.2.2 and separated using SDS-PAGE electrophoresis.

3.2.2.4 <u>Treatment of skin/ECM molecules with larval products in the presence of anti worm IgG</u>

Skin extracts and ECM molecules were incubated overnight at 37˚C with 20 µg of post-infection anti worm IgG antibodies per sample. Larval EF/ES products were then added at 2 µg per sample and incubated overnight at 37˚C. Skin extracts and ECM molecules were then processed as described in section 3.2.2.2 and subjected to separation using SDS-PAGE electrophoresis.

3.2.3 Visualisation of *Necator americanus* larval activity

3.2.3.1 <u>Western Blot</u>

Proteins separated on SDS-PAGE gels were transferred onto nitrocellulose membrane at a constant voltage of 26 V overnight, using a BioRad Mini Protean II Transfer Cell. Westerns blots were then blocked with 5% dried milk powder in TBS for 2 hours before being incubated overnight at 4˚C with a primary antibody as shown in Table 3.1. All antibodies were used at a concentration of 0.8 µg/mL and diluted in blocking buffer. Blots were extensively washed with TBS containing 0.05% Tween 20, then incubated for 2 hours with a secondary antibody conjugated to either peroxidase or alkaline phosphatase and diluted in blocking buffer as shown in Table 3.1. Following two TBS/0.05% Tween 20 washes, each lasting for 20 minutes, antibody binding was visualised by incubating blots with horseradish peroxidase substrate chlornapthol (5 mg of chlornapthol dissolved in 5 mL of 1: 5 (v/v) ethanol/TBS and 3 µL of hydrogen peroxide added before use) or alkaline phophatase substrate (20 mL of 0.75 M Tris (pH 9.6) containing 82.5 µg/mL of 5-bromo-4-chloro-3indolyl phosphate and 154 µg/mL of nitroblue tetrazolium (NTZ)). The reaction was then stopped by washing blots in distilled water.

Table 3.1   Antibodies used to visualise proteins transferred to Western blots.

Protein	Primary antibody	Secondary antibody
Collagen I	Goat anti human collagen I	Anti goat- alkaline phosphatase (1:500)
Collagen III	Goat anti human collagen III	Anti goat- alkaline phosphatase (1:500)
Collagen IV	Goat anti human collagen IV	Anti goat- alkaline phosphatase (1:500)
Collagen V	Goat anti human collagen V	Anti goat- alkaline phosphatase (1:500)
Fibronectin	Rabbit anti human fibronectin	Anti rabbit- alkaline phosphatase (1:2500)
Laminin	Rabbit anti human laminin	Anti rabbit- alkaline phosphatase (1:2500)

3.2.3.2   Coomassie Blue staining

Gels were fixed for 30 minutes in destain solution before being stained with Coomassie Brilliant Blue R250 overnight, on a rocking platform. Proteins separated on SDS-PAGE gels were visualised by destaining the gels for 5—6 hours and were observed as blue bands against a clear background.

3.2.4   Assay of transglutaminase activity

Transglutaminase activity was detected following a method by Slaughter *et al* (1992). Dimethyl casein was dissolved in 0.1 M Tris-HCl (pH 8.5) at a concentration of 10 mg/mL. Following heating at 80˚C for 30 minutes, insoluble dimethyl casein was removed by centrifugation at 13000 x g for 20 minutes and the supernatant solution was used to coat the wells of a 96 well Nunc MaxiSorb plate overnight at 4˚C (50 µL per well). Excess dimethyl casein was removed by careful aspiration then the wells were blocked with 3% bovine serum albumin (BSA) in 0.1 M Tris-HCl (pH 8.5) for 30 minutes at room temperature. The wells were washed twice with 0.1 M Tris-HCl (pH 8.5). Transglutaminase activity was assayed in triplicate by adding 200 µL per well of a mixture containing 5 mM $CaCl_2$, 10 mM dithiothreitol (DTT), 0.5 mM 5'-Biotinoyl-amino hexanoylamino-pentylamine, EF/ES products between 5% and 50% (v/v) and 0.1 M Tris-HCl (pH 8.5). The plate was incubated for 45 minutes at 37˚C and the reaction stopped by washing the wells with 0.2 M EDTA then 0.1 M Tris-HCl, pH 8.5. Extravidin-peroxidase was diluted 1:1000 (v/v) in 3% BSA/0.1 M Tris-HCl (pH 8.5), added at 200 µL per well and incubated for 1 hour at room temperature. The wells were then washed once with 0.01% Triton X-100 and twice with 0.1 M sodium acetate, pH 6. Activity was then visualised by the addition of 100 µL of 3,3',5,5'-tetramethylbenidine dihydrochloride per well (TMB, prepared by dissolving 1 tablet in 10 mL of 0.1 M sodium acetate (pH 6) and 2 µL of 30% hydrogen peroxide). After 10 minutes, the reaction was stopped by adding 50 µL per well of 2.5 M sulphuric acid and the absorbance measured using DYNEX MRX Microplate Reader at 450 nm.

3.2.5   Statistical analysis

Data were analyzed with GraphPad Prism version 5.01. Values are presented as means ± SEM and statistical significance ($P < 0.05$) was determined by two-way ANOVA tests followed by Bonferroni post-tests.

3.3 Results

3.3.1 Degradation of extracellular matrix (ECM) molecules by *Necator americanus* larval products

The digestion of extracellular matrix macromolecules (ECM) was investigated as a function of *Necator americanus* proteolytic activity. No hydrolysis of collagen type I was observed although bands of small molecular weight (~ 84 and 55 kDa) disappeared on treatment with both EF (Lane 3) and ES (Lane 2) products (Figure 3.1, a and a'). The breakdown of collagen type III was not observed with Coomassie Blue staining (Figure 3.1, b) while Western blots showed an evident degradation with ES products as mirrored by the appearance of protein bands at 55 and 29 kDa (Figure 3.1, b'). Besides the 37 kDa band, protein products of smaller molecular weights were relatively weak following treatment with ES products and disappeared with EF products (Figure 3.1, b'). Unlike collagen type III, minimal degradation of collagen type IV was observed on Western blots, featuring the disappearance of proteins at 29 and 24 kDa with ES and EF products, respectively (Figure 3.1, c'). Major changes in the breakdown of collagen IV by EF products were observed with Coomassie Blue staining as demonstrated by the fading of the 135 kDa protein and the appearance of strong protein bands at 123 and 37 kDa. Bands at 78 and 52 kDa were missing with both EF and ES products whereas the 100 kDa protein band was only absent with ES products. Treatment with ES products also caused smaller proteins to disappear as shown in Figure 3.1 (c). No degradation of collagen type V was observed, as shown in Figure 3.1 (d). The formation of proteins at 208 kDa was noticeable with EF products, additional to fading of proteins at 145 and 14 kDa and the disappearance of bands at 17, 20 and 21

kDa (Figure 3.1, d). Proteins with molecular weights of 20—50 kDa also disappeared in the presence of EF and ES products while bands at 84 and 52 kDa were only observed with ES products (Figure 3.1, d'). Both larval EF and ES products also exhibited the presence of distinct protein bands at 100 and 62 kDa.
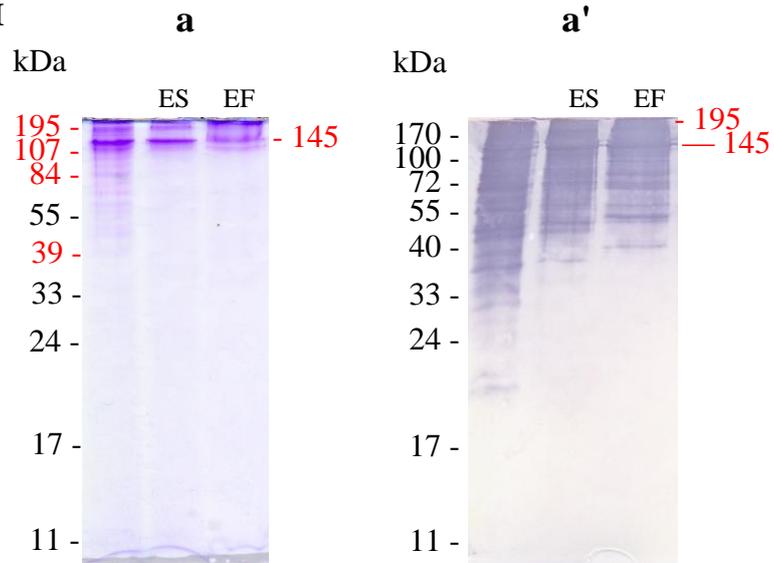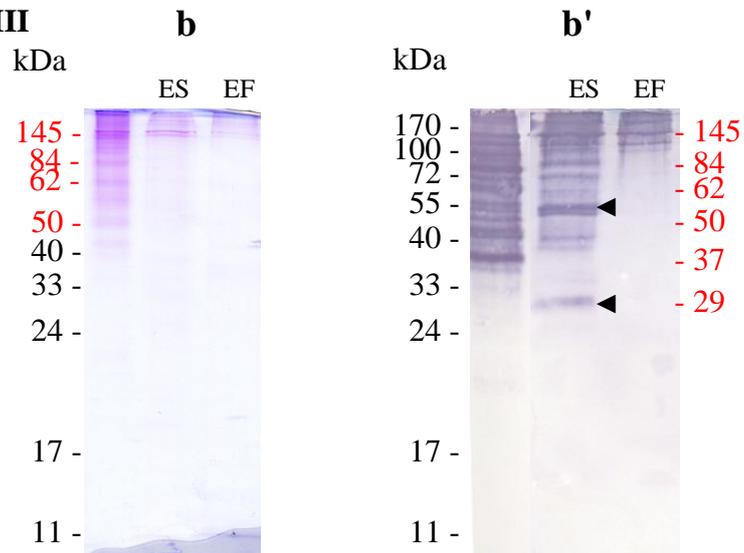
Collagen IV
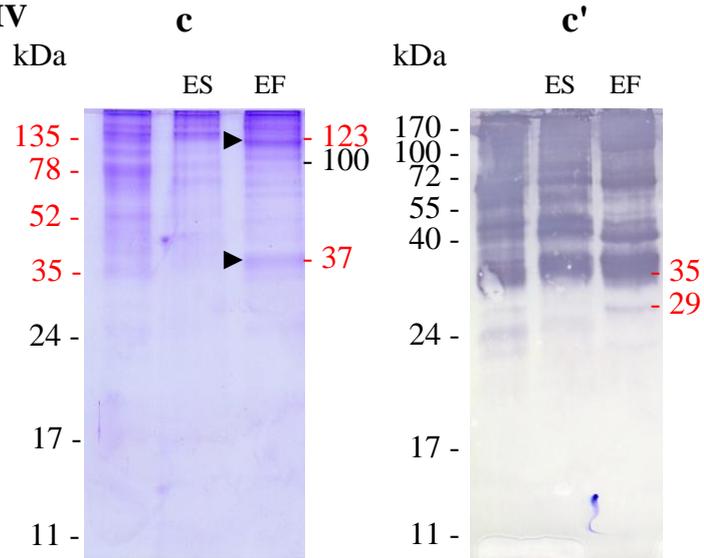
Collagen V
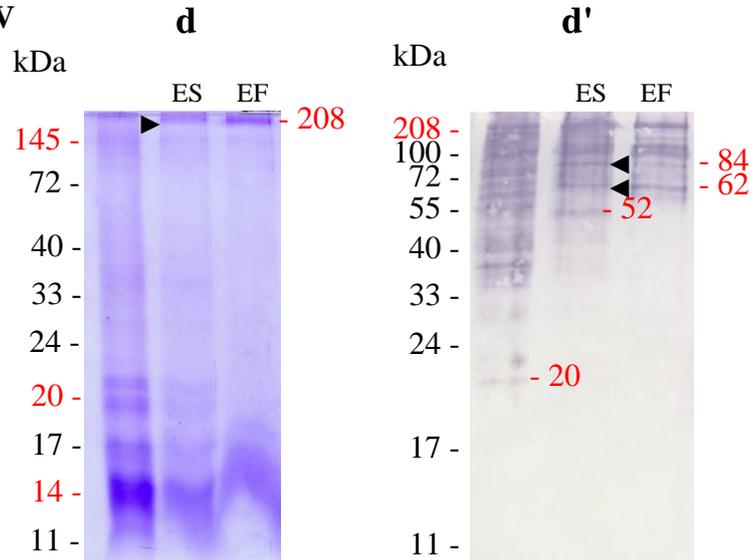
Fibronectin
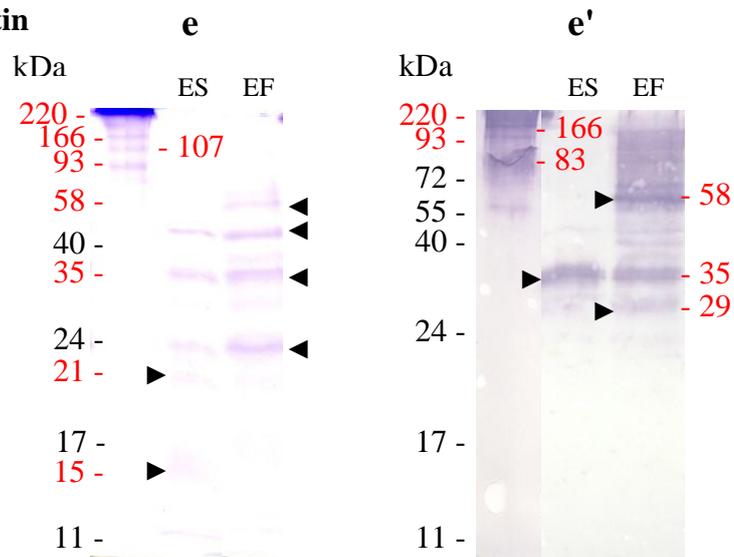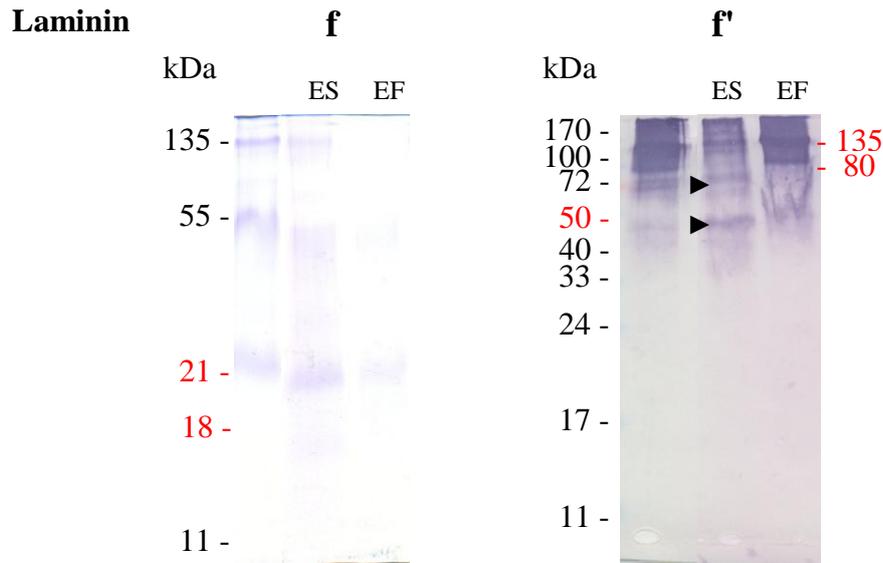
Figure 3.1   **The breakdown of extracellular matrix (ECM) by** *Necator americanus* **larval products described in: (a—f) gels stained with Coomassie Blue and (a'—f') Western blots. Gels were labelled for protein molecular weight (black), extra protein bands (red) and arrowheads point at breakdown products.**

Lane 1, ECM molecules as controls;

Lane 2, ECM molecules + ES products;

Lane 3, ECM molecules + EF products.

Hydrolysis of fibronectin was evident with both EF and ES products as demonstrated by the total disappearance of proteins at 220, 166, 107 and 93 kDa (Figure 3.1, e). Proteins of smaller molecular weights were formed at 40, 35 and 24 kDa, stronger with EF products. Individual bands were observed at 58 kDa (EF only) and at 21 and 15 kDa (ES products). On Western blots, the degradation of fibronectin resulted in a single band at 35 kDa with ES products while the presence of proteins at 58, 35 and 29 kDa was noted with EF products (Figure 3.1, e').

Degradation of laminin was minimal as illustrated in Figure 3.1 (f). Protein bands at 135, 55, 21 and 18 kDa were relatively weak with ES products while only proteins at 55 and 21 kDa were observed with EF products. Figure 3.1 (f ') shows an evident breakdown of laminin with ES products, described by the fading of the 135 kDa protein and the strong presence of proteins at 80 and 50 kDa. However, breakdown products by EF products were absent at 80 kDa and weaker at 50 kDa (Figure 3.1, f ').

a- Collagen I

kDa

170 -
100 -
72 -
55 -
40 -

33 -

24 -

17 -

11 -

— 195
— 145

1   Control
2   ES
3   EF
'   Post-infection IgG
"   All inhibitors

1   2   3   2'   3'   2"   3"

b- Collagen III

kDa

170 -
100 -
72 -
55 -
40 -

33 -
29 -
24 -

145
84
62
50
37

17 -

11 -

1   Control
2   ES
3   EF
'   Post-infection IgG
"   All inhibitors

1   2   3   2'   3'   2"   3"

c- Collagen IV

kDa

170 -
100 -
72 -
55 -
40 -
35 -
29 -
24 -

17 -

11 -

1   Control
2   ES
3   EF
'   Post-infection IgG
"   All inhibitors

1   2   3   2'   3'   2"   3"

d- Collagen V

kDa

| 208 - |
| 100 - |
| 72 - |
| 55 - |
| 40 - |
| 33 - |
| 24 - |
| 20 - |
| 17 - |
| 11 - |

52 -
40 -

1 Control
2 ES
3 EF
' Post-infection IgG
" All inhibitors

1   2   3   2'   3'   2"   3"

e- Fibronectin

kDa

220 -
93 -   - 166
72 -
55 -
40 -
35 -
29 -
24 -

- 166
- 83
- 58

17 -

11 -

1 Control
2 ES
3 EF
' Post-infection IgG
" All inhibitors

1   2   3   2'   3'   2"   3"

f- Laminin

kDa

170 -
100 -
72 -
50 -
40 -
33 -
24 -

- 135
- 80

17 -

11 -

1 Control
2 ES
3 EF
' Post-infection IgG
" All inhibitors

1   2   3   2'   3'   2"   3"

111

Figure 3.2 **Western blots showing degradation of ECM by *Necator americanus* larval products. (a) Collagen I; (b) Collagen III; (c) Collagen IV; (d) Collagen V; (e) Fibronectin; (f) Laminin. Molecular weights are shown either in black (protein ladder) or red (extra bands) and arrowheads point at recovered protein bands.**
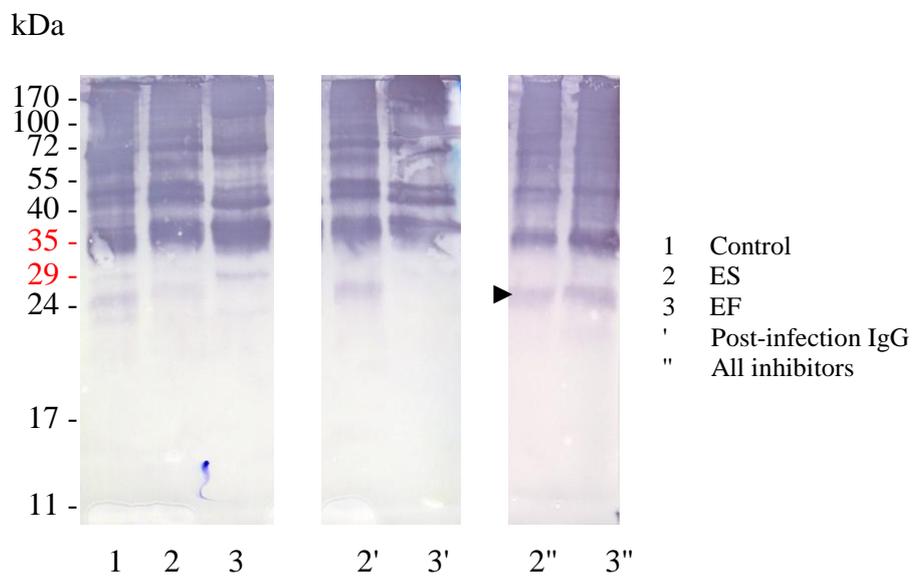
Lane 1, ECM molecules as controls;

Lane 2, ECM molecules + ES products;

Lane 3, ECM molecules + EF products;

Lane 2', ECM molecules + ES + post-infection IgG;

Lane 3', ECM molecules + EF + post-infection IgG;

Lane 2'', ECM molecules + ES + All inhibitors;

Lane 3'', ECM molecules + EF + All inhibitors.

Inhibition of *Necator americanus* proteolytic activity was investigated using either post-infection anti worm IgG antibodies or a mixture of serine, cysteine, aspartyl and metalloprotease inhibitors. No changes in the hydrolysis of both collagens I and V were observed when pre-treated with either post-infection IgG or a mixture of all inhibitors (Figure 3.2, a and d, Lanes 2'—3"). Degradation of collagen IV and laminin was not altered in the presence of post-infection IgG antibodies while minimal inhibition of proteolytic breakdown was observed using all inhibitors in combination. Changes in collagen IV hydrolysis included the reappearance of proteins of 24 kDa with both EF and ES products and the disappearance of the 29 kDa bands with EF products only (Figure 3.2, c, Lanes 2" and 3"). Inhibition of laminin breakdown eliminated the 50 kDa band with EF products while proteins at this molecular weight faded leading to the appearance of a strong band at 80 kDa with ES products (Figure 3.2, f, Lanes 2" and 3"). Anti worm IgG antibodies produced no change in the degradation of collagen III except for the reappearance of weak bands at 55 and 37 kDa (Figure 3.2, b, Lanes 2' and 3'). However, degradation of collagen III was greatly inhibited in the presence of all protease inhibitors as demonstrated by the reappearance of proteins of small molecular weights including 84, 62, 50, 40 and 37 kDa. Protein band at 29 kDa was not observed with ES products while bands at 55 kDa were relatively weaker and associated with an increase in the intensity of proteins at 145 kDa (Figure 3.2, b, Lanes 2" and 3"). Similarly, fibronectin proteolysis was partially inhibited by protease inhibitors as evidenced by the emergence of protein bands at 166 and 83 kDa and the absence of proteins at low molecular weight (i.e. 35 kDa) with EF products (Figure 3.2, e, Lanes 2" and 3"). Post-infection IgG antibodies

produced less inhibition of fibronectin breakdown as illustrated by the presence of proteins of low molecular weights including 58, 40 and 24 kDa for both ES and EF, respectively (Figure 3.2, e, Lanes 2' and 3').

In line with previous findings, in which treatment of collagen V with larval products induced the formation of a new, larger proteins (208 kDa), the presence of transglutaminases in *Necator americanus* larval products was investigated. Transglutaminase activity was significantly present in EF products and significantly higher in ES products as shown in Figure 3.3.
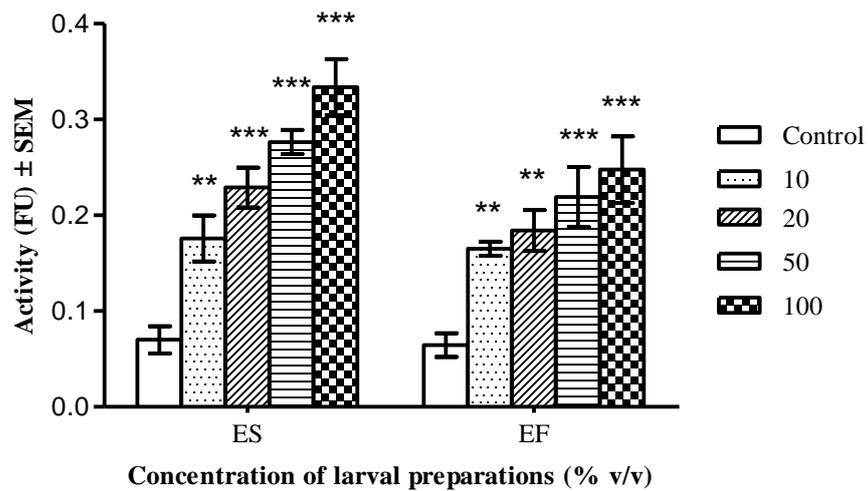
Figure 3.3   Transglutaminase activity in *Necator americanus* larval products. Activity is compared to controls containing no larval products. Activity is presented as the mean ± SEM and *** = P < 0.001; ** = P < 0.01.

3.3.2 Degradation of human skin by *Necator americanus* larval products

Electrophoretic separation of skin extracts demonstrated the presence of a strong protein band at 68 kDa and relatively weak bands at 100, 55, 40, 24 and 14 kDa (Figure 3.4, Control). Incubation of human skin with *Necator americanus* larval EF and ES products for 2 hours at 37˚C was found to cause no major changes in the protein profile of human skin. In addition to the marked reduction in the intensity of the 68 kDa protein band, EF products resulted in the disappearance of the 100, 55, 40 and 14 kDa protein bands (Figure 3.4, Lane 2) while ES products caused the bands at 40, 37 and 14 kDa to disappear.
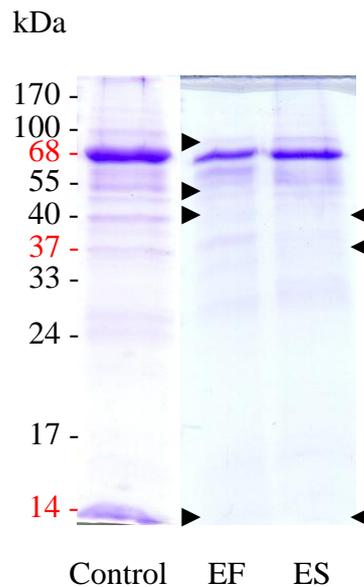
Figure 3.4   SDS-PAGE gels showing the effect of *Necator americanus* larval products on human skin. Optimal extraction of skin samples was obtained using 0.1M phosphate buffer as described in the Methods. Molecular weight of protein ladder (black), extra protein bands (red) and arrowheads point at changes in protein profile.

Human skin was shown to contain different extracellular matrix macromolecules including collagens I and III, fibronectin and laminin (Figure 3.5, a—f, Lane 2). The presence of collagen I was mirrored by characteristic protein bands at 145, 135 and 58 kDa (Figure 3.5, a) while the presence of collagen III was confirmed following the detection of proteins, most importantly at 145, 135 and 93 kDa (Figure 3.5, b). While fibronectin was detected as a single band at 58 kDa, laminin involved a strong protein band at 135 kDa, with a less intense band at 80 kDa (Figure 3.5, e and f, respectively). Collagens IV and V were not significantly present in human skin extracts as shown in Figure 3.5 (c and d). Human skin was compared to ECM proteins run as controls in Lanes 1 (a—f).

Necator americanus larval products were found to cause minimal or no breakdown of collagen I, fibronectin and laminin in the skin, as shown in Figure 3.6 (a, c and d; Lanes 3 and 4). Changes included the disappearance of protein bands at 100 and 58 kDa (collagen I) and fading of the 40 kDa (fibronectin) with ES products. However, collagen III was considerably hydrolysed as featured by the loss of most protein bands except for proteins at 135 kDa (with both EF and ES products), at 145 kDa (only with EF products) and traces of proteins at 50 kDa (Figure 3.6, b; Lane 3 and 4). These changes were not inhibited in the presence of either a mixture of protease inhibitors or post-infection IgG antibodies (Figure 3.6, a—d; Lane 3'—4").
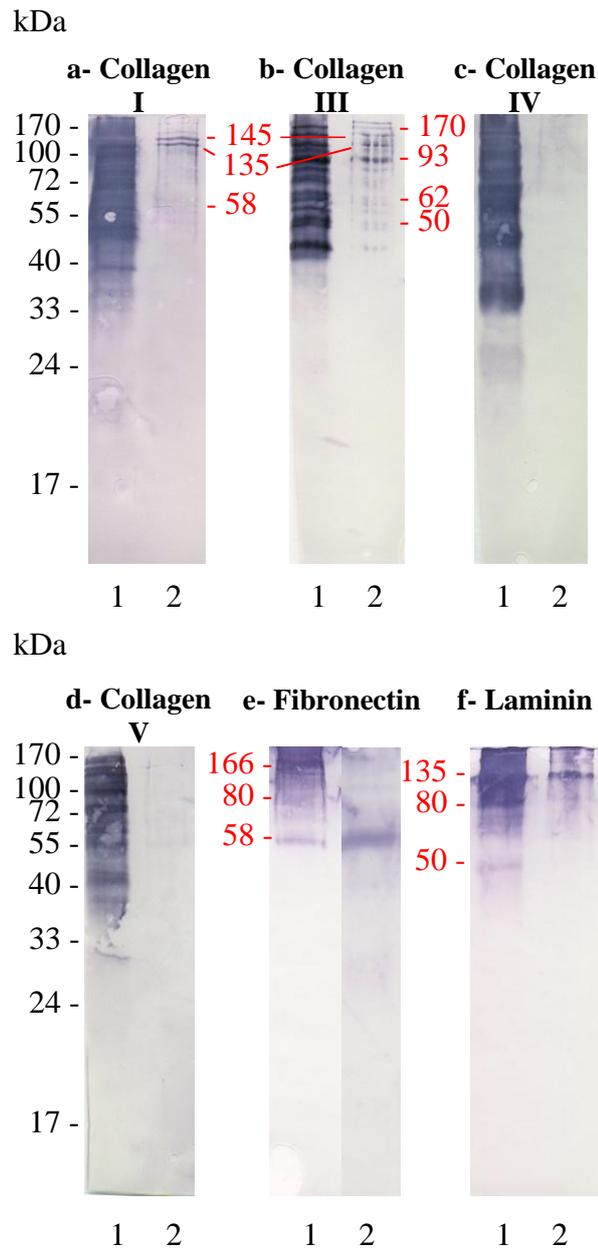
Figure 3.5 Western blots showing the presence of ECM molecules in the human skin. Molecular weights are shown either in black (protein ladder) or red (extra protein bands).

Lane 1, ECM molecules as controls;

Lane 2, human skin.

a- Collagen I

kDa

170 -
100 -
72 -
55 -
40 -
33 -
24 -
17 -
11 -

— 145
— 135
— 58

1	Control ECM
2	Control Skin
3	ES
4	EF
'	Post-infection IgG
"	All inhibitors

1   2   3   4   3'   4'   3"   4"

b- Collagen III

kDa

170 -
100 -
72 -
55 -
40 -
33 -
24 -
17 -
11 -

— 145
— 135
— 50

1	Control ECM
2	Control Skin
3	ES
4	EF
'	Post-infection IgG
"	All inhibitors

1   2   3   4   3'   4'   3"   4"

c- Fibronectin

kDa

170 -
100 -
72 -
55 -
40 -
33 -
24 -
17 -
11 -

— 58
— 40
— 24

1	Control ECM
2	Control Skin
3	ES
4	EF
'	Post-infection IgG
"	All inhibitors

1   2   3   4   3'   4'   3"   4"

d- Laminin

kDa

1	Control ECM	
2	Control Skin	
3	ES	
4	EF	
'	Post-infection IgG	
"	All inhibitors	

Figure 3.6   Effect of *Necator americanus* larval products on human skin macromolecules. Molecular weights are shown either in black (protein ladder) or red (extra protein bands).

Lane 1, ECM molecules as control;

Lane 2, human skin as control;

Lane 3, human skin + ES products;

Lane 4, human skin + EF products;

Lane 3', human skin + ES + post-infection IgG;

Lane 4', human skin + EF + post-infection IgG;

Lane 3'', human skin + ES + All inhibitors;

Lane 4'', human skin + EF + All inhibitors.

3.3.3 Comparison of the effects of *Necator americanus* larval products on ECM and human skin

The difference in the degradation of laminin, fibronectin, collagen I and III by larval products is summarised in Figure 3.7. *Necator americanus* larval EF and ES products demonstrated a great ability to digest most extracellular matrix proteins when used in isolation (Lanes 1—3), while ECM molecules present in human skin were not so easily digested (Lanes 1'—3'). Degradation of both collagen I and III was greater with ES products, featured by the disappearance of protein bands at 100 and 58 kDa (collagen I) and 145 and 100 kDa (collagen III) from human skin as opposed to proteins of small molecular masses when collagens were used in isolation (Figure 3.7, a and b; Lanes 1—3). Collagen III, both in human skin and alone, was also degraded by EF products as shown in Figure 3.7 (b). Unlike collagen I and III, fibronectin and laminin from the human skin were not degraded by larval products while these molecules, when used separatly, were greatly degraded by ES products as previously described in Figure 3.1.

a- Collagen I

b- Collagen III

kDa

c- Fibronectin

kDa

d- Laminin

kDa
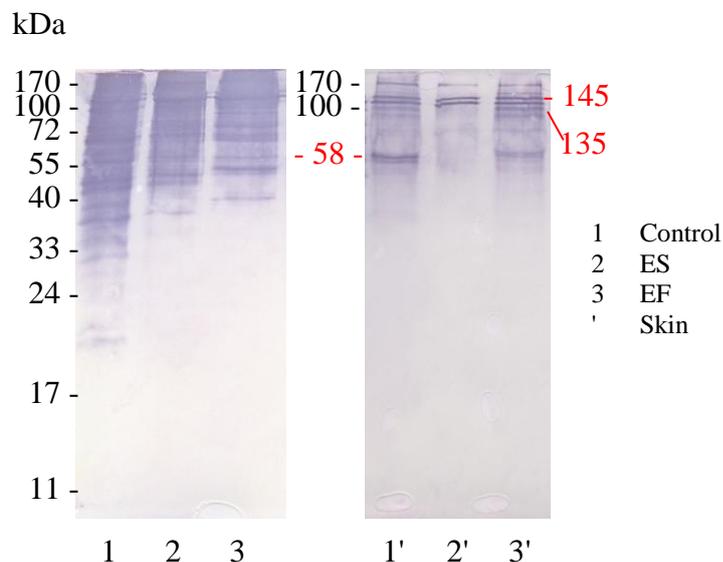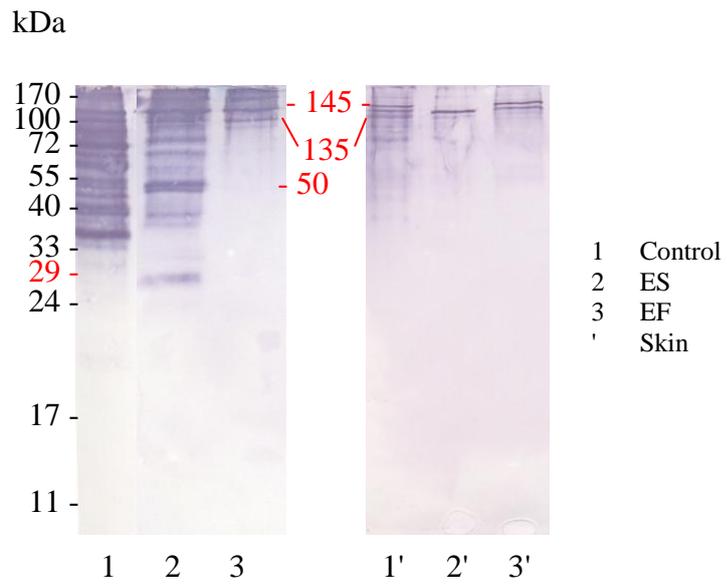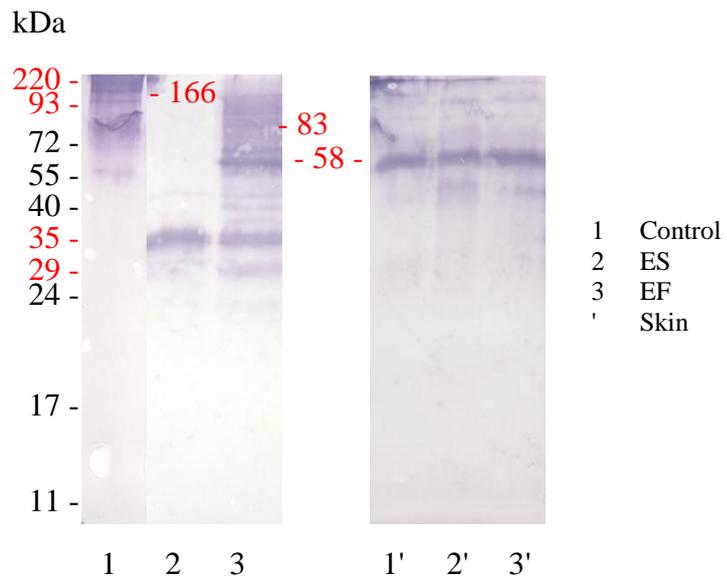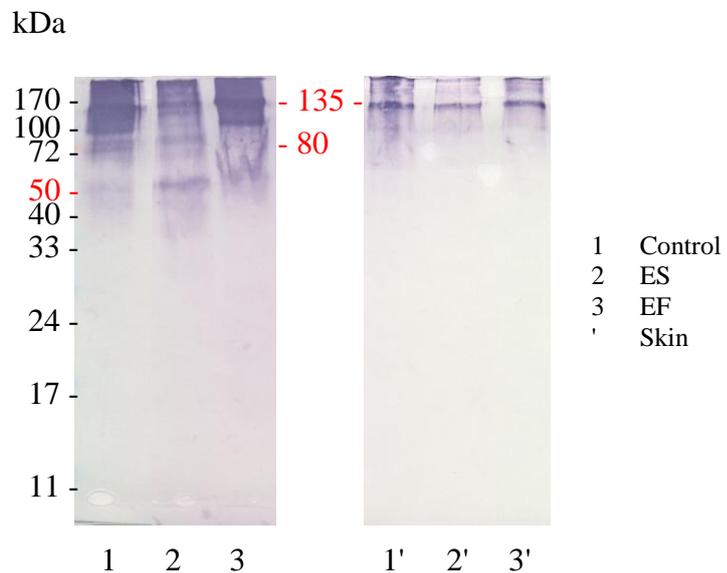
Figure 3.7 **Western blots comparing degradation of extracellular matrix (Lanes 1—3) and human skin macromolecules (Lanes 1'—3') by** *Necator americanus* **larval products. Molecular weights are shown either in black (protein ladder) or red (extra protein bands).**

Lane 1, ECM molecules as control;

Lane 2, ECM molecules + ES products;

Lane 3, ECM molecules + EF products;

Lane 1', human skin as control;

Lane 2', human skin + ES products;

Lane 3', human skin + EF products.

3.4 Discussion

In order to invade the human host, *Necator americanus* larvae have to penetrate the skin and migrate through the dermal connective tissue to reach the microcirculation. In this work, *Necator americanus* larval products demonstrated a great ability to digest most extracellular matrix (ECM) macromolecules including collagens III and IV, fibronectin and laminin, as tested by SDS-PAGE and Western blots (Figures 3.1). Unlike previous work by Brown *et al* (1999), no degradation was observed with collagens I and V, indicating that larval enzymes are selective towards specific ECM molecules. Collagens I and III are predominantly present in the connective tissue and the walls of blood vessels in the skin. The molecular structure of collagen I is complex and accounts for its resistance to non-specific proteolytic degradation, making collagen III a suitable alternative target for larval proteases. In addition, degradation of fibronectin and laminin suggested a possible loss of their ability to interact with other ECM molecules and maintain the structural stability of the skin, as previously proposed by Hotez *et al* (1990) and most recently by Williamson *et al* (2006). Since collagen IV and laminin are the main components of basement membranes (Timpl and Brown, 1996; Timpl, 1996), the breakdown of these molecules indicated that larval proteolytic activities can also create an access point for the larvae to penetrate all basement membranes as well as the walls of the blood vessels in the skin. Thus, our findings suggested that *Necator americanus* larval products target these molecules to disturb the structure of the skin and create an opening for larvae to migrate to the blood circulation.

The digestion of ECM proteins was significantly different with larval products, described by a selective degradation of collagen III and laminin with ES products and a greater affinity for collagen IV by EF products. The degradation of fibronectin was also different showing a single, strong protein with ES products opposed to multiple protein bands of lesser intensity with EF products. The characteristic variation in the degradation of individual ECM proteins might be explained by the characteristic divergence in larval enzymes, previously described in chapter 2. Besides exsheathment, results indicated that EF products, which showed a considerable ability to degrade matrix macromolecules, might also be involved in early stages of larval penetration allowing *Necator americanus* species to advance in the skin, as previously reported by Kumar and Pritchard (1992a). ES products, however, are most likely responsible for further larval migration deep down the skin and gaining access into the microcirculation.

Unlike other matrix proteins, treatment of collagen V with larval products resulted in the disappearance of protein bands of small molecular weight and the emergence of new proteins with high molecular weight (Figure 3.1, d). This was indicative of the possible involvement of larval enzymes in the cross-linking of small proteins and the creation of strong protein bands which are resistant to proteolytic cleavage (Collighan and Griffin, 2009). Further investigation confirmed the presence of transglutaminase activity in both EF and ES products, as suggested by Kasper *et al* (2001). The presence of transglutaminase has been reported in a number of parasites including *Onchocerca volvulus* (Lustigman *et al*, 1995), *Plasmodium falciparum* (Adini

et al, 2001) and others, the inhibition of which was found to prevent the moulting of L3 larvae to L4 stage larvae (Lustigman *et al*, 1995; Rao *et al*, 1999; Chandrashekar and Mehta, 2000). Transglutaminase activity, which was significantly higher in ES products, therefore suggested an important role in the long-term maintenance and survival of *Necator americanus* species as well as the progression of the parasitic infection.

Total inhibition of the enzymatic breakdown of ECM proteins with EF and ES products was never observed. Treatment with post-infection anti worm IgG antibodies demonstrated no inhibitory effect on the hydrolysis of most ECM molecules exclusive of fibronectin. Results suggested that the competitive binding of these antibodies to larval enzymes, as previously described in chapter 2, might account for the low inhibition of the enzymatic activity. However, the hydrolysis of collagens III, IV, fibronectin and laminin was greatly inhibited in the presence of all protease inhibitors in combination, as illustrated by the reappearance of original proteins bands (Figure 3.2, a—f). Inhibition of ECM degradation suggested that larval proteases are primarily involved in the hydrolysis of matrix proteins, therefore playing a major role in the degradation of connective tissue and migration of *Necator americanus* larvae in the skin (Brown *et al*, 1999). Thus, targeting larval proteases using specific protease inhibitors would prevent larval penetration and be beneficial in the course of treatment of *Necator americanus* infection, as suggested by Kumar and Pritchard (1992a) and Brown *et al* (1999). Protease inhibitors produced no change in the degradation of collagen V, indicating that larval

proteases are relatively selective and confirming that other enzymes were involved in the hydrolysis of collagen V.

Although investigating the effect of larval products on individual matrix macromolecules has been informative, it might give different views of what really happen in the human skin due to the complex nature of the latter. No major degradation of skin extracts was observed with EF and ES products, compared to matrix molecules (Figure 3.4). This is likely due to the fact that using ECM proteins in isolation ignored the major protective role of the skin as featured by the complex molecular structure and the presence of tissue-derived protease inhibitors, which are possibly responsible for the low degradation profile of skin macromolecules by larval products. Protease inhibitors, which have been shown to exist in the skin including cysteine (Zeeuwen *et al*, 2009) and serine inhibitors (Rao *et al*, 1995; Rao *et al*, 1998) are believed to provide important regulatory and protective functions against uncontrolled proteolytic degradation from host and external pathogens. To date, the presence of aspartyl and metalloproteases inhibitors in the skin was not confirmed, which might account for the significant involvement of these protease classes in the skin penetration, as described by Brown *et al* (1999).

The presence of collagens I, III, fibronectin and laminin in the skin extracts was confirmed using Western blots (Figure 3.5). Collagen IV was not observed while traces of collagen V were hardly detectable. Larval products demonstrated an ability to degrade skin-collagen III which was significantly greater with ES products while minimal digestion of collagen I and fibronectin

was observed. Results suggested that larval products target molecules with low complexity (e.g. collagen III) to create a fast and easy breach for the larvae to enter the host. Targeting other skin macromolecules including collagen I, fibronectin and laminin might require stronger proteolytic activity and larger numbers of species due to their complex structure, mainly responsible for the protective nature of the skin. In addition, degradation of skin macromolecules was primarily related to the characteristic presence of proteolytic enzymes in *Necator americanus* larval products, as described above. Total inhibition of proteolytic activities on skin macromolecules was not observed suggesting a potential involvement of other enzymes in the digestion process, which should be addressed in the future. EF products, causing noticeable breakdown in the skin-ECM molecules, confirmed their potential involvement in the initial stages of larval migration in the skin while ES products were proved essential for further progression towards the underlying vasculature.

In summary,

- Individual macromolecules including collagen III and IV, fibronectin and laminin showed a great susceptibility to larval products, suggesting that *Necator americanus* larvae might target these proteins to disturb the stability of the skin.

- Skin-originated collagen III was more susceptible to larval proteolytic activity compared to collagen I and fibronectin, suggesting that skin macromolecules might be resistant to proteolysis by larval products.

- Transglutaminase activity was present in both EF and ES products, possibly with a role to play in the maintenance of *Necator americanus*.

4. Interaction of *Necator americanus* larval products and the vascular endothelium

4.1 Introduction

The vascular endothelium forms the intact, innermost layer of the vessel wall, which acts as a physical barrier to maintain vascular homeostasis and regulate vascular permeability. As part of the infection process, *Necator americanus* larvae are required to enter the vasculature, presumably by disrupting the vascular endothelium, as has been shown for other parasites such as *Dirofilaria* (Boreham, 1984) and *Schistosoma* (Fallon *et al*, 1996). Migration of *Schistosoma mansoni* through/ during the lung-stage was shown to be activated by excretory/secretory products during which parasites attach to endothelial cells (Trottein *et al*, 1999). *Schistosoma*-related studies revealed that parasitic enzymes induced a decrease in vascular permeability using bovine brain capillary endothelial cells (BBCEC) *in vitro* (Trottein *et al*, 1999), while intradermal administration of *Schistosoma* extracts was associated with increased vascular permeability and local oedema *in vivo* (Teixeira *et al*, 1993; Fallon *et al*, 1996). Other studies highlighted the potential involvement of proteases secreted by *Schistosoma mansoni* (Han *et al,* 2002; Hansell *et al*, 2008) and *Porphyromonas gingivalis* (Imamura *et al*, 1995), in parasite-induced increase in vascular permeability. Several studies have shown vascular permeability to change in response to physiological and pathological factors including permeability increasing agents such as vascular endothelial growth factor (VEGF) and inflammatory mediators including histamine and thrombin (Lampugnani *et al*, 1995; Esser *et al*, 1998; Vogel *et al*, 2001), as well as cytokines such as IL-6 and IL-8 (Ali *et al*, 1999; Petreaca *et al*, 2007). Most of these mediators have been reported to trigger series of phosphorylation cascades leading to increased permeability, which is described in section 1.3.4.

Human umbilical vein endothelial cells (HUVEC) have been used successfully to model interactions between the malaria parasite *Plasmodium falciparum* and the ova of the bilharzia fluke *Schistosoma mansoni* and vascular endothelium (Cooke and Nash, 1995; Lejoly-Boisseau *et al*, 1999). In these studies, live *Schistosoma mansoni* eggs were shown to adhere to endothelial cells, particularly in post-capillary venules, using an *in vitro* flow assay using HUVEC cultures, while *Plasmodium falciparum* parasitized red blood cells were shown to adhere to HUVEC through intercellular adhesion molecule (ICAM-1). The HUVEC model, which is known to maintain the general properties of all endothelial cells including plasticity and molecular structure, has been used here to address the interaction of *Necator americanus* larval enzymes with the endothelium for the first time. This interaction was studied by exposing HUVEC monolayers to well defined hookworm larval exsheathing fluid (EF) and secretions (ES), with cell monolayer integrity being examined using transendothelial electrical resistance (TEER) and tracer permeability.

4.2 Methods

4.2.1 Isolation of human umbilical vein endothelial cells (HUVEC)

Human umbilical vein endothelial cells (HUVEC) were isolated from freshly collected umbilical cords, obtained at elective caesarean section from normal pregnancies, using the method of Jaffe *et al* (1973). Umbilical cords were collected in sterile 0.9% (w/v) NaCl saline containing 200 IU/mL penicillin and 200 μg/mL streptomycin and stored at 4°C for up to 24 hours before use. The vein at each end of the umbilical cord was cannulated with a three-ways stopcock and secured by tying Vincryl suture (2/0, 75 cm) around the cord at these ends. The vein was then perfused with pre-warmed sterile 0.9% (w/v) saline to remove any residual blood contents and ensure the cord is not damaged at any point. HUVEC were harvested by means of collagenase type II digestion whereby the umbilical vein was filled with Medium M199 supplemented with 200 IU/mL penicillin, 200 μg/mL streptomycin, 2 μg/mL fungizone and 0.5 mg/mL collagenase type II. Following incubation of the cord for 10 minutes at 37°C and under 5% CO_2 in a water bath containing pre-warmed sterile 0.9% (w/v) saline plus 200 IU/mL penicillin and 200 μg/mL streptomycin, the collagenase solution was passed back and forth through the vein using 10 mL syringes attached to stopcocks at each end of the cord to ensure that endothelial cells were detached from the vessel wall. The resulting endothelial cell suspension was collected in M20 (M199 supplemented with 100 IU/mL penicillin, 100 μg/mL streptomycin, 2 μg/mL fungizone and 20% (v/v) heat inactivated fetal bovine serum (FBS)), centrifuged at 1000 rpm for 5 minutes at room temperature and resuspended in growth medium (M20 supplemented with 50 μg/mL endothelial cell growth supplement (ECGS) and

50 µg/mL heparin) and allowed to attach to a 1% (w/v) gelatin coated 25 cm^2 tissue culture flask.

4.2.2   Maintenance, subculture and seeding of HUVEC on Transwells

Cells were cultured on 1% gelatinised T25 cm^2 flasks in growth medium M20; Medium 199 supplemented with 20% (v/v) heat inactivated fetal bovine serum (FBS), 100 IU/mL penicillin, 100 µg/mL streptomycin, 2 µg/mL fungizone, 150 µg/mL endothelial cell growth supplement (ECGS), and 50 µg/mL heparin, at 37˚C and 5% CO_2 in air. At 90—100% confluence, HUVEC were detached by incubating endothelial cells with 0.05% trypsin/ 0.02% EDTA for 5 minutes at 37˚C and the reaction was stopped by adding growth medium. HUVEC were then collected by centrifugation (1000 rpm for 5 minutes) and the pellet was resuspended in growth medium plus ECGS at 150 µg/mL, and heparin at 50 µg/mL. HUVEC were seeded on 1% (w/v) gelatin coated transwells (12 mm, 0.4 µm) at a density of 10^5 cells per well and growth medium was refreshed every 24 hours (200 µL and 700 µL in the apical and basal chamber, respectively).

4.2.3   Experimental design

4.2.3.1   Treatment of HUVEC monolayers with EF/ES products

For studies on endothelial barrier function, HUVEC cells were used up to the third passage. At confluence, HUVEC monolayers were incubated with EF/ES products for 2 hours at 37˚C and 5% CO_2 in air. Growth medium was carefully aspirated from the apical chamber and replaced with EF/ES products while medium in the basal chamber was refreshed. To avoid fetal bovine serum (FBS) inhibiting the enzymatic activity of larval products, EF/ES products

were diluted in M0 (M199 supplemented with 100 IU/mL penicillin, 100 µg/mL streptomycin and 2 µg/mL fungizone with no added FBS) and assayed at different concentrations (0.05—1.5 µg/mL). α- thrombin, a serine protease was used as a positive control at 0.15 U/mL. HUVEC monolayers with no added EF/ES products were used as controls and compared to HUVEC monolayers treated with larval products in this assay.

4.2.3.2   Apical/basal treatment of HUVEC monolayers with EF/ES products

The apical/basal treatment of HUVEC monolayers was based on replacing growth medium in the apical, basal or both chambers with larval products. EF/ES products were diluted in medium M0 (to a concentration of 1.5 µg/mL) and incubated with confluent HUVEC monolayers for 2 hours at 37˚C and 5% CO_2 in air. Treatment-free HUVEC monolayers, with no added EF/ES products, were used as controls and compared to treated HUVEC monolayers.

4.2.3.3   Treatment of HUVEC monolayers with protease inhibitors

EF/ES products were pre-incubated with protease inhibitors individually or in a mixture for 30 minutes at 37˚C. Protease inhibitors were diluted with RPMI-1640 medium to a typical working concentration following manufacturers' recommendations, as shown in Table 4.1. EF/ES products, pre-treated with protease inhibitors, were added to the apical and basal sides of confluent HUVEC monolayers at a concentration of 1.5 µg/mL and incubated for 2 hours at 37˚C and 5% CO_2 in air. Control HUVEC monolayers were treated with EF/ES products, free of inhibitors, and used for comparison to monolayers treated in the presence of protease inhibitors. The effect of treatment of

HUVEC monolayers with protease inhibitors, individually or in combination, with no larval products was investigated and is described in Appendix 3.

Table 4.1   List of protease inhibitors used.

Protease inhibitors	Concentrations used
E64 (cysteine proteases)	1 µM
Pepstatin A (aspartyl proteases)	1 µM
1, 10- Phenanthroline (metalloproteases)	1 mM
Phenyl methane sulphonyl fluoride (PMSF, serine proteases)	1 mM

4.2.3.4   Treatment of HUVEC monolayers with post-infection anti worm IgG antibody

EF/ES products (1.5 µg/mL) were incubated overnight at 37˚C with 20 µg/mL of either control or post-infection anti hookworm IgG, previously described in section 2.2.7.1. EF/ES products, pre-treated with IgG, were added to the apical and basal sides of confluent HUVEC monolayers and incubated for 2 hours at 37˚C and 5% CO_2 in air. HUVEC monolayers, treated with EF/ES products only, were used as controls, compared to monolayers treated with larval products in the presence of IgG.

4.2.4   Assays of endothelial permeability

4.2.4.1   Transendothelial electrical resistance (TEER)

After HUVEC were seeded on gelatin coated transwells, the transendothelial electrical resistances (TEER) of the monolayers were monitored over a period of 6 days, using an EVOM resistance meter (World Precision Instruments) as shown in Figure 1 until they reached a steady level ($\sim$ 72—74 Ω.cm^2). Measurements were made 20 minutes after refreshing the medium. During treatment with EF/ES products (described in section 4.2.3), the resistance across HUVEC monolayers was measured in triplicate at 20 minutes intervals. Specific TEER values were then calculated by subtracting the resistance of a cell-free transwell insert from the resistance measured across individual monolayers. At the end of the 2 hours period, medium from the apical and basal chambers were collected and stored at -20˚C for further analysis and the wells were transferred to a new plate to study the leakage of tracer across HUVEC monolayers.

0.4 μm 12 mm transwell plate
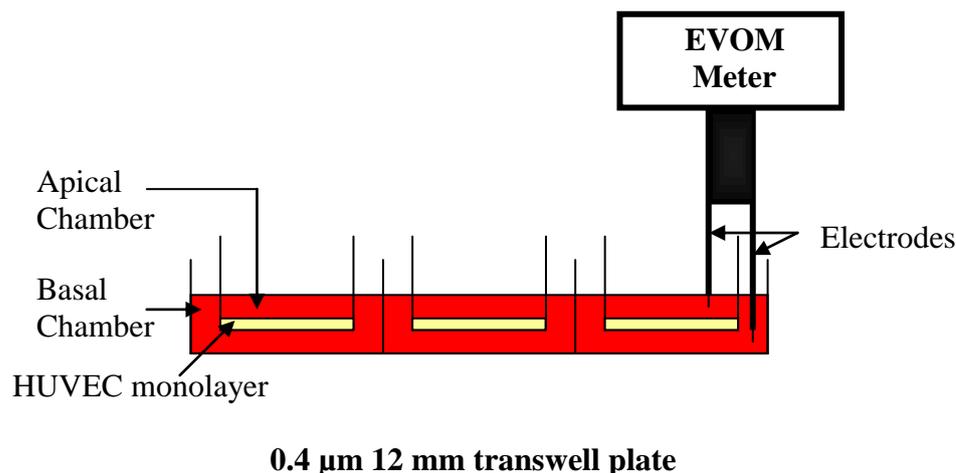
Figure 4.1   Schematic representation of the experimental apparatus used to measure transendothelial electrical resistance (TEER). Electrodes measure the electrical current, carried by ions across HUVEC monolayers, as the change in voltage between the apical and basal compartments of the transwells.

4.2.4.2   Leakage of TRITC- Albumin

The leakage of tetramethylrhodamine isothiocyanate TRITC-albumin (~ 68 kDa) across pre-treated HUVEC monolayers was assessed, described in sections 4.2.3.1—4.2.3.4. TRITC-albumin tracer was dissolved in RPMI-1640 phenol red-free medium with 20% FBS to a concentration of 50 mM and added to the apical chamber (200 μL each). Cells were incubated and alternated between 37˚C and room temperature (on an orbital shaker to ensure homogenous distribution of tracer) over a total period of 2 hours. Triplicate, 20 μL aliquots were collected from the basal chamber at 20—30 minutes intervals and made up to 100 μL with RPMI-1640 medium with 20% FBS. Retrieved aliquots from the basal chamber were immediately replaced. The amount of

tracer-fluorescence crossing individual monolayers was then measured using DYNEX Microtiter Plate MFX Fluorometer (excitation = 530 nm, emission = 590 nm) and values were converted to concentrations of the tracer, TRITC-albumin. The leakage of TRITC-albumin across cell-free transwell inserts was measured by collecting 20 µL aliquots from the basal chamber at 20—30 minutes intervals. Retrieved aliquots were immediately replaced and made up to 100 µL with RPMI 1640 medium with 20% FBS.

1. Take 3 x 20 µl samples per time point

Tracer/RPMI

HUVEC layer

RPMI 1640 + 20% FBS

2. Replace with 60 µl of RPMI-1640 + 20% FBS

0.4 µm 12 wells transwell plate
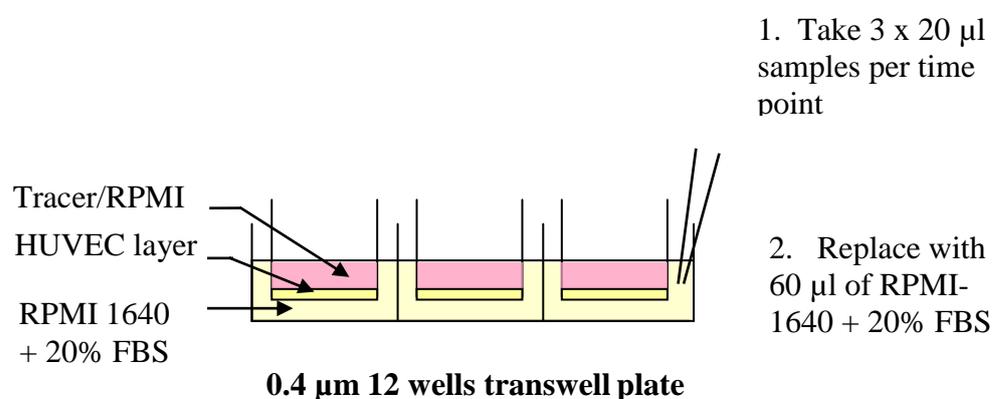
Figure 4.2   Schematic of the experimental apparatus used to measure the leakage of tracer across HUVEC monolayers.

4.2.4.3   Standard curve for TRITC-albumin tracer

TRITC-albumin tracer was dissolved in RPMI 1640 phenol red-free medium with 20% FBS to a known concentration (0—100 mM) and added to the apical chamber of the insert (200 µL each). The amount of tracer-fluorescence was measured using DYNEX Microtiter Plate MFX Fluorometer (excitation = 530 nm, emission = 590 nm) and plotted against the concentration of TRITC-albumin to generate a standard curve.

4.2.5   Immunocytochemistry

HUVEC monolayers were gently washed and fixed for 10 minutes in 1% (w/v) paraformaldehyde (PFA) in PBS (pH 7.2), permeabilised for 10 minutes with 0.15% (v/v) Triton X-100, and blocked for 30 minutes in phosphate buffered saline (PBS) containing 5% (v/v) normal human serum, all at room temperature. Cells were incubated overnight at 4˚C with a primary antibody as shown in Table 4.2. After washing with 0.1% BSA/PBS, cells were incubated for 2 hours at room temperature, in the dark, with a secondary antibody (Table 4.2). Both primary and secondary antibodies were diluted to the appropriate concentration with bovine serum albumin (0.1% BSA/PBS), unless otherwise stated. Staining for F-actin was performed by incubating cells with FITC conjugated phalloidin (50 µg/mL in PBS) for 2 hours at room temperature, in the dark. HUVEC cells were washed twice with 0.1% BSA/PBS followed by one wash with PBS and finally mounted in Vectorshield with propidium iodide to visualise the nuclei. Cells were then observed using a Leica TCS SP2 confocal laser scanning microscope (n = 3).

Table 4.2   List of antibodies used in immunocytochemistry.

Junctional molecules	Primary antibody	Secondary antibody
VE-Cadherin	Monoclonal anti-CD 144 (used at 10 µg/mL)	FITC conjugated anti-mouse IgG, diluted to 1:50 (v/v)
Occludin	Polyclonal anti-occludin (used at 25 µg/mL)	TRITC conjugated anti-rabbit IgG, diluted to 1:10 (v/v)

4.2.6   Microscopy

4.2.6.1   <u>Phase microscopy</u>

HUVEC monolayers were grown to confluence on 1% (w/v) gelatin coated tissue culture flasks and the morphology of cells was visualised using a Nikon phase-contrast microscope. The confluence of HUVEC cultures was checked before any experiment and imaging was performed using a Nikon Coolpix 995 digital camera at different magnifications.

4.2.6.2   <u>Confocal microscopy</u>

Leica TCS SP2 confocal laser scanning microscope was used to image HUVEC monolayers following immunocytochemistry. Cell monolayers were scanned using the glycerol immersion lens with an objective magnification of 63 x. The viewer window was used to arrange, manipulate and produce images with the maximum intensity. Finally both multi-channel and single images were named accordingly and saved as snapshots.

4.2.7   Statistical analysis

Where appropriate, data were analyzed with GraphPad Prism version 5.01. Values are presented as means (n = 3) ± SEM and statistical significance was determined by two-way ANOVA tests followed by Bonferroni post-tests. Statistical significance was defined as $P < 0.05$.

4.3   Results

4.3.1   Characterisation of human umbilical vein endothelial cell monolayers (HUVEC)

4.3.1.1   Integrity of normal HUVEC monolayers

Transendothelial electrical resistance (TEER) and solute permeability assays were used to evaluate the physical integrity of endothelial monolayers, not stimulated by *Necator americanus* larval product. TEER showed a rapid increase during the first 48 hours, followed by a plateau of 72—74 $\Omega.cm^2$ when HUVEC monolayers reached confluence (Figure 4.3).
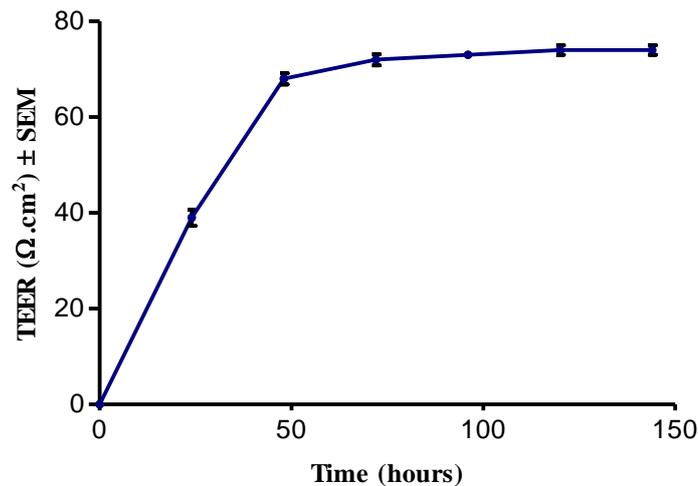
Figure 4.3   Transendothelial electrical resistance across HUVEC monolayers. TEER was measured, in triplicates, using EVOM resistance meter and values are presented as the mean ± SEM.

Conversion of fluorescence units to concentration of TRITC-albumin (i.e. the number of TRITC moles per mole of albumin) aimed at eliminating any sources of variation in our data. The standard curve, shown in Figure 4.4,

described the relationship between fluorescence and concentration of tracer between 0 and 100 mM. The linearity of the standard curve, as evidenced by an R^2 value of 0.9992, allowed the use of a straight line equation to determine unknown concentrations of TRITC-albumin, in subsequent experiments.
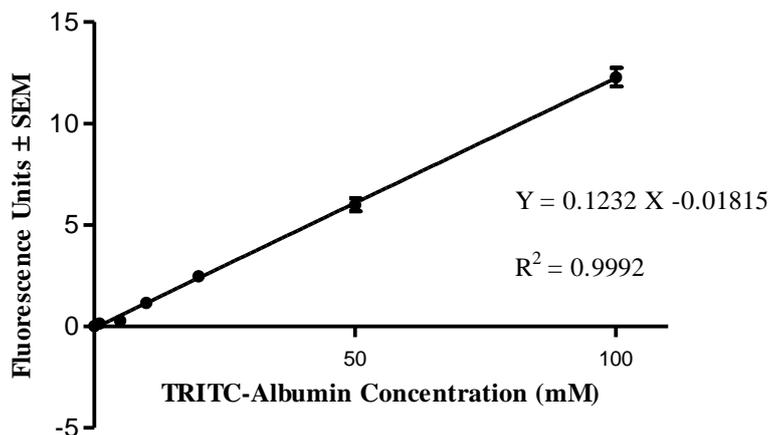
Figure 4.4 Standard curve for TRITC-albumin. Values are presented as the mean ± SEM. The relationship between TRITC-albumin concentrations and fluorescence was linear.

To investigate the effect of medium in the permeability assay, TRITC-albumin was dissolved in media with or without phenol red at a concentration of 50 mM, and the amount of fluorescence was measured, as described in section 4.2.4.2. Figure 4.5 summarises that the yield of TRITC-albumin was significantly higher (63 mM) when dissolved in Medium 20 (M199 with phenol red, containing 20% FBS), compared to RPMI-1640 (with 20% FBS), phenol red-free (49.9 mM). Media containing phenol red was shown to interfere with fluorescence, resulting in inaccurate readings, therefore the use of RPMI-1640, phenol-red free, was approved for the following experiments.
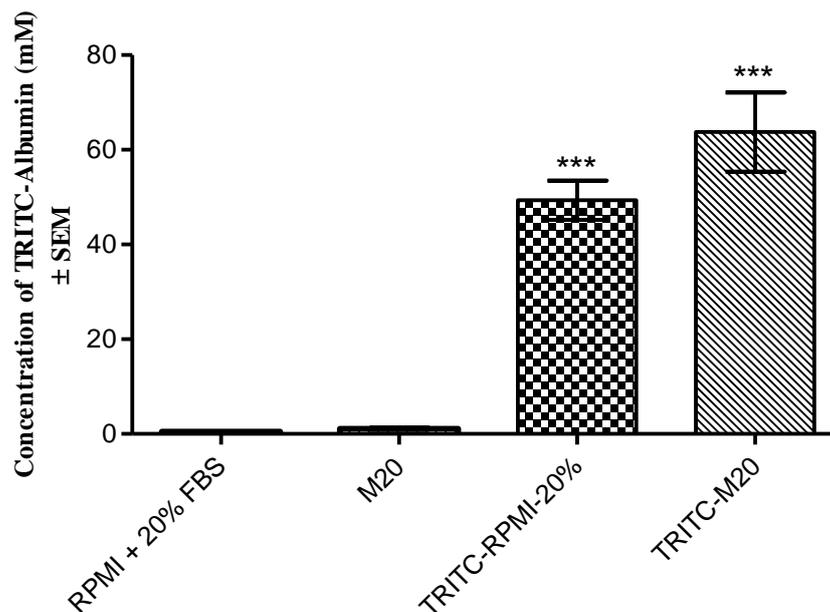
Figure 4.5 **Effect of media on TRITC-albumin concentration. The concentration of tracer, dissolved in different media, was measured and values are presented as the mean of concentration ± SEM, *** = P < 0.001, compared to RPMI-1640 + 20% FBS.**

The quantity of TRITC-albumin crossing the transwell inserts increased over the 2 hour-period and was significantly higher in the absence of cell monolayers (Figure 4.6). The presence of confluent HUVEC monolayers, as assessed by TEER, significantly reduced the leakage of TRITC-albumin by ~ 81% after 2 hours, as opposed to cell-free inserts. The percentage of TRITC-albumin recovered from the basal compartment was calculated (Equation 4.1).

$$\frac{\text{Concentration of TRITC} - \text{albumin crossing monolayers}}{\text{Original input of TRITC} - \text{albumin (50 mM)}} \times 100$$

Equation 4.1 Formula of percentage leakage of TRITC-albumin to the original input

Table 4.3   Percentage of TRITC-albumin leakage across transwell inserts, calculated using equation 4.1.

Transwell inserts	% of TRITC-albumin recovered from the basal chamber after 120 minutes
Cell-free	22.3
HUVEC monolayer	4.3

A recovery of 22.3% of the original tracer input was observed with cell-free inserts, as compared to a 4.3% with confluent HUVEC monolayers (Table 4.3). Equilibrium was never achieved over the 2 hour-study indicating the importance of endothelial cells in regulating solute permeability across HUVEC monolayers.
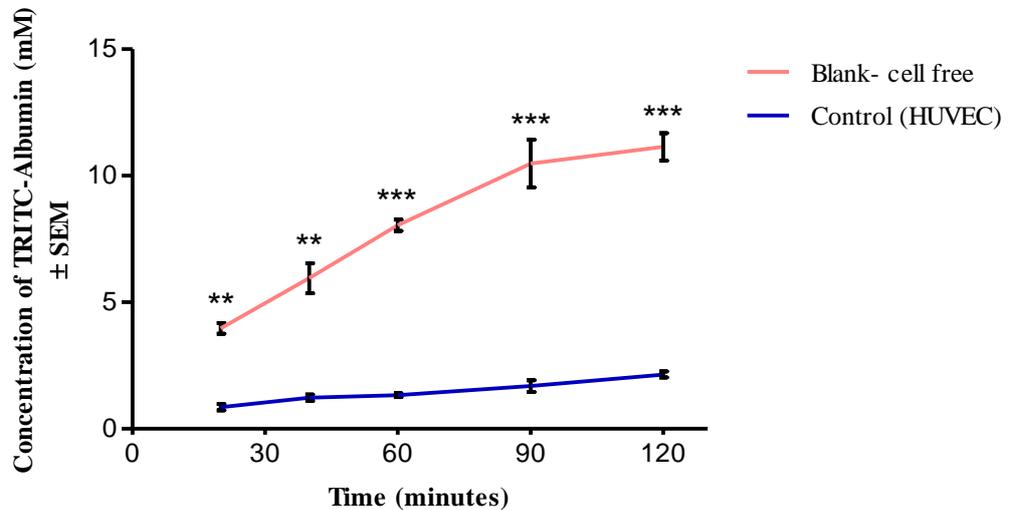
Figure 4.6   Leakage of TRITC-albumin across HUVEC monolayers. TRITC-albumin concentrations are presented as the mean ± SEM. *** = $P < 0.001$ and ** = $P < 0.01$ compared to cell monolayers.

Plotting TEER against tracer leakage, both measured across HUVEC monolayers, demonstrated a strong inverse relationship and linear relationship as demonstrated by an R^2 of 0.7439 between these two parameters of endothelial permeability (Figure 4.7). Hence, high resistance across HUVEC monolayers is mirrored by low solute/tracer leakage, indicating high confluence of these monolayers.
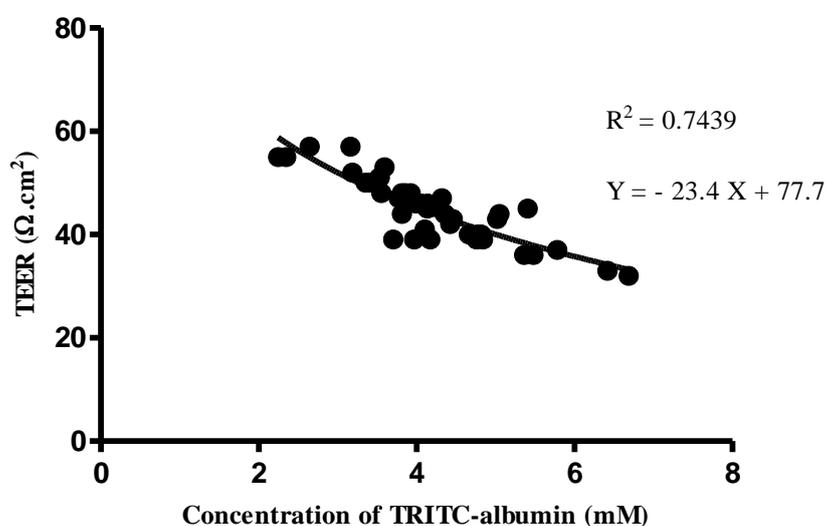
Figure 4.7   A plot of TEER across HUVEC monolayers against their permeability to TRITC-albumin.

4.3.1.2   Morphology of HUVEC monolayers

Morphological features of HUVEC cultures were investigated using phase-contrast microscopy. Early in their growth, HUVEC cells showed an elongated morphology (Figure 4.8, a). At confluence, reached by 48—72 hours, cells exhibited typical cobblestone morphology as shown in Figure 4.8 (b).
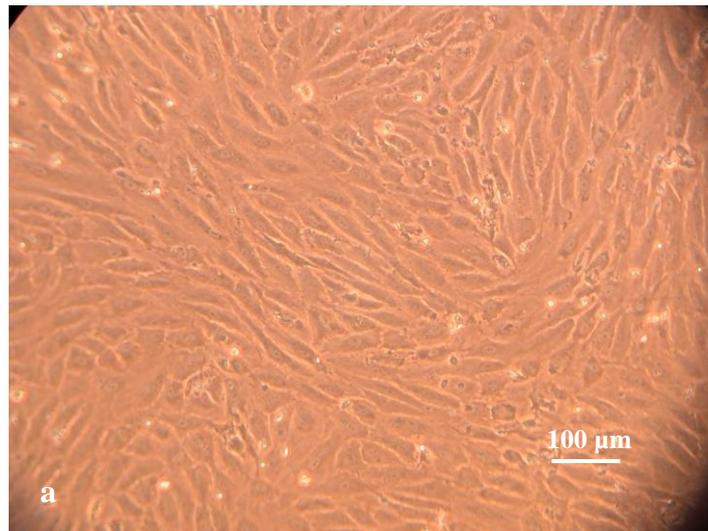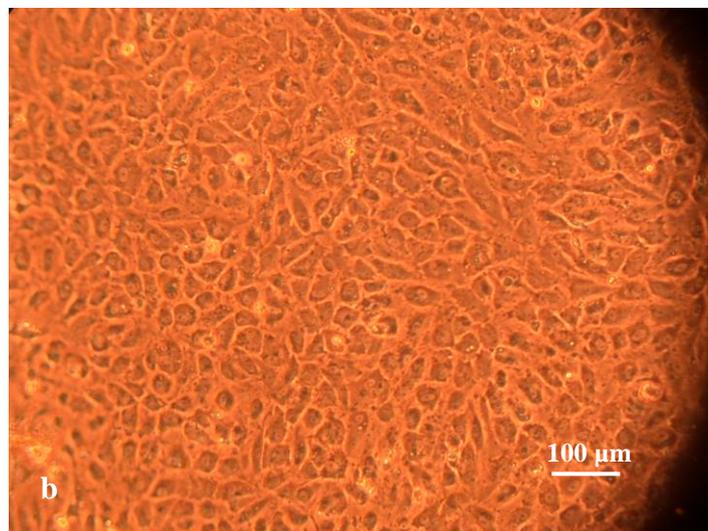
Figure 4.8   Phase contrast micrograph of HUVEC cells grown to a) 90% confluence and b) 100% confluence. Bars = 100 μm.

4.3.1.3   Junctional molecules present in HUVEC monolayers

The organisation of cell to cell junctions in confluent HUVEC monolayers was studied using confocal microscopy. Confluent endothelial monolayers exhibited a significant presence and continuity of the adherens junction protein, VE-Cadherin, while the tight junction molecule, occludin, was present but weak, showing a patchy distribution (Figure 4.9, a and b). F-actin filaments were mostly localised at the periphery, cell-cell border (Figure 4.9, d), with some stress fibers (Figure 4.9, c). Changes in junctional integrity in response to *Necator americanus* larval EF/ES products are described in chapter 5.
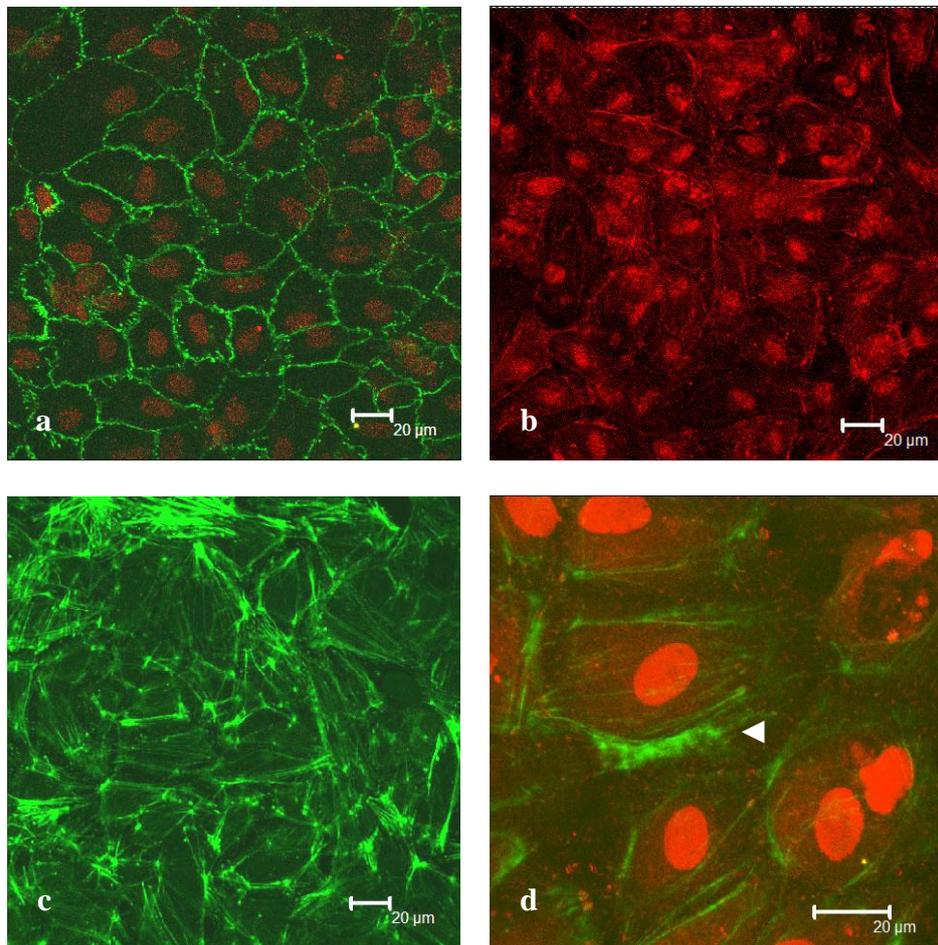
Figure 4.9   Immunostaining of HUVEC monolayers against junctional molecules. a) VE-Cadherin, b) occludin, c) and d) F-actin. Nuclei were stained with propidium iodide (red) in (a), (b) and (d). Bars = 20 µm.

4.3.2 Interaction of *Necator americanus* larval products with human umbilical vein endothelial cell monolayers (HUVEC)

4.3.2.1   Effects of concentration of larval products on monolayer permeability

Changes in endothelial permeability as assessed by a decrease in resistance (TEER) and an increase in tracer leakage across endothelial monolayers were related to concentration of EF/ES products in the culture medium. The decrease in monolayer resistance was dose-dependent and continued over a period of 2 hours, as shown in Figures 4.10 (a and b). Both EF and ES products caused a statistically significant reduction of TEER from control values (- 46.8% and - 50.9%, $P < 0.001$ respectively) when used at a final concentration of 1.5 µg/mL ($P < 0.001$, Figure 4.10, c). The serine protease, α-thrombin was also found to induce a reduction in TEER across HUVEC monolayers ($P < 0.001$).

a- EF products

b- ES products

c- EF vs ES products
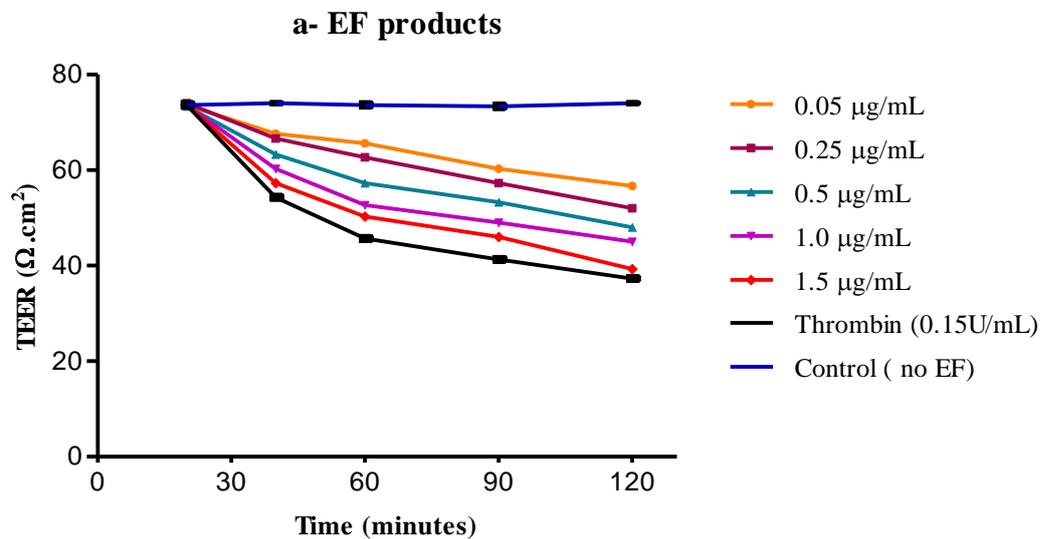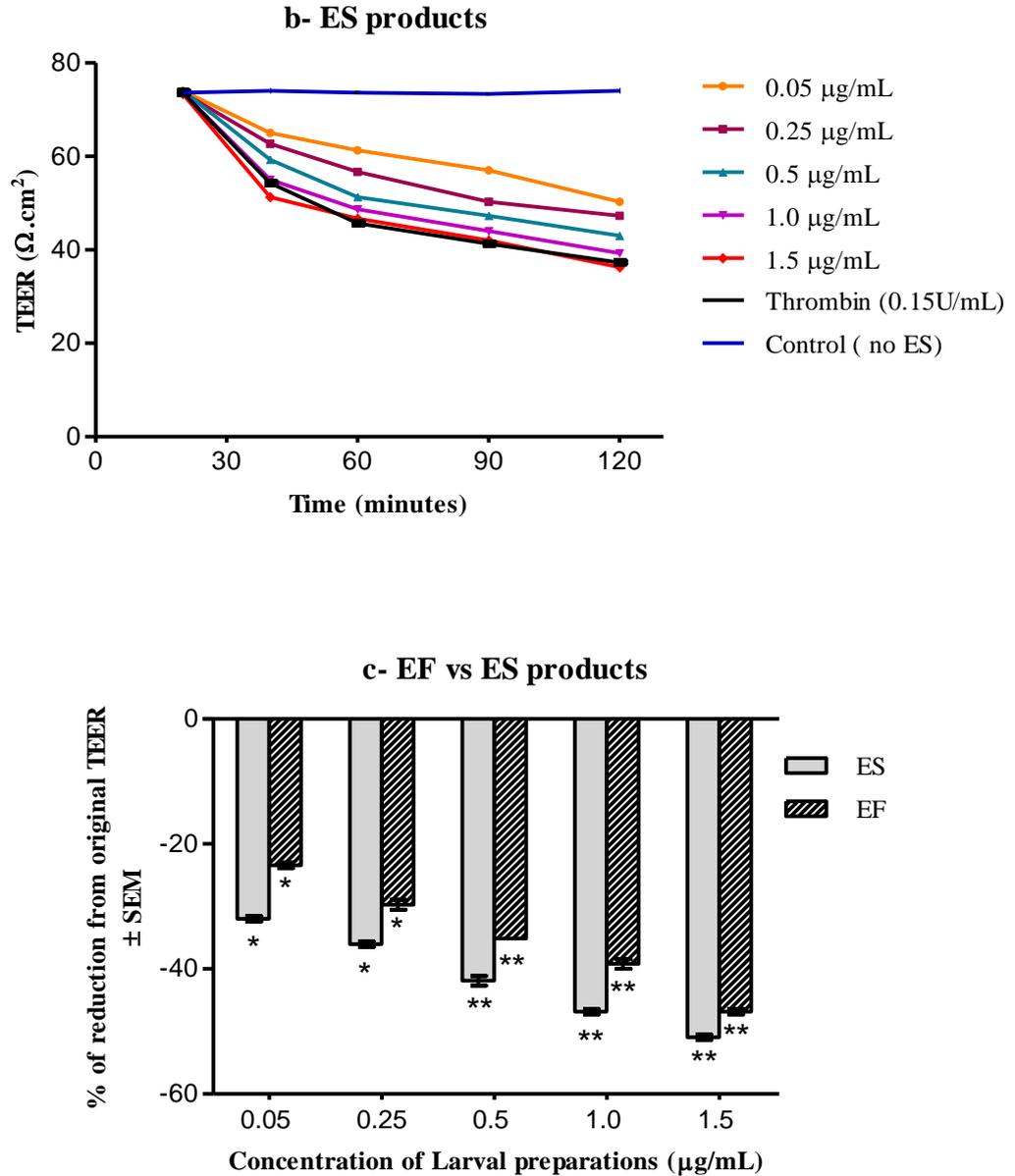
Figure 4.10 **Changes in transendothelial electrical resistance (TEER) across HUVEC monolayers following treatment with larval, a) EF products and b) ES products. c) Percentage changes from control TEER at different concentrations of EF/ES products at the end of the 2 hour-study. TEER values are presented as a percentage of reduction in original TEER ± SEM. * = P < 0.01, ** = P < 0.001 compared to original resistance of untreated controls.**

Changes in HUVEC resistance correlated with a dose-dependent (0.05—1.5 µg/mL) and time-related increase in levels of TRITC-albumin crossing treated monolayers over the 2 hour-study, compared to untreated monolayers (Figure 4.11, a and b). Although similar in pattern, ES products significantly demonstrated greater tracer leakage at any one dose compared to EF products and α-thrombin (Figure 4.11, (c); Table 4.4). The percentage of increase in TRITC-albumin leakage across treated monolayers, as opposed to control HUVEC monolayers was calculated using Equation 4.2.

$$\frac{\text{Conc. of tracer crossing control monolayers} - \text{Conc. of tracer crossing treated monolayers}}{\text{Conc. of tracer crossing control monolayers}} \times 100$$

Equation 4.2 Formula of percentage of TRITC-albumin leakage to control HUVEC monolayers

a- EF products

b- ES products

c- EF vs ES products

Concentration of Larval preparation (µg/mL)
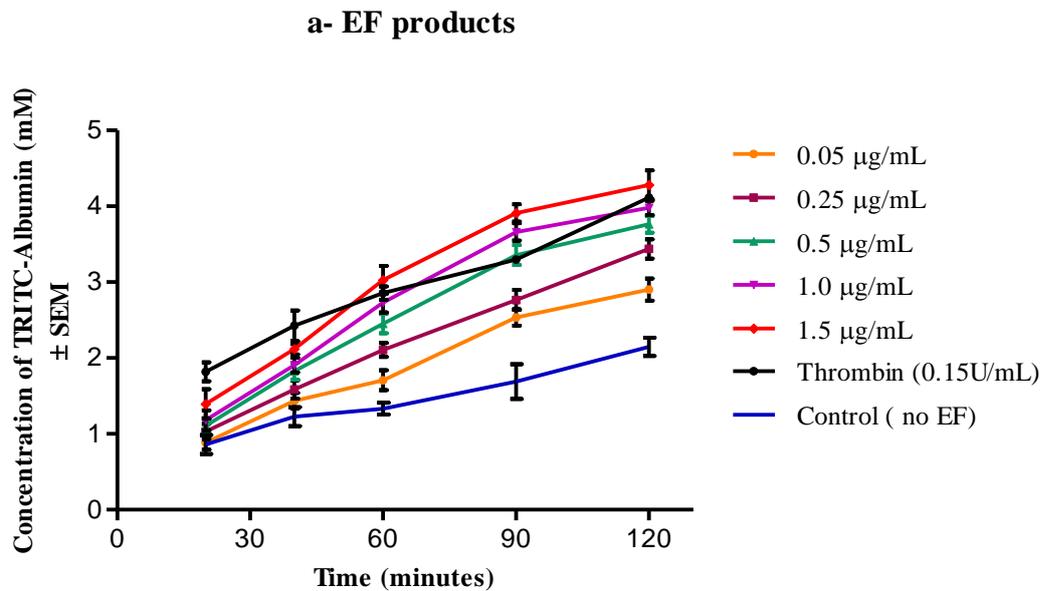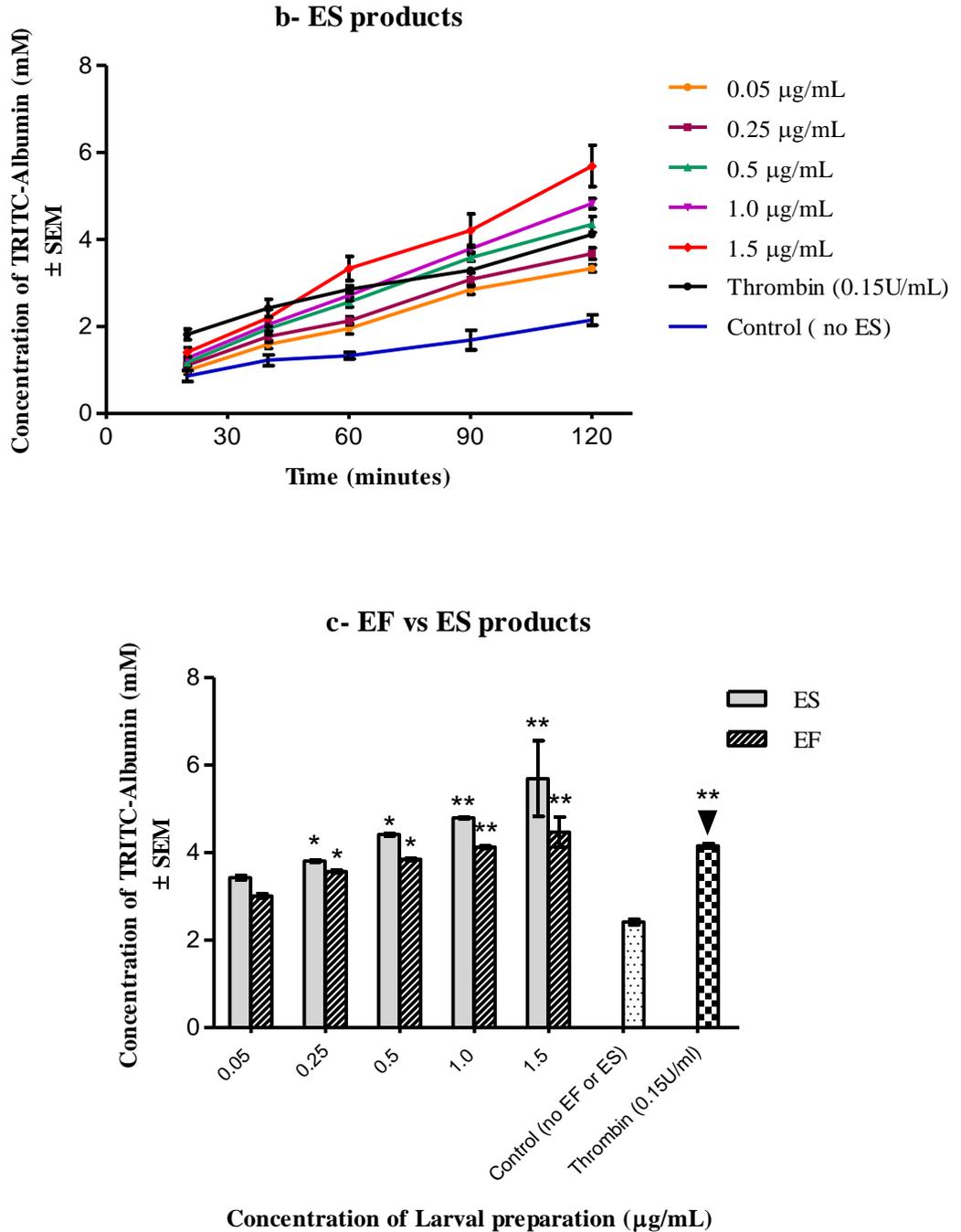
Figure 4.11 **Leakage of TRITC-albumin across HUVEC monolayers following treatment with a) EF products, b) ES products and c) EF vs. ES products at the end of the 2 hours-study. TRITC-albumin concentrations were calculated by subtracting tracer leakage across a blank monolayer and reported as the mean ± SEM. Significance was defined as * = P < 0.01 and ** = P < 0.001, compared to untreated controls.**

Table 4.4 describes permeability at the end of the 2 hour-period as the percentage increase in TRITC-albumin leakage across treated monolayers compared to untreated HUVEC monolayers, calculated using equation 4.2. A gradual increase in tracer leakage was observed as a function of the concentration of larval products in medium (0.05—1.5 µg/mL). For all the following experiments, larval EF and ES products were used at a concentration of 1.5 µg/mL, which caused a significant increase of 85.1% and 135.6%, respectively, compared to an increase of 72.2% caused by the positive control, α-thrombin.

Table 4.4   Percentage of increase in TRITC-albumin leakage across treated HUVEC monolayers, compared to control HUVEC monolayers after 2 hours.

Concentration of larval products (µg/mL)	% of increase in TRITC-albumin leakage	
	EF	**ES**
0.05	+ 24.5	+ 42
0.25	+ 47.8	+ 57.8
0.5	+ 59.3	+ 82.8
1.0	+ 70.9	+ 98.5
1.5	+ 85.1	+ 135.6
Thrombin (0.15 U/mL)	+ 72.2	

4.3.2.2   Effects of apical/basal administration of larval products on monolayer permeability

The increase in endothelial permeability was significantly higher than basally-treated monolayers (P < 0.001) when larval products were administered to the apical chamber and highest when applied to both chambers of transwells. The latter resulted in a reduction in TEER compared to control values (- 46.8% (EF) and - 50.9% (ES)) as opposed to the reduction of - 37.3% (EF) and - 40.5% (ES), observed with apical treatment of HUVEC monolayers as shown in Figure 4.12 (a). This was associated with an increase in tracer leakage (74.8% vs. 85.1% for EF, 130.3% vs. 135.6% for ES) following larval treatment of the apical and both chambers, as described in Table 4.5. Tracer leakage, shown in Figure 4.12 (b), displayed a biphasic pattern with a slow increase in TRITC-albumin crossing HUVEC monolayers, which were treated on the apical and both chambers, over the first 40 minutes of the permeability assay. Significant tracer leakage was then observed as early as 60 minutes post-treatment (apical and both chambers only, P < 0.01) and was found to increase over the 2 hour-study (Figure 4.12, b).
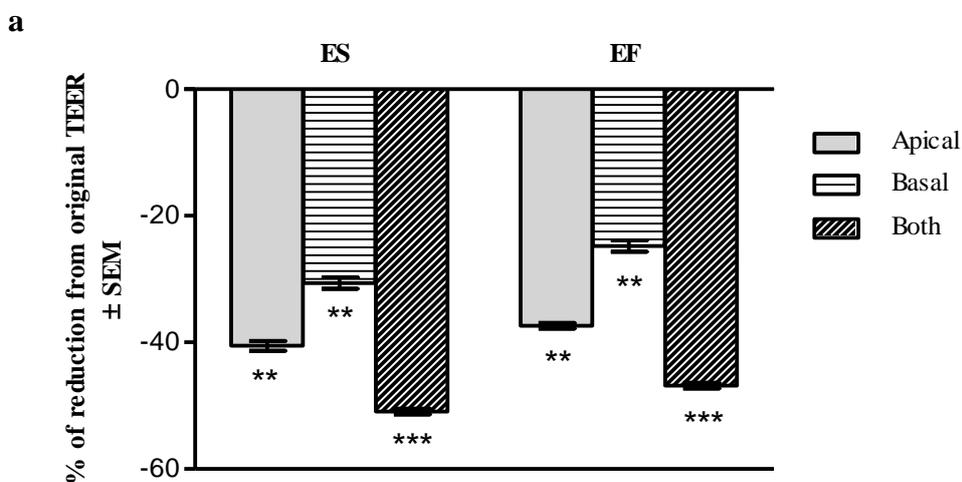
b
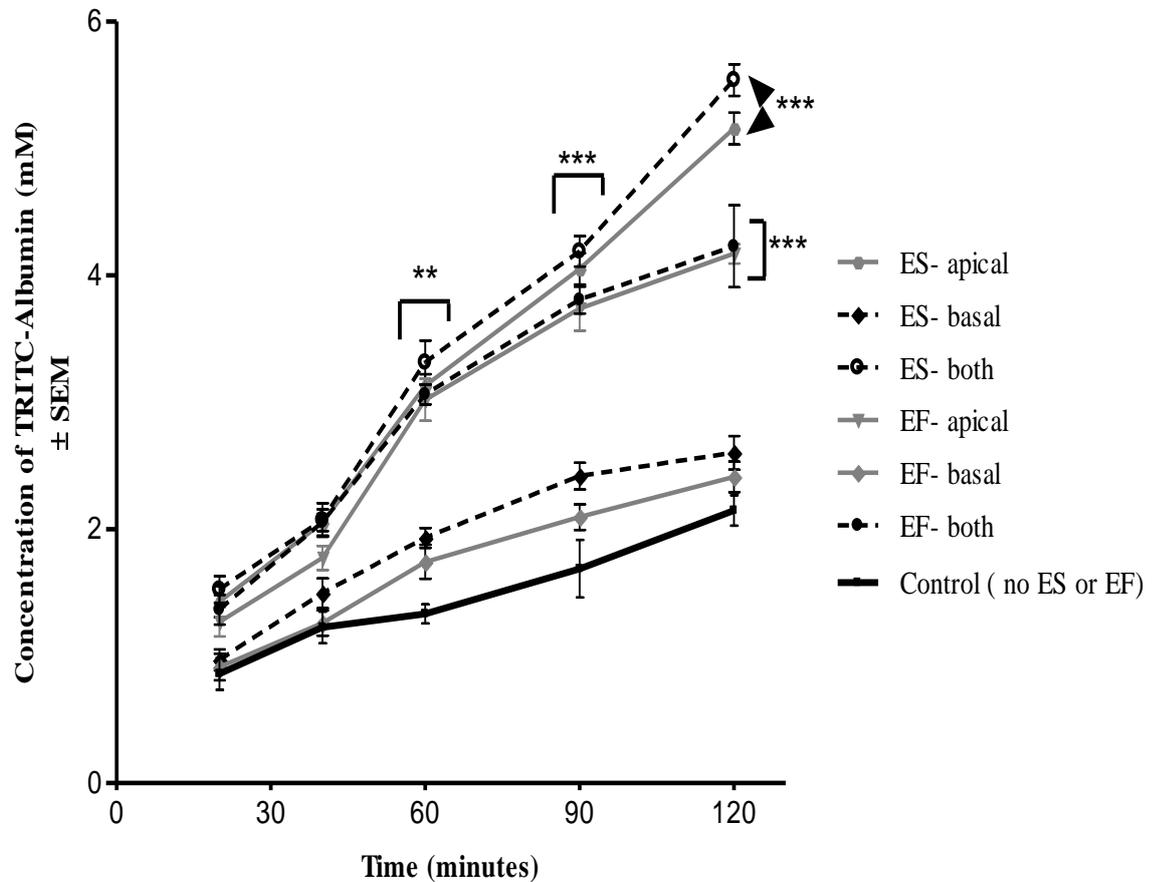
Figure 4.12   Effects of apical/basal administration of larval products on monolayer permeability. a) Percentage of reduction in TEER from untreated HUVEC monolayers, during treatment with larval products. TEER values are presented as a percentage of reduction in TEER ± SEM, ** = P < 0.01 and *** = P < 0.001 compared to original TEER of untreated controls. b) Leakage of TRITC-albumin over time with larval products at the apical, basal or both chambers. TRITC-albumin concentrations are reported as the mean ± SEM. ** = P < 0.01, *** = P < 0.001 compared to untreated controls.

In contrast, the presence of both larval products individually in the basal chamber caused a significant decrease in monolayer resistance (- 24.7% for EF, - 30.6% for ES, P < 0.01) as shown in Figure 4.12 (a), and a slow increase in tracer leakage which continued over the 2 hour-assay (Figure 4.12, b). A minor increase in TRITC-albumin levels (1.4% for EF, 8.6% for ES) was observed after the 2 hour-permeability assay, compared to untreated monolayers (Table 4.5).

Table 4.5   Percentage of increase in TRITC-albumin leakage across treated monolayers, calculated following equation 4.2. Significance was defined as P < 0.05 compared to untreated HUVEC monolayers with *** = P < 0.001.

Administration of larval products	% of increase in TRITC-albumin leakage	
	EF	ES
Apical (***)	+ 74.8	+ 130.3
Basal	+ 1.4	+ 8.6
Both Chambers (***)	+ 85.1	+ 135.6

4.3.2.3   Effects of protease inhibition of larval products on monolayer
           permeability

The use of protease inhibitors singly and in combination prior to treatment of
HUVEC monolayers with larval EF/ES products resulted in a better
preservation of endothelial barrier properties as revealed by improved TEER
and reduced tracer leakage across treated monolayers. Inhibitors, used together,
were the most effective treatment resulting in a minimal reduction in TEER
(16.6% for EF, 18.4% for ES) compared to the resistance of individually-
treated (especially with PMSF; 27.9% for EF, 33.3% for ES) and inhibitor-free
(46.8% for EF, 50.9% for ES) monolayers (Figure 4.13, a). The measured
TEER values agreed with the subsequent, statistically significant reduction in
tracer leakage values measured post-treatment and summarised in Table 4.6.
The use of inhibitor cocktails resulted in an increase in tracer leakage of 28.4%
vs. 85.1% (EF) and 32.5% vs. 135.6% (ES), compared to inhibitor-free
monolayers. Individual inhibitors also showed a significant reduction in tracer
leakage, such as PMSF associated with leakage of 60.8% vs. 85.1% (EF) and
84.9% vs. 135.6% (ES) compared to untreated, inhibitor-free monolayers, as
demonstrated in Figure 4.13 (b).

a

b
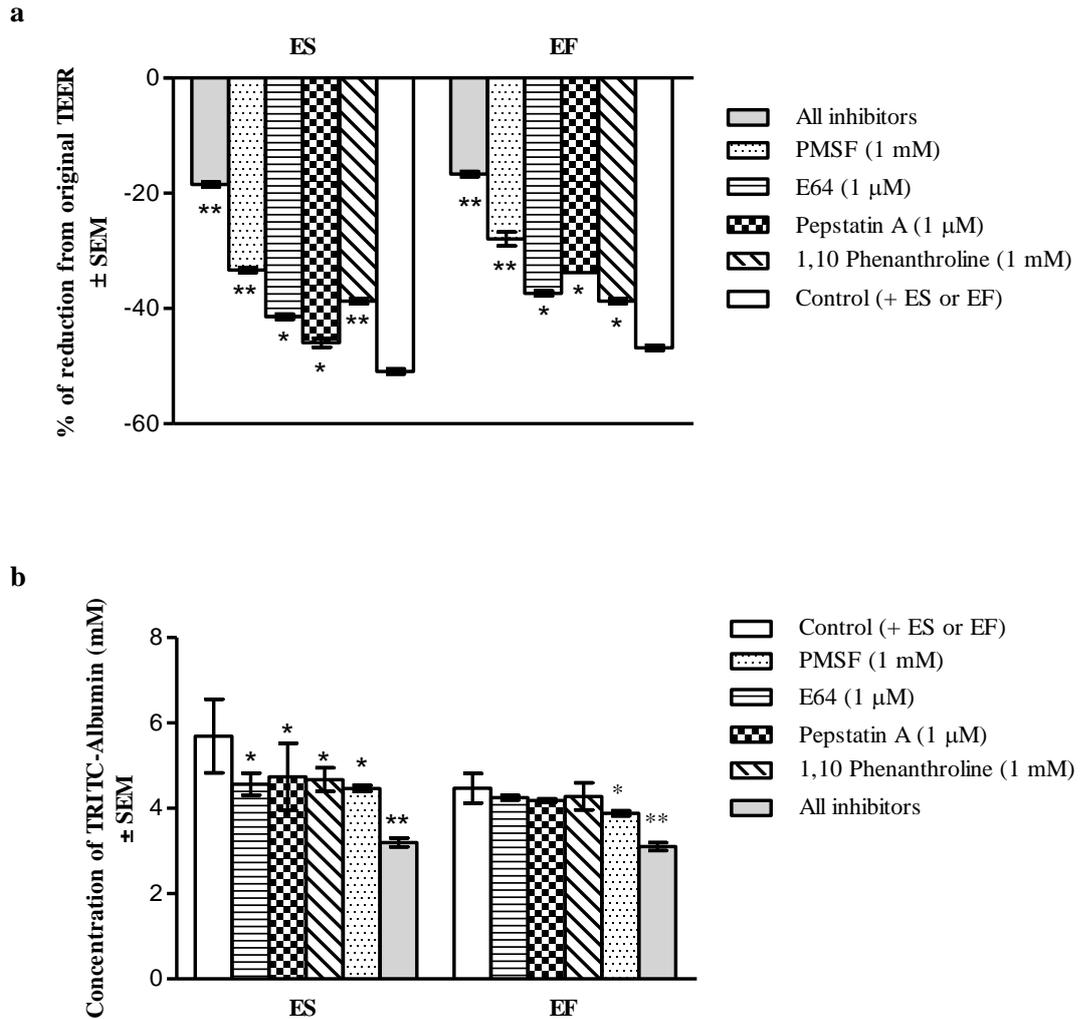
Figure 4.13 Effects of protease inhibition of larval products on monolayer permeability. a) Percentage change in transendothelial electrical resistance (TEER) from control resistance during treatment with larval products. TEER values are presented as a percentage of reduction in resistance ± SEM, ** = P < 0.01 and *** = P < 0.001, compared to reduction in TEER of EF/ES treated controls. b) TRITC-albumin leakage across HUVEC monolayers post-treatment with protease inhibitors. Tracer concentrations are reported as the mean ± SEM. * = P < 0.05 and ** = P < 0.01, compared to EF/ES treated controls.

Table 4.6 describes the percentage increase in tracer leakage across HUVEC monolayers, treated with larval products in the presence of protease inhibitors. Inhibitors, used individually, were associated with a moderate increase in tracer leakage while treatment with all inhibitors, in combination, demonstrated the lowest leakage of TRITC-albumin (shown in red), compared to monolayers treated with larval EF/ES products only (shown in bold). Of note was that preservation of endothelial permeability was greater with inhibition of ES products than EF products ($P < 0.05$).

Table 4.6   Percentage of increase in TRITC-albumin leakage across treated monolayers, after the 2 hour-permeability assay.

Concentration of larval products (µg/mL)	% of increase in TRITC-albumin leakage	
	EF	**ES**
E64	+ 75.9	+ 89.1
Pepstatin A	+ 73.1	+ 96
1, 10 phenanthroline	+ 77.2	+ 93.3
PMSF	+ 60.8	+ 84.9
All inhibitors	+ 28.4	+ 32.5
Controls (+ EF or ES)	**+ 85.1**	**+ 135.6**

4.3.2.4   Effects of post-infection IgG antibodies on monolayer permeability

The use of IgG antibodies, taken from individuals naturally infected with *Necator americanus*, induced no change in the disruption of endothelial monolayers caused by *Necator americanus* larval products. In Figure 4.14 (a and b) describing larval-induced reduction in monolayer resistance, both post-infection IgG and control sera (from healthy, non infected individuals) were unable to prevent the significant decrease in TEER, previously described with larval EF and ES products. TEER, measured after the 2 hour-treatment, was significantly reduced to ~ 45% and 51%, with EF and ES respectively (Figure 4.14, c).

b- ES products

c- EF vs ES products
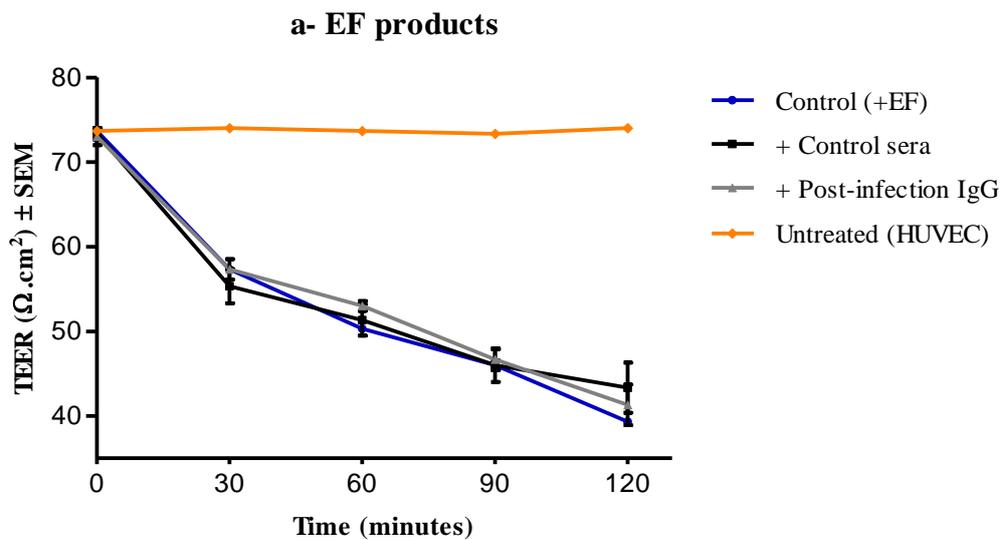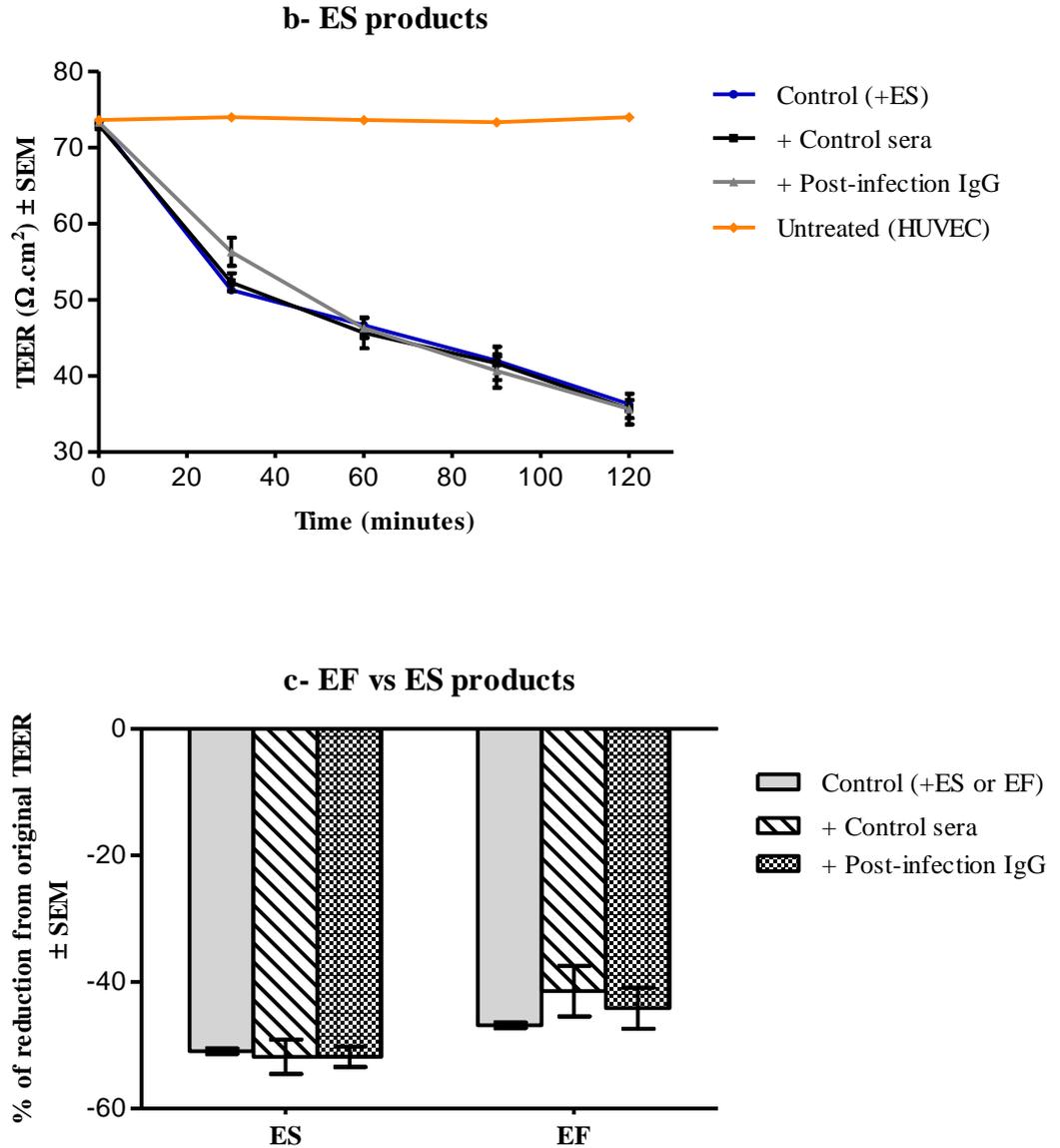
Figure 4.14 **Changes in TEER across HUVEC monolayers, following treatment of larval products with post-infection IgG antibodies; a) EF products and b) ES products. c) Percentage of reduction from control TEER for EF and ES products at the end of the 2 hour-treatment. TEER values are presented as a percentage of reduction in original TEER ± SEM and statistically compared to EF/ES treated controls.**

In accordance with changes in monolayer resistance, treatment with post-infection IgG and control sera was associated with a significant, continuous increase in TRITC-albumin leakage, compared to antibody-free monolayers (Figure 4.15, a and b). At the end of the 2 hour- permeability assay, tracer leakage was significantly higher than that across untreated HUVEC monolayers, except for those ES-treated monolayers in the presence of post-infection IgG (Figure 4.15, c). Although a modest inhibition of larval-induced increase in tracer leakage was observed, these results indicated that post-infection IgG were unable to preserve monolayer integrity by inhibiting larval activities.

b- ES products
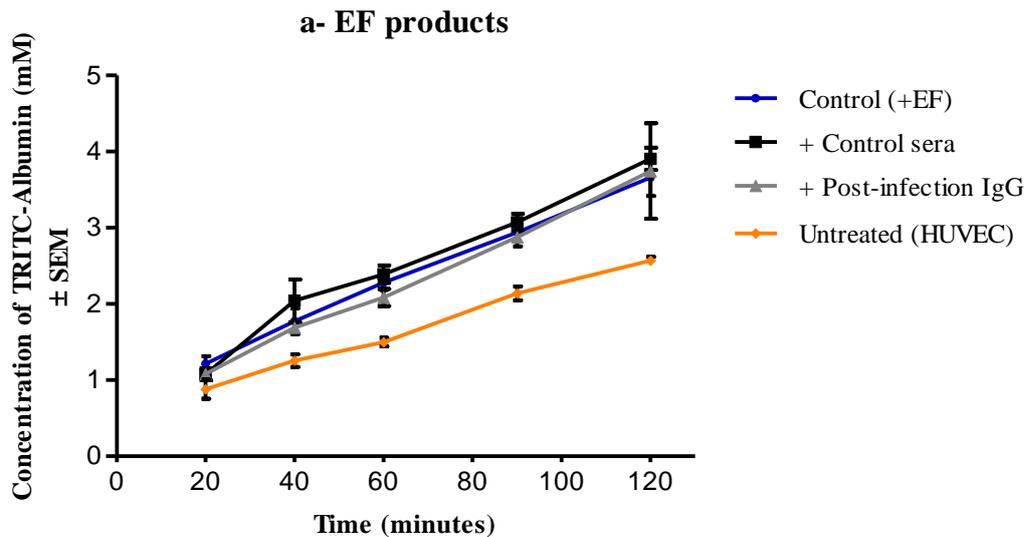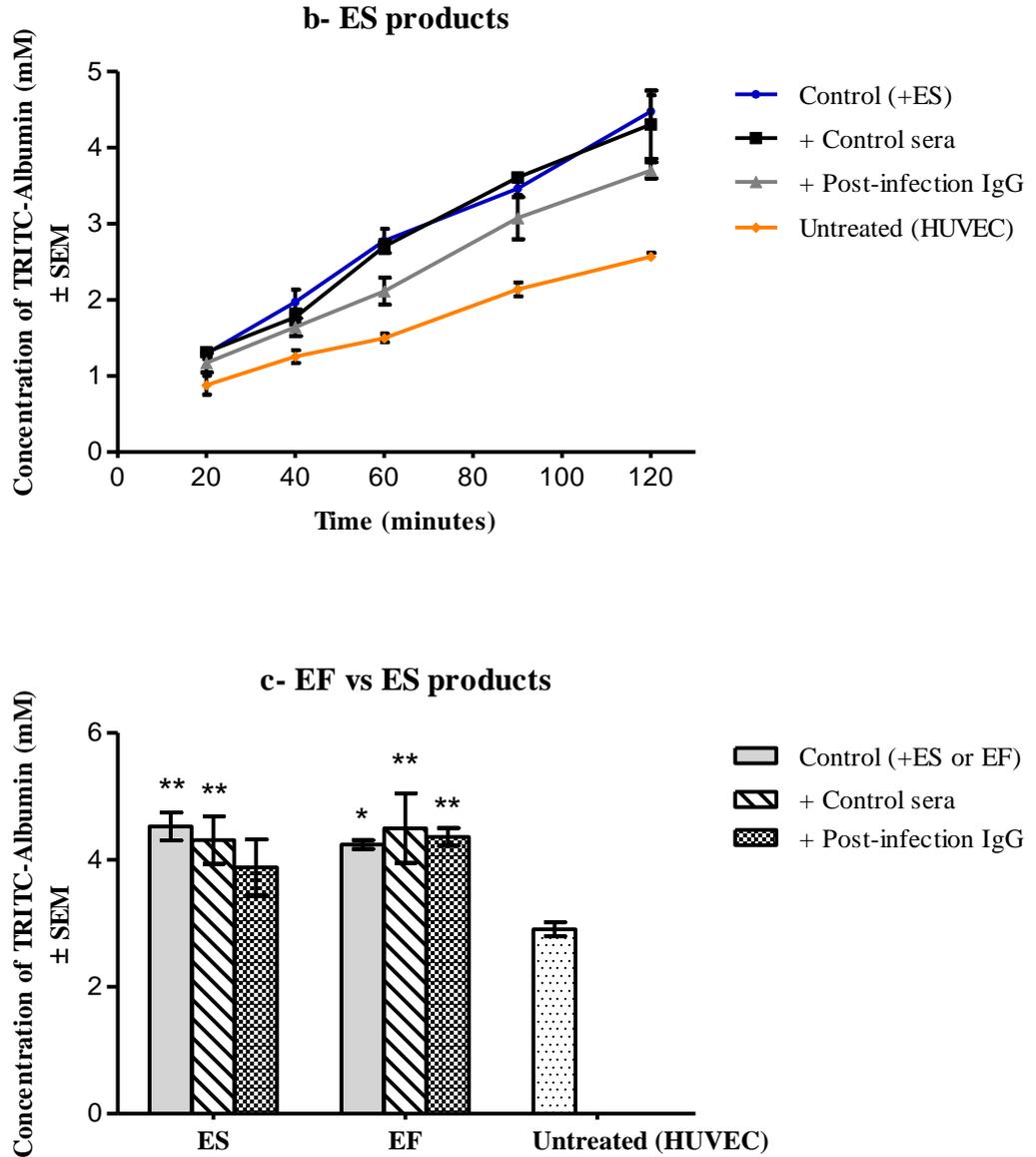
c- EF vs ES products

Figure 4.15 **Leakage of TRITC-albumin across HUVEC monolayers post-treatment with post-infection anti worm IgG antibodies, in response to; a) EF products, b) ES products and c) EF vs. ES products at the end of the 2 hour-study. TRITC-albumin concentrations are presented as the mean ± SEM. * = P < 0.05 and ** = P < 0.01, compared to untreated HUVEC controls.**

4.4 Discussion

Human umbilical vein endothelial cells (HUVECs) were used as an *in vitro* model of the human endothelium to study the interaction between *Necator americanus* larval enzymes and the vascular endothelium. The physical integrity of HUVEC monolayers was examined using transendothelial electrical resistance (TEER) and solute permeability assays. A rapid increase in TEER values was characteristic of the 48 hours post-seeding on transwell inserts and indicative of the continuous growth of HUVEC monolayers. Once confluent, the resistance across HUVEC monolayers reached a ceiling of 72 to74 $\Omega.cm^2$ which was maintained over the following 72 hours (Figure 4.3). The resistance measured in these HUVEC monolayers was higher than that demonstrated in a study by Blum *et al* (1997), in which TEER values of confluent HUVEC monolayers reached a maximum of 20 $\Omega.cm^2$. The difference between these studies may be due to growing HUVEC monolayers at different passages, as described by Man *et al* (2008). All the cultures used in this study were used at passages 1—3, ensuring restrictive, confluent HUVEC monolayers with all molecular occupancy of endothelial junctions (Figure 4.9). However, HUVEC monolayers exhibited lower resistance than other cell lines including human brain endothelial cells (150—155 $\Omega.cm^2$), as reported by Blum *et al* (1997). This is primarily due to the almost-total absence of tight junctions-associated proteins in HUVEC monolayers, previously described in the literature (Stins *et al*, 1997), and re-examined in this thesis. Figure 4.9 (b) showed that occludin, the tight junction molecule which is abundantly present in endothelial cells from vascular beds with restrictive permeability, was moderately observed in HUVEC endothelial monolayers, mostly accounting

for the considerably low resistance of these monolayers and re-emphasising the molecular heterogeneity observed in the endothelium, as described in section 1.3.3.

Resistance across HUVEC monolayers had a strong inverse linear relationship with tracer leakage, suggesting that the integrity of endothelial monolayers at confluence was associated with the highest resistance and the lowest solute permeability (Dewi *et al*, 2004; Dewi *et al*, 2008). The great ability of confluent HUVEC monolayers to reduce tracer leakage compared to cell-free inserts (by 81%), allowed these monolayers to be used as a predictor of putative substances that can enhance endothelial permeability.

The morphology of HUVECs changed from elongated, early in their growth, to a typical cobblestone shape with more cell to cell contacts once monolayers reached confluence. These observations emphasised that the increase in the integrity of endothelial monolayers accounted for the increase in their resistance and subsequently, their barrier functions. VE-cadherin, the adhesion molecule which is detected only in vascular endothelial cells (Liaw *et al*, 1990; Lampugnani *et al*, 1992; Leach *et al*, 1993), is believed to increase the stabilisation of junctional structure by being anchored to the actin cytoskeleton (Dejana *et al*, 2000; Firth, 2002). In this study, confluent HUVEC monolayers exhibited a continuous presence of VE-cadherin at cellular junctions while F-actin was localised peripherally, at cell to cell borders (Figure 4.9).

In this chapter, studies were focused on investigating changes in the vascular permeability related to larval enzymatic activity. Results demonstrated a dose related increase (0.05—1.5 µg/mL) in HUVEC monolayer permeability to albumin following treatment with larval products, as shown by reduced transendothelial electrical resistance (TEER) and increased leakage of TRITC-albumin (Figures 4.10 and 4.11, respectively). Disruption of endothelial barrier functions (i.e. permeability) was most significant upon treatment with larval ES products emphasising the potential involvement of excretory/secretory (ES) products in the penetration process and the interaction between *Necator americanus* larvae and the endothelium. Bacteria, such as *Prophyromonas gingivalis*, were also shown to gain access to the host by inducing an increase in vascular permeability in response to parasitic proteinases (Imamura *et al*, 1995). In addition, treatment of HUVEC monolayers with larval products at high doses was also associated with significant alterations in their barrier properties, observed as early as 40 minutes post-treatment, indicating that a strong presence of larval products may associate with an earlier disruption of the endothelium and faster entry of larvae into the host's microcirculation. However, the use of larval products at low doses (i.e. 0.05 µg/mL) induced a significant reduction in monolayer resistance but had no major effect on tracer leakage across treated monolayers, implying that TEER is a more sensitive marker to changes in endothelial permeability.

A two-phase increase in monolayer permeability was induced by larval products applied to the apical chamber or following apical and basal simultaneous treatments of HUVEC monolayers and is described as a slow

increase in tracer leakage during the first 40 minutes and a subsequent rapid increase over the last 60 minutes of the assay. However, basal treatments of HUVEC monolayers were associated with a slow, non significant increase in permeability (i.e. tracer leakage). These changes suggest that direct bathing with larval products allowed them to negotiate and disturb endothelial monolayers faster compared to monolayers treated from the basal side. The increase in permeability upon basal treatments may be delayed due to the need to navigate multiple layers (i.e. plastic membrane and gelatin coating in the experimental setup), before reaching the cells. *In vivo*, larval-induced permeability upon apical application may account for larval migration from the blood into the surrounding tissue during the lung-stage, possibly with similarity to transendothelial migration of leukocytes during inflammatory reactions (Moll *et al*, 1998) while increased permeability following basal application may facilitate larval entry into the microcirculation. Larvae are therefore required to breach the basement membrane before reaching the endothelium which is possibly facilitated by the ability of *Necator americanus* larval enzymes to digest skin macromolecules including collagen IV and laminin, the main components of all basement membranes, as described in chapter 3.

The use of enzyme inhibitors demonstrated the importance of the combined effect of serine, cysteinyl, aspartyl and metalloproteases in modulating endothelial permeability (Figure 4.13). Although the use of all inhibitors in combination exhibited the highest protection of endothelial integrity, a total preservation of endothelial barrier functions was never seen which suggests that other larval enzymes may also be involved, therefore requiring further

characterisation of larval EF and ES products. This also suggests that enzyme inhibitors are not wholly effective, even as cocktails, against mixed enzyme populations. In addition, treatment with larval products might also trigger the activation of matrix metalloproteinases (MMPs) from endothelial cells which in turn, can be partially responsible for inducing an increase in vascular permeability (Lafleur *et al*, 2001; Alexander, 2002; Johannsson *et al*, 2007). Inactivation of tissue-associated protease inhibitors might also be triggered in the presence of *Necator americanus* larval enzymes leading to an increase in vascular permeability, as previously observed with *Schistosoma mansoni* species (Hansell *et al*, 2008). Furthermore, post-infection IgG were unable to prevent larval-induced endothelial permeability, indicating that these antibodies act as a competitive substrate to larval enzymes, not affecting the functionality of these enzymes as suggested in chapters 2 and 3, and that antibodies against specific larval enzymes may be required to provide better protection against hookworm infection at early stages. Due to the significance of larval migration during early stages of the hookworm infection, mechanisms underlying larval-induced permeability will be addressed in chapter 5.

5. Cellular mechanisms underlying endothelial responses to

Necator americanus larval products

5.1 Introduction

Vascular permeability has been shown to change in response to pathophysiological stimuli including permeability increasing agents such as vascular endothelial growth factor (VEGF), proteases and inflammatory mediators including histamine and thrombin (Imamura *et al*, 1995; Esser *et al*, 1998; Vogel *et al*, 2001; Hansell *et al*, 2008). The pro-inflammatory effects of thrombin, a serine protease of major importance in the coagulation cascade, and gingipains, cysteine proteases derived from *Porphyromonas gingivalis*, have been shown to be mediated by activation of endothelial cells to promote the production of acute inflammatory cytokines including IL-6 (Day *et al*, 2006) and IL-8 (Inomata *et al*, 2007), respectively. Neutrophil derived proteolytic activities have also been shown to mediate increased vascular permeability and enhanced transmigration of monocytes through the activation of endothelial cells and IL-8 release (Lukacs *et al*, 1995; Moll *et al*, 1998).

On a morphological and a functional basis, one of the major structures regulating vascular permeability is the inter-endothelial cleft. Junctional adhesion molecules located in this cleft are essential for establishing strong homotypic and heterotypic connections and anchoring junctional molecules to the cellular actin cytoskeleton, promoting stabilisation of junctions (Dejana *et al*, 2000; Firth, 2002). Protease-related alterations in vascular permeability concurred with reorganisation of actin filaments and formation of intercellular gaps in the endothelial barrier, as described previously by Moll *et al* (1998) and Young *et al* (2003). In addition, disruption of essential adhesion molecules at endothelial cell to cell contacts has been reported, evidenced by the

remodelling of VE-cadherin in response to actin modulating stimuli (Hordijk *et al*, 1999). The involvement of junctional components in modulating the vascular permeability has been described in section 1.3.4.

In chapter 4, *Necator americanus* larval enzymes induced an increase in vascular permeability, which might be related to cytotoxic effects of larval enzymes causing endothelial cells to detach and leading to a degree of disruption in the endothelial integrity. However, junctional structures present another potential gateway for *Necator americanus* larvae to breach the endothelium and enter the blood circulation. In this chapter, the effects of *Necator americanus* larval EF and ES products on the viability of cells and on cell to cell junctions were investigated. The latter involved staining for actin filaments and VE-cadherin, the main junctional components with a major role to play in modulating permeability, as described in section 1.3.4. In addition, larval-induced activation of endothelial cells was determined by measuring cellular secretions of cytokines (IL-6 and IL-8) and VEGF, which have been implicated in protease-induced vascular permeability.

5.2 Methods

5.2.1 Quantification of cellular responses using Enzyme Linked ImmunoSorbent Assay (ELISA)

Following treatment with EF/ES products, cell supernatants were collected, centrifuged for 10 minutes at 13000 x g to remove cell debris, and stored at -20˚C pending analysis. Human VEGF, IL-6 DuoSet$^{®}$ ELISA Development kit and IL-8 ELISA kit were used to quantify VEGF, IL-6 and IL-8 in the supernatants according to the manufacturers' recommendations (Table 5.1). In brief, a capture antibody was diluted to an appropriate working concentration and used to coat a 96 well Nunc MaxiSorb plate (100 µL per well). The plate was sealed and incubated overnight at room temperature or at 4˚C (IL-8 only) after which time wells were extensively washed with PBS containing 0.05% Tween 20 and blocked for 1 hour at room temperature with 1% bovine serum albumin in PBS (300 µL of 1% BSA/PBS per well). Following three washes with PBS/0.05% Tween 20, standards and cell supernatants were diluted in 1% BSA/PBS, added as 100 µL per well and incubated for 2 hours at room temperature. The wells were carefully aspirated and washed with PBS/0.05% Tween 20 and 100 µL of an appropriate detection antibody was added per well and incubated for 2 hours at room temperature. After careful washing, 100 µL of Streptavidin-Horseradish Peroxidase (HRP, diluted 1:200 (v/v) in 1% BSA/PBS) was added per well and incubated for 30 minutes at room temperature. Extensive washing of the wells was followed by the incubation of 100 µL of TMB substrate solution per well (prepared as described in section 2.2.7.3) for 20 minutes at room temperature and the reaction was stopped by adding 50 µL of 2.5 M sulphuric acid per well.

Table 5.1   Summary of materials used in the ELISA procedure.

Step	VEGF	IL-6	IL-8
Capture antibody	Diluted with PBS and used at 1 µg/mL	Diluted with PBS and used at 2 µg/mL	Diluted in 0.1 M phosphate buffer, pH 9.0 and used at 1 µg/mL
Standards	Diluted with 1% BSA/PBS, concentration range 1—60 pg/mL, overnight at room temperature	Diluted with 1% BSA/PBS, concentration range 1—75 pg/mL, overnight at room temperature	Diluted with 1% BSA/PBS/0.05% Tween 20, concentration range 0.1—100 pg/mL, overnight at 4˚C
Samples	Diluted 1:2 (v/v) with 1% BSA/PBS	Diluted 1:2 (v/v) with 1% BSA/PBS	Diluted 1:2 (v/v) with 1% BSA/PBS/ 0.05% Tween 20
Detection antibody	Diluted with 1% BSA/PBS and used at 100 ng/mL	Diluted with 1% BSA/PBS and used at 200 ng/mL	Diluted with 1% BSA/PBS/0.05% Tween 20 and used at 1 µg/mL
Detection limits	1—2000 pg/mL	1—600 pg/mL	0.1—1000 pg/mL

The optical density of each plate was immediately determined using a DYNEX MRX Microplate Reader at 450 nm. Samples were assessed in duplicate and results are expressed as means ± standard error of the mean (SEM).

5.2.2   Estimation of cell viability

Cells were grown to confluence on 1% gelatin coated-96 well plates and treated with EF/ES products at 1.5 µg/mL, as described in section 4.2.3.2. Treated HUVEC monolayers were then exposed to 100 µL/well of resazurin solution used at a concentration of 10 µg/mL (in pre-warmed Hank's Balanced Salt Solution) and incubated at 37°C and 5% CO_2 in air for 1 hour (Kim *et al*, 2009). Viability was determined as the ability of live cells to oxidise resazurin to the fluorescent resorufin. Fluorescence was measured using FLUOstar Galaxy Microplate Plate Reader (excitation = 530 nm, emission detection = 590 nm) and values were expressed as the percentage of the fluorescence compared to untreated HUVEC controls.

5.2.3   Immunocytochemistry

5.2.3.1   <u>Staining</u>

Post-treatment, HUVEC monolayers were gently washed and fixed for 10 minutes in 1% (w/v) paraformaldehyde (PFA), permeabilised for 10 minutes with 0.15% (v/v) Triton X-100, and blocked for 30 minutes in phosphate buffered saline (PBS) containing 5% (v/v) normal human serum, at room temperature (described in section 4.2.5). Cells, stained for VE-cadherin, were incubated overnight at 4°C with monoclonal anti-CD 144 (at 10 µg/mL) followed by extensive washing with 0.1% BSA/PBS. The secondary antibody, FITC conjugated anti-mouse IgG (diluted to 1:50 (v/v)) was then added and

cells were incubated for 2 hours at room temperature, in the dark. Staining for F-actin was performed by incubating cells with FITC conjugated phalloidin (50 μg/mL in PBS) for 2 hours at room temperature, in the dark. Both primary and secondary antibodies were diluted to the appropriate concentration with bovine serum albumin (0.1% BSA/PBS). Finally, cells were washed twice with 0.1% BSA/PBS followed by one wash with PBS and mounted in Vectorshield with propidium iodide to visualise the nuclei. Cells were then observed and imaged using a Leica TCS SP2 confocal laser scanning microscope, as described in section 4.2.6.2.

5.2.3.2   Quantification of VE-Cadherin immunocytochemistry

Quantification of VE-Cadherin staining was carried out using a systematic random selection method (Gunderson *et al*, 1999), in Adobe Photoshop 7. Four representative images per sample were analysed for certain features of junctional adhesion using grid counting including continuous, discontinuous (or stitch) and total loss of junctional VE-Cadherin from cell to cell contacts. Images were outlined and a grid superimposed. The size of the single grid box was 5 x 5 cm^2. A number was chosen, blind, from 1—8 and used as a starting point. Counting was carried out on grid boxes falling at the chosen number, by counting left to right, top to bottom and so on. Once four grid boxes in each image were counted, counting was stopped. These numbers were averaged then converted to a percentage of the staining feature to the total number of VE-cadherin junctions counted per sample.

5.2.4 Statistical analysis

Data were tested for significant differences using two-way ANOVA tests, followed by Bonferroni post-tests, and statistical significance was defined as $P < 0.05$. Analysis was carried out using GraphPad Prism version 5.01 and values are presented as means ± SEM.

5.3 Results

5.3.1 Viability of endothelial cells

Necator americanus larval products exhibited no cytotoxic effects on endothelial cells, as demonstrated by no significant changes in the metabolism of resazurin by HUVEC cells post-treatment with larval EF and ES products, compared to untreated control cells (Figure 5.1). Visual examination of HUVEC monolayers also proved that both untreated and larval-treated monolayers showed no cell detachment or disaggregation of HUVEC monolayers.
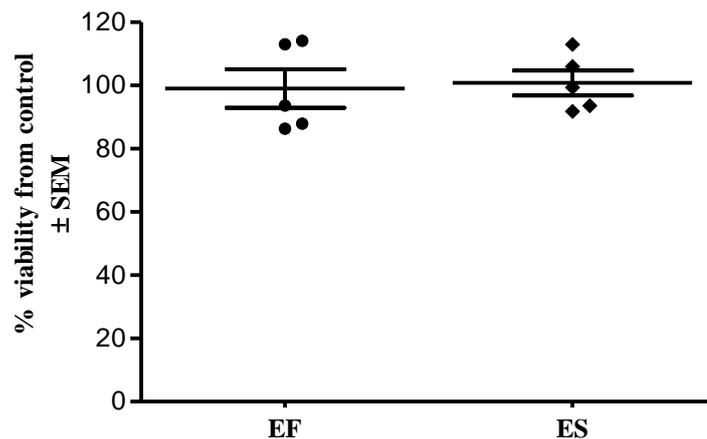
Figure 5.1 **Effects of *Necator americanus* larval activity on cell viability using resazurin metabolism assay. Viability, determined as the ability of viable cells to oxidise resazurin to the fluorescent resorufin, was measured in HUVEC monolayers post-treatment with EF/ES products. Results are presented as the percentage of resorufin fluorescence from HUVEC monolayers post-treated compared to untreated controls ± SEM. The optical reading of fluorescent resorufin in untreated HUVEC controls was 644.13 ± 57.36. Treatment with both EF and ES products demonstrated no statistically significant changes in cell viability (P > 0.05).**

5.3.2 Quantification of endothelial cell responses to *Necator americanus* larval activities

5.3.2.1 <u>Effects of concentration of larval products on endothelial cell responses</u>

The values of the optical density obtained from the ELISA standards were plotted against their concentrations and used to construct standard curves for VEGF and cytokines. Conversion of the optical density to concentration of secretions (pg/mL) aimed at eliminating any sources of variation in our data and generated semi-logarithmic graphs for VEGF, IL-6, and IL-8 as shown in Figure 5.2 (a—c). An equation of a straight trendline was also generated and used to determine unknown concentrations of VEGF, IL-6, and IL-8 in subsequent experiments.

a- VEGF

$$Y = 0.0256 \times Ln (X) + 0.0844$$

176

b- IL-6

$$Y = 0.1214 \times Ln(X) + 0.0048$$

c- IL-8

$$Y = 0.2758 \times Ln(X) + 0.7530$$
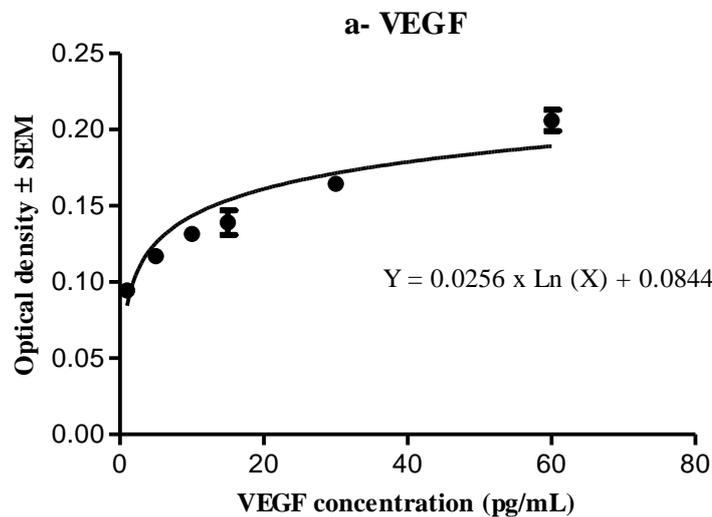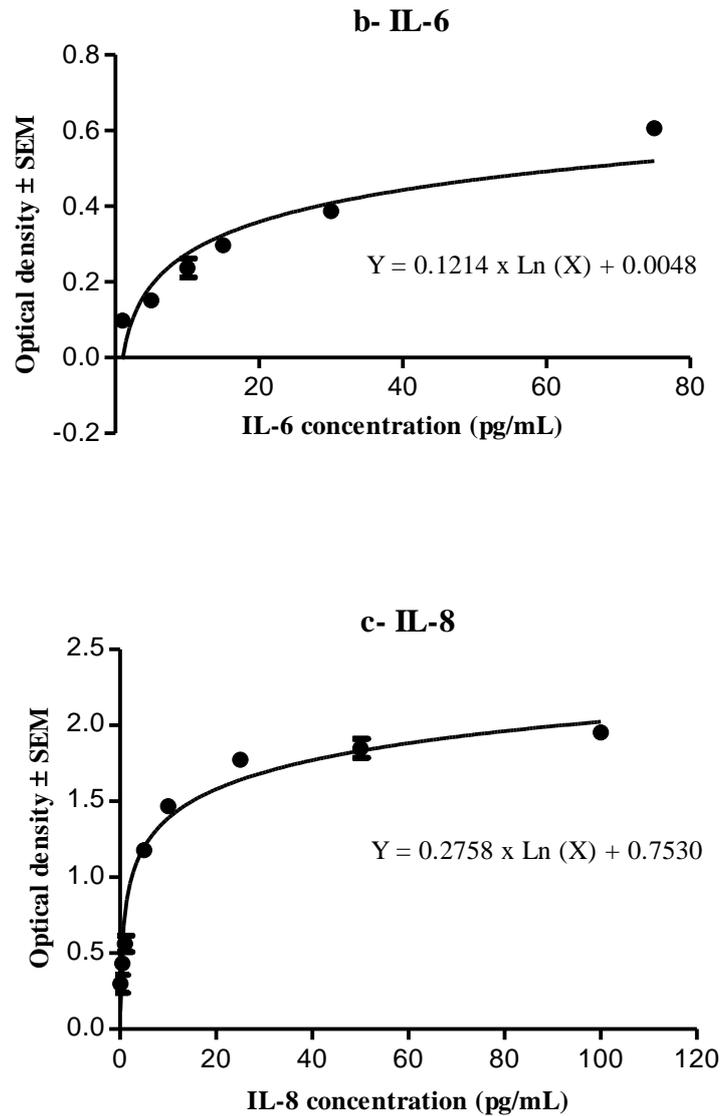
Figure 5.2 **Standard curves of the optical density plotted against the concentration of a) VEGF, b) IL-6, and c) IL-8. Values are expressed as the mean of the optical density ± SEM. A semi-logarithmic equation for each graph was generated.**

To assess the effects of larval products on the release of VEGF and cytokines from endothelial cells, levels of VEGF, IL-6, and IL-8 were determined in culture supernatants from cells pre-treated with EF/ES products, using ELISA. While larval products (both EF and ES) caused almost no change in VEGF release from HUVEC cultures (Figure 5.3, a), a significant increase in endothelial secretion of IL-6 (~ 2 fold) and IL-8 (~ 9 fold) was observed post-treatment with larval ES products at a final concentration of 1.5 µg/mL (Figure 5.3, b and c).

a- VEGF

Concentration of EF/ES preparation (µg/mL)

b- IL-6

Concentration of EF/ES preparation (µg/mL)
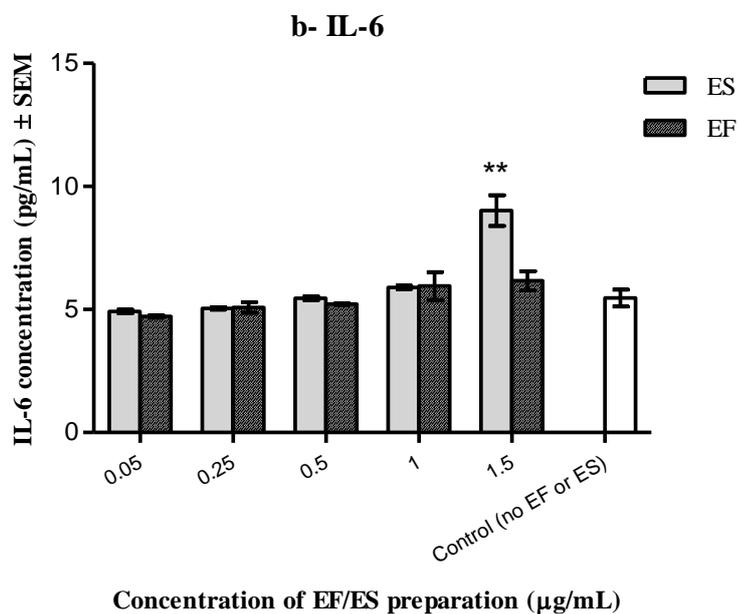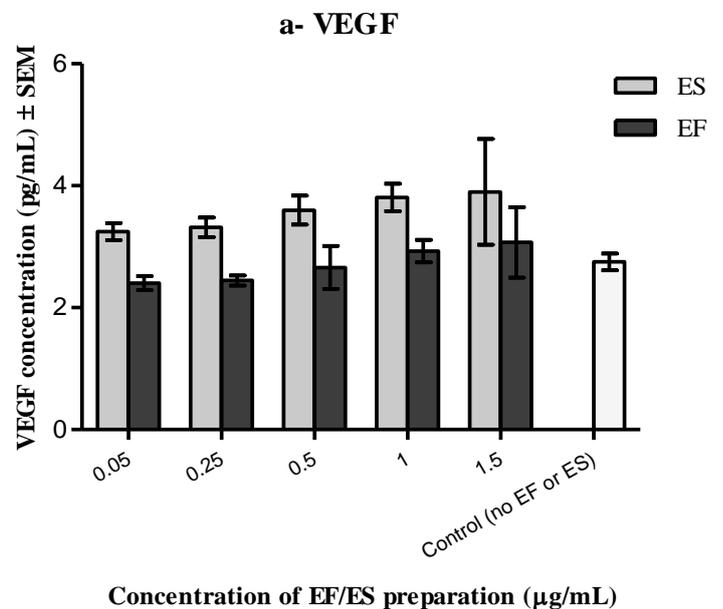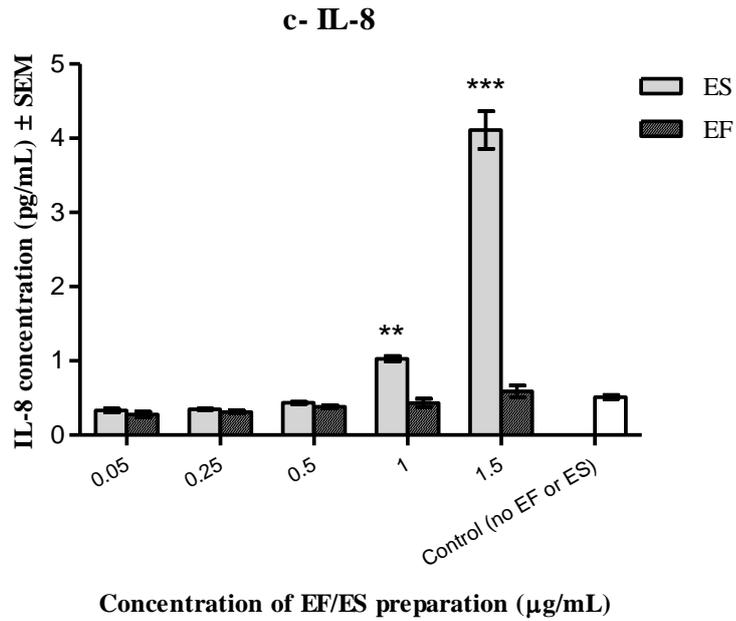
c- IL-8

Figure 5.3 **Quantification of a) VEGF, b) IL-6, and c) IL-8 secretions from HUVEC cells following treatment of monolayers with *Necator americanus* larval EF and ES products. Secretions were measured in duplicates and values are expressed as the mean of their concentrations (pg/mL) in the culture supernatants ± SEM. Statistical significance was determined as ** = P < 0.01 and *** = P < 0.001 compared to cytokine secretions from untreated HUVEC controls (no EF or ES).**

Changes in VE-cadherin staining were associated with alterations in monolayer permeability and endothelial cytokine secretions. Different concentrations of larval EF (Figure 5.4, a—e) and ES products (Figure 5.4, a'—e') induced a dose-dependent fragmentation of the continuous, junctional VE-cadherin, ultimately leading to total loss of VE-cadherin staining and the formation of wide intercellular gaps at higher concentrations (Figure 5.4). Quantification of VE-cadherin patterns emphasised the dose-dependent effects of larval EF and ES products on the integrity of HUVEC monolayers, as described by the significant decrease in the percentage of cellular junctions expressing continuous VE-cadherin (Figure 5.5, a) and the associated increase in the total loss of junctional VE-cadherin (Figure 5.5, c). The latter was significantly detected in the presence of ES products at a concentration as low as 0.5 µg/mL, opposed to EF products (1 µg/mL, Figure 5.5, c). However, the percentage of cellular junctions exhibiting discontinuous VE-cadherin was significantly higher than control monolayers and illustrated no dose-related response to larval products. Additionally, larval EF and ES products caused dose-related changes in F-actin localisation, loss of cortical actin, and increase in stress fibres and perinuclear actin, as seen in Figure 5.6. Thrombin, a serine protease, was used as a positive control which resulted in similar changes in the junctional VE-cadherin and F-actin localisation (Figures 5.4 and 5.6).

EF ES

EF   ES

0.5 µg/mL

1.0 µg/mL
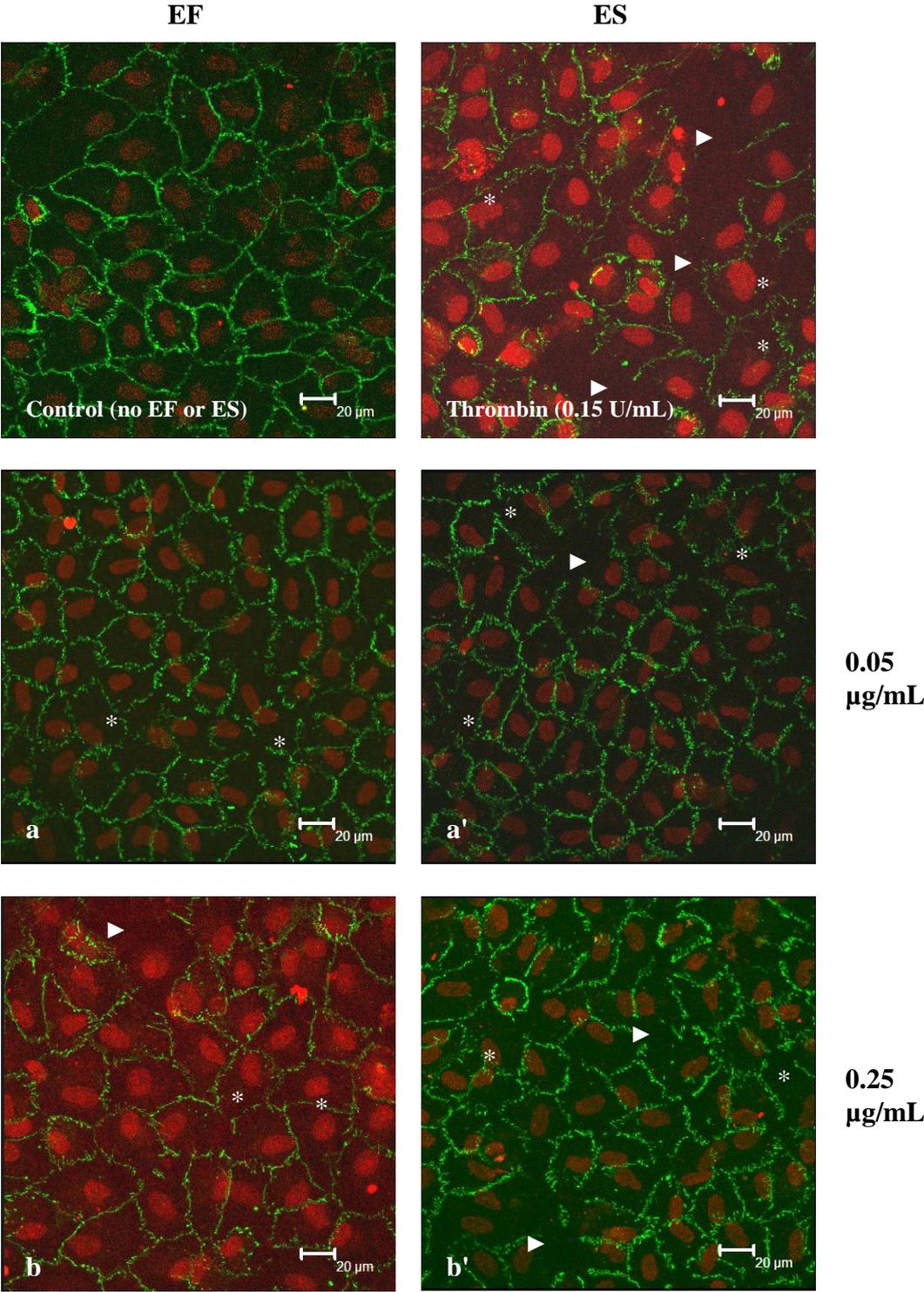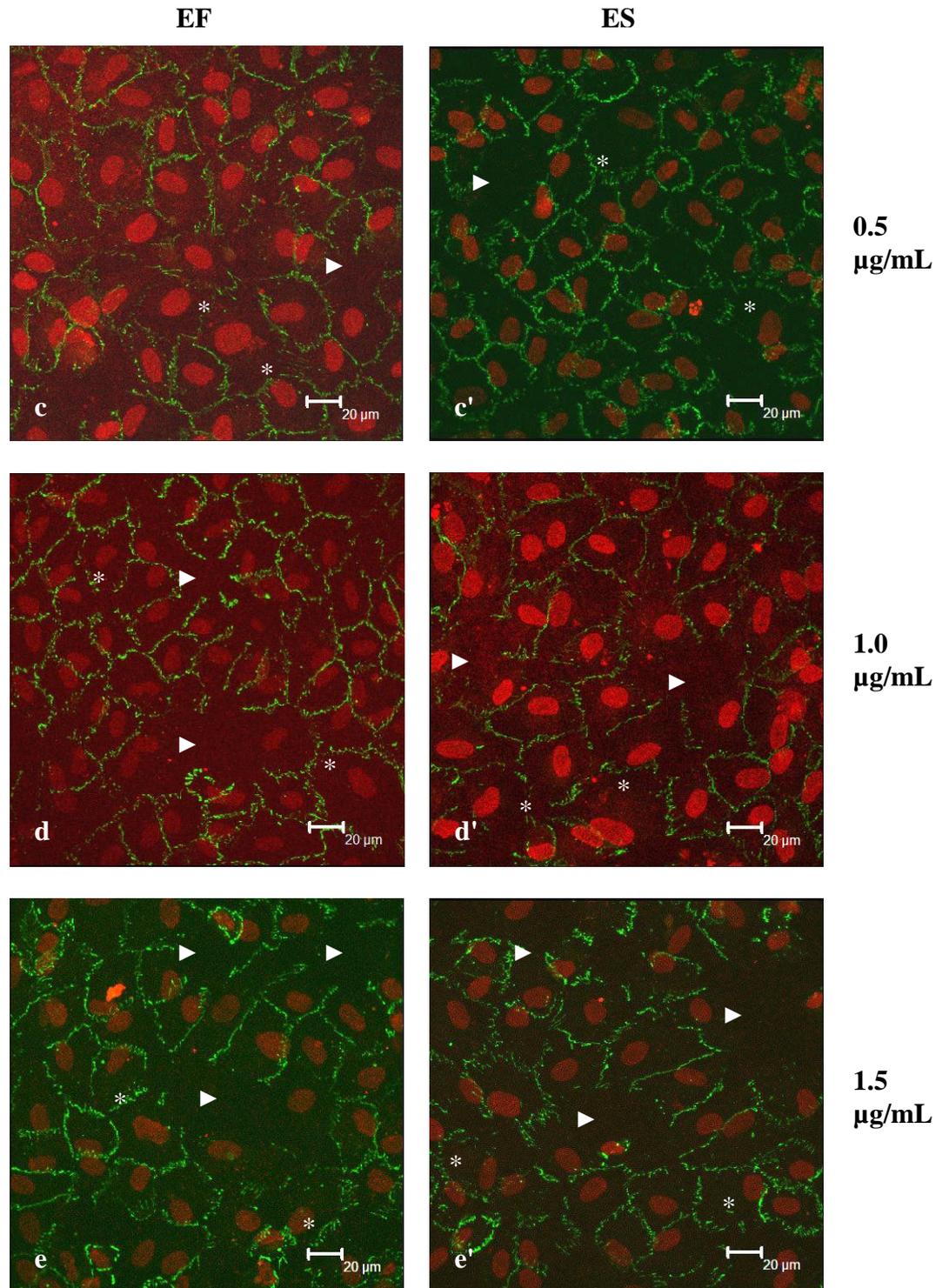
1.5 µg/mL

Figure 5.4   **Micrographs showing localisation of VE-cadherin at cellular junctions in monolayers treated with either EF (a—e) or ES products (a'—e'). HUVEC monolayers were pre-treated with larval EF/ES products at 0.05 µg/mL (a, a'), at 0.25 µg/mL (b, b'), at 0.5 µg/mL (c, c'), at 1 µg/mL (d, d'), and at 1.5 µg/mL (e, e'). Nuclei were stained with propidium iodide**

(red) and Bars = 20 μm. Arrowheads point at gaps in the monolayer, and *

shows regions of discontinuous VE-cadherin.
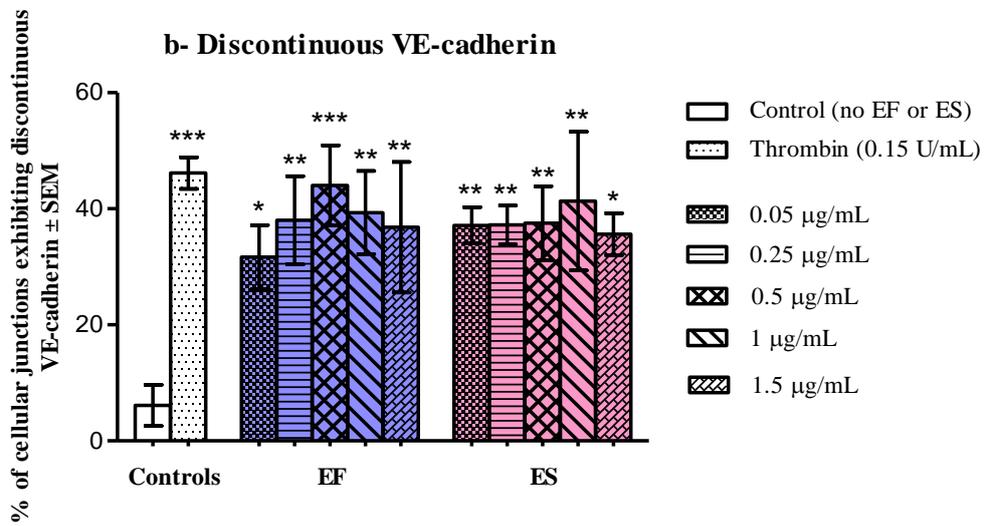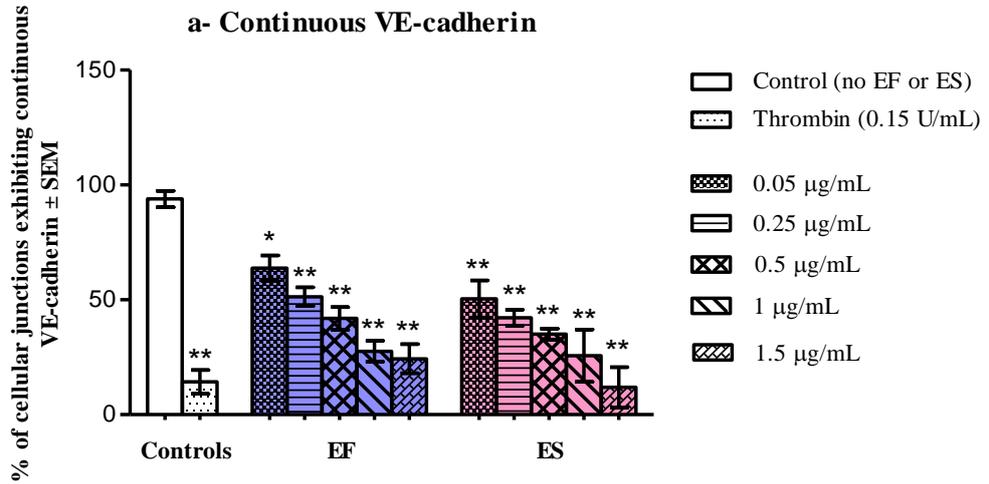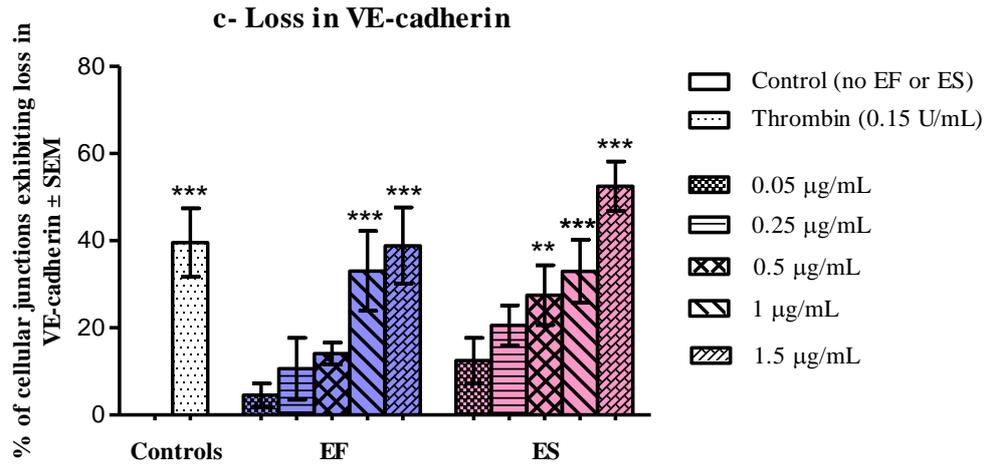
Figure 5.5 **Effects of *Necator americanus* larval activities on the pattern of VE-cadherin expression in HUVEC monolayers, described as continuous (a), discontinuous (b), and total loss of junctions (c). VE-cadherin expression is presented as the percentage of each pattern to the total number of junctions, counted per sample, ± SEM. Significance was defined as *** = P < 0.001, ** = P < 0.01, and * = P < 0.05 compared to untreated controls (no EF or ES).**

EF

ES

Control (no EF or ES)   20 µm

Thrombin (0.15 U/mL)   20 µm
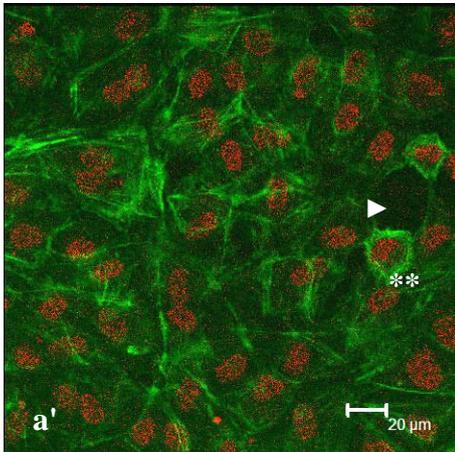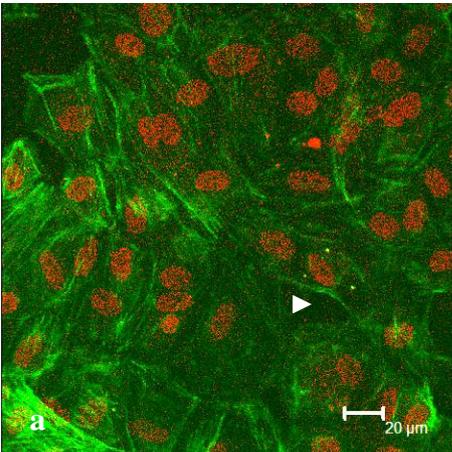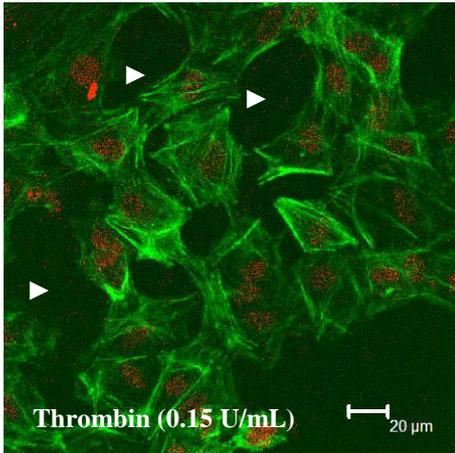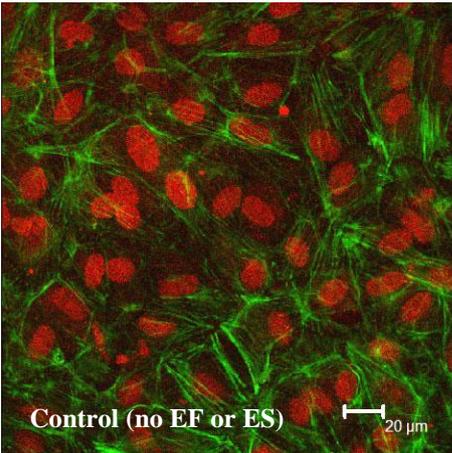
0.05 µg/mL
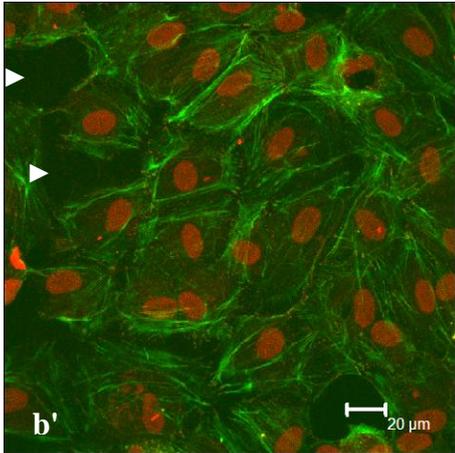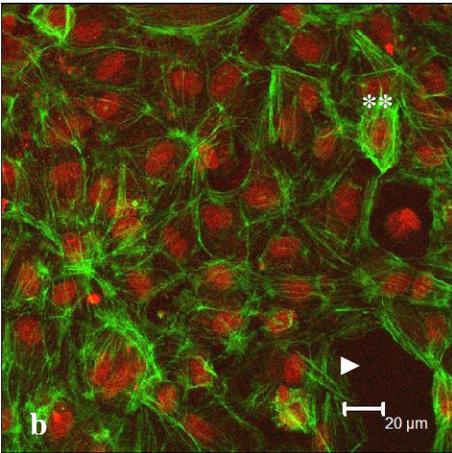
0.25 µg/mL
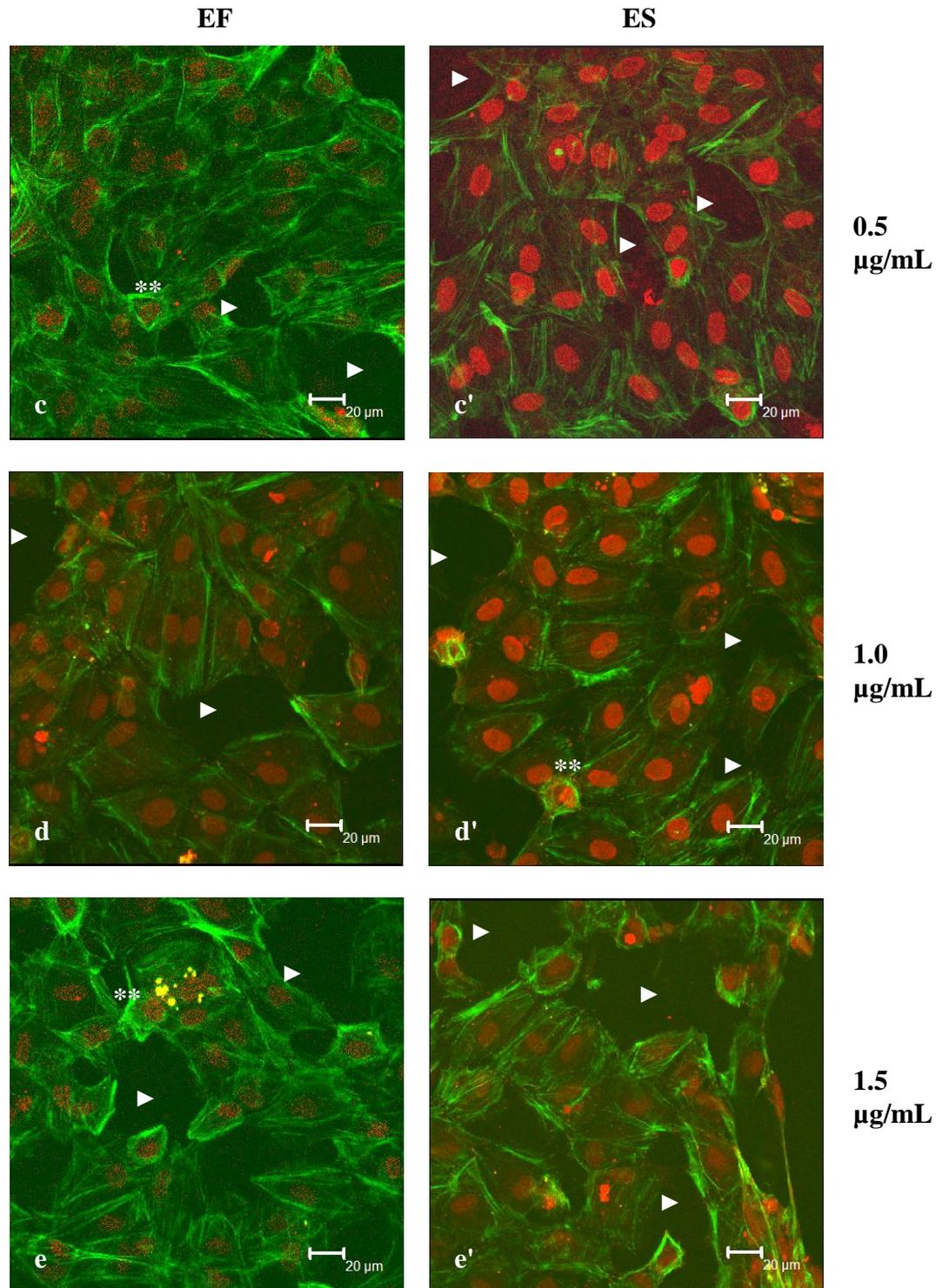
Figure 5.6 **Effects of *Necator americanus* larval activities on localisation of F-actin filaments at cellular junctions in monolayers treated with either EF (a—e) or ES products (a'—e'). HUVEC monolayers were pre-treated with larval EF/ES products at 0.05 μg/mL (a, a'), at 0.25 μg/mL (b, b'), at 0.5 μg/mL (c, c'), at 1 μg/mL (d, d'), and at 1.5 μg/mL (e, e'). Nuclei were stained with propidium iodide (red). Bars = 20 μm, arrowheads point at gaps in the monolayer and ** shows appearance of perinuclear actin.**

5.3.2.2 Effects of apical/basal administration of larval products on endothelial

cell responses

Treatment of HUVEC monolayers with larval ES products from the apical,

basal and both chambers induced a significant increase in the levels of secreted

IL-6 ($P < 0.01$) and IL-8 ($P < 0.001$), as shown in Figure 5.7. Although all

significant, alterations in IL-6 and IL-8 secretions were highest following

treatment in both chambers (~ 2 fold and ~ 13 fold, respectively) compared to

cytokine levels observed with the apical-treatment only (~ 1.6 fold and ~ 8

fold, respectively). These results signify a direct correlation between IL-6 and

IL-8 release and changes in endothelial permeability, mainly caused by larval

ES products. Treatment with EF products exhibited similar levels of secreted

IL-6 and IL-8 compared to untreated HUVEC controls ($P > 0.05$).
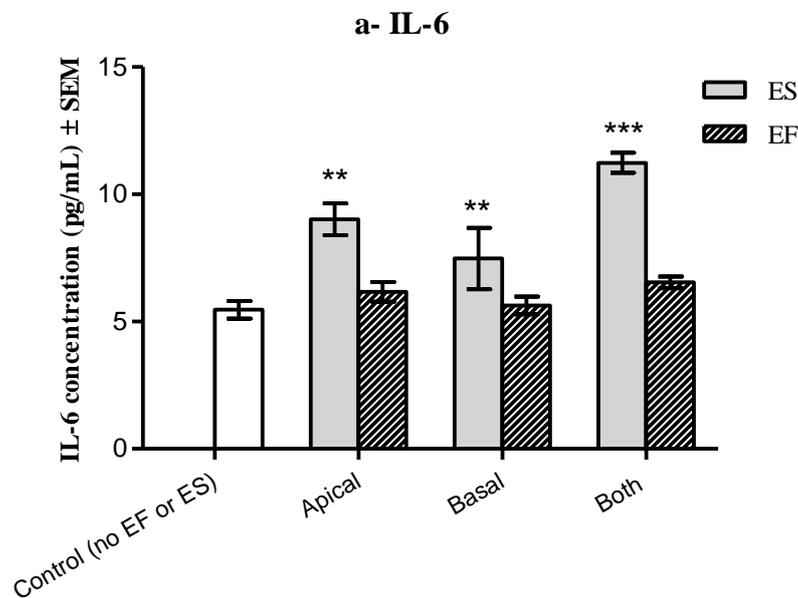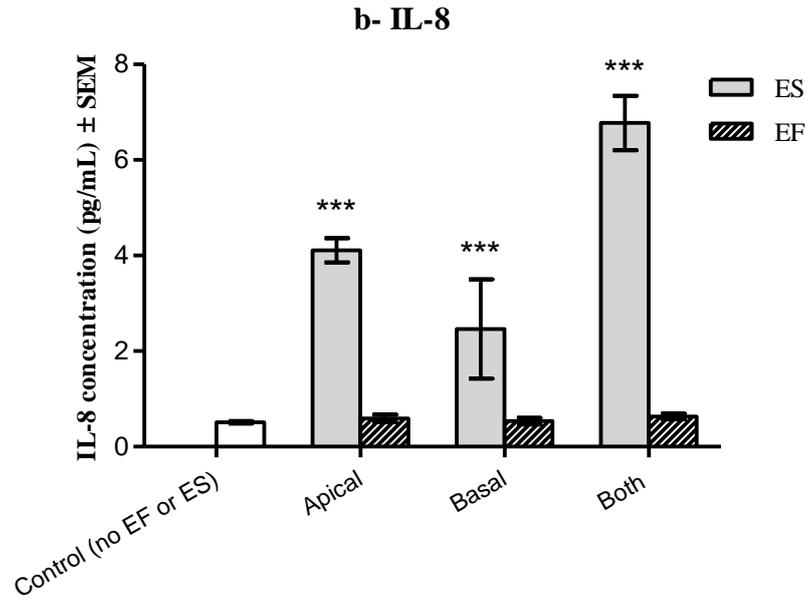
b- IL-8

Figure 5.7 **Effects of the apical/basal administration of larval products on HUVEC secretions of a) IL-6 and b) IL-8. Values are expressed as the mean of cytokine concentrations (pg/mL) ± SEM and significance is presented as ** = P < 0.01 and *** = P < 0.001, compared to cytokine production by untreated HUVEC monolayers (no EF or ES).**

Consistent with changes in monolayer permeability and cytokine secretions, junctional VE-cadherin and F-actin filaments were also observed to be disrupted subsequent to treatment of HUVEC monolayers with larval products in the apical or both chambers (Figures 5.8 and 5.10, respectively). This is consistent with the significant reduction in the percentage of cellular junctions expressing continuous VE-cadherin and the major increase in the total loss of VE-cadherin upon treatment with larval products in the apical and both chambers (Figure 5.9, a and c). Basal treatment with both EF and ES products appeared to have a lesser effect on junctional structure (Figure 5.8; b, b') and caused no significant loss of VE-cadherin staining (Figure 5.9, b). The percentage of discontinuous VE-cadherin staining in treated monolayers was significantly higher than untreated monolayers at any one time, except for monolayers treated with EF products in the basal chamber (Figure 5.9, b).
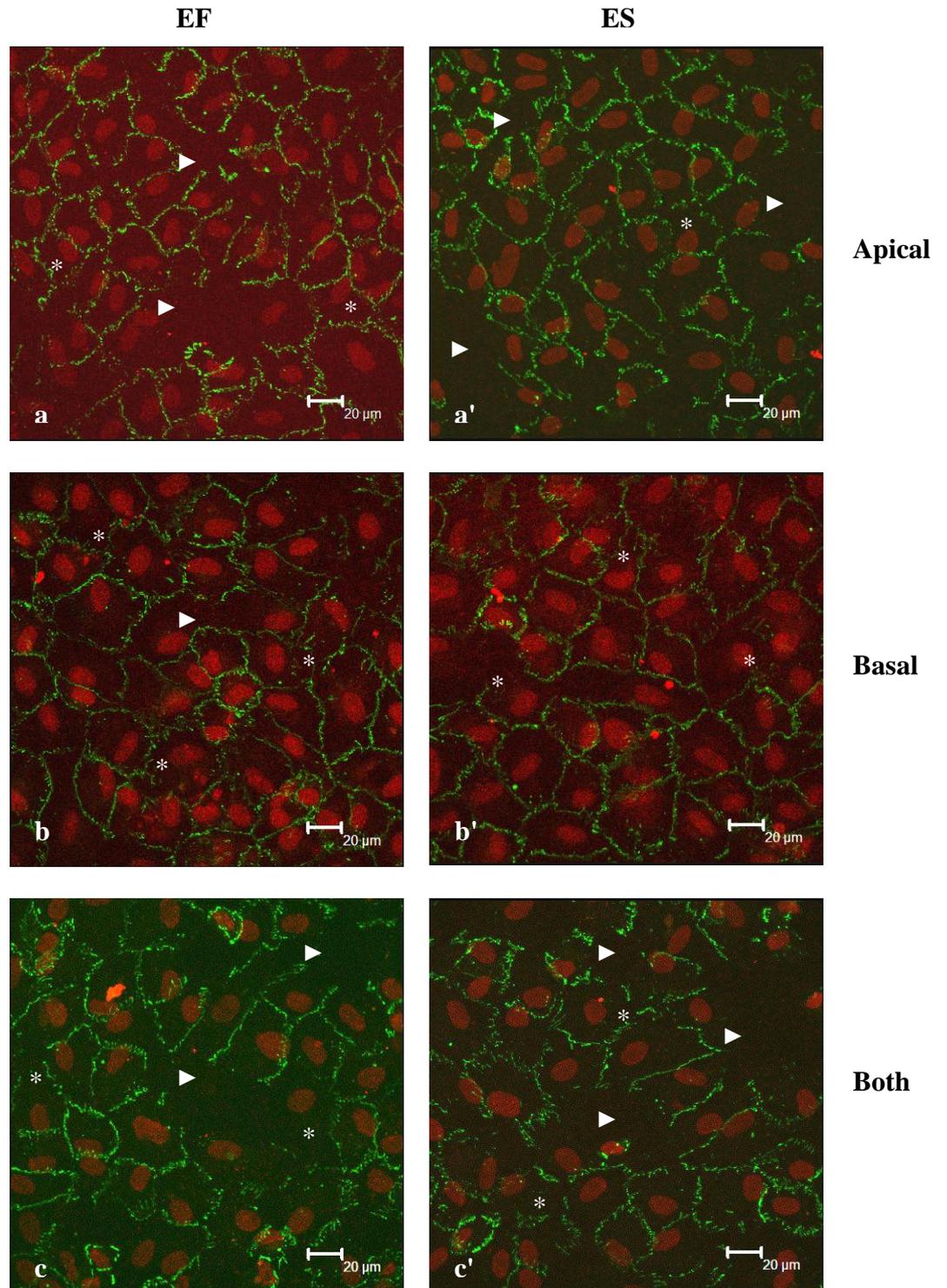
Figure 5.8   **Changes in localisation of VE-cadherin at cellular junctions in response to apical/basal administration of *Necator americanus* larval EF (a—c) or ES products (a'—c'). Confluent HUVEC monolayers were treated with larval products as described in section 4.2.3.2, in the apical (a, a'), basal (b, b'), and both chambers (c, c'). Nuclei were stained with**

propidium iodide (red). Bar = 20 μm, arrowheads point at gaps in the monolayer, and * indicates discontinuous VE-cadherin.
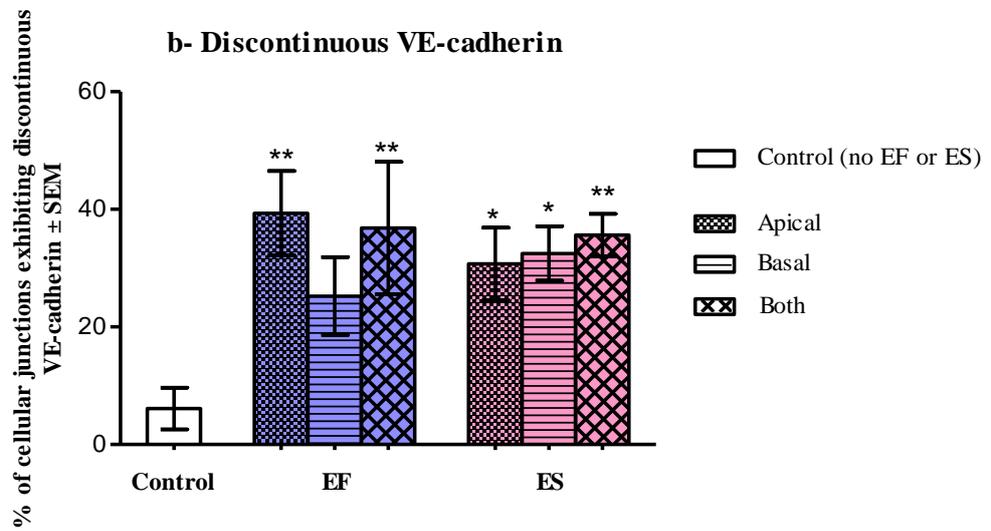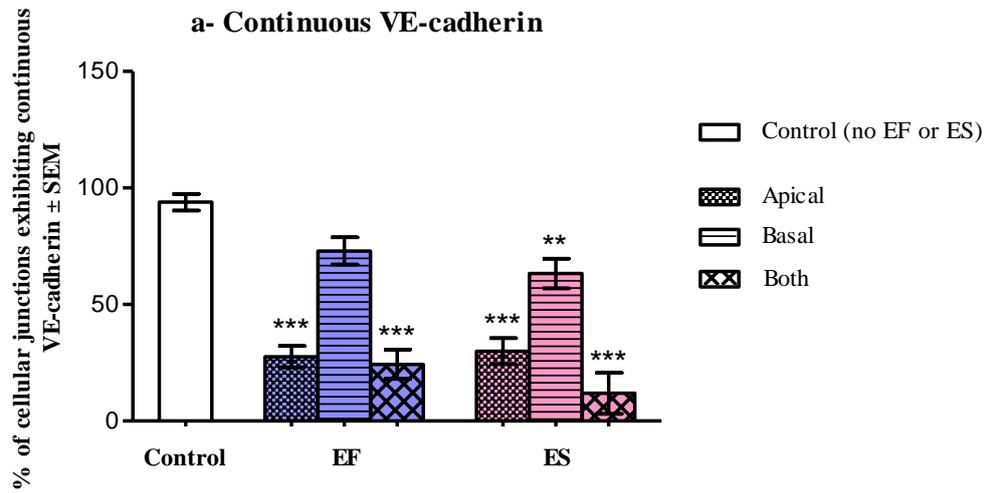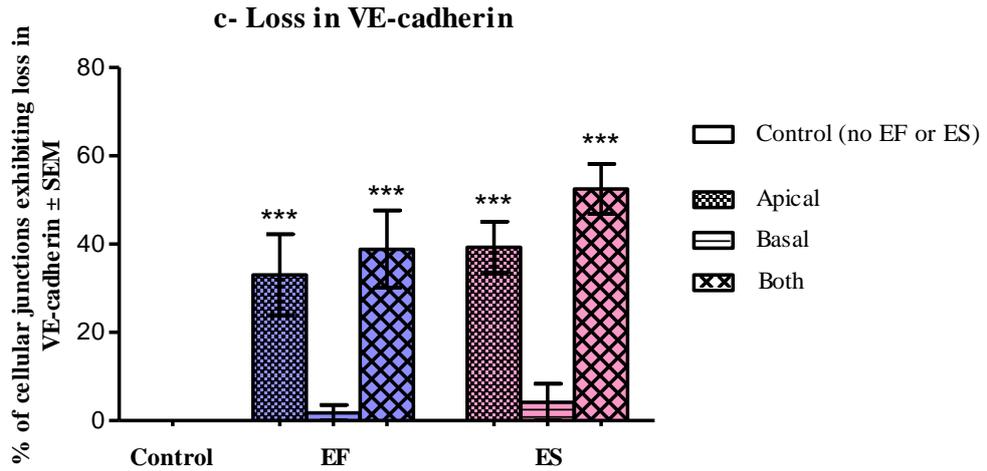
Figure 5.9 **Effects of the apical/basal administration of *Necator americanus* larval products on the pattern of VE-cadherin expression in HUVEC monolayers, described as continuous (a), discontinuous (b), and total loss of junctions (c). VE-cadherin expression is presented as the percentage of each pattern to the total number of junctions, counted per sample, ± SEM and statistical significance is defined as *** = P < 0.001, ** = P < 0.01, and * = P < 0.05 compared to untreated controls (no EF or ES).**

EF   ES
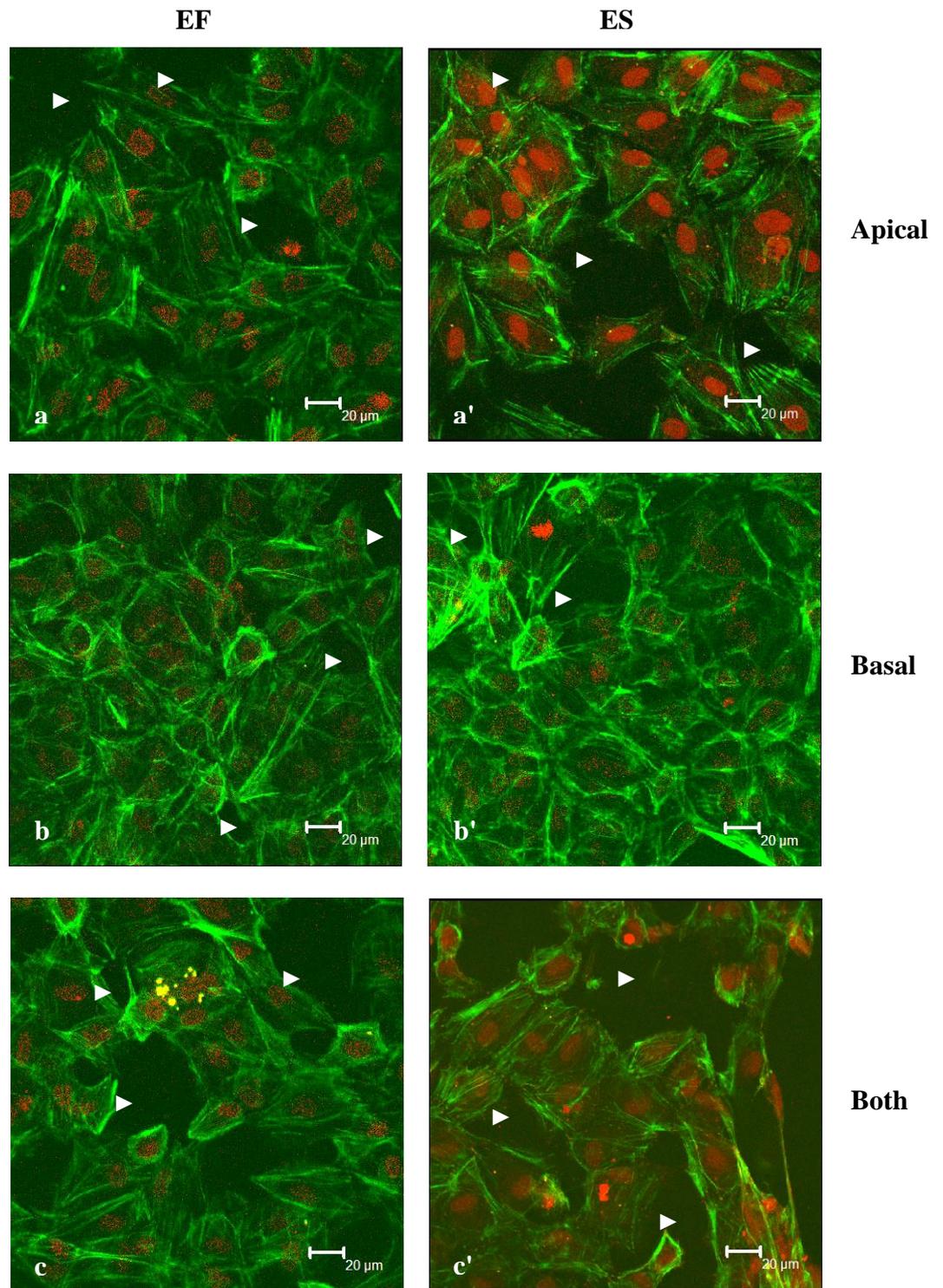
Figure 5.10 Effects of the apical/basal administration of *Necator americanus* larval EF (a—c) or ES products (a'—c') on the localisation of F-actin filaments. Confluent HUVEC monolayers were treated with larval products in the apical (a, a'), basal (b, b'), and both chambers (c, c'). Bar = 20 μm, arrowheads point at gaps in the monolayer.

5.3.2.3   Effects of protease inhibition of larval products on endothelial cell responses

Measuring VEGF and cytokines release from HUVEC monolayers, pre-treated with four protease inhibitors individually or in a mixture, showed that both EF and ES products induced significant alterations in IL-6 and IL-8 production (Figure 5.11, a and b). The use of inhibitors separately to block protease activities in EF and ES products caused a decrease in IL-6 and IL-8 release by endothelial cells (ranging from 0—25%), with PMSF resulting in the highest reduction in cytokine production (26% and 42% for IL-6 and IL-8 responses to ES products, respectively). However, the use of all inhibitors together demonstrated a greater reduction in the levels of secreted IL-6 (40.7%, P < 0.001) and IL-8 (52.0%, P < 0.0001) in response to larval ES products only. Hence, alterations in the endothelial permeability are largely dependent on the differential contributions of all studied protease classes. Again, cells treated with EF products resulted in no significant increase in secreted IL-6 and IL-8 (P > 0.05).
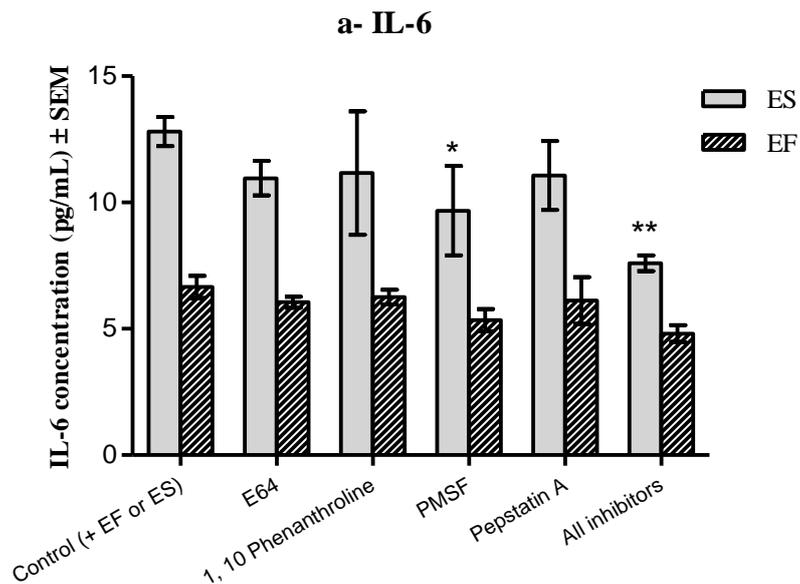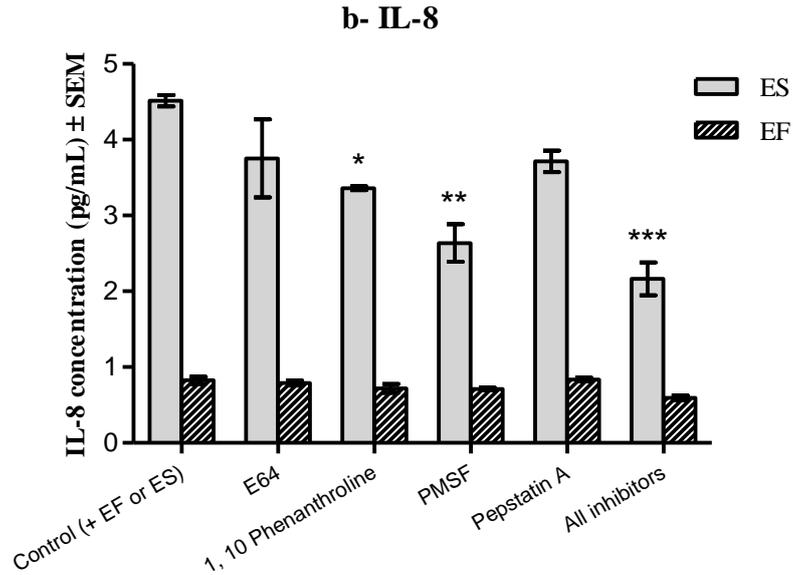
a- IL-6

b- IL-8

Figure 5.11   Effects   of   protease   inhibition   of   larval   activities   on endothelial secretions of a) IL-6 and b) IL-8. HUVEC monolayers were treated with larval EF/ES products pre-incubated with protease inhibitors as described in section 4.2.3.3. Values are presented as the mean of the concentration of secreted cytokines (pg/mL) ± SEM and statistically compared to cytokine secretions from HUVEC monolayers treated with EF/ES products in the absence of protease inhibitors (* = P < 0.05, ** = P < 0.001, and *** = P < 0.0001).

Protease inhibition of larval products reduced loss of monolayer integrity when inhibitors were used in combination, with minimal disruption of both VE-cadherin (Figure 5.12, a and b) and F-actin (Figure 5.14, a and b) at cell—cell junctions being observed. Pre-treatment of larval products with a mixture of all inhibitors illustrated a significant preservation in monolayer integrity, described by an increase in the number of junctions expressing continuous VE-cadherin (up to 50—90% vs. ~ 25% with EF/ES treated monolayers) and the associated reduction in the total loss of VE-cadherin junctions (to less than 10% compared to ~ 40—50% with EF/ES treated monolayers) as shown in Figure 5.13 (a and c). Additionally, a significant increase in the percentage of cellular junctions with a continuous VE-cadherin pattern was observed upon treatment of HUVEC monolayers with larval products in the presence of the protease inhibitors E64 (ES only) or PMSF (both EF and ES). Changes in the number of cellular junctions with a discontinuous VE-cadherin pattern were not significant with the exception of monolayers treated with ES products in the presence of a cocktail of all inhibitors (Figure 5.13, b), indicating that the proteases studied are jointly responsible for the VE-cadherin and F-actin disruption and eventually alterations in endothelial integrity and permeability. Monolayers with the lowest preservation of continuous VE-cadherin in the presence of 1, 10 phenanthroline and pepstatin A, exhibited higher levels of cellular junctions with a discontinuous VE-cadherin expression (Figure 5.13, a and b).

a- EF products
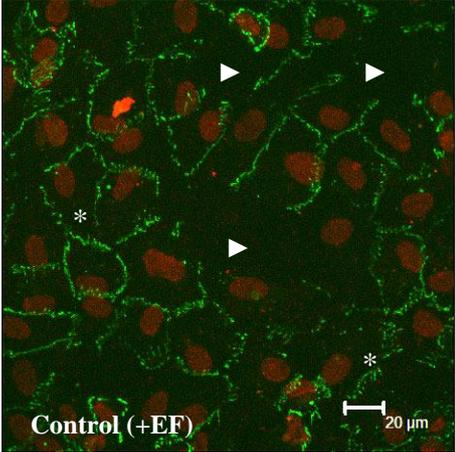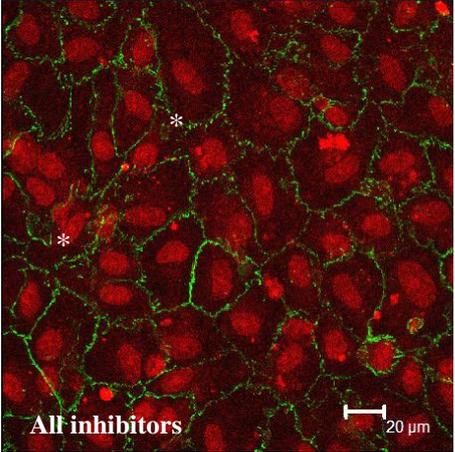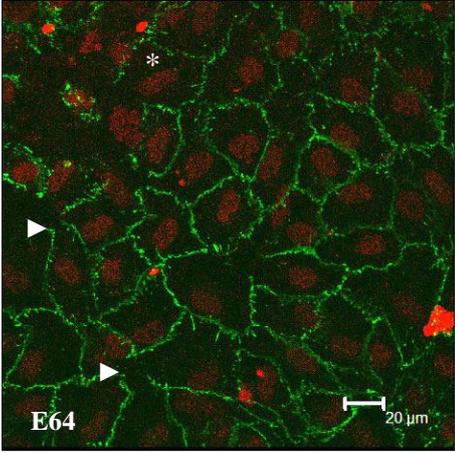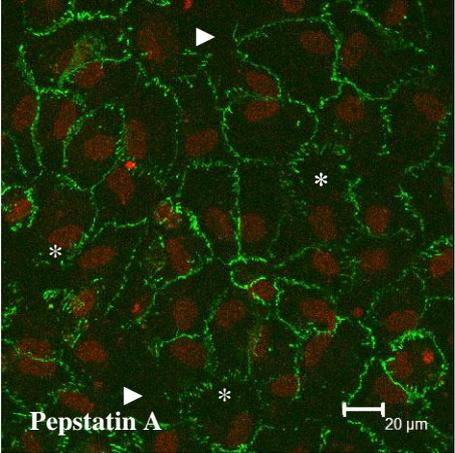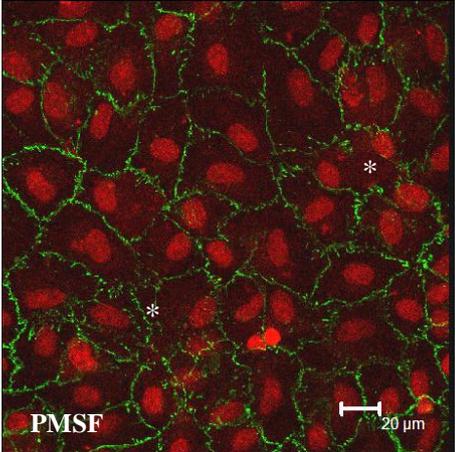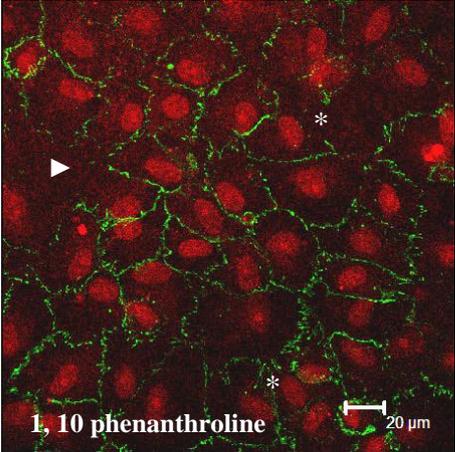
b- ES products
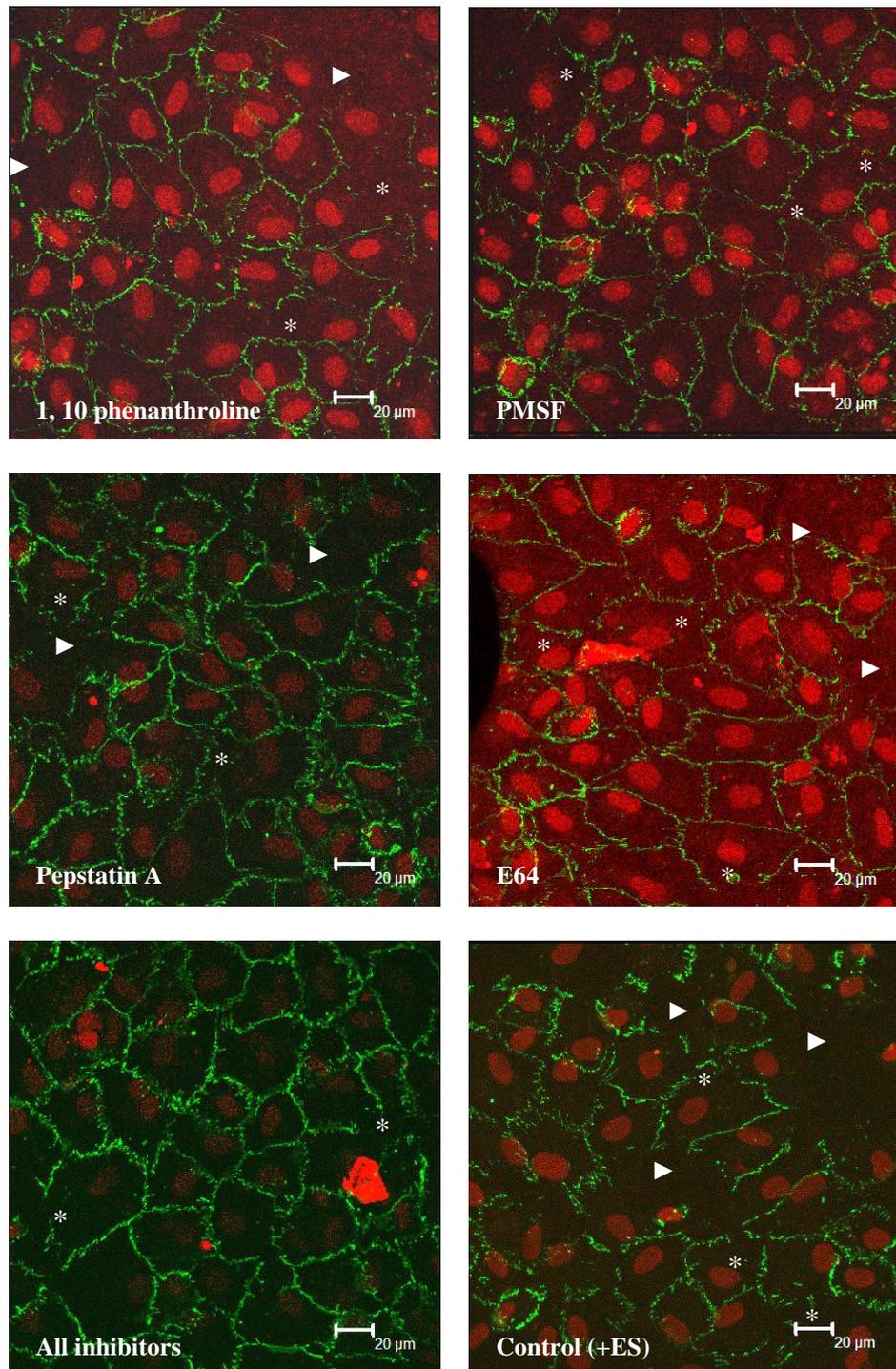
Figure 5.12   Immunostaining of HUVEC monolayers for junctional VE-cadherin following administration of a) EF and b) ES products, pre-treated with protease inhibitors, individually; 1 mM 1, 10 phenanthroline, 1 mM PMSF, 1 μM pepstatin A, and 1 μM E64; or in combination. Nuclei

were stained with propidium iodide (red). Bar = 20 μm, arrowheads point at gaps in the monolayer, and * shows regions of discontinuous VE-cadherin.

a- Continuous VE-cadherin

Legend:
- Control (+ EF or ES)
- 1,10 Phenanthroline (1 mM)
- PMSF (1 mM)
- Pepstatin A (1 μM)
- E64 (1 μM)
- All inhibitors

b- Discontinuous VE-cadherin

Legend:
- Control (+ EF or ES)
- 1,10 Phenanthroline (1 mM)
- PMSF (1 mM)
- Pepstatin A (1 μM)
- E64 (1 μM)
- All inhibitors
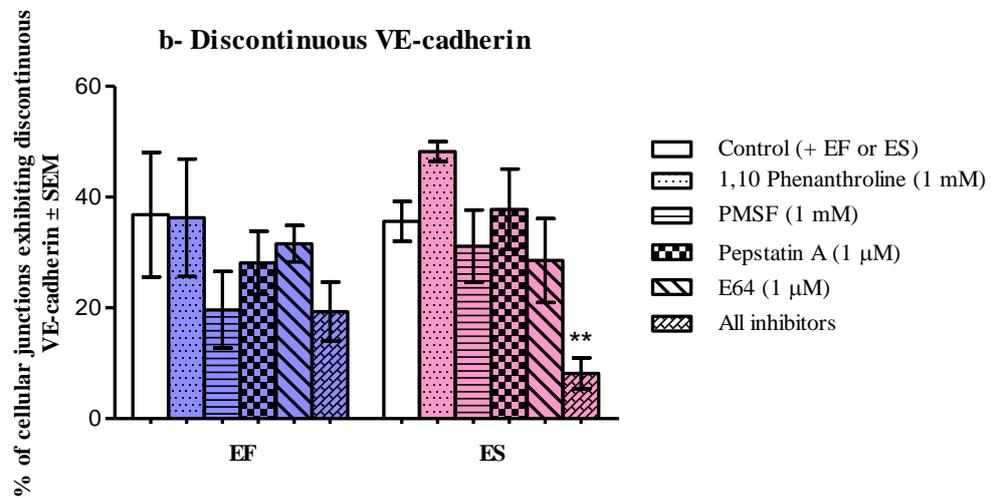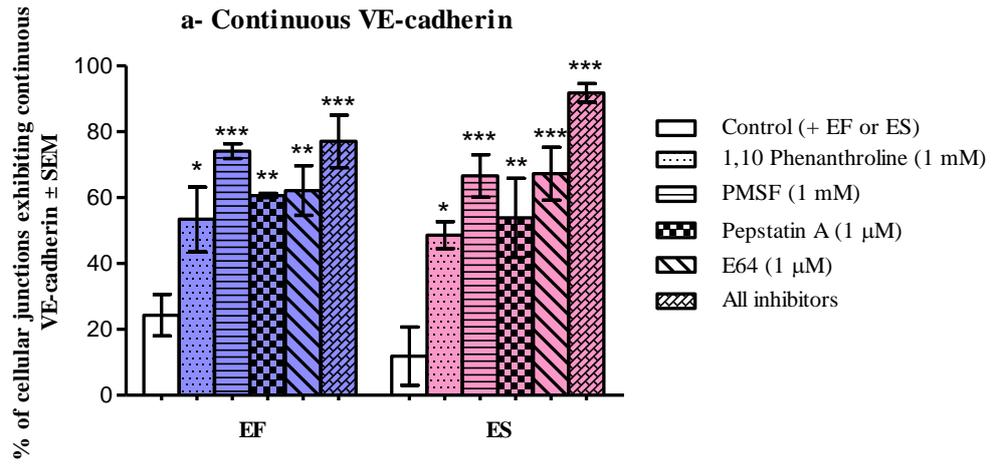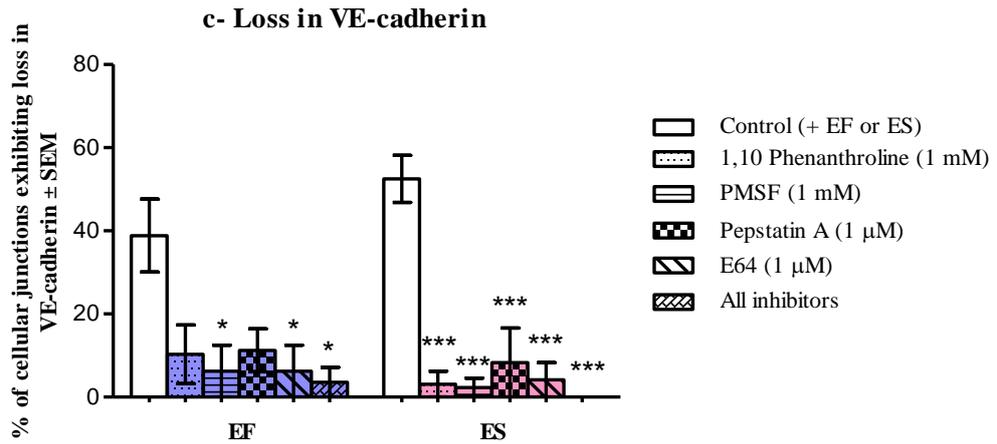
Figure 5.13 **Effects of protease inhibition of larval products on the pattern of VE-cadherin expression in HUVEC monolayers, described as continuous (a), discontinuous (b), and total loss of junctions (c). VE-cadherin expression is presented as the percentage of each pattern to the total number of junctions, counted per sample, ± SEM and statistical significance is defined as *** = P < 0.001, ** = P < 0.01, and * = P < 0.05 compared to treated controls (with EF or ES only).**

a- EF products
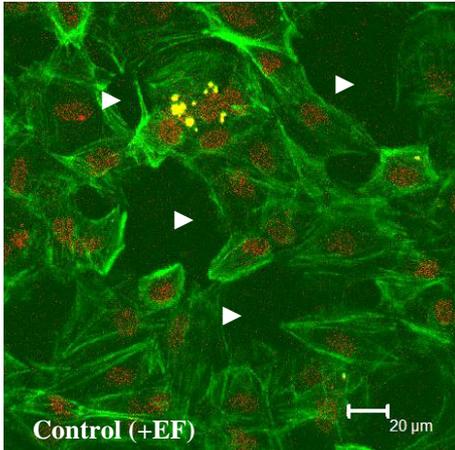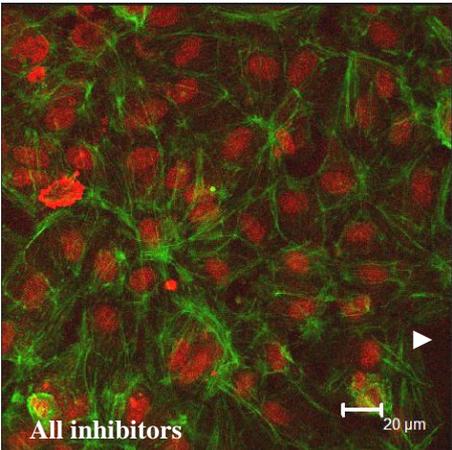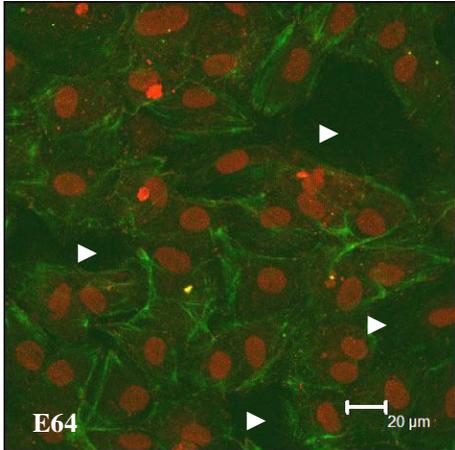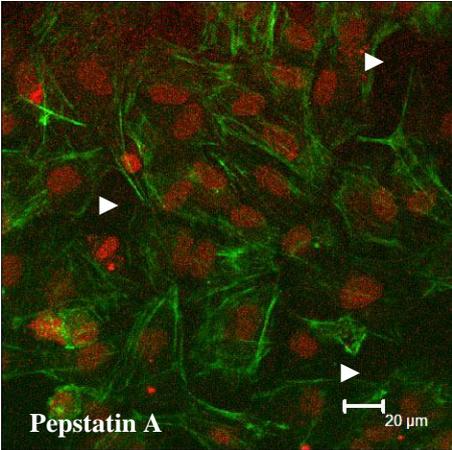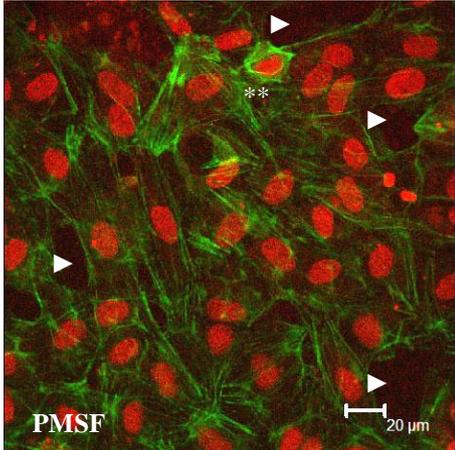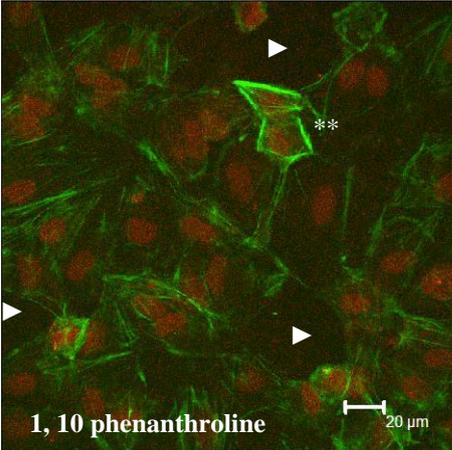
b- ES products
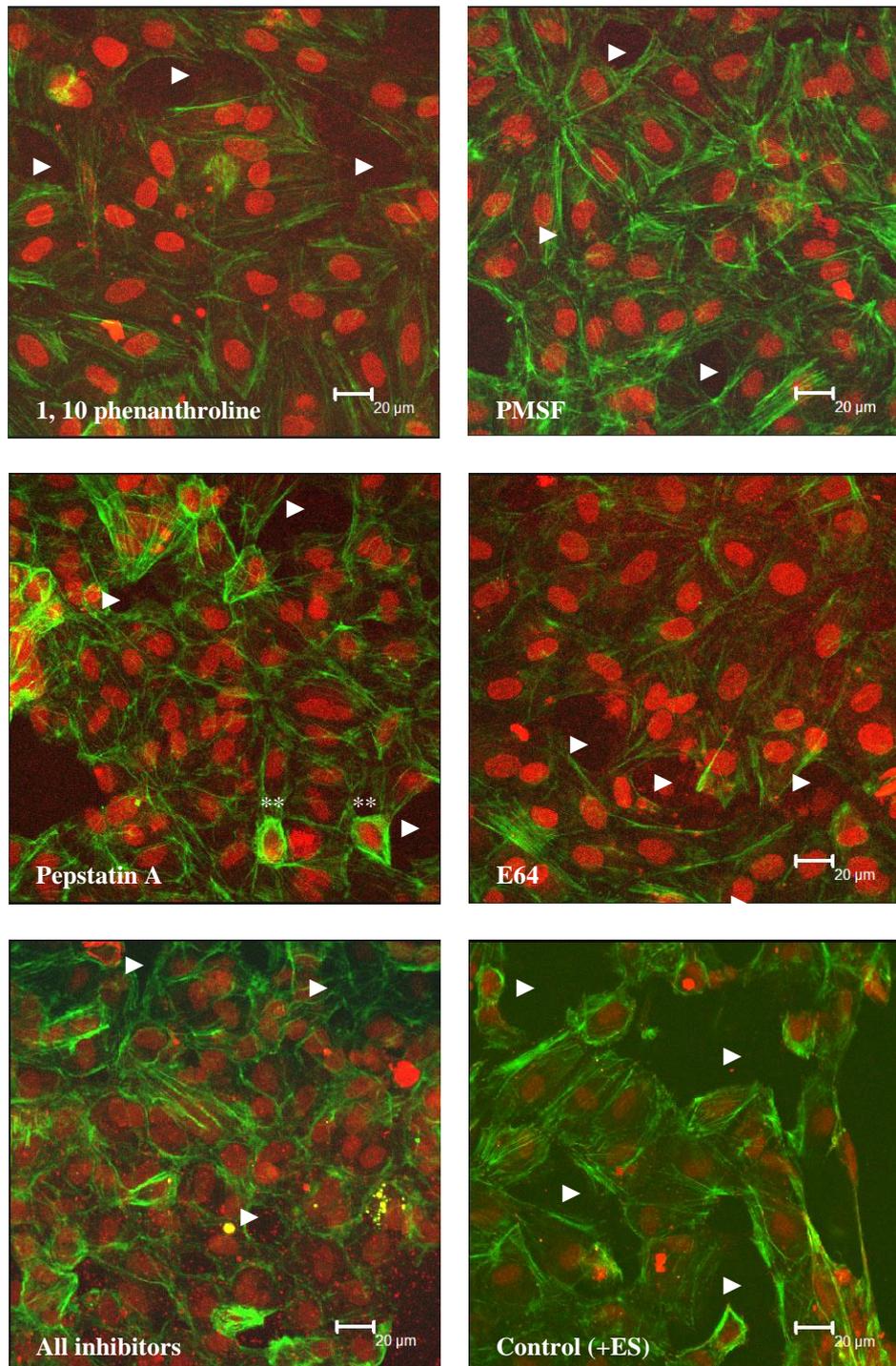
Figure 5.14 **Immunostaining of HUVEC monolayers for F-actin filaments following administration of a) EF and b) ES products, pre-treated with protease inhibitors, individually; 1 mM 1, 10 phenanthroline, 1 mM PMSF, 1 μM pepstatin A, and 1 μM E64; or in combination. Bar = 20 μm, arrowheads point at gaps in the monolayer and ** shows rearrangement into perinuclear actin.**

5.3.2.4   Effects of post-infection IgG antibodies on endothelial cell responses

Treatment of HUVEC monolayers with larval products in the presence of post-infection IgG had no significant effect on cytokine production compared to monolayers which were treated with larval products only (Figure 5.15, a and b). The use of post-infection IgG antibodies caused a similar increase in secreted IL-6 and IL-8 compared to EF/ES treated monolayers while the presence of control sera resulted in significantly higher levels of both cytokines in the culture supernatants in response to ES products indicating that post-infection IgG has very weak anti-larval activity.
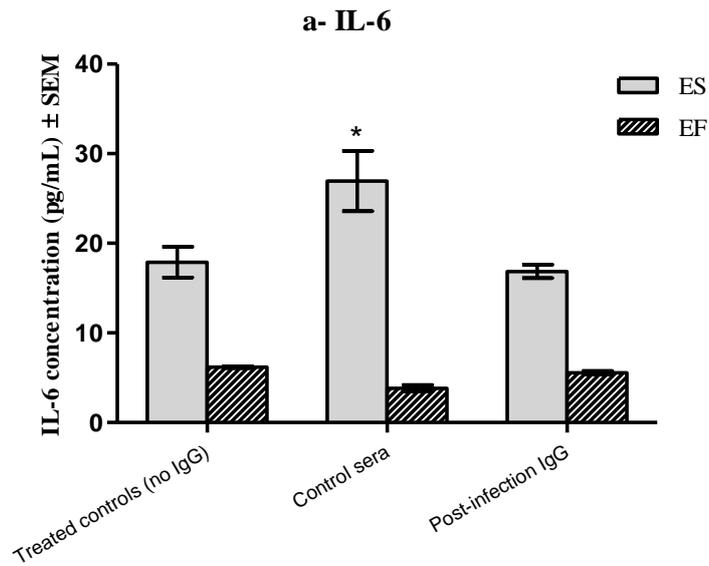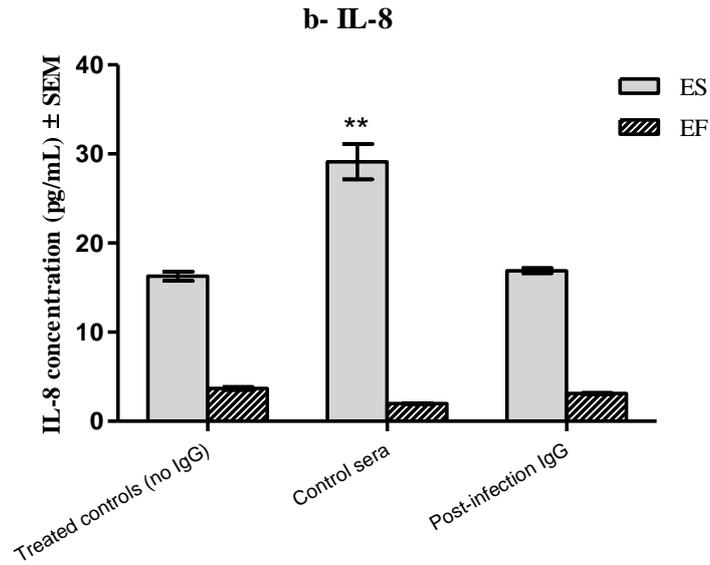
a- IL-6

b- IL-8

Figure 5.15   Effects of larval products, pre-treated with post-infection IgG antibodies, on endothelial secretions of a) IL-6 and b) IL-8. HUVEC monolayers were treated as described in section 4.2.3.4 and their secretions are expressed as the mean of cytokine concentrations (pg/mL) ± SEM. Significance is presented as * = P < 0.05 and ** = P < 0.01, compared to treated HUVEC controls (+ EF or ES only).

In line with changes in endothelial permeability and cytokine secretions, post-infection IgG antibodies demonstrated no ability to inhibit disruption of junctional VE-cadherin and F-actin, associated with larval proteolytic activities (Figure 5.16 and 5.18). Quantification of junctional VE-cadherin reflected previous observations and demonstrated no significant preservative effect of these antibodies on the number of junctions expressing continuous VE-cadherin staining (Figure 5.17, a). The use of post-infection IgG antibodies was also found to cause no major alterations in the number of discontinuous VE-cadherin junctions compared to EF/ES treated monolayers (no IgG), although a significant reduction in the total loss of VE-cadherin junctions was observed in the presence of ES products (Figure 5.17, c).

EF   ES
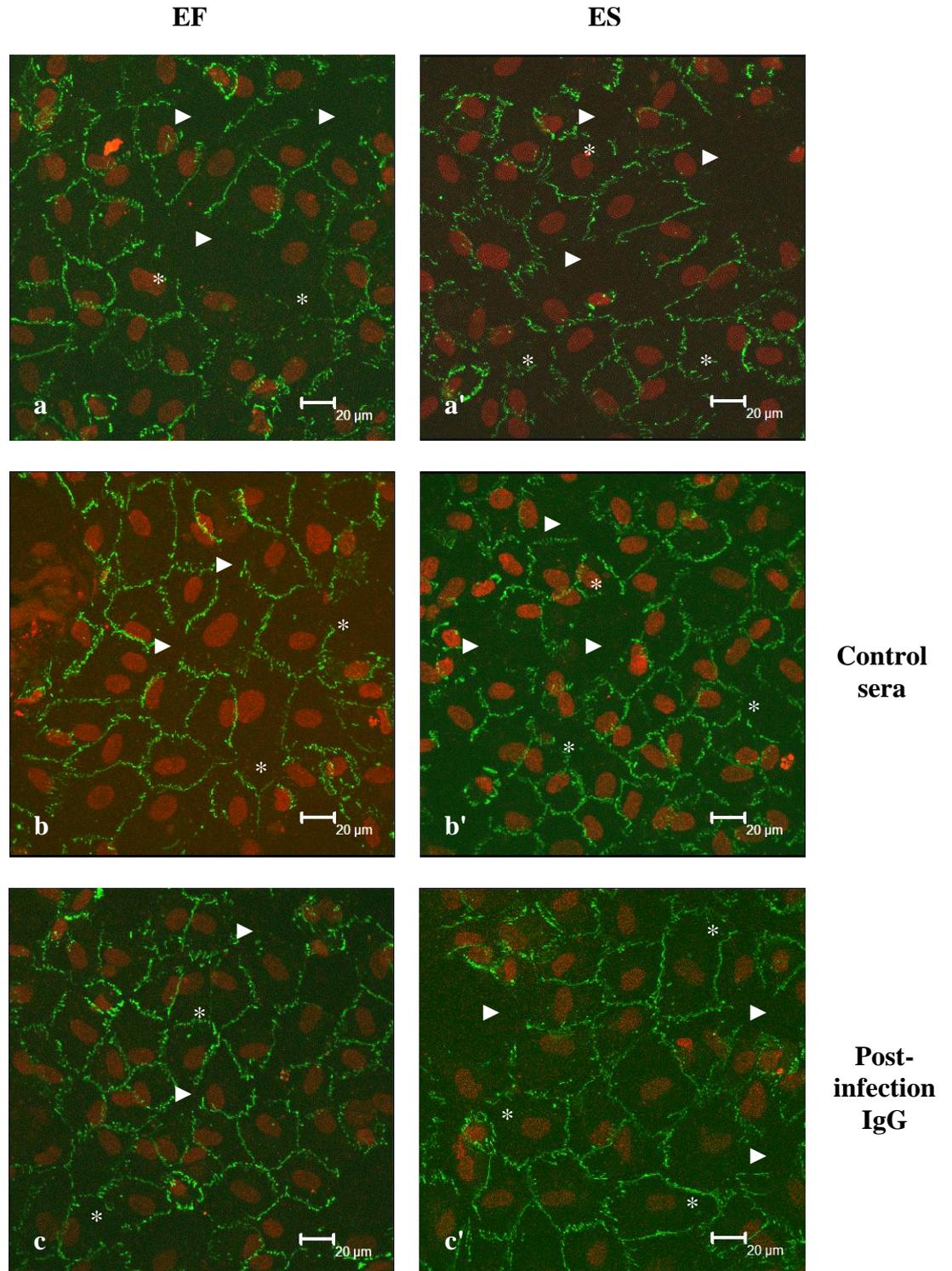
Figure 5.16   Changes in the localisation of VE-cadherin in HUVEC monolayers in response to larval EF (a—c) and ES products (a'—c'). Monolayers were treated with larval products only (a, a'), or larval products pre-incubated with either control sera (b, b') or post-infection

IgG antibodies (c, c'). Nuclei were stained with propidium iodide (red). Bar = 20 μm, arrowheads point at gaps in the monolayer, and * indicates discontinuous VE-cadherin.
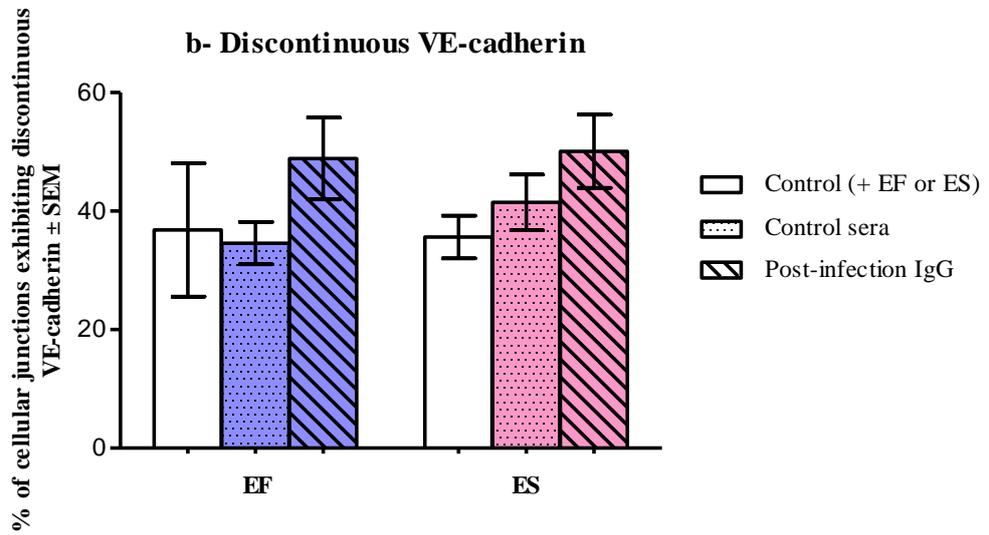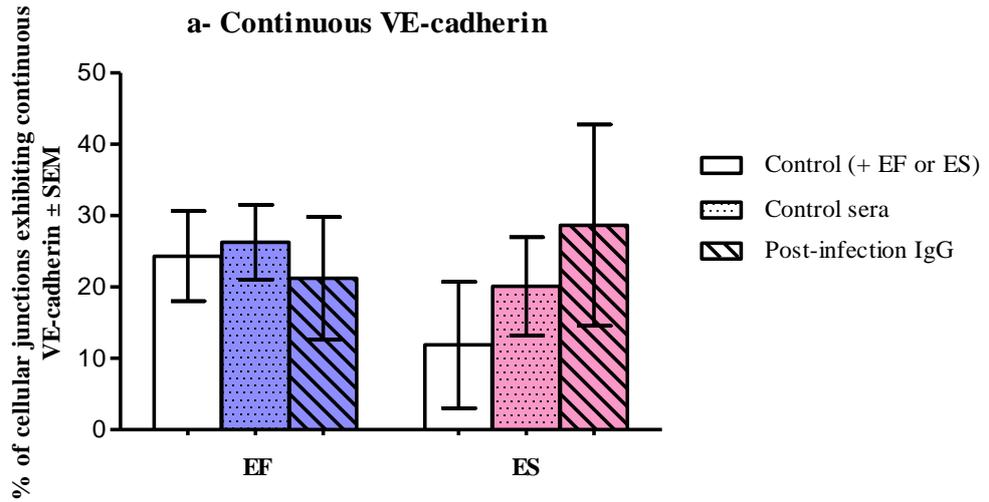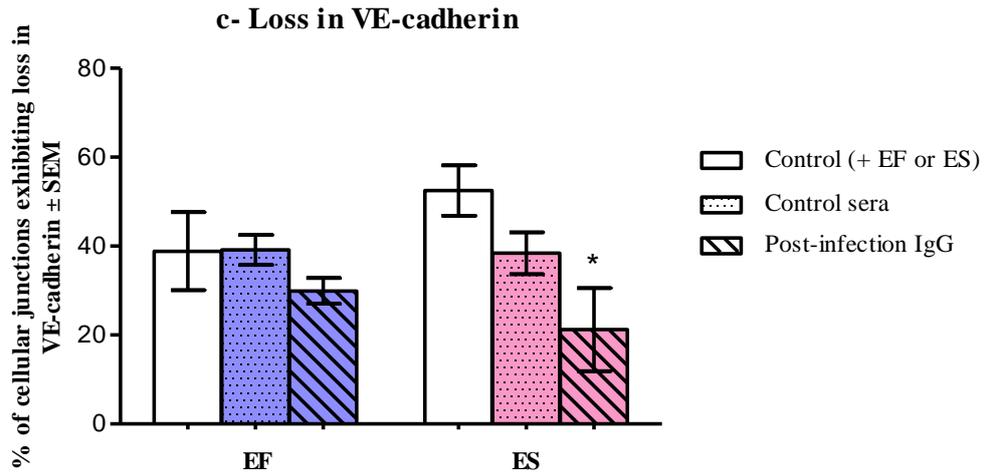
Figure 5.17 **Changes in the pattern of VE-cadherin expression in HUVEC monolayers, post-treatment with post-infection IgG antibodies; continuous (a), discontinuous (b), and total loss of junctions (c). VE-cadherin expression is presented as the percentage of each pattern to the total number of junctions, counted per sample, ± SEM and statistical significance is defined as * = P < 0.05 compared to treated controls (with EF or ES only).**

EF   ES
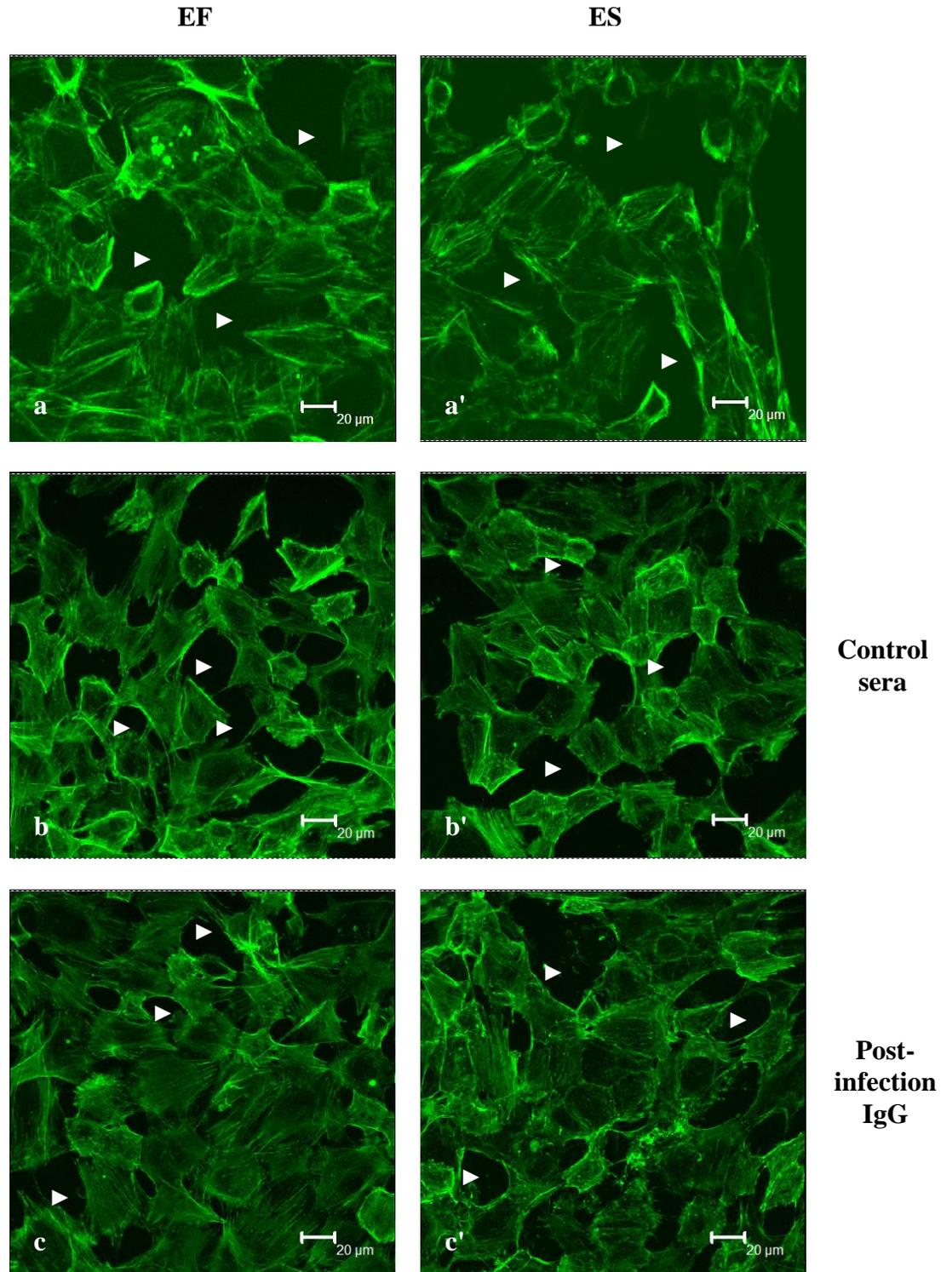
Figure 5.18   Changes in the localisation of F-actin filaments in HUVEC monolayers in response to larval EF (a—c) and ES products (a'—c'). Monolayers were treated with larval products only (a, a'), or larval products pre-incubated with either control sera (b, b') or post-infection IgG antibodies (c, c'). Bar = 20 μm and arrowheads point at gaps in the monolayer.

5.4 Discussion

Necator americanus larval exsheathing products and secretions exhibited no direct cytotoxicity against endothelial cells, suggesting that the penetration process is not associated with cellular death and emphasising that larval enzymes are most likely to cause structural disturbance of the endothelial barrier to allow larvae to enter the host.

In all experiments, the increase in endothelial permeability was associated with a moderate, but significant, increase in IL-6 and a large, significant increase in IL-8 secretion (Figure 5.3, b and c), with no increase in VEGF release (Figure 5.3, a). Larval ES products caused a dose related increase in IL-6 and IL-8 release from HUVEC cells suggesting a major role of both cytokines in modulating endothelial permeability and barrier properties in response to *Necator americanus* larval secretions. These results agree with previous work, in which endothelial permeability was shown to be mediated in part by IL-6 (Ali *et al*, 1999; Dewi *et al*, 2004) and most significantly by IL-8, in a VEGF independent manner (Petreaca *et al*, 2007). EF products, which have also been shown to induce endothelial permeability, resulted in no significant increase in IL-6 and IL-8 secretions suggesting that EF-induced permeability is not mediated by cytokines. In addition, activation of endothelial cells in response to ES products only, which is determined by cytokine production, might be related to the differential contribution of proteases and possibly other enzymes in ES but not in EF proteolytic activities, as described in chapter 2.

The increase in cytokine secretions also mirrored intercellular gap formation in endothelial monolayers at VE-cadherin rich junctions. Larval products caused a dose dependent disruption of endothelial junctional structures described as a significant increase in the loss of VE-cadherin (Figures 5.4 and 5.5) and a non dose related increase in the number of VE-cadherin junctions showing a discontinuous pattern, suggesting that larval enzymes are likely to facilitate migration by inducing fragmentation of junctional VE-cadherin molecules, ultimately leading to total loss of these junctions and the formation of intercellular gaps. Additionally, disruption of F-actin filaments which is thought to be triggered by secreted cytokines including IL-6 and IL-8 (Blum *et al*, 1997), eventually led to rearrangement into actin stress fibers, cell retraction and emergence of noticeable gaps. These results highlight the potential role of larval enzymes in the penetration process as they navigate the endothelium and gain access by targeting the stability of cellular junctions.

A significant increase in secretions of IL-6 and IL-8 was also observed following administration of larval products to the apical and both apical and basal sides of HUVEC monolayers (Figure 5.7), together with a significant elevation in the loss of VE-cadherin junctions and the formation of wide gaps in the treated monolayers (Figures 5.8—5.10). Basal treatments, however, caused a relatively considerable increase in cytokine release in response to larval ES products only, again highlighting the important role of larval ES activity in mediating the interaction between *Necator americanus* larvae and the endothelium and their ability to create gateways for the larvae during the penetration stage. The significant increase in the number of discontinuous VE-

cadherin junctions observed with basal treatments emphasised that the delayed disruption of endothelial monolayers upon basal treatment is potentially related to the need to navigate a multi-layered structure to reach the cells while the more rapid structural disturbance observed upon apical administration is most likely caused by direct interaction of endothelial cells with larval products, possibly accounting for larval migration from the blood into the surrounding tissues.

The use of protease inhibitors aimed at investigating their ability to protect the endothelial integrity of HUVEC monolayers in the presence of larval products. Protease inhibitors, when used in a cocktail, demonstrated a significantly great ability to reduce the levels of secreted IL-6 and IL-8 following treatment with ES products confirming the differential contribution of all proteases in the activation of cellular production of cytokines during the penetration process. These changes were mirrored by a significant preservation of monolayer properties as indicated by less disruption of junctional stability (Figure 5.12 and 5.14). Although the presence of enzyme inhibitors prevented further loss of monolayer integrity as described by a significant reduction in the total loss of VE-cadherin junctions and the formation of gaps, a complete inhibition of cytokine production and fragmentation of junctional molecules was not observed, suggesting that other enzymes may also be involved in modulating endothelial permeability and that enzyme inhibitors are not wholly effective, even as cocktails, against this mixed enzyme population. Activation of matrix metalloproteinases (MMPs) from endothelial cells by larval products is also possible and can be partially responsible for triggering an increase in

endothelial permeability (Lafleur *et al*, 2001; Alexander, 2002; Johannsson *et al*, 2007). The use of post-infection IgG antibodies resulted in no significant changes in the release of IL-6 and IL-8 and junctional disruption, suggesting that enzyme-specific antibodies might be required for a pronounced inhibitory role and to provide protection against *Necator americanus* infection. Moreover, failure of post-infection IgG to prevent disruption of the endothelial barrier suggests that infected individuals are not producing an appropriate response to eliminate these parasites, hence possibly accounting for the high rates of re-infection.

Stimulation of endothelial cells by inflammatory agents such as thrombin has been shown to induce endothelial barrier dysfunction by activating a number of phosphorylation cascades, eventually triggering conformational changes in the barrier structure and creating an opening of the paracellular pathway (Yuan, 2002). This is primarily driven via actomyosin contraction initiated by myosin light chain (MLC) phosphorylation, which is tightly linked to actin microfilament reorganisation previously described by Garcia *et al* (1995) and Verin *et al* (2001). Phosphorylation of most adhesion molecules linking VE-cadherin to actin by protein kinase C (PKC) was also shown to mediate disruption of VE-cadherin junctions and therefore is most likely involved in the mechanisms of increased endothelial permeability (Bogatcheva *et al*, 2002; Sandoval *et al*, 2001). Our results confirmed that larval enzymes triggered a series of intracellular signalling reactions by targeting endothelial junctional molecules including VE-cadherin and F-actin. Cytokine-induced tyrosine phosphorylation of junctional molecules (Nwariaku *et al*, 2004) and

modulation of the actin-myosin contractile system (Blum *et al*, 1997; Hordijk *et al*, 1999) have been suggested as potential mechanisms for regulating adherens junctions, thereby altering endothelial barrier functions and paracellular permeability (Leach *et al*, 1995; Budworth *et al*, 1999). IL-6 release from endothelial cells in inflammatory state demonstrated a critical involvement of reactive oxygen species (ROS) and phosphorylation of adhesion molecules by protein kinase C (Ali *et al*, 1999; Desai *et al*, 2002), therefore inducing functional alteration in vascular permeability which was associated with morphological dissociation of VE-cadherin-catenin complex from their cytoskeletal anchor (Desai *et al*, 2002; Yuan, 2002). However, IL-8 seems to induce permeability as a result of cytoskeletal actin filaments rearrangement by activating phosphorylation of actomyosin contraction and stimulating transactivation of the IL-8 receptors CXCR1 and CXCR2 (Schraufstatter *et al*, 2001; Gavard *et al*, 2009) and VEGFR2 which in turn, is required for endothelial gap formation (Petreaca *et al*, 2007). Future investigations of cytokine-induced permeability may lead to elucidation of the mechanisms highlighted in this project.

In conclusion, we have demonstrated that *Necator americanus* larval products were capable of interacting with the endothelial monolayer causing increased endothelial permeability in parallel with elevated IL-6 and IL-8 release. At the cellular mechanistic level, larval products also caused junctional disruption and gap formation, which in reality would permit *Necator americanus* larvae to pass through the endothelium and enter the microcirculation. The contribution of a repertoire of larval enzymes to this process suggests that multiple enzymes may have to be targeted to prevent the infection process.

6. General Discussion, Conclusions and Future work

The primary aim of this work was to understand the importance of larval secretions in penetrating the skin and the underlying vasculature during *Necator americanus* infection. The hypothesis in this thesis suggested that *Necator americanus* L3 larvae produce exsheathing and secretory proteases which disrupt junctional integrity via paracellular routes causing a breach in the endothelial barrier and allowing entry of larvae to the bloodstream. Thus, understanding the enzymatic profiles of *Necator americanus* larval secretions and studying their immunological and biological impacts on an *in vitro* model of the endothelium were the main aims of this thesis.

The second chapter focused on generating detailed protein profiles of *Necator americanus* larval exsheathing fluids (EF) and excretory/secretory (ES) products. The involvement of proteases in larval EF and ES products was studied using substrate gel electrophoresis and further characterised using enzyme assays. Results demonstrated a pH related protease activity against FITC-casein which was optimal between pH 6 and 8.5 for both the exsheathing fluid (EF) and the excretory/secretory products (ES). The proteolytic effects at pH 6.5 suggested a major role of larval enzymes in both EF and ES products at the early stages of migrating through the skin surface, pH of which ranges between 4.5 and 6.5 (Yosipovitch *et al*, 1993), while the significant enzymatic activity in ES products at pH 6.5 to 8 highlighted their potential role in the penetration process, allowing larvae to move deeper in the skin and reach the microcirculation. The predominant presence of serine and cysteine proteases in EF products suggested an important role of these proteases during the exsheathment of *Necator americanus* larvae as previously described by Kumar

and Pritchard (1992a), while their considerable presence in ES products signified their potential role during larval migration in the skin, as described above. The involvement of serine, cysteine and metalloproteases in the gelatinolytic activity of both EF and ES products confirmed the major importance of these proteases in negotiating the different layers of the skin (Kumar and Pritchard, 1992a). However, the modest presence of aspartyl proteases in larval EF and ES products indicated that these proteases might be partially involved in skin penetration and possibly mediate different developmental processes of *Necator americanus* larvae at this stage. The high presence of aminopeptidases in EF products also suggested an important role of these enzymes during and after exsheathment as proposed by Kumar and Pritchard (1992a) while the presence of leucine aminopeptidases in ES products indicated their potential involvement in the hydrolysis of both skin and serum molecules (Williamson *et al*, 2003). Hence, the characteristic contribution of all proteolytic activities in the larval products suggested that the penetration process may be mediated by the activity of more than one protease, likely due to the complex nature of the skin and the need to survive the host's immune system as proposed by Pritchard *et al* (1990). Proteolysis of haemoglobin, possibly in a multi-protease cascade (Williamson *et al*, 2002), also suggested that proteases in EF and ES products are of major importance in the feeding behaviour of larvae as reported by Williamson *et al* (2003a).

The absence of hyaluronidase activity in larval EF and ES products, as described in chapter 2, indicated that unlike the infective *Ancylostoma* species (Hotez *et al*, 1992), *Necator americanus* larval migration through the skin

might not be mediated by the activity of hyaluronidase, an enzyme responsible for the degradation of hyaluronic acid which serves as cell to cell adhesion bridges in the different layers of the skin (Miyake *et al*, 1990). Therefore, chapter 3 focused on studying the proteolytic effects of larval EF and ES products on skin macromolecules. *Necator americanus* larval products demonstrated a selective degradation of collagen III and laminin with ES products, a greater affinity for collagen IV by EF products and a different pattern of hydrolysis of fibronectin by larval EF and ES products suggesting that the characteristic difference in larval enzymes is responsible for variation in the degradation of individual extracellular matrix (ECM) proteins. These results also indicated that EF products, which are of major importance during the exsheathment of larvae, might play an additional role in early stages of larval penetration allowing *Necator americanus* species to advance in the skin, as previously reported by Kumar and Pritchard (1992a) while ES products are most likely responsible for further larval migration through the deeper layers of the skin. Degradation of collagen IV and laminin, the main components of all basement membranes (Timpl and Brown, 1996; Timpl, 1996), and fibronectin and collagen III by larval proteases suggested that *Necator americanus* larvae disturb the structure of the skin possibly by directing larval proteolytic activities to target the skin molecules and create an opening for larvae to migrate to the blood circulation.

The proteolysis of skin macromolecules upon treatment with larval EF and ES products was minimal as featured by the modest digestion of collagen I and fibronectin while degradation of collagen III was significant and greater with

ES products, as described in chapter 3. This is likely due to the complex structure of the skin, which unlike individual ECM proteins, was shown to contain tissue-derived protease inhibitors such as cysteine and serine protease inhibitors (Rao *et al*, 1995; Rao *et al*, 1998; Zeeuwen *et al*, 2009), with a role to play in the regulatory and protective functions of the skin against uncontrolled proteolysis from host or environmental pathogens. Hydrolysis of collagen III suggested that larval products might target proteins with low molecular complexity to create a fast and easy breach for the larvae to enter the host while targeting other skin macromolecules including collagen I, fibronectin and laminin might require stronger proteolytic activity and larger numbers of species due to their complex structures. Degradation of ECM and skin macromolecules, which was primarily related to the characteristic presence of proteolytic enzymes in *Necator americanus* larval products, supported the potential role of EF products in the initial stages of larval migration and highlighted the major role of ES products in negotiating the connective tissue and progressing towards the underlying vasculature.

Unlike other matrix proteins, treatment of collagen V with larval products indicated a possible involvement of larval enzymes in the cross-linking of small proteins and the creation of strong protein bands which were resistant to proteolytic cleavage (Collighan and Griffin, 2009). Transglutaminase, responsible for the cross-linking of peptides, has been reported in a number of parasites including *Onchocerca volvulus* (Lustigman *et al*, 1995), *Plasmodium falciparum* (Adini *et al*, 2001) and in *Necator americanus* larval EF and ES products, as described in chapter 3. The inhibition of transglutaminase was

found to prevent the moulting of L3 larvae to L4 stage larvae (Lustigman *et al*, 1995; Rao *et al*, 1999; Chandrashekar and Mehta, 2000), therefore suggesting an important role of these enzymes in the long-term maintenance and survival of *Necator americanus* species as well as the progression of the parasitic infection.

In order to study the effect of *Necator americanus* species on the vasculature, human umbilical vein endothelial cells (HUVEC) were used as an *in vitro* model of the vascular endothelium, as described in chapter 4. The HUVEC model is known to establish no phenotypic features and to maintain the general properties of endothelial cells from different vascular beds. Since *Necator americanus* larvae encounter the vascular endothelium at different stages of their journey in the host (i.e. including the skin and lungs), the HUVEC model was used to describe the basic interaction of larvae with the endothelium. In this work, the electrical resistance of HUVEC monolayers reached a maximum of 72 to 74 $\Omega.cm^2$ at confluence which was significantly higher than that reported by Blum *et al* (1997) and concur with recent work by Man *et al* (2008), a significant difference possibly related to using HUVEC cultures at different passages. High transendothelial electrical resistance (TEER) across HUVEC monolayers was associated with typical cobblestone morphology of cells. At a molecular level, confluent HUVEC monolayers demonstrated a continuous strong expression of vascular endothelial cadherin (VE-cadherin) at cellular junctions and a clear presence of actin filaments (F-actin) but a weaker occludin was observed. The latter was not therefore studied. Results here emphasised the role of VE-cadherin and actin filaments in maintaining the

integrity of the endothelial junctions as previously described in the literature (Dejana *et al*, 2000; Firth, 2002). Hence, based on the hypothesis, *Necator americanus* larvae are believed to facilitate their entry to the microcirculation by disturbing the molecular integrity of HUVEC monolayers, eventually mediating alterations in endothelial permeability.

Changes in the endothelial barrier functions, featured as the permeability of endothelial monolayers, were examined in relation to larval enzymatic activity. Studies were carried by measuring transendothelial electrical resistance (TEER) and tracer leakage across HUVEC monolayers during and post-treatment with larval products, respectively. Larval enzymes caused a concentration related increase in endothelial permeability, leading to earlier disruption of the endothelium at high doses, possibly as a result of targeting the integrity of monolayers to facilitate entry of *Necator americanus* larvae into the blood circulation. However, the use of larval products at low doses resulted in modest increase in permeability, described by a significant reduction in monolayer resistance with no significant changes in tracer leakage across treated monolayers, indicating that TEER is a more sensitive marker to changes in endothelial barrier functions. In addition, the greater changes in permeability, observed with larval ES products, might be due to the characteristic presence of proteolytic activities in ES compared to EF products, earlier described in chapter 2. This is in line with previous research in which bacteria such as *Prophyromonas gingivalis* and parasites such as *Schistosoma mansoni* were shown to adhere to endothelial cells *in vitro* which allowed them to modulate vascular permeability in response to parasitic triggers and gain

access to the host (Imamura *et al*, 1995; Timpl and Martin, 1997; Hansell *et al*, 2008).

Treatment of HUVEC monolayers with larval products in the apical or both chambers resulted in a significant increase in permeability compared to those treated in the basal chamber only. The direct interaction between endothelial cells and larval products applied to the apical chamber, resulted in a faster disruption of the endothelial barrier while the basal administration of larval products was associated with a delayed increase in permeability, possibly due to the need to cross multiple layers, both *in vitro* and *in vivo,* before reaching the cells. Negotiating the basement membrane, which is possibly facilitated by the ability of *Necator americanus* larval enzymes to digest its main components including collagen IV and laminin as described in chapter 3, may therefore account for this delayed increase in permeability following basal treatments. As argued in chapter 4, the apical-induced permeability is likely to mediate breaking out from the blood vessel during the lung-associated migration, while migrating from the skin into the dermal microcirculation, through the vascular basement membrane, may be mediated by larval-induced permeability similar to that observed following basal administration.

Finally, treatment of HUVEC monolayers with larval products in the presence of protease inhibitors aimed at exploring which proteases are involved in this interaction and determining if protease inhibitors are able to prevent larval-associated increase in endothelial permeability. The increase in monolayer permeability, in response to larval products, demonstrated a joint contribution

of serine, cysteinyl, aspartyl and metalloproteases, the inhibition of which resulted in a significant preservation of monolayer permeability. A total protection of endothelial barrier functions was never seen which suggests that additional enzymatic activity may also be involved and that treatment with larval products might also trigger the activation of matrix metalloproteinases (MMPs) from endothelial cells which in turn, can be partially responsible for inducing an additional increase in vascular permeability (Lafleur *et al*, 2001; Alexander, 2002; Johannsson *et al*, 2007). Inactivation of tissue-associated protease inhibitors, previously observed with *Schistosoma mansoni* species (Hansell *et al*, 2008), might also be triggered in the presence of *Necator americanus* larval enzymes leading to a further increase in vascular permeability.

Parasites, such as *Plasmodium falciparum*, have been shown to induce apoptosis in endothelial cells as an important mechanism during host invasion (Pino *et al*, 2003). In this work, *Necator americanus* larvae induced no cytotoxicity against endothelial cells suggesting that larval migration into the microcirculation is not mediated by the activation of cell apoptosis and highlighting that, as proposed in the hypothesis, larvae are most likely to cause structural disturbance of the endothelial paracellular junctions, enough to allow larvae to enter the host. The transcellular routes of transport across the endothelium were not addressed in this thesis, primarily due to the large size of *Necator americanus* larvae which ranges between 550 and 580 μm in length (Adenusi and Ogunyomi, 2003).

The increase in monolayer permeability, described in chapter 4, was associated with a significant increase in cytokine production and loss of monolayer integrity. Larval ES products caused a dose related increase in IL-6 and IL-8 release from HUVEC cells, but no significant increase in VEGF levels, possibly implicating these cytokines in modulating monolayer permeability and endothelial barrier properties in response to *Necator americanus* larval secretions (Ali *et al*, 1999; Dewi *et al*, 2004; Petreaca *et al*, 2007). At a cellular level, larval products also induced a dose related disruption of junctional integrity of HUVEC monolayer, described as a significant loss of VE-cadherin junctions, retraction of endothelial cells and the formation of intracellular gaps. Analysis of endothelial integrity suggested that, as described in chapter 5, larval enzymes might induce release of IL-6 and IL-8 from endothelial cells to trigger retraction of actin filaments and dissociation of VE-cadherin from other adhesion molecules (Blum *et al*, 1997; Yuan, 2002), eventually leading to rearrangement of actin cytoskeleton, increase in monolayer permeability and loss of barrier regulatory functions. However, the use of antibodies against IL-6 and IL-8 to determine the importance of these cytokines in larval-induced permeability was not studied due to time limitations.

Modulation of endothelial permeability in response to inflammatory agents such as thrombin, a serine protease primarily involved in the coagulation cascade, has been shown to involve the activation of multiple phosphorylation cascades including myosin light chain (MLC) phosphorylation (Garcia *et al*, 1995; Verin *et al*, 2001) and protein kinase C (PKC) phosphorylation of VE-cadherin complexes (Sandoval *et al*, 2001; Bogatcheva *et al*, 2002). In this

work, larval proteases were shown to trigger a series of intracellular signalling reactions by targeting endothelial junctional molecules including VE-cadherin and F-actin. The no change in VEGF levels indicated that larval enzymes activate endothelial cells, via cytokines, in a VEGF-independent mechanism, as has been shown for IL-8 (Petreaca *et al*, 2007). Therefore, alterations to endothelial barrier functions and paracellular permeability are most likely a result of cytokine-induced tyrosine phosphorylation of junctional molecules (Nwariaku *et al*, 2004) and modulation of the actin-myosin contractile system (Blum *et al*, 1997; Hordijk *et al*, 1999), which in theory, would allow *Necator americanus* larvae to enter the host.

The significant increase in IL-6 and IL-8 production and the subsequent loss of VE-cadherin expression at cellular junctions was consistent with the increase in monolayer permeability following the apical treatment of HUVEC monolayers with larval products. The apical treatment was also shown to cause greater loss of junctional VE-cadherin while the basal treatment of HUVEC monolayers was associated with significant fragmentation of VE-cadherin molecules, emphasising that the modest increase in endothelial permeability upon basal treatment is primarily related to the delayed interaction with the monolayer due to multi-layered apparatus and, in reality, the complex structure of the skin and the underlying vasculature. Treatment of endothelial monolayers with larval products, pre-treated with protease inhibitors, resulted in significant reduction in IL-6 and IL-8 release and considerable preservation of junctional integrity, particularly when protease inhibitors were used as a cocktail. Results, therefore, highlighted the major role of larval proteases in the interaction of

Necator americanus larvae with the endothelial barrier and suggested that targeting these proteases would prevent larval entry into the host's bloodstream, hence providing an early protection against *Necator americanus* infection.

Post-infection anti hookworm IgG, which was expected to prevent protease-associated disruption of endothelial integrity, was used to probe larval products on Western blots, as described in chapter 2, and highlighted modest similarities between adult and larval ES antigens while no similarity, featured as no capturing of antigens, with EF products. These observations were confirmed using ELISA and are supported by the presence of certain antigens in adult and larval ES products such as calreticulin (Pritchard *et al*, 1999; Kasper *et al*, 2001), aspartic Na-APR-1 (Williamson *et al*, 2002; Pearson *et al*, 2009) and cysteine Na-ASP-2 (Hawdon *et al*, 1999) proteases. Post-infection anti worm IgG was functional in that it binds parasitic analogues in a competitive manner. However, post-infection IgG did not inhibit the processes measured in this work including proteolysis of FITC-casein and digestion of ECM and skin macromolecules (chapter 3). Post-infection IgG antibodies were also shown to cause no significant protection of monolayer permeability and endothelial integrity, suggesting that these antibodies have no anti-larval activity and that enzyme-specific antibodies might be required to target specific larval EF and ES proteases for a pronounced inhibitory role and to provide protection against these species.

In conclusion, this study has demonstrated that *Necator americanus* larval products are capable of degrading skin macromolecules and interacting with the endothelial monolayer, causing increased IL-6 and IL-8 release and subsequent disruption in endothelial permeability. In addition, larval products also caused junctional disruption and gap formation, theoretically allowing *Necator americanus* larvae to enter the microcirculation and migrate from the bloodstream into the surrounding tissue. The characteristic contribution of a repertoire of larval enzymes to this process suggests that multiple enzymes may have to be targeted to prevent and treat the *Necator americanus* infection.

Future Work

This thesis laid the groundwork for a good understanding of the interaction between *Necator americanus* larvae and the vascular endothelium. However, certain extensions to this work would help expand and strengthen the current knowledge to be able to provide protection against hookworm infections.

In this thesis, the HUVEC model has been used to provide a general understanding of the interaction between *Necator americanus* larvae and the endothelium. The use of endothelial cells from vascular beds of significant relevance to hookworm infection, including the skin and lungs, would describe the specific mechanisms allowing larvae to migrate through the endothelial barrier in these organs. Using real time imaging to visualise live larvae migrating through an *in vitro* apparatus of endothelial cells grown on a matrix, also present an opportunity to study the penetration process and the interaction with the vascular endothelium. Unfortunately, the IgG used here was active against adult worms but barely active against larvae. The use of anti worm IgG of high specific activity against larval products is believed to inhibit their proteolytic activities and provide early protection against *Necator americanus* species and therefore should be investigated as an extension to this thesis.

Alterations in endothelial permeability and barrier integrity, which were described in chapters 4 and 5, highlighted the need to study the signalling processes which are activated during *Necator americanus* larval invasion. Proteases, including thrombin and trypsin, have been reported to activate vascular endothelial cells through protease-activated receptors (PARs) as

previously described by Inomata *et al* (2007) and Day *et al* (2006). Investigations of the potential involvement of PARs in regulating larval-induced increase in vascular permeability (Klarenbach *et al*, 2003) would therefore afford an understanding of the molecular mechanisms underlying hookworm-endothelium interactions and, probably, play a role in the prevention and treatment of *Necator americanus* infection. In addition, the interaction between larval calreticulin and the vascular endothelium is an interesting area for future work. Calreticulin, an antigen observed in *Necator americanus* larval and adult products, has been shown to interact with cell surface adhesion molecules, known as integrins (Reilly *et al*, 2004). The close co-operation between integrins and VE-cadherin is known to promote stability of the endothelium by connecting cells to the surrounding extracellular matrix molecules (Cheresh and Stupack, 2008), the disruption of which is likely to mediate larval-induced permeability and allow *Necator americanus* larvae to enter the body.

Furthermore, there is an increased interest in understanding the potential therapeutic effects of *Necator americanus* infection on allergic disorders such as asthma, atopic dermatitis and eczema (Cooper *et al*, 2003; Falcone and Pritchard, 2005; Leonardi-Bee *et al*, 2006; Wordemann *et al*, 2008). Recent work by McLean and Hull (2007) demonstrated that both asthma and atopic dermatitis are related to genetic abnormalities in filament aggregation proteins (filaggrin), which under the normal conditions, are extensively cross-linked to epidermal proteins by tissue transglutaminases to form an impermeable barrier at the outer layer of the skin (McGrath and Uitto, 2008). Therefore, the effects

of larval EF and ES products in which transglutaminase activity was detected, as described in chapter 3, on filaggrin and other epidermal proteins present another bright area for future work which should be investigated in relation to the therapeutic importance of *Necator americanus* infection to different allergies.

References

Adenusi AA, Ogunyomi EA (2003). Relative prevalence of the human hookworm species, Necator americanus and Ancylostoma duodenale in an urban community in Ogun State, Nigeria. African J of Biotech; **2**(11):470-473.

Adini A, Krugliak M, Ginsburg H, Li L, Lavie L, Warburg A (2001). Transglutaminase in Plasmodium parasites: activity and putative role in oocysts and blood stages. Mol Biochem Parasitol; **117**(2):161-168.

Aird WC (2007). Phenotypic heterogeneity of the endothelium: I. Structure, function, and mechanisms. Circ Res; **100**(2):158-173.

Aird WC (2007a). Phenotypic heterogeneity of the endothelium: II. Representative vascular beds. Circ Res; **100**(2):174-190.

Albelda SM, Muller WA, Buck CA, Newman PJ (1991). Molecular and cellular properties of PECAM-1 (endoCAM/CD31): a novel vascular cell-cell adhesion molecule. J Cell Biol; **114**(5):1059-1068.

Albonico M, Bickle Q, Ramsan M, Montresor A, Savioli L, Taylor M (2003). Efficacy of mebendazole and levamisole alone or in combination against intestinal nematode infections after repeated targeted mebendazole treatment in Zanzibar. Bull World Health Organ; **81**(5):343-352.

Albonico M, Ramsan M, Wright V, Jape K, Haji HJ, Taylor M, et al (2002). Soil-transmitted nematode infections and mebendazole treatment in Mafia Island schoolchildren. Ann Trop Med Parasitol; **96**(7):717-726.

Albonico M, Smith PG, Ercole E, Hall A, Chwaya HM, Alawi KS, et al (1995). Rate of reinfection with intestinal nematodes after treatment of children with mebendazole or albendazole in a highly endemic area. Trans R Soc Trop Med Hyg; **89**(5):538-541.

Albonico M, Stoltzfus RJ, Savioli L, Tielsch JM, Chwaya HM, Ercole E, et al (1998). Epidemiological evidence for a differential effect of hookworm species, Ancylostoma duodenale or Necator americanus, on iron status of children. Int J Epidemiol; **27**(3):530-537.

Alexander J (2002). Extracellular matrix, junctional integrity and matrix metalloproteinase interactions. J Anat; **200**(5):525.

Ali MH, Schlidt SA, Chandel NS, Hynes KL, Schumacker PT, Gewertz BL (1999). Endothelial permeability and IL-6 production during hypoxia: role of ROS in signal transduction. Am J Physiol; **277**(5 Pt 1):L1057-1065.

Andriopoulou P, Navarro P, Zanetti A, Lampugnani MG, Dejana E (1999). Histamine induces tyrosine phosphorylation of endothelial cell-to-cell adherens junctions. Arterioscler Thromb Vasc Biol; **19**(10):2286-2297.

Asojo OA, Goud G, Dhar K, Loukas A, Zhan B, Deumic V, et al (2005). X-ray structure of Na-ASP-2, a pathogenesis-related-1 protein from the nematode

parasite, Necator americanus, and a vaccine antigen for human hookworm infection. J Mol Biol; **346**(3):801-814.

Aurrand-Lions M, Johnson-Leger C, Imhof BA (2002). Role of interendothelial adhesion molecules in the control of vascular functions. Vascul Pharmacol; **39**(4-5):239-246.

Ayalon O, Sabanai H, Lampugnani MG, Dejana E, Geiger B (1994). Spatial and temporal relationships between cadherins and PECAM-1 in cell-cell junctions of human endothelial cells. J Cell Biol; **126**(1):247-258.

Balda MS, Whitney JA, Flores C, Gonzalez S, Cereijido M, Matter K (1996). Functional dissociation of paracellular permeability and transepithelial electrical resistance and disruption of the apical-basolateral intramembrane diffusion barrier by expression of a mutant tight junction membrane protein. J Cell Biol; **134**(4):1031-1049.

Bazzoni G (2006). Endothelial tight junctions: permeable barriers of the vessel wall. Thromb Haemost; **95**(1):36-42.

Bazzoni G, Dejana E (2004). Endothelial cell-to-cell junctions: molecular organization and role in vascular homeostasis. Physiol Rev; **84**(3):869-901.

Bazzoni G, Martinez Estrada O, Dejana E (1999). Molecular structure and functional role of vascular tight junctions. Trends Cardiovasc Med; **9**(6):147-152.

Beaver PC, Jung RC, Cupp EW (1984). Clinical parasitology. Philadelphia, Lea and Febiger (eds): 269-301.

Behnke JM (1991). In: Human parasitic Diseases: Hookworm Infection. Gilles HM, Ball PAJ (eds): 93-155.

Behnke JM, Paul V, Rajasekariah GR (1986). The growth and migration of Necator americanus following infection of neonatal hamsters. Trans R Soc Trop Med Hyg; **80**(1):146-149.

Bethony J, Brooker S, Albonico M, Geiger SM, Loukas A, Diemert D, et al (2006). Soil-transmitted helminth infections: ascariasis, trichuriasis, and hookworm. Lancet; **367**(9521):1521-1532.

Bethony J, Chen J, Lin S, Xiao S, Zhan B, Li S, et al (2002). Emerging patterns of hookworm infection: influence of aging on the intensity of Necator infection in Hainan Province, People's Republic of China. Clin Infect Dis; **35**(11):1336-1344.

Bethony J, Loukas A, Smout M, Brooker S, Mendez S, Plieskatt J, et al (2005). Antibodies against a secreted protein from hookworm larvae reduce the intensity of hookworm infection in humans and vaccinated laboratory animals. FASEB J; **19**(12):1743-1745.

Bin Z, Hawdon J, Qiang S, Hainan R, Huiqing Q, Wei H, et al (1999). Ancylostoma secreted protein 1 (ASP-1) homologues in human hookworms. Mol Biochem Parasitol; **98**(1):143-149.

Blum MS, Toninelli E, Anderson JM, Balda MS, Zhou J, O'Donnell L, et al (1997). Cytoskeletal rearrangement mediates human microvascular endothelial tight junction modulation by cytokines. Am J Physiol; **273**(1 Pt 2):H286-294.

Bogatcheva NV, Garcia JG, Verin AD (2002). Molecular mechanisms of thrombin-induced endothelial cell permeability. Biochemistry (Mosc); **67**(1):75-84.

Bonaldo P, Russo V, Bucciotti F, Doliana R, Colombatti A (1990). Structural and functional features of the alpha 3 chain indicate a bridging role for chicken collagen VI in connective tissues. Biochemistry; **29**(5):1245-1254.

Bonnefoy A, Harsfalvi J, Pfliegler G, Fauvel-Lafeve F, Legrand C (2001). The subendothelium of the HMEC-1 cell line supports thrombus formation in the absence of von Willebrand factor and collagen types I, III and VI. Thromb Haemost; **85**(3):552-559.

Boreham PF (1984). Activation in vitro of some biological systems by extracts of adult worms and microfilariae of Dirofilaria immitis. J Helminthol; **58**(3):207-212.

Bos JD, Kapsenberg ML. The immune system of the skin (1995). Ned Tijdschr Geneeskd; **139**(31):1587-1591.

Bower MA, Constant SL, Mendez S (2008). Necator americanus: the Na-ASP-2 protein secreted by the infective larvae induces neutrophil recruitment in vivo and in vitro. Exp Parasitol; **118**(4):569-575.

Braverman IM (2000). The cutaneous microcirculation. J Investig Dermatol Symp Proc; **5**(1):3-9.

Briggaman RA, Wheeler CE, Jr (1968). Epidermal-dermal interactions in adult human skin: role of dermis in epidermal maintenance. J Invest Dermatol; **51**(6):454-465.

Brooker S, Bethony J, Hotez PJ (2004). Human hookworm infection in the 21st century. Adv Parasitol; **58**:197-288.

Brophy PM, Patterson LH, Brown A, Pritchard DI (1995). Glutathione S-transferase (GST) expression in the human hookworm Necator americanus: potential roles for excretory-secretory forms of GST. Acta Trop; **59**(3):259-263.

Brown A, Burleigh JM, Billett EE, Pritchard DI (1995). An initial characterization of the proteolytic enzymes secreted by the adult stage of the human hookworm Necator americanus. Parasitology; **110** (Pt 5):555-563.

Brown A, Girod N, Billett EE, Pritchard DI (1999). Necator americanus (human hookworm) aspartyl proteinases and digestion of skin macromolecules during skin penetration. Am J Trop Med Hyg; **60**(5):840-847.

Brown AP (2000). Necator americanus: Characterisation of secreted proteinases and vaccine development; PhD thesis.

Brown JC, Mann K, Wiedemann H, Timpl R (1993). Structure and binding properties of collagen type XIV isolated from human placenta. J Cell Biol; **120**(2):557-567.

Budworth RA, Anderson M, Clothier RH, Leach L (1999). Histamine-induced Changes in the Actin Cytoskeleton of the Human Microvascular Endothelial Cell line HMEC-1. Toxicol in vitro; **13**(4-5):789-795.

Campbell WC, Benz GW (1984). Ivermectin: a review of efficacy and safety. J Vet Pharmacol Ther; **7**(1):1-16.

Carr A, Pritchard DI (1986). Identification of hookworm (Necator americanus) antigens and their translation in vitro. Mol Biochem Parasitol; **19**(3):251-258.

Chandrashekar R, Mehta K (2000). Transglutaminase-catalyzed reactions in the growth, maturation and development of parasitic nematodes. Parasitol Today; **16**(1):11-17.

Cheresh DA, Stupack DG (2008). Regulation of angiogenesis: apoptotic cues from the ECM. Oncogene; **27**(48):6285-6298.

Cline BL, Little MD, Bartholomew RK, Halsey NA (1984). Larvicidal activity of albendazole against Necator americanus in human volunteers. Am J Trop Med Hyg; **33**(3):387-394.

Collighan RJ, Griffin M (2009). Transglutaminase 2 cross-linking of matrix proteins: biological significance and medical applications. Amino Acids; **36**(4):659-670.

Cooke BM, Nash GB (1995). Plasmodium falciparum: characterization of adhesion of flowing parasitized red blood cells to platelets. Exp Parasitol; **80**(1):116-123.

Cooper PJ, Chico ME, Rodrigues LC, Ordonez M, Strachan D, Griffin GE, et al (2003). Reduced risk of atopy among school-age children infected with geohelminth parasites in a rural area of the tropics. J Allergy Clin Immunol; **111**(5):995-1000.

Cordenonsi M, D'Atri F, Hammar E, Parry DA, Kendrick-Jones J, Shore D, et al (1999). Cingulin contains globular and coiled-coil domains and interacts with ZO-1, ZO-2, ZO-3, and myosin. J Cell Biol; **147**(7):1569-1582.

Croese J, Wood MJ, Melrose W, Speare R (2006). Allergy controls the population density of Necator americanus in the small intestine. Gastroenterology; **131**(2):402-409.

Crompton DW (2000). The public health importance of hookworm disease. Parasitology; **121**:S39-50.

Culley FJ, Brown A, Conroy DM, Sabroe I, Pritchard DI, Williams TJ (2000). Eotaxin is specifically cleaved by hookworm metalloproteases preventing its action in vitro and in vivo. J Immunol; **165**(11):6447-6453.

Culley FJ, Brown A, Girod N, Pritchard DI, Williams TJ (2002). Innate and cognate mechanisms of pulmonary eosinophilia in helminth infection. Eur J Immunol; **32**(5):1376-1385.

Daub J, Loukas A, Pritchard DI, Blaxter M (2000). A survey of genes expressed in adults of the human hookworm, Necator americanus. Parasitology; **120**(Pt 2):171-184.

Day JR, Taylor KM, Lidington EA, Mason JC, Haskard DO, Randi AM, et al (2006). Aprotinin inhibits proinflammatory activation of endothelial cells by thrombin through the protease-activated receptor 1. J Thorac Cardiovasc Surg; **131**(1):21-27.

Dejana E, Bazzoni G, Lampugnani MG (1999). The role of endothelial cell-to-cell junctions in vascular morphogenesis. Thromb Haemost; **82**(2):755-761.

Dejana E, Corada M, Lampugnani MG (1995). Endothelial cell-to-cell junctions. FASEB J; **9**(10):910-918.

Dejana E, Lampugnani MG, Martinez-Estrada O, Bazzoni G (2000). The molecular organization of endothelial junctions and their functional role in vascular morphogenesis and permeability. Int J Dev Biol; **44**(6):743-748.

Dejana E, Orsenigo F, Lampugnani MG (2008). The role of adherens junctions and VE-cadherin in the control of vascular permeability. J Cell Sci; **121**(Pt 13):2115-2122.

Dejana E, Tournier-Lasserve E, Weinstein BM (2009). The control of vascular integrity by endothelial cell junctions: molecular basis and pathological implications. Dev Cell; **16**(2):209-221.

Del Forno C, Cerimele D, Serri F (1978). Histochemistry of the dermal ground substance of initial psoriatic lesions. Arch Dermatol Res; **262**(3):311-321.

DeLisser HM, Newman PJ, Albelda SM (1994). Molecular and functional aspects of PECAM-1/CD31. Immunol Today; **15**(10):490-495.

Desai TR, Leeper NJ, Hynes KL, Gewertz BL (2002). Interleukin-6 causes endothelial barrier dysfunction via the protein kinase C pathway. J Surg Res; **104**(2):118-123.

Desakorn V, Suntharasamai P, Pukrittayakamee S, Migasena S, Bunnag D (1987). Adherence of human eosinophils to infective filariform larvae of Necator americanus in vitro. Southeast Asian J Trop Med Public Health; **18**(1):66-72.

Devaney E (2005). The end of the line for hookworm? An update on vaccine development. PLoS Med; **2**(10):e327.

Dewi BE, Takasaki T, Kurane I (2004). In vitro assessment of human endothelial cell permeability: effects of inflammatory cytokines and dengue virus infection. J Virol Methods; **121**(2):171-180.

Dewi BE, Takasaki T, Kurane I (2008). Peripheral blood mononuclear cells increase the permeability of dengue virus-infected endothelial cells in association with downregulation of vascular endothelial cadherin. J Gen Virol; **89**(Pt 3):642-652.

Dondorp AM, Pongponratn E, White NJ (2004). Reduced microcirculatory flow in severe falciparum malaria: pathophysiology and electron-microscopic pathology. Acta Trop; **89**(3):309-317.

Dudek SM, Garcia JG (2001). Cytoskeletal regulation of pulmonary vascular permeability. J Appl Physiol; **91**(4):1487-1500.

Dvorak AM, Feng D (2001). The vesiculo-vacuolar organelle (VVO). A new endothelial cell permeability organelle. J Histochem Cytochem; **49**(4):419-432.

Edens HA, Parkos CA (2000). Modulation of epithelial and endothelial paracellular permeability by leukocytes. Adv Drug Deliv Rev; **41**(3):315-328.

Esser S, Lampugnani MG, Corada M, Dejana E, Risau W (1998). Vascular endothelial growth factor induces VE-cadherin tyrosine phosphorylation in endothelial cells. J Cell Sci; **111**(Pt 13):1853-1865.

Falcone FH, Pritchard DI (2005). Parasite role reversal: worms on trial. Trends Parasitol; **21**(4):157-160.

Fallon PG, Teixeira MM, Neice CM, Williams TJ, Hellewell PG, Doenhoff MJ (1996). Enhancement of Schistosoma mansoni infectivity by intradermal injections of larval extracts: a putative role for larval proteases. J Infect Dis; **173**(6):1460-1466.

Fichard A, Tillet E, Delacoux F, Garrone R, Ruggiero F (1997). Human recombinant alpha1(V) collagen chain. Homotrimeric assembly and subsequent processing. J Biol Chem; **272**(48):30083-30087.

Firth J (2002). Endothelial barriers: from hypothetical pores to membrane proteins. J Anat; **200**(5):524-525.

Flohr C, Quinnell RJ, Britton J (2009). Do helminth parasites protect against atopy and allergic disease? Clin Exp Allergy; **39**(1):20-32.

Furuse M, Fujita K, Hiiragi T, Fujimoto K, Tsukita S (1998). Claudin-1 and -2: novel integral membrane proteins localizing at tight junctions with no sequence similarity to occludin. J Cell Biol; **141**(7):1539-1550.

Furuse M, Hirase T, Itoh M, Nagafuchi A, Yonemura S, Tsukita S (1993). Occludin: a novel integral membrane protein localizing at tight junctions. J Cell Biol; **123**(6 Pt 2):1777-1788.

Furuse M, Itoh M, Hirase T, Nagafuchi A, Yonemura S, Tsukita S (1994). Direct association of occludin with ZO-1 and its possible involvement in the localization of occludin at tight junctions. J Cell Biol; **127**(6 Pt 1):1617-1626.

Garcia JG, Davis HW, Patterson CE (1995). Regulation of endothelial cell gap formation and barrier dysfunction: role of myosin light chain phosphorylation. J Cell Physiol; **163**(3):510-522.

Garlanda C, Dejana E (1997). Heterogeneity of endothelial cells. Specific markers. Arterioscler Thromb Vasc Biol; **17**(7):1193-1202.

Garrone R, Lethias C, Le Guellec D (1997). Distribution of minor collagens during skin development. Microsc Res Tech; **38**(4):407-412.

Gavard J, Gutkind JS (2006). VEGF controls endothelial-cell permeability by promoting the beta-arrestin-dependent endocytosis of VE-cadherin. Nat Cell Biol; **8**(11):1223-1234.

Gavard J, Hou X, Qu Y, Masedunskas A, Martin D, Weigert R, et al (2009). A role for a CXCR2/phosphatidylinositol 3-kinase gamma signaling axis in acute and chronic vascular permeability. Mol Cell Biol; **29**(9):2469-2480.

Geiger SM, Caldas IR, Mc Glone BE, Campi-Azevedo AC, De Oliveira LM, Brooker S, et al (2007). Stage-specific immune responses in human Necator americanus infection. Parasite Immunol; **29**(7):347-358.

Geiger SM, Massara CL, Bethony J, Soboslay PT, Correa-Oliveira R (2004). Cellular responses and cytokine production in post-treatment hookworm patients from an endemic area in Brazil. Clin Exp Immunol; **136**(2):334-340.

Ghohestani RF, Li K, Rousselle P, Uitto J (2001). Molecular organization of the cutaneous basement membrane zone. Clin Dermatol; **19**(5):551-562.

Girard JP, Springer TA (1995). High endothelial venules (HEVs): specialized endothelium for lymphocyte migration. Immunol Today; **16**(9):449-457.

Girod N, Brown A, Pritchard DI, Billett EE (2003). Successful vaccination of BALB/c mice against human hookworm (Necator americanus): the immunological phenotype of the protective response. Int J Parasitol; **33**(1):71-80.

Girolomoni G, Caux C, Lebecque S, Dezutter-Dambuyant C, Ricciardi-Castagnoli P (2002). Langerhans cells: still a fundamental paradigm for studying the immunobiology of dendritic cells. Trends Immunol; **23**(1):6-8.

Gonnet F, Lemaitre G, Waksman G, Tortajada J (2003). MALDI/MS peptide mass fingerprinting for proteome analysis: identification of hydrophobic proteins attached to eucaryote keratinocyte cytoplasmic membrane using different matrices in concert. Proteome Sci; **1**(1):2.

Gonzalez-Mariscal L, Tapia R, Chamorro D (2008). Crosstalk of tight junction components with signaling pathways. Biochim Biophys Acta;**1778**(3):729-756.

Goode BL, Eck MJ (2007). Mechanism and function of formins in the control of actin assembly. Annu Rev Biochem; **76**:593-627.

Gordon MK, Olsen BR (1990). The contribution of collagenous proteins to tissue-specific matrix assemblies. Curr Opin Cell Biol; **2**(5):833-838.

Goud GN, Bottazzi ME, Zhan B, Mendez S, Deumic V, Plieskatt J, et al (2005). Expression of the Necator americanus hookworm larval antigen Na-ASP-2 in Pichia pastoris and purification of the recombinant protein for use in human clinical trials. Vaccine; **23**(39):4754-4764.

Gunderson HJ, Jensen EB, Kieu K, Nielson J (1999). The efficiency of systematic sampling in stereology-recognised. J Microsc; **193**:199-211.

Haas W, Haberl B, Syafruddin, Idris I, Kallert D, Kersten S, et al (2005). Behavioural strategies used by the hookworms Necator americanus and Ancylostoma duodenale to find, recognize and invade the human host. Parasitol Res; **95**(1):30-39.

Haas W, Haberl B, Syafruddin, Idris I, Kersten S (2005a). Infective larvae of the human hookworms Necator americanus and Ancylostoma duodenale differ in their orientation behaviour when crawling on surfaces. Parasitol Res; **95**(1):25-29.

Han ED, MacFarlane RC, Mulligan AN, Scafidi J, Davis AE (2002). Increased vascular permeability in C1 inhibitor-deficient mice mediated by the bradykinin type 2 receptor. J Clin Invest; **109**(8):1057-1063.

Hansell E, Braschi S, Medzihradszky KF, Sajid M, Debnath M, Ingram J, et al (2008). Proteomic analysis of skin invasion by blood fluke larvae. PLoS Negl Trop Dis; **2**(7):e262.

Harhaj NS, Antonetti DA (2004). Regulation of tight junctions and loss of barrier function in pathophysiology. Int J Biochem Cell Biol; **36**(7):1206-1237.

Hawdon JM, Datu B (2003). The second messenger cyclic GMP mediates activation in Ancylostoma caninum infective larvae. Int J Parasitol; **33**(8):787-793.

Hawdon JM, Hotez PJ (1996). Hookworm: developmental biology of the infectious process. Curr Opin Genet Dev; **6**(5):618-623.

Hawdon JM, Jones BF, Perregaux MA, Hotez PJ (1995). Ancylostoma caninum: metalloprotease release coincides with activation of infective larvae in vitro. Exp Parasitol; **80**(2):205-211.

Hawdon JM, Narasimhan S, Hotez PJ (1999). Ancylostoma secreted protein 2: cloning and characterization of a second member of a family of nematode secreted proteins from Ancylostoma caninum. Mol Biochem Parasitol; **99**(2):149-165.

Hawdon JM, Schad GA (1990). Serum-stimulated feeding in vitro by third-stage infective larvae of the canine hookworm Ancylostoma caninum. J Parasitol; **76**(3):394-398.

Hawdon JM, Volk SW, Rose R, Pritchard DI, Behnke JM, Schad GA (1993). Observations on the feeding behaviour of parasitic third-stage hookworm larvae. Parasitology; **106** (Pt 2):163-169.

Heaphy MR, Winkelmann RK (1977). The human cutaneous basement membrane--anchoring fibril complex: preparation and ultrastructure. J Invest Dermatol; **68**(4):177-178.

Hewitt CR, Brown AP, Hart BJ, Pritchard DI (1995). A major house dust mite allergen disrupts the immunoglobulin E network by selectively cleaving CD23: innate protection by antiproteases. J Exp Med; **182**(5):1537-1544.

Hoagland KE, Schad GA (1978). Necator americanus and Ancylostoma duodenale: life history parameters and epidemiological implications of two sympatric hookworms of humans. Exp Parasitol; **44**(1):36-49.

Holbrook KA, Odland GF (1975). The fine structure of developing human epidermis: light, scanning, and transmission electron microscopy of the periderm. J Invest Dermatol; **65**(1):16-38.

Hordijk PL, Anthony E, Mul FP, Rientsma R, Oomen LC, Roos D (1999). Vascular-endothelial-cadherin modulates endothelial monolayer permeability. J Cell Sci; **112**(Pt 12):1915-1923.

Horton J (2003). Human gastrointestinal helminth infections: are they now neglected diseases? Trends Parasitol; **19**(11):527-531.

Hotez P (2008). Hookworm and poverty. Ann N Y Acad Sci; **1136**:38-44.

Hotez P, Haggerty J, Hawdon J, Milstone L, Gamble HR, Schad G, et al (1990). Metalloproteases of infective Ancylostoma hookworm larvae and their possible functions in tissue invasion and ecdysis. Infect Immun; **58**(12):3883-3892.

Hotez PJ, Bethony J, Bottazzi ME, Brooker S, Buss P (2005). Hookworm: "the great infection of mankind". PLoS Med; **2**(3):e67.

Hotez PJ, Brooker S, Bethony JM, Bottazzi ME, Loukas A, Xiao S (2004). Hookworm infection. N Engl J Med; **351**(8):799-807.

Hotez PJ, Narasimhan S, Haggerty J, Milstone L, Bhopale V, Schad GA, et al (1992). Hyaluronidase from infective Ancylostoma hookworm larvae and its possible function as a virulence factor in tissue invasion and in cutaneous larva migrans. Infect Immun; **60**(3):1018-1023.

Hotez PJ, Pritchard DI (1995). Hookworm infection. Sci Am; **272**(6):68-74.

Hotez PJ, Zhan B, Bethony JM, Loukas A, Williamson A, Goud GN, et al (2003). Progress in the development of a recombinant vaccine for human hookworm disease: the Human Hookworm Vaccine Initiative. Int J Parasitol; **33**(11):1245-1258.

Hsieh GC, Loukas A, Wahl AM, Bhatia M, Wang Y, Williamson AL, et al (2004). A secreted protein from the human hookworm necator americanus binds selectively to NK cells and induces IFN-gamma production. J Immunol; **173**(4):2699-2704.

Huttelmaier S, Harbeck B, Steffens O, Messerschmidt T, Illenberger S, Jockusch BM (1999). Characterization of the actin binding properties of the vasodilator-stimulated phosphoprotein VASP. FEBS Lett; **451**(1):68-74.

Huxley VH, Curry FE (1991). Differential actions of albumin and plasma on capillary solute permeability. Am J Physiol; **260**(5 Pt 2):H1645-1654.

Ilan N, Cheung L, Pinter E, Madri JA (2000). Platelet-endothelial cell adhesion molecule-1 (CD31), a scaffolding molecule for selected catenin family members whose binding is mediated by different tyrosine and serine/threonine phosphorylation. J Biol Chem; **275**(28):21435-21443.

Imamura T, Potempa J, Pike RN, Travis J (1995). Dependence of vascular permeability enhancement on cysteine proteinases in vesicles of Porphyromonas gingivalis. Infect Immun; **63**(5):1999-2003.

Inomata M, Into T, Ishihara Y, Nakashima M, Noguchi T, Matsushita K (2007). Arginine-specific gingipain A from Porphyromonas gingivalis induces Weibel-Palade body exocytosis and enhanced activation of vascular endothelial

cells through protease-activated receptors. Microbes Infect; **9**(12-13):1500-1506.

Ishida-Yamamoto A, Iizuka H (1998). Structural organization of cornified cell envelopes and alterations in inherited skin disorders. Exp Dermatol; **7**(1):1-10.

Jackson DE, Kupcho KR, Newman PJ (1997). Characterization of phosphotyrosine binding motifs in the cytoplasmic domain of platelet/endothelial cell adhesion molecule-1 (PECAM-1) that are required for the cellular association and activation of the protein-tyrosine phosphatase, SHP-2. J Biol Chem; **272**(40):24868-24875.

Jaffe EA, Nachman RL, Becker CG, Minick CR (1973). Culture of human endothelial cells derived from umbilical veins. Identification by morphologic and immunologic criteria. J Clin Invest; **52**(11):2745-2756.

Jian X, Shu-Hua X, Hui-Qing Q, Sen L, Hotez P, Bing-Gui S, et al (2003). Necator americanus: maintenance through one hundred generations in golden hamsters (Mesocricetus auratus). II. Morphological development of the adult and its comparison with humans. Exp Parasitol; **105**(3-4):192-200.

Jiang WG, Bryce RP, Horrobin DF, Mansel RE (1998). Regulation of tight junction permeability and occludin expression by polyunsaturated fatty acids. Biochem Biophys Res Commun; **244**(2):414-420.

Jimbow K, Quevedo WC, Jr., Fitzpatrick TB, Szabo G (1976). Some aspects of melanin biology: 1950-1975. J Invest Dermatol; **67**(1):72-89.

Johannsson E, Henriksen T, Iversen PO (2007). Increase in matrix metalloproteinases from endothelial cells exposed to umbilical cord plasma from high birth weight newborns. Am J Physiol Regul Integr Comp Physiol; **292**(4):R1563-1568.

Karnovsky MJ (1967). The ultrastructural basis of capillary permeability studied with peroxidase as a tracer. J Cell Biol; **35**(1):213-236.

Karnovsky MJ (1968). The Ultrastructural Basis of Transcapillary Exchanges. J Gen Physiol; **52**(1):64-95.

Kasper G, Brown A, Eberl M, Vallar L, Kieffer N, Berry C, et al (2001). A calreticulin-like molecule from the human hookworm Necator americanus interacts with C1q and the cytoplasmic signalling domains of some integrins. Parasite Immunol; **23**(3):141-152.

Keiser J, Utzinger J (2008). Efficacy of current drugs against soil-transmitted helminth infections: systematic review and meta-analysis. JAMA; **299**(16):1937-1948.

Kidd RL, Krawczyk WS, Wilgram GF (1971). The Merkel cell in human epidermis: its differentiation from other dendritic cells. Arch Dermatol Forsch; **241**(4):374-384.

Kiistala U, Mustakallio KK (1968). The presence of Langerhans cells in human dermis with special reference to their potential mesenchymal origin. Acta Derm Venereol; **48**(2):115-122.

Kim EA, Kim JA, Park MH, Jung SC, Suh SH, Pang MG, et al (2009). Lysophosphatidylcholine induces endothelial cell injury by nitric oxide production through oxidative stress. J Matern Fetal Neonatal Med; **22**(4):325-331.

Klarenbach SW, Chipiuk A, Nelson RC, Hollenberg MD, Murray AG (2003). Differential actions of PAR2 and PAR1 in stimulating human endothelial cell exocytosis and permeability: the role of Rho-GTPases. Circ Res; **92**(3):272-278.

Kowalczyk AP, Navarro P, Dejana E, Bornslaeger EA, Green KJ, Kopp DS, et al (1998). VE-cadherin and desmoplakin are assembled into dermal microvascular endothelial intercellular junctions: a pivotal role for plakoglobin in the recruitment of desmoplakin to intercellular junctions. J Cell Sci; **111**(Pt 20):3045-3057.

Kucharz EJ (1992). The collagens: biochemistry and patho-physiology. New York, Springer (eds).

Kumar N, Gupta PS, Saha K, Misra RC, Agarwal DS, Chuttani HK (1980). Serum and intestinal immunoglobulins in patients of ancylostomiasis. Indian J Med Res; **71**:531-537.

Kumar S, Pritchard DI (1992). Skin penetration by ensheathed third-stage infective larvae of Necator americanus, and the host's immune response to larval antigens. Int J Parasitol; **22**(5):573-579.

Kumar S, Pritchard DI (1992a). The partial characterization of proteases present in the excretory/secretory products and exsheathing fluid of the infective (L3) larva of Necator americanus. Int J Parasitol; **22**(5):563-572.

Kumar S, West DC, Ager A (1987). Heterogeneity in endothelial cells from large vessels and microvessels. Differentiation; **36**(1):57-70.

Lacour JP, Dubois D, Pisani A, Ortonne JP (1991). Anatomical mapping of Merkel cells in normal human adult epidermis. Br J Dermatol; **125**(6):535-542.

Lafleur MA, Hollenberg MD, Atkinson SJ, Knauper V, Murphy G, Edwards DR (2001). Activation of pro-(matrix metalloproteinase-2) (pro-MMP-2) by thrombin is membrane-type-MMP-dependent in human umbilical vein endothelial cells and generates a distinct 63 kDa active species. Biochem J; **357**(Pt 1):107-115.

Lampugnani MG, Corada M, Caveda L, Breviario F, Ayalon O, Geiger B, et al (1995). The molecular organization of endothelial cell to cell junctions: differential association of plakoglobin, beta-catenin, and alpha-catenin with vascular endothelial cadherin (VE-cadherin). J Cell Biol; **129**(1):203-217.

Lampugnani MG, Dejana E (1997). Interendothelial junctions: structure, signalling and functional roles. Curr Opin Cell Biol; **9**(5):674-682.

Lampugnani MG, Resnati M, Raiteri M, Pigott R, Pisacane A, Houen G, et al (1992). A novel endothelial-specific membrane protein is a marker of cell-cell contacts. J Cell Biol; **118**(6):1511-1522.

Lavker RM, Matoltsy AG (1971). Substructure of keratohyalin granules of the epidermis as revealed by high resolution electron microscopy. J Ultrastruct Res; **35**(5):575-581.

Leach L (2002). The phenotype of the human materno-fetal endothelial barrier: molecular occupancy of paracellular junctions dictate permeability and angiogenic plasticity. J Anat; **200**(6):599-606.

Leach L, Clark P, Lampugnani MG, Arroyo AG, Dejana E, Firth JA (1993). Immunoelectron characterisation of the inter-endothelial junctions of human term placenta. J Cell Sci; **104**(Pt 4):1073-1081.

Leach L, Eaton BM, Westcott ED, Firth JA (1995). Effect of histamine on endothelial permeability and structure and adhesion molecules of the paracellular junctions of perfused human placental microvessels. Microvasc Res; **50**(3):323-337.

Leach L, Firth JA (1995). Advances in understanding permeability in fetal capillaries of the human placenta: a review of organization of the endothelial paracellular clefts and their junctional complexes. Reprod Fertil Dev; **7**(6):1451-1456.

Leach L, Taylor A, Sciota F (2009). Vascular dysfunction in the diabetic placenta: causes and consequences. J Anat; **215**(1):69-76.

Lejoly-Boisseau H, Appriou M, Seigneur M, Pruvost A, Tribouley-Duret J, Tribouley J (1999). Schistosoma mansoni: in vitro adhesion of parasite eggs to the vascular endothelium. Subsequent inhibition by a monoclonal antibody directed to a carbohydrate epitope. Exp Parasitol; **91**(1):20-29.

Leonardi-Bee J, Pritchard D, Britton J (2006). Asthma and current intestinal parasite infection: systematic review and meta-analysis. Am J Respir Crit Care Med; **174**(5):514-523.

Liaw CW, Cannon C, Power MD, Kiboneka PK, Rubin LL (1990). Identification and cloning of two species of cadherins in bovine endothelial cells. EMBO J; **9**(9):2701-2708.

Loukas A, Constant SL, Bethony JM (2005). Immunobiology of hookworm infection. FEMS Immunol Med Microbiol; **43**(2):115-124.

Loukas A, Bethony JM, Mendez S, Fujiwara RT, Goud GN, Ranjit N, et al (2005a). Vaccination with recombinant aspartic hemoglobinase reduces parasite load and blood loss after hookworm infection in dogs. PLoS Med; **2**(10):e295.

Loukas A, Dowd AJ, Prociv P, Brindley PJ (2000). Purification of a diagnostic, secreted cysteine protease-like protein from the hookworm Ancylostoma caninum. Parasitol Int; **49**(4):327-333.

Loukas A, Opdebeeck J, Croese J, Prociv P (1996). Immunoglobulin G subclass antibodies against excretory/secretory antigens of Ancylostoma caninum in human enteric infections. Am J Trop Med Hyg; **54**(6):672-676.

Loukas A, Prociv P (2001). Immune responses in hookworm infections. Clin Microbiol Rev; **14**(4):689-703.

Lukacs NW, Strieter RM, Elner V, Evanoff HL, Burdick MD, Kunkel SL (1995). Production of chemokines, interleukin-8 and monocyte chemoattractant protein-1, during monocyte: endothelial cell interactions. Blood; **86**(7):2767-2773.

Lum H, Malik AB (1994). Regulation of vascular endothelial barrier function. Am J Physiol; **267**(3 Pt 1):L223-241.

Lustigman S, Brotman B, Huima T, Castelhano AL, Singh RN, Mehta K, et al (1995). Transglutaminase-catalyzed reaction is important for molting of Onchocerca volvulus third-stage larvae. Antimicrob Agents Chemother; **39**(9):1913-1919.

Lynley AM, Dale BA (1983). The characterization of human epidermal filaggrin. A histidine-rich, keratin filament-aggregating protein. Biochim Biophys Acta; **744**(1):28-35.

Mackenzie IC (1975). Ordered structure of the epidermis. J Invest Dermatol; **65**(1):45-51.

Majno G, Palade GE (1961). Studies on inflammation. 1. The effect of histamine and serotonin on vascular permeability: an electron microscopic study. J Biophys Biochem Cytol; **11**:571-605.

Man S, Ubogu EE, Williams KA, Tucky B, Callahan MK, Ransohoff RM (2008). Human brain microvascular endothelial cells and umbilical vein endothelial cells differentially facilitate leukocyte recruitment and utilize chemokines for T cell migration. Clin Dev Immunol; **2008**:384982.

Marinkovich MP, Lunstrum GP, Keene DR, Burgeson RE (1992). The dermal-epidermal junction of human skin contains a novel laminin variant. J Cell Biol; **119**(3):695-703.

Martin GR, Timpl R (1987). Laminin and other basement membrane components. Annu Rev Cell Biol; **3**:57-85.

Matthews BE (1975). Mechanism of skin penetration by Ancylostoma tubaeforme larvae. Parasitology; **70**(1):25-38.

Matthews BE (1982). Skin penetration by Necator americanus larvae. Z Parasitenkd; **68**(1):81-86.

McGrath JA, Eady RAJ, Pope FM (2008). Anatomy and Organization of Human Skin. In: Rook's Textbook of Dermatology. New York, Blackwell Science Ltd (eds):45-128.

McGrath JA, Uitto J (2008). The filaggrin story: novel insights into skin-barrier function and disease. Trends Mol Med; **14**(1):20-27.

McLaren DJ (1974). The anterior glands of adult Necator americanus (Nematoda: Strongyloidea). I. Ultrastructural studies. Int J Parasitol; **4**(1):25-37.

McLean WH, Hull PR (2007). Breach delivery: increased solute uptake points to a defective skin barrier in atopic dermatitis. J Invest Dermatol; **127**(1):8-10.

Meeusen EN, Balic A (2000). Do eosinophils have a role in the killing of helminth parasites? Parasitol Today; **16**(3):95-101.

Mehta D, Malik AB (2006). Signaling mechanisms regulating endothelial permeability. Physiol Rev; **86**(1):279-367.

Minshall RD, Tiruppathi C, Vogel SM, Malik AB (2002). Vesicle formation and trafficking in endothelial cells and regulation of endothelial barrier function. Histochem Cell Biol; **117**(2):105-112.

Miyake K, Underhill CB, Lesley J, Kincade PW (1990). Hyaluronate can function as a cell adhesion molecule and CD44 participates in hyaluronate recognition. J Exp Med; **172**(1):69-75.

Miyasaka M, Tanaka T (2004). Lymphocyte trafficking across high endothelial venules: dogmas and enigmas. Nat Rev Immunol; **4**(5):360-370.

Moll T, Dejana E, Vestweber D (1998). In vitro degradation of endothelial catenins by a neutrophil protease. J Cell Biol; **140**(2):403-407.

Mortimer K, Brown A, Feary J, Jagger C, Lewis S, Antoniak M, et al (2006). Dose-ranging study for trials of therapeutic infection with Necator americanus in humans. Am J Trop Med Hyg; **75**(5):914-920.

Muller SL, Portwich M, Schmidt A, Utepbergenov DI, Huber O, Blasig IE, et al (2005). The tight junction protein occludin and the adherens junction protein alpha-catenin share a common interaction mechanism with ZO-1. J Biol Chem; **280**(5):3747-3756.

Muller WA (2003). Leukocyte-endothelial-cell interactions in leukocyte transmigration and the inflammatory response. Trends Immunol; **24**(6):327-334.

Muro S, Koval M, Muzykantov V (2004). Endothelial endocytic pathways: gates for vascular drug delivery. Curr Vasc Pharmacol; **2**(3):281-299.

Narvaez D, Kanitakis J, Faure M, Claudy A (1996). Immunohistochemical study of CD34-positive dendritic cells of human dermis. Am J Dermatopathol; **18**(3):283-288.

Navarro P, Caveda L, Breviario F, Mandoteanu I, Lampugnani MG, Dejana E (1995). Catenin-dependent and -independent functions of vascular endothelial cadherin. J Biol Chem; **270**(52):30965-30972.

Nawroth R, Poell G, Ranft A, Kloep S, Samulowitz U, Fachinger G, et al (2002). VE-PTP and VE-cadherin ectodomains interact to facilitate regulation of phosphorylation and cell contacts. EMBO J; **21**(18):4885-4895.

Newman PJ (1999). Switched at birth: a new family for PECAM-1. J Clin Invest; **103**(1):5-9.

Nishiyama T, Amano S, Tsunenaga M, Kadoya K, Takeda A, Adachi E, et al (2000). The importance of laminin 5 in the dermal-epidermal basement membrane. J Dermatol Sci; **24**:S51-59.

Nishiyama T, McDonough AM, Bruns RR, Burgeson RE (1994). Type XII and XIV collagens mediate interactions between banded collagen fibers in vitro and may modulate extracellular matrix deformability. J Biol Chem; **269**(45):28193-28199.

Noda M, Yasuda-Fukazawa C, Moriishi K, Kato T, Okuda T, Kurokawa K, et al (1995). Involvement of rho in GTP gamma S-induced enhancement of phosphorylation of 20 kDa myosin light chain in vascular smooth muscle cells: inhibition of phosphatase activity. FEBS Lett; **367**(3):246-250.

Nwariaku FE, Liu Z, Zhu X, Nahari D, Ingle C, Wu RF, et al (2004). NADPH oxidase mediates vascular endothelial cadherin phosphorylation and endothelial dysfunction. Blood; **104**(10):3214-3220.

Odland GF (1991). Structure of the skin. In: Goldsmith LA, ed. Physiology, Biochemistry, and Molecular Biology of the Skin. New York, Oxford University Press:3-62.

Odland GF, Holbrook K (1981). The lamellar granules of epidermis. Curr Probl Dermatol; **9**:29-49.

Orlova VV, Economopoulou M, Lupu F, Santoso S, Chavakis T (2006). Junctional adhesion molecule-C regulates vascular endothelial permeability by modulating VE-cadherin-mediated cell-cell contacts. J Exp Med; **203**(12):2703-2714.

Palmer DR, Bradley M, Bundy DA (1996). IgG4 responses to antigens of adult Necator americanus: potential for use in large-scale epidemiological studies. Bull World Health Organ; **74**(4):381-386.

Pappenheimer JR, Renkin EM, Borrero LM (1951). Filtration, diffusion and molecular sieving through peripheral capillary membranes; a contribution to the pore theory of capillary permeability. Am J Physiol; **167**(1):13-46.

Pearce RH (1968). Proteins of the ground substance of human dermis. Biochem Pharmacol: 156-7.

Pearson MS, Bethony JM, Pickering DA, de Oliveira LM, Jariwala A, Santiago H, et al (2009). An enzymatically inactivated hemoglobinase from Necator americanus induces neutralizing antibodies against multiple hookworm species and protects dogs against heterologous hookworm infection. FASEB J; **23**(9):3007-3019.

Peltonen J, Larjava H, Jaakkola S, Gralnick H, Akiyama SK, Yamada SS, et al (1989). Localization of integrin receptors for fibronectin, collagen, and laminin in human skin. Variable expression in basal and squamous cell carcinomas. J Clin Invest; **84**(6):1916-1923.

Petreaca ML, Yao M, Liu Y, Defea K, Martins-Green M (2007). Transactivation of vascular endothelial growth factor receptor-2 by interleukin-8 (IL-8/CXCL8) is required for IL-8/CXCL8-induced endothelial permeability. Mol Biol Cell; **18**(12):5014-5023.

Pino P, Vouldoukis I, Kolb JP, Mahmoudi N, Desportes-Livage I, Bricaire F, et al (2003). Plasmodium falciparum--infected erythrocyte adhesion induces caspase activation and apoptosis in human endothelial cells. J Infect Dis; **187**(8):1283-1290.

Pit DS, Polderman AM, Baeta S, Schulz-Key H, Soboslay PT (2001). Parasite-specific antibody and cellular immune responses in human infected with Necator americanus and Oesophagostomum bifurcum. Parasitol Res; **87**(9):722-729.

Plopper G (2007). The extracellular matrix and cell adhesion. In: Cells. Sudbury, MA: Jones and Barlett.

Predescu D, Palade GE (1993). Plasmalemmal vesicles represent the large pore system of continuous microvascular endothelium. Am J Physiol; **265**(2 Pt 2):H725-733.

Pritchard DI (1995). Gastrointestinal nematodes: the Karkar experience. P N G Med J; **38**(4):295-299.

Pritchard DI, Brown A (2001). Is Necator americanus approaching a mutualistic symbiotic relationship with humans? Trends Parasitol; **17**(4):169-172.

Pritchard DI, Brown A, Kasper G, McElroy P, Loukas A, Hewitt C, et al (1999). A hookworm allergen which strongly resembles calreticulin. Parasite Immunol; **21**(9):439-450.

Pritchard DI, Leggett KV, Rogan MT, McKean PG, Brown A (1991). Necator americanus secretory acetylcholinesterase and its purification from excretory-secretory products by affinity chromatography. Parasite Immunol; **13**(2):187-199.

Pritchard DI, Quinnell RJ, Slater AF, McKean PG, Dale DD, Raiko A, et al (1990). Epidemiology and immunology of Necator americanus infection in a community in Papua New Guinea: humoral responses to excretory-secretory and cuticular collagen antigens. Parasitology; **100** (Pt 2):317-326.

Pritchard DI, Quinnell RJ, Walsh EA (1995). Immunity in humans to Necator americanus: IgE, parasite weight and fecundity. Parasite Immunol;**17**(2):71-75.

Pritchard DI, Walsh EA (1995). The specificity of the human IgE response to Necator americanus. Parasite Immunol; **17**(11):605-607.

Pritchard DI, Walsh EA, Quinell RJ, Raiko A, Edmonds P, Keymer AE (1992). Isotypic variation in antibody responses in a community in Papua New Guinea to larval and adult antigens during infection, and following reinfection, with the hookworm Necator americanus. Parasite Immunol; **14**(6):617-631.

Quinnell RJ, Pritchard DI, Raiko A, Brown AP, Shaw MA (2004). Immune responses in human necatoriasis: association between interleukin-5 responses and resistance to reinfection. J Infect Dis; **190**(3):430-438.

Quinnell RJ, Bethony J, Pritchard DI (2004a). The immunoepidemiology of human hookworm infection. Parasite Immunol; **26**(11-12):443-454.

Quinnell RJ, Slater AF, Tighe P, Walsh EA, Keymer AE, Pritchard DI (1993). Reinfection with hookworm after chemotherapy in Papua New Guinea. Parasitology; **106**(Pt 4):379-385.

Rao CN, Cook B, Liu Y, Chilukuri K, Stack MS, Foster DC, et al (1998). HT-1080 fibrosarcoma cell matrix degradation and invasion are inhibited by the

matrix-associated serine protease inhibitor TFPI-2/33 kDa MSPI. Int J Cancer; **76**(5):749-756.

Rao CN, Liu YY, Peavey CL, Woodley DT (1995). Novel extracellular matrix-associated serine proteinase inhibitors from human skin fibroblasts. Arch Biochem Biophys; **317**(1):311-314.

Rao UR, Chapman MR, Singh RN, Mehta K, Klei TR (1999). Transglutaminase activity in equine strongyles and its potential role in growth and development. Parasite; **6**(2):131-139.

Reddy A, Fried B (2007). The use of Trichuris suis and other helminth therapies to treat Crohn's disease. Parasitol Res; **100**(5):921-927.

Reddy A, Fried B (2009). An update on the use of helminths to treat Crohn's and other autoimmunune diseases. Parasitol Res; **104**(2):217-221.

Reilly D, Larkin D, Devocelle M, Fitzgerald DJ, Moran N (2004). Calreticulin-independent regulation of the platelet integrin alphaIIbbeta3 by the KVGFFKR alphaIIb-cytoplasmic motif. Platelets; **15**(1):43-54.

Reynolds AB, Carnahan RH (2004). Regulation of cadherin stability and turnover by p120ctn: implications in disease and cancer. Semin Cell Dev Biol; **15**(6):657-663.

Roberts WG, Palade GE (1995). Increased microvascular permeability and endothelial fenestration induced by vascular endothelial growth factor. J Cell Sci; **108**(Pt 6):2369-2379.

Rodrigo FG, Cotta-Pereira G (1979). Connective fibers involved in the dermoepidermal anchorage. An electron microscopical study. Dermatologica; **158**(1):13-23.

Rogers WP, Brooks F (1977). The mechanism of hatching of eggs of Haemonchus contortus. Int J Parasitol; **7**(1):61-65.

Rogers WP, Brooks F (1978). Leucine aminopeptidase in exsheathing fluid of North American and Australian Haemonchus contortus. Int J Parasitol; **8**(1):55-58.

Rogers WP, Sommerville RI (1963). The Infective Stage of Nematode Parasites and Its Significance in Parasitism. Adv Parasitol; **1**:109-177.

Rubin LL, Staddon JM (1999). The cell biology of the blood-brain barrier. Annu Rev Neurosci; **22**:11-28.

Ruffer C, Strey A, Janning A, Kim KS, Gerke V (2004). Cell-cell junctions of dermal microvascular endothelial cells contain tight and adherens junction proteins in spatial proximity. Biochemistry; **43**(18):5360-5369.

Ruggiero F, Champliaud MF, Garrone R, Aumailley M (1994). Interactions between cells and collagen V molecules or single chains involve distinct mechanisms. Exp Cell Res; **210**(2):215-223.

Ruggiero F, Roulet M, Bonod-Bidaud C (2005). Dermis collagens: beyond their structural properties. J Soc Biol; **199**(4):301-311.

Ruoslahti E (1988). Fibronectin and its receptors. Annu Rev Biochem; **57**:375-413.

Rutten MJ, Hoover RL, Karnovsky MJ (1987). Electrical resistance and macromolecular permeability of brain endothelial monolayer cultures. Brain Res; **425**(2):301-310.

Saalbach A, Aneregg U, Bruns M, Schnabel E, Herrmann K, Haustein UF (1996). Novel fibroblast-specific monoclonal antibodies: properties and specificities. J Invest Dermatol; **106**(6):1314-1319.

Salafsky B, Fusco A, Siddiqui A (1990). Necator americanus: factors influencing skin penetration by larvae. In: Schad GA, Warren KS (eds) Hookworm disease: current status and new directions. London, Taylor and Francis:329-339.

Sandoval R, Malik AB, Minshall RD, Kouklis P, Ellis CA, Tiruppathi C (2001). Ca(2+) signalling and PKCalpha activate increased endothelial permeability by disassembly of VE-cadherin junctions. J Physiol; **533**(Pt 2):433-445.

Sasa M, Shirasaka R, Tanaka H, Miura A, Yamamoto H, Katahira K (1960). Observation on the behavior of infective larvae of hookworms and related nematode parasites, with notes on the effect of carbon dioxide in the breath as the stimulant. Jpn J Exp Med; **30**:433-447.

Schad GA (1991). Presidential address. Hooked on hookworm: 25 years of attachment. J Parasitol; **77**(2):176-186.

Schad GA, Chowdhury AB, Dean CG, Kochar VK, Nawalinski TA, Thomas J, et al (1973). Arrested Development in Human Hookworm Infections: An Adaptation to a Seasonally Unfavorable External Environment. Science; **180**(4085):502-504.

Schechter NM (1989). Structure of the dermal-epidermal junction and potential mechanisms for its degradation: the possible role of inflammatory cells. Immunol Ser; **46**:477-507.

Schmelz M, Moll R, Kuhn C, Franke WW (1994). Complexus adhaerentes, a new group of desmoplakin-containing junctions in endothelial cells: II. Different types of lymphatic vessels. Differentiation; **57**(2):97-117.

Schraufstatter IU, Chung J, Burger M (2001). IL-8 activates endothelial cell CXCR1 and CXCR2 through Rho and Rac signaling pathways. Am J Physiol Lung Cell Mol Physiol; **280**(6):L1094-1103.

Schubert W, Frank PG, Razani B, Park DS, Chow CW, Lisanti MP (2001). Caveolae-deficient endothelial cells show defects in the uptake and transport of albumin in vivo. J Biol Chem; **276**(52):48619-48622.

Sciacca J, Forbes WM, Ashton FT, Lombardini E, Gamble HR, Schad GA (2002). Response to carbon dioxide by the infective larvae of three species of parasitic nematodes. Parasitol Int; **51**(1):53-62.

Shienvold FL, Kelly DE (1976). The hemidesmosome: new fine structural features revealed by freeze-fracture techniques. Cell Tissue Res; **172**(3):289-307.

Simionescu M (2000). Structural biochemical and functional differentiation of the vascular endothelium. In: Morphogenesis of Endothelium. Edited by W Risau and G M Rubanyi. Amesterdam, Harwood Academic:1-21.

Simionescu N, Simionescu M, Palade GE (1978). Open junctions in the endothelium of the postcapillary venules of the diaphragm. J Cell Biol; **79**(1):27-44.

Slaughter TF, Achyuthan KE, Lai TS, Greenberg CS (1992). A microtiter plate transglutaminase assay utilizing 5-(biotinamido)pentylamine as substrate. Anal Biochem; **205**(1):166-171.

Smith CA, Wood EJ (1991). Fibrous proteins. In Biological Molecules. London, Chapman and Hall:65-82.

Smith JM (1976). Comparative ultrastructure of the oesophageal glands of third stage larval hookworms. Int J Parasitol; **6**(1):9-13.

Sollberg S, Peltonen J, Uitto J (1992). Differential expression of laminin isoforms and beta 4 integrin epitopes in the basement membrane zone of normal human skin and basal cell carcinomas. J Invest Dermatol; **98**(6):864-870.

Spring KR (1998). Routes and mechanism of fluid transport by epithelia. Annu Rev Physiol; **60**:105-119.

Staiano-Coico L, Higgins PJ, Darzynkiewicz Z, Kimmel M, Gottlieb AB, Pagan-Charry I, et al (1986). Human keratinocyte culture. Identification and staging of epidermal cell subpopulations. J Clin Invest; **77**(2):396-404.

Stevens T, Garcia JG, Shasby DM, Bhattacharya J, Malik AB (2000). Mechanisms regulating endothelial cell barrier function. Am J Physiol Lung Cell Mol Physiol; **279**(3):L419-422.

Stins MF, Gilles F, Kim KS (1997). Selective expression of adhesion molecules on human brain microvascular endothelial cells. J Neuroimmunol; **76**(1-2):81-90.

Sun QH, DeLisser HM, Zukowski MM, Paddock C, Albelda SM, Newman PJ (1996). Individually distinct Ig homology domains in PECAM-1 regulate homophilic binding and modulate receptor affinity. J Biol Chem; **271**(19):11090-11098.

Sun TT, Green H (1978). Keratin filaments of cultured human epidermal cells. Formation of intermolecular disulfide bonds during terminal differentiation. J Biol Chem; **253**(6):2053-2060.

Swanson JL, Helwig EB (1968). Special fibrils of human dermis. J Invest Dermatol; **50**(2):195-199.

Swerlick RA, Lee KH, Wick TM, Lawley TJ (1992). Human dermal microvascular endothelial but not human umbilical vein endothelial cells express CD36 in vivo and in vitro. J Immunol; **148**(1):78-83.

Szabo G (1954). The number of melanocytes in human epidermis. Br Med J; **1**(4869):1016-1017.

Taddei A, Giampietro C, Conti A, Orsenigo F, Breviario F, Pirazzoli V, et al (2008). Endothelial adherens junctions control tight junctions by VE-cadherin-mediated upregulation of claudin-5. Nat Cell Biol; **10**(8):923-934.

Talavera D, Castillo AM, Dominguez MC, Gutierrez AE, Meza I (2004). IL8 release, tight junction and cytoskeleton dynamic reorganization conducive to permeability increase are induced by dengue virus infection of microvascular endothelial monolayers. J Gen Virol; **85**(Pt 7):1801-1813.

Taylor MD, LeGoff L, Harris A, Malone E, Allen JE, Maizels RM (2005). Removal of regulatory T cell activity reverses hyporesponsiveness and leads to filarial parasite clearance in vivo. J Immunol; **174**(8):4924-4933.

Teixeira-Carvalho A, Fujiwara RT, Stemmy EJ, Olive D, Damsker JM, Loukas A, et al (2008). Binding of excreted and/or secreted products of adult hookworms to human NK cells in Necator americanus-infected individuals from Brazil. Infect Immun; **76**(12):5810-5816.

Telo P, Breviario F, Huber P, Panzeri C, Dejana E (1998). Identification of a novel cadherin (vascular endothelial cadherin-2) located at intercellular junctions in endothelial cells. J Biol Chem; **273**(28):17565-17572.

Terranova VP, Rohrbach DH, Martin GR (1980). Role of laminin in the attachment of PAM 212 (epithelial) cells to basement membrane collagen. Cell; **22**(3):719-726.

Tillet E, Wiedemann H, Golbik R, Pan TC, Zhang RZ, Mann K, et al (1994). Recombinant expression and structural and binding properties of alpha 1(VI) and alpha 2(VI) chains of human collagen type VI. Eur J Biochem; **221**(1):177-185.

Timothy LM, Behnke JM (1993). Necator americanus in inbred mice: a re-evaluation of primary infection kinetics. Parasitology; **107**(Pt 4):425-431.

Timpl R (1996). Macromolecular organization of basement membranes. Curr Opin Cell Biol; **8**(5):618-624.

Timpl R, Brown JC (1996). Superamolecular assembly of basement membranes. Bioessays; **18**(2):123-132.

Timpl R, Martin JR (1997). Components of basement membranes. In: Immunochemistry of the extracellular matrix. CRC Press:119-150.

Toyofuku T, Yabuki M, Otsu K, Kuzuya T, Hori M, Tada M (1998). Direct association of the gap junction protein connexin-43 with ZO-1 in cardiac myocytes. J Biol Chem; **273**(21):12725-12731.

Trottein F, Descamps L, Nutten S, Dehouck MP, Angeli V, Capron A, et al (1999). Schistosoma mansoni activates host microvascular endothelial cells to acquire an anti-inflammatory phenotype. Infect Immun; **67**(7):3403-3409.

Twining SS (1984). Fluorescein isothiocyanate-labeled casein assay for proteolytic enzymes. Anal Biochem; **143**(1):30-34.

Van der Rest M, Garrone R (1991). Collagen family of proteins. FASEB J; **5**(13):2814-2823.

Vandenbroucke E, Mehta D, Minshall R, Malik AB (2008). Regulation of endothelial junctional permeability. Ann N Y Acad Sci; **1123**:134-145.

Verin AD, Birukova A, Wang P, Liu F, Becker P, Birukov K, et al (2001). Microtubule disassembly increases endothelial cell barrier dysfunction: role of MLC phosphorylation. Am J Physiol Lung Cell Mol Physiol; **281**(3):L565-574.

Vestweber D (2000). Molecular mechanisms that control endothelial cell contacts. J Pathol; **190**(3):281-291.

Villasante A, Pacheco A, Ruiz A, Pellicer A, Garcia-Velasco JA (2007). Vascular endothelial cadherin regulates vascular permeability: Implications for ovarian hyperstimulation syndrome. J Clin Endocrinol Metab; **92**(1):314-321.

Vogel SM, Easington CR, Minshall RD, Niles WD, Tiruppathi C, Hollenberg SM, et al (2001). Evidence of transcellular permeability pathway in microvessels. Microvasc Res; **61**(1):87-101.

Weber C, Fraemohs L, Dejana E (2007). The role of junctional adhesion molecules in vascular inflammation. Nat Rev Immunol; **7**(6):467-477.

Weis S, Shintani S, Weber A, Kirchmair R, Wood M, Cravens A, et al (2004). Src blockade stabilizes a Flk/cadherin complex, reducing edema and tissue injury following myocardial infarction. J Clin Invest; **113**(6):885-894.

Wilkins JA, Lin S (1986). A re-examination of the interaction of vinculin with actin. J Cell Biol; **102**(3):1085-1092.

Williams MC, Wissig SL (1975). The permeability of muscle capillaries to horseradish peroxidase. J Cell Biol; **66**(3):531-555.

Williamson AL, Brindley PJ, Abbenante G, Datu BJ, Prociv P, Berry C, et al (2003). Hookworm aspartic protease, Na-APR-2, cleaves human hemoglobin and serum proteins in a host-specific fashion. J Infect Dis; **187**(3):484-494.

Williamson AL, Brindley PJ, Abbenante G, Prociv P, Berry C, Girdwood K, et al (2002). Cleavage of hemoglobin by hookworm cathepsin D aspartic proteases and its potential contribution to host specificity. FASEB J; **16**(11):1458-1460.

Williamson AL, Brindley PJ, Loukas A (2003a). Hookworm cathepsin D aspartic proteases: contributing roles in the host-specific degradation of serum proteins and skin macromolecules. Parasitology; **126**(Pt 2):179-185.

Williamson AL, Lecchi P, Turk BE, Choe Y, Hotez PJ, McKerrow JH, et al (2004). A multi-enzyme cascade of hemoglobin proteolysis in the intestine of blood-feeding hookworms. J Biol Chem; **279**(34):35950-35957.

Williamson AL, Lustigman S, Oksov Y, Deumic V, Plieskatt J, Mendez S, et al (2006). Ancylostoma caninum MTP-1, an astacin-like metalloprotease secreted by infective hookworm larvae, is involved in tissue migration. Infect Immun; **74**(2):961-967.

Winter JA, Davies OR, Brown AP, Garnett MC, Stolnik S, Pritchard DI (2005). The assessment of hookworm calreticulin as a potential vaccine for necatoriasis. Parasite Immunol; **27**(4):139-146.

Wolff K, Schreiner E (1968). An electron microscopic study on the extraneous coat of keratinocytes and the intercellular space of the epidermis. J Invest Dermatol; **51**(6):418-430.

Wordemann M, Diaz RJ, Heredia LM, Collado Madurga AM, Ruiz Espinosa A, Prado RC, et al (2008). Association of atopy, asthma, allergic rhinoconjunctivitis, atopic dermatitis and intestinal helminth infections in Cuban children. Trop Med Int Health; **13**(2):180-186.

Wright TJ, Leach L, Shaw PE, Jones P (2002). Dynamics of vascular endothelial-cadherin and beta-catenin localization by vascular endothelial

growth factor-induced angiogenesis in human umbilical vein cells. Exp Cell Res; **280**(2):159-168.

Wright V, Bickle Q (2005). Immune responses following experimental human hookworm infection. Clin Exp Immunol; **142**(2):398-403.

Wu ZX, Fang YY, Liu YS (2006). Effect of a novel drug--enteric coated tribendimidine in the treatment of intestinal nematode infections. Zhongguo Ji Sheng Chong Xue Yu Ji Sheng Chong Bing Za Zhi; **24**(1):23-26.

Xiao K, Allison DF, Buckley KM, Kottke MD, Vincent PA, Faundez V, et al (2003). Cellular levels of p120 catenin function as a set point for cadherin expression levels in microvascular endothelial cells. J Cell Biol; **163**(3):535-545.

Xiao S, Zhan B, Xue J, Goud GN, Loukas A, Liu Y, et al (2008). The evaluation of recombinant hookworm antigens as vaccines in hamsters (Mesocricetus auratus) challenged with human hookworm, Necator americanus. Exp Parasitol; **118**(1):32-40.

Xiao SH, Hui-Ming W, Tanner M, Utzinger J, Chong W (2005). Tribendimidine: a promising, safe and broad-spectrum anthelmintic agent from China. Acta Trop; **94**(1):1-14.

Xu Y, Swerlick RA, Sepp N, Bosse D, Ades EW, Lawley TJ (1994). Characterization of expression and modulation of cell adhesion molecules on an immortalized human dermal microvascular endothelial cell line (HMEC-1). J Invest Dermatol; **102**(6):833-837.

Xue H, Liu S, Ren H, Qiang H, Xiao S, Feng Z, et al (1999). Enzyme-linked immunoelectrotransfer blotting analysis of human serologic responses to infective hookworm larval antigen. Chin Med J (Engl); **112**(3):249-250.

Xue J, Hui-Qing Q, Jun-Ming Y, Fujiwara R, Zhan B, Hotez P, et al (2005). Necator americanus: optimization of the golden hamster model for testing anthelmintic drugs. Exp Parasitol; **111**(4):219-223.

Yamada KM. Fibronectin domains and receptors (1988). In: Fibronectin. D. F. Mosher. New York, Academic Press Inc:47-121.

Yan JX, Wait R, Berkelman T, Harry RA, Westbrook JA, Wheeler CH, et al (2000). A modified silver staining protocol for visualization of proteins compatible with matrix-assisted laser desorption/ionization and electrospray ionization-mass spectrometry. Electrophoresis; **21**(17):3666-3672.

Yasuno H, Maeda M, Sato M, Nishimura A, Shimizu C, Miyamoto Y, et al (1980). Organ culture of adult human skin. J Dermatol; **7**(1):37-47.

Yen A, Braverman IM (1976). Ultrastructure of the human dermal microcirculation: the horizontal plexus of the papillary dermis. J Invest Dermatol; **66**(3):131-142.

Yoshioka K, Sugimoto N, Takuwa N, Takuwa Y (2007). Essential role for class II phosphoinositide 3-kinase alpha-isoform in Ca2+-induced, Rho- and Rho kinase-dependent regulation of myosin phosphatase and contraction in isolated vascular smooth muscle cells. Mol Pharmacol; **71**(3):912-920.

Yosipovitch G, Tur E, Morduchowicz G, Boner G (1993). Skin surface pH, moisture, and pruritus in haemodialysis patients. Nephrol Dial Transplant; **8**(10):1129-1132.

Young BA, Sui X, Kiser TD, Hyun SW, Wang P, Sakarya S, et al (2003). Protein tyrosine phosphatase activity regulates endothelial cell-cell interactions, the paracellular pathway, and capillary tube stability. Am J Physiol Lung Cell Mol Physiol; **285**(1):L63-75.

Yuan SY (2002). Protein kinase signaling in the modulation of microvascular permeability. Vascul Pharmacol; **39**(4-5):213-223.

Zeeuwen PL, Cheng T, Schalkwijk J (2009). The biology of cystatin M/E and its cognate target proteases. J Invest Dermatol; **129**(6):1327-1338.

Zhan B, Hotez PJ, Wang Y, Hawdon JM (2002). A developmentally regulated metalloprotease secreted by host-stimulated Ancylostoma caninum third-stage infective larvae is a member of the astacin family of proteases. Mol Biochem Parasitol; **120**(2):291-296.

Zhan B, Liu S, Perally S, Xue J, Fujiwara R, Brophy P, et al (2005). Biochemical characterization and vaccine potential of a heme-binding glutathione transferase from the adult hookworm Ancylostoma caninum. Infect Immun; **73**(10):6903-6911.

Appendix 1: Materials

A1.1 **Sigma- Aldrich**

Acrylamide/Bis-acrylamide, 29:1 (A-2792)
Agarose (A-9539)
Albumin from Bovine Serum (A-7906)
Albumin, tetramethyl-rhodamine isothiocyanate bovine (A-2289)
2-amino-2-methyl-1,3-propanediol (A-9754)
Ammonium Persulfate (A-3678)
Anti Goat IgG (whole molecule)- Alkaline Phosphatase (A-4187)
Anti Laminin (L-9393)
Anti Mouse IgG (whole molecule)- Alkaline Phosphatase (A-3562)Anti
Anti Rabbit IgG (whole molecule)- Alkaline Phosphatase (A-9919)
Anti Rabbit IgG (whole molecule)- TRITC (T-6778)
5' Biotinoyl- amino hexanoylamino-pentylamine trifluoroacetate salt (B-7306)
Calcium Chloride, anhydrous (C-4901)
Casein (C-5890)
Citric acid, trisodium salt dehydrate (C-7254)
Collagen from human placenta, type I (C-7774)
Collagen from human placenta, type III (C-4407)
Collagen from human placenta, type IV (C-7521)
Collagen from human placenta, type V (C-3657)
4-Chloro-1-Naphthol (C5,780-4)
4-Chloro-1-Naphthol (C-8890)
L-Cysteine (C-7755)
Dimethyl Sulfoxide (D-8418)
DL-Dithiothretol (D-9163)
Endothelial Cell Growth Supplement from bovine neural tissue (E-2759)
Ethylenediaminetetraacetic acid, anhydrous (E-6758)
E-TOXATE kit (ET0200)
ExtrAvidin® Peroxidase conjugate (E-2886)
Formaldehyde, 37% w/w solution (F-1268)
Formamide, > 99% (F-7503)
Gelatin, type A (G-8150)
Gelatin, type B (G-9391)
Hank's balanced salt solution (H-8264)
Hemoglobin, human (H-7379)
Heparin Sodium salt, grade 1-A (H-3149)
Hyaluronic acid potassium salt from human umbilical cord (H-1504)
Hyaluronidase from bovine testes, type I-S (H-3506)
Hydrogen Peroxide, 30% w/w solution (H-1009)
Magnesium Chloride, anhydrous (M-8266)
Microtiter plate, poly 96-well (M-9685)
Mouse IgG (whole molecule)- FITC (F-0257)
Neutral Red solution (N-2889)
Papain from papaya latex (P-4762)
Paraformaldehyde (P-6148)
Phalloidin- FITC (P-5282)
1,10-Phenanthroline, monohydrate (P-9375)
Phenylmethane Sulfonyl Fluoride (P-7626)

Phosphate Buffered Saline tablets (P-4417)
RPMI-1640 Medium (R-7509)
Silver Stain kit (AG-25)
Sodium Acetate, trihydrate (S-7670)
Sodium Bicarbonate (S-8875)
Sodium Chloride (S-3160/63)
Sodium Citrate, tribasic dehydrate (S-4641)
Sodium Phosphate, dibasic (S-9390)
Streptomycin Sulfate salt (S-9137)
Stains-All (E-9379)
3,3',5,5'-tetramethylbenidine dihydrochloride tablets (T-3405)
N,N,N',N'-tetramethylethylene-diamine (T-9281)
Triton, t-Octylphenoxypolythoxy ethanol (X-100)
Trizma$^®$ base (T-1503)
Trizma$^®$ hydrochloride (T-3253)
Whatman Chromatography papers, 3 MM (Z-270849)

A1.2   Fisher Scientific
Acetone (A-0560/17)
5-Bromo-4-Chloro-3-Indolyl Phosphate P- Toluidine salt, BCIP (B-PE1610/100)
Bromophenol Blue (B-P620/44)
Citric Acid (C-6200/60)
Glycine (B-P381/5)
Silver Nitrate (S-1280/48)
Sodium Dodecyl Sulfate (S-P530/53)
Sodium Thiosulfate (S-7240/53)

A1.3   BioRad
Equilibration Buffer I (163-2107)
Equilibration Buffer II (163-2108)
Glycerol, 30% solution
Mineral Oil (163-2129)
Precision Plus Protein^{TM} Standards, Dual Color (161-0374)
Protein Assay Dye Reagent Concentrate (500-0006)
ReadyStrip^{TM} IPG strips, 7 cm, Ph 3-10 (163-2000)
2-D Rehydration Sample Buffer I (163-2083)

A1.4   Southern Biotech
Goat Anti type III Collagen (1330-01)
Goat Anti type IV Collagen (1340-01)

A1.5   Calbiochem
Casein, N, N-Dimethylated, Bovine (311511)
E64 Protease Inhibitor (324890)
Thrombin, Human Plasma (605190)

A1.6   AbD Serotec
Goat Anti Human Collagen I (131001)
Goat Anti Human Collagen V (135001)

Native Human Laminin (5620-0604)
Rabbit Anti Human Fibronectin (4470-2204)

A1.7   BD Biosciences
Biotin Mouse Anti Human IL-8 (554718)
Fibronectin, Human (354008)
Mouse Anti Human CD144 (555661)
Mouse Anti Human IL-8 (554716)
Recombinant Human IL-8 (554609)

A1.8   Fluka
Coomassie Brilliant Blue R-250 (14745)
Pepstatin A (77170)
Polyethylene Glycol 20'000 (81300)
Sodium Chloride (71381)

A1.9   Gibco (Invitrogen)
Medium 199 X 1 (22340)
Trypsin-EDTA, 0.05% (25300)

A1.10   Biogenesis, UK
Rabbit Anti Human Fibronectin (4470-2204)

A1.11   The Binding Site, UK
Anti Human IgG (AFF)-Perox (AP004)

A1.12   Whatman PROTRAN
NitroCellulose Transfer Membrane (0.1 μm)

A1.13   Vector Laboratories, Inc
Vectashield Mounting Medium for Fluorescence with Propidium Iodide (H-1300)

A1.14   R&D Systems
Human IL-6 DuoSet® ELISA Development System (DY206)
Human VEGF DuoSet® ELISA Development System (DY293B)

A1.15   MERCK
Tert-Amyl-alcohol (8.06193)

A1.16   HyClone
Characterized Fetal Bovine Serum, heat inactivated (SH-30071)

A1.17   Costar, Corning
Transwell Permeable Supports, 12 mm inserts (3460)
25 cm^2 Tissue flasks (163371)

A1.19   VYCON
Lipid Resistant 3-way Stopcock (875.00)

Appendix 2: Buffers and Media

A2.1 SDS-PAGE buffers

A2.1.1 1.5 M Tris-HCl pH 8.8
Tris   90.83 g
Dissolved in distilled water, pH adjusted to 8.8 with concentrated HCl and made up to 500 mL.

A2.1.2 0.5 M Tris-HCl pH 6.8
Tris   30.30 g
Dissolved in distilled water, pH adjusted to 6.8 with concentrated HCl and made up to 500 mL.

A2.1.3 10% Sodium dodecyl sulphate (SDS)
Sodium dodecyl sulphate   10 g
Dissolved in distilled water to 100 mL.

A2.1.4 10% Ammonium persulphate (APS)
Ammonium persulphate   1 g
Dissolved in distilled water to 10 mL, stored at -20 ˚C in 200 µL aliquots.

A2.1.5 Resolving gel	6%	10%	12%
Acrylamide/Bis-acrylamide (29:1)	2.4 mL	4 mL	4.8 mL
1.5 M Tris-HCl, pH 8.8	3 mL	3 mL	3 mL
10% SDS	120 µL	120 µL	120 µL
Distilled water	6.48 mL	4.88 mL	4.08 mL

To 12 mL of resolving gel, add:
10% APS   60 µL
TEMED   6 µL

A2.1.6 4% Stacking gel
Acrylamide/Bis-acrylamide (29:1)   6.25 mL
0.5 M Tris-HCl, pH 6.8   12.5 mL
10% SDS   0.5 mL
Distilled water to 50 mL, and store at 4 ˚C. To 1 mL of stacking gel, add:
10% APS   10 µL
TEMED   4 µL

A2.1.7 2 x Reducing sample buffer (RSB)
0.5 M Tris-HCl, pH 6.8   2 mL
Glycerol   2 mL
10% SDS   4 mL
1% Bromophenol Blue   20 µL
Dithiothreitol (100 mM DTT)   154 g
Distilled water   2 mL

A2.1.8 2 x Non reducing sample buffer (NRSB)
0.5 M Tris-HCl, pH 6.8   2 mL
Glycerol   2 mL
10% SDS   4 mL
1% Bromophenol Blue   20 µL

Distilled water	2 mL

A2.1.9   SDS-PAGE electrode buffer

Tris	30 g
Glycine	144 g
SDS	10 g

Distilled water to 10 L.

A2.2   Staining and destaining buffers

A2.2.1   Fixative and destain

Methanol	250 mL
Glacial Acetic acid	100 mL
Distilled water	650 mL

A2.2.2   1% Coomassie Brilliant Blue R250 stain

Coomassie Brilliant Blue R250	0.5 g
Methanol	125 mL
Glacial Acetic acid	50 mL

Distilled water to 500 mL, filtered before use and stored in the dark at room temperature.

A2.2.3   0.1% Stains-All

Stains-All	1 mg
Formamide (50%)	1 mL

0.25% Agarose

Agarose	25 mg
0.5 M Tris-HCl, pH 6.8	10 mL

A2.2.4   0.02% Sodium thiosulphate

Sodium thiosulphate	0.1 g
Distilled water	500 mL

Keep at 4 ˚C.

A2.2.5   0.2% Silver nitrate

Silver nitrate	1 g
Distilled water	500 mL

Keep at 4 ˚C.

A2.2.6   Developing solution

Sodium carbonate	15 g
Sodium thiosulphate	2 mg
Formaldehyde (37%)	0.25 mL

Distilled water to 500 mL, stored at 4 ˚C.

A2.2.7   2% Ethylene-diaminetetraacetic acid (EDTA)

EDTA	10 g
Distilled water	500 mL

Stored at 4 ˚C.

A2.3   Western blotting buffers

A2.3.1   Tris buffered Saline (TBS)
NaCl   90 g
Tris   62.1 g
Dissolved in approximately 200 mL of distilled water, pH adjusted to 7.4 and made up to 10 L.

A2.3.2   Blocking buffer
Skimmed milk powder   5 g
TBS   100 mL

A2.3.3   Washing buffer (TBS/0.05% Tween)
Tween 20   250 µL
TBS   500 mL

A2.3.4   Transfer buffer
Glycine   144.1 g
Tris   30.25 g
SDS   10 g
Methanol   2 L
Made up with distilled water to 10 L, and stored at room temperature.

A2.3.5   Alkaline phosphatase substrate solution
        <u>Substrate buffer</u>
Tris   45.41 g
Dissolved in 330 mL of distilled water, pH adjusted to 9.6 with concentrated HCl and made up to 500 mL.
        <u>Nitro Blue Tetrazolium (NBT)</u>
Nitro blue tetrazolium   75 mg
Dissolved in 1 mL of 70% dimethyl-sulfoxide, and stored at -20 ˚C in 44 µL aliquots.
        <u>5 Bromo-4-chloro-3-indolyl phosphate p-toluidine salt (BCIP)</u>
BCIP salt   50 mg
Made up to 1 mL with 100% dimethyl-sulfoxide, and stored at -20 ˚C in 33 µL aliquots.
        <u>Alkaline phosphatase substrate</u>
Substrate buffer   20 ml
NBT   44 µL
BCIP   33 µL

A2.3.6   Horseradish peroxidase substrate solution
Chlornaptol   50 mg
Dissolved in 10 mL of ethanol, and made up to 50 mL with TBS.
30 µL of hydrogen peroxide added before use.

A2.4   General buffers

A2.4.1   Phosphate buffered saline (PBS)

NaCl   80 g
KCl   2 g
Na_2HPO_4 14.4 g
KH_2PO_4 2.4 g

Dissolved in approximately 500 mL of distilled water, pH adjusted to 7.2 and made up to 10 L.

A2.4.2   Washing buffer (PBS/0.05% Tween)

Tween 20   250 μL
PBS   500 mL

A2.4.3   0.1 M Citrate/Sodium citrate buffer

Sodium citrate   14.7 g
Citric acid   10.52 g

Each made up with distilled water to 500 mL, and titrated against each other to the required pH.

A2.4.4   0.1 M Sodium phosphate buffer

$NaH_2PO_4.2H_2O$ 7.8 g
Na_2HPO_4 7.09 g

Each made up with distilled water to 500 mL, and titrated against each other to the required pH.

A2.4.5   0.05 M 2-amino-2-methyl-1:3-propanediol-HCl buffer

2-amino-2-methyl-1:3-propanediol   2.6 g

Made up with distilled water to 500 mL, pH adjusted as required with concentrated HCl.

A2.4.6   0.5 M Tris-HCl pH 8.5

Tris   30.30 g

Dissolved in distilled water, pH adjusted to 8.5 with concentrated HCl and made up to 500 mL.

A2.4.7   0.1 M Tris-HCl pH 8.5

Tris   6.06 g

Dissolved in distilled water, pH adjusted to 8.5 with concentrated HCl and made up to 500 mL.

A2.4.8   0.05 M Carbonate/Bicarbonate buffer pH 9.6

Na_2CO_3 0.8 g
$NaHCO_3$ 1.47 g

Dissolved in 100 mL distilled water, pH adjusted to 9.6 with 1 M HCl and made up to 500 mL.

A2.4.9   0.1 M Sodium acetate pH 6

Sodium acetate   8.2 g

Dissolved in 800 mL distilled water, pH adjusted to 6 with glacial acetic acid and made up to 1 L.

A2.4.10   2.5 M Sulphuric acid
Concentrated sulphuric acid	18 mL
Distilled water	82 mL

A2.4.11   Blocking buffer (for ELISA)
Bovine albumin serum (BSA)	3 g
PBS	100 mL

A2.5   Cell culture materials

A2.5.1   1% Gelatin
Gelatin	1 g
Milli Q water	100 ml

Autoclaved to dissolve and sterilise, and stored at 4 ˚C.

A2.5.2   0.9% Saline
NaCl	4.5 g
Distilled water	500 mL

Autoclaved, and stored at room temperature.

A2.5.3   Medium M0
Medium 199	500 mL
Penicillin	1000 U
Streptomycin	1 g
Fungizone	1 mg

Stored at 4 ˚C.

A2.5.4   M20 Growth medium
M0	80 mL
Fetal bovine serum (FBS)	20 mL

A2.5.5   1% Collagenase
Collagenase type II	100 mg
Hank's balanced salt solution (HBSS)	10 mL

Mixed, filter sterilized and stored at -20 ˚C into 500 µL aliquots. In HUVEC isolation, collagenase is used at 0.1% in M0.

A2.5.6   50 mM Albumin-TRITC
Albumin-TRITC	1 mg
RPMI-1640 without phenol red	2 mL

A2.5.7   0.1% BSA/PBS
BSA	0.1 g
PBS	100 mL

Appendix 3: Supplementary results

A3.1   Effect of protease inhibitors alone on endothelial integrity
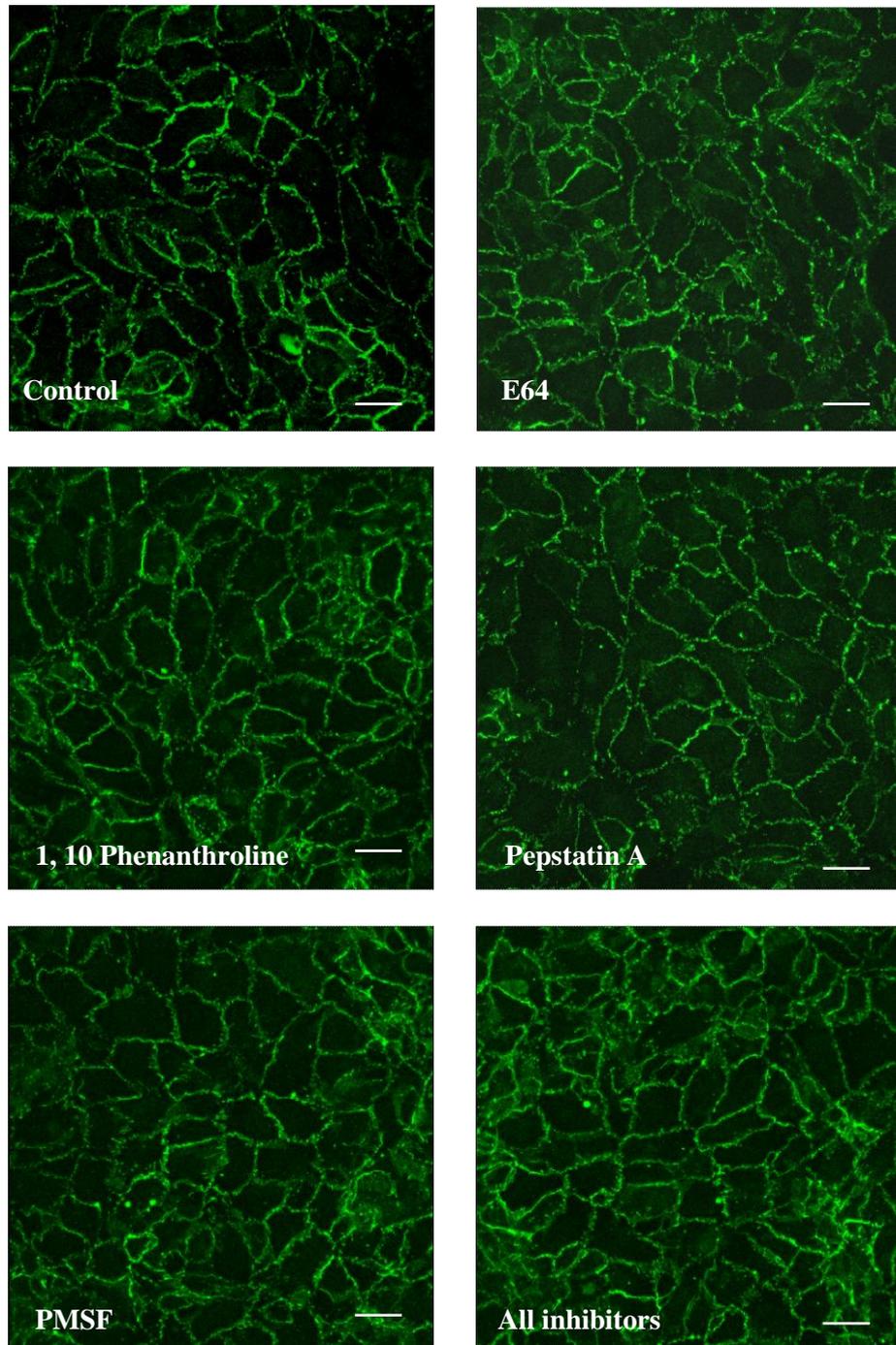
Figure A3.1.1   Effect of protease inhibitors on endothelial integrity as confluent HUVEC monolayers were treated with protease inhibitors, individually or in combination, and stained for VE-cadherin as described in section 4.2.5. Inhibitors alone induced no change in endothelial integrity as junctional VE-cadherin showed a continuous expression which is comparable to control, inhibitor-free monolayers.